

MICROCOPY RESOLUTION TEST CHART  
NATIONAL BUREAU OF STANDARDS-1963-A

AFWAL-TR-82-2092

DYNAMIC SIMULATION OF AIRBORNE HIGH POWER SYSTEMS

R. W. Gilchrist, Et al

Clemson University  
Clemson, South Carolina 29631

November 1982

Final Report for Period August 1979 - June 1982

Approved for public release; distribution unlimited.



ADA 123 730

DTIC FILE COPY

AERO PROPULSION LABORATORY  
AIR FORCE WRIGHT AERONAUTICAL LABORATORIES  
AIR FORCE SYSTEMS COMMAND  
WRIGHT-PATTERSON AIR FORCE BASE, OHIO 45433

DTIC  
SELECTED

JAN 24 1983

A

120

NOTICE

When Government drawings, specifications, or other data are used for any purpose other than in connection with a definitely related Government procurement operation, the United States Government thereby incurs no responsibility nor any obligation whatsoever; and the fact that the government may have formulated, furnished, or in any way supplied the said drawings, specifications, or other data, is not to be regarded by implication or otherwise as in any manner licensing the holder or any other person or corporation, or conveying any rights or permission to manufacture use, or sell any patented invention that may in any way be related thereto.

This report has been reviewed by the Office of Public Affairs (ASD/PA) and is releasable to the National Technical Information Service (NTIS). At NTIS, it will be available to the general public, including foreign nations.

This technical report has been reviewed and is approved for publication.



GERALD D. CLARK, Captain, USAF  
Project Engineer



PAUL R. BERTHEAUD  
Technical Area Manager  
Power Systems Branch  
Aerospace Power Division

FOR THE COMMANDER



D. DAVID RANDOLPH, MAJOR, USAF  
Deputy Director, Aerospace Power Division  
Aero Propulsion Laboratory

"If your address has changed, if you wish to be removed from our mailing list, or if the addressee is no longer employed by your organization please notify AFWAL/POOS, W-PAFB, OH 45433 to help us maintain a current mailing list".

Copies of this report should not be returned unless return is required by security considerations, contractual obligations, or notice on a specific document.

UNCLASSIFIED

SECURITY CLASSIFICATION OF THIS PAGE (When Data Entered)

REPORT DOCUMENTATION PAGE		READ INSTRUCTIONS BEFORE COMPLETING FORM
1. REPORT NUMBER AFWAL-TR-82-2092	2. GOVT ACCESSION NO. AD-A123 730	3. RECIPIENT'S CATALOG NUMBER
4. TITLE (and Subtitle) DYNAMIC SIMULATION OF AIRBORNE HIGH POWER SYSTEM		5. TYPE OF REPORT & PERIOD COVERED Final Report 15 August 79 - June 82
		6. PERFORMING ORG. REPORT NUMBER
7. AUTHOR(s) R.W. Gilchrist, H. Almaula, C.J. Alajajian G.F. Bell, D.D. Miller, E.S. Chen, F.C. Lee, C.Y. Chen, R.L. Avant, R. Ramanathan		8. CONTRACT OR GRANT NUMBER(s) F33615-79-C-2047
9. PERFORMING ORGANIZATION NAME AND ADDRESS Electrical and Computer Engineering Department Clemson University Clemson, S.C. 29631		10. PROGRAM ELEMENT, PROJECT, TASK AREA & WORK UNIT NUMBERS 3145 3249
11. CONTROLLING OFFICE NAME AND ADDRESS Aero Propulsion Laboratory (AFWAL/P005-2) Air Force Wright Aeronautical Laboratories (AFSC) Wright-Patterson Air Force Base, Ohio 45433		12. REPORT DATE November 1982
		13. NUMBER OF PAGES 246
14. MONITORING AGENCY NAME & ADDRESS (if different from Controlling Office)		15. SECURITY CLASS. (of this report)
		15a. DECLASSIFICATION/DOWNGRADING SCHEDULE UNCLASSIFIED
16. DISTRIBUTION STATEMENT (of this Report) Approved for public release; distribution unlimited.		
17. DISTRIBUTION STATEMENT (of the abstract entered in Block 20, if different from Report)		
18. SUPPLEMENTARY NOTES		
19. KEY WORDS (Continue on reverse side if necessary and identify by block number) Generator modeling including saturation, Resonant charging, AC and DC Direct phase variables Transformer modeling SCR modeling		
20. ABSTRACT (Continue on reverse side if necessary and identify by block number) > This report describes work done in modeling components and in simulating AC and DC charging systems using these components. The components modeled were three phase AC generators, three phase transformers, SCR's and SCR's in AC and DC resonant charging arrays. Mathematical and circuit models were developed and simulations were conducted using SCEPTRE, a CAD program.  > The generator model is in terms of phase variables and allows for consideration of direct and quadrature axis damping, nonlinearities due to saturation,		

→ variation in speed and is formulated so that prime mover and control components may be added later.

→ The transformer model is a circuit model which allows inclusion of coupling between phases and saturation effects,

→ The SCR model is a conversion of the SPICE 2 model to a SCEPTRE model with features to account for turn-off and turn-on transients encountered in AC and DC charging applications,

→ The generator and transformer operation was simulated under steady state and severe transient conditions to test component operation.

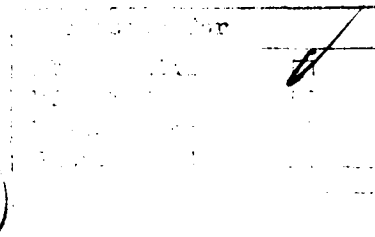
→ Simulations were conducted with the SCR models in AC and DC charging arrays. Snubbers and other compensating networks were designed to suppress undesirable transients and assure proper turn-on and turn-off ↗

Problems arising due to the system "stiff" differential equations are analyzed.

## Foreword

This final report was submitted by Clemson University, Clemson, S.C. 29631 under contract F33615-79-2047. The effort was sponsored by the Aero Propulsion Laboratory, Air Force Wright Aeronautical Laboratories, Air Force Systems Command, Wright Patterson AFB, Ohio 45433 under Project 3145. Capt. Fred Brockhurst was the Project Engineer at the beginning of the project. Capt. Jerry Clark is currently the Project Engineer. The time period covered by the report is August 15, 1979 through June 30, 1982.

Dr. R.W. Gilchrist (Principal Investigator), Dr. Haren Almaula, Dr. Charles J. Alajajian, G. Frank Bell, D.D. Miller, and E.S. Chen Performed the part of the work done at Clemson. The work Subcontracted to VPI and SU was performed by Dr. Fred C. Lee (Principal Investigator), Dr. G.Y. Chen, R.L. Avant and R. Ramanathan.



A

## TABLE OF CONTENTS

SECTION	PAGE
I INTRODUCTION	1
II THE GENERATOR MODEL	3
2.1 OBJECTIVE	3
2.2 GENERATOR MATHEMATICAL MODEL	3
2.3 CHOICE OF GENERATOR VARIABLES	4
2.4 FORMULATION FOR NON-LINEAR INDUCTANCE	5
2.5 SCEPTRE EQUIVALENT CIRCUIT	11
2.6 INCLUSION OF PRIME-MOVER AND EXCITATION CONTROL MODEL	13
2.7 AN ALTERNATIVE GENERATOR MODEL	13
III THE TRANSFORMER MODEL	23
3.1 OBJECTIVE	23
3.2 THE TRANSFORMER MODEL	23
3.3 SCEPTRE MODELING	28
IV THE RESONANT CHARGING CIRCUITS	30
4.1 OBJECTIVE	30
4.2 THE SCR MODEL IN SPICE 2	30
4.3 THE MODIFIED HU-KI MODEL OF THE SCR FOR SPICE 2	37
4.4 THE SCR MODEL IN SCEPTRE	48
V CHOICE OF VARIABLES	70
5.1 OBJECTIVE	70
5.2 CHOICE OF VARIABLES	70
5.3 SCEPTRE VARIABLES	74
VI NUMERICAL METHODS FOR STIFF DIFFERENTIAL EQUATIONS	75
6.1 INTRODUCTION	75

## TABLE OF CONTENTS (Continued)

SECTION	PAGE	
6.2	INTEGRATION METHODS	75
6.3	INTEGRATION METHODS OF SCEPTRE	77
VII	SYSTEM INTEGRATION	78
VIII	GENERATOR AND TRANSFORMER SIMULATION RESULTS	80
8.1	INTRODUCTION	80
8.2	THE SIMULATION RUNS	81
8.3	RESULTS	82
IX	AC AND DC CHARGING CIRCUIT SIMULATION RESULTS	104
9.1	INTRODUCTION	104
9.2	SPICE 2 SINGLE LOOP SIMULATION	105
9.3	SPICE 2 SIMULATION OF A TWO LOOP AC RESONANT CHARGING CIRCUIT	105
9.4	SPICE 2 SIMULATION OF A SINGLE LOOP AC RESONANT CHARGING CIRCUIT USING TWO SCR'S IN PARALLEL	115
9.5	SPICE 2 SIMULATION OF A SINGLE LOOP AC RESONANT CHARGING CIRCUIT USING TWO SCR'S IN SERIES	115
9.6	AC RESONANT CHARGING CIRCUIT SIMULATIONS IN SCEPTRE	121
9.7	AN AC RESONANT CHARGING CIRCUIT WITH THREE SCRS AND A DIODE IN SERIES	126
9.8	A THREE PHASE AC RESONANT CHARGING CIRCUIT	128
9.9	A DC RESONANT CHARGING SYSTEM	142
X	CONCLUSION	148
10.1	INTRODUCTION	148
10.2	SYSTEM VARIABLES	148
10.3	NUMERICAL METHODS FOR STIFF DIFFERENTIAL EQUATIONS	149

## TABLE OF CONTENTS (Concluded)

SECTION	PAGE
10.4 THE GENERATOR MODEL	149
10.5 THE TRANSFORMER MODEL	150
10.6 AC AND DC RESONANT CHARGING CIRCUITS	151
APPENDIX A THE GENERATOR MODEL	154
A.1 EQUIVALENT CIRCUIT EQUATIONS	154
A.2 SATURATION EFFECTS	157
A.3 THE TORQUE EQUATION	161
APPENDIX B SATURATED GENERATOR MODEL	163
B.1 SATURATED GENERATOR EQUATIONS	163
APPENDIX C GENERATOR DATA USED	170
C.1 UNSATURATED GENERATOR DATA	170
C.2 SATURATION DATA	171
C.3 MEASUREMENT OF THE UNSATURATED INDUCTANCES	172
APPENDIX D USERS MANUAL	177
D.1 INTRODUCTION	177
D.2 THREE PHASE GENERATOR MODEL	177
D.3 TRANSFORMER MODEL	210
D.4 THE RESONANT CHARGING PROGRAMS	216
REFERENCES	231

## LIST OF ILLUSTRATION

FIGURE		PAGE
1.	VARIATION OF $L_{AA}$ WITH $i_x$	7
2.	EQUIVALENT CIRCUIT FOR PHASE "a"	12
3.	DC CIRCUIT FOR NODAL ANALYSIS	14
4.	GENERAL DC NETWORK ELEMENT	16
5.	PHASE A BACKWARD EULER NODAL CIRCUIT	20
6.	THREE LEG THREE PHASE TRANSFORMER	25
7.	SCEPTRE EQUIVALENT CIRCUIT FOR PHASE A	28
8.	A SPICE 2 SCR MODEL	31
9.	THE SPICE 2 SCR MODEL	32
10.	SPICE AC RESONANT CHARGING CIRCUIT	38
11.	SPICE AC RESONANT CHARGING RESULTS	39
12.	MODIFIED HU-KI MODEL	41
13.	SCR JUNCTION CAPACITANCES	42
14.	SPICE 2 HU-KI MODEL	45
15.	SCR V-I CHARACTERISTIC CURVE	47
16.	SCEPTRE TWO-TRANSISTOR SCR NETWORK	50
17.	SCEPTRE 3-JUNCTION SCR MODEL	52
18.	SCEPTRE 3-JUNCTION SCR MODEL	53
19.	SCEPTRE PROGRAM SCR MODEL	59
20.	JUNCTION CAPACITANCE SUBPROGRAM	60
21.	JUNCTION BREAKDOWN CURRENT SUBPROGRAM	60
22.	REDUCED SCEPTRE SCR MODEL	66
23.	SCEPTRE PROGRAM FOR REDUCED SCR MODEL	67
24.	SUBPROGRAM FOR PX1 AND PX2	67

LIST OF ILLUSTRATIONS (Continued)

FIGURE		PAGE
25.	CALAHAN'S EXAMPLE CIRCUIT	73
26.	PHASE A LINE CURRENT LINEAR MODEL STEADY STATE	84
27.	SPEED VS TIME LINEAR MODEL STEADY STATE	85
28.	DIRECT AXIS DAMPER CURRENT	86
29.	PHASE A LINE CURRENT SATURATED MODEL STEADY STATE	87
30.	SPEED VS TIME SATURATED MODEL STEADY STATE	88
31.	DIRECT AXIS DAMPER CURRENT	89
32.	PHASE A CURRENT SYMMETRICAL SHORT CIRCUIT	90
33.	FIELD CURRENT SYMMETRICAL SHORT CIRCUIT	91
34.	DIRECT AXIS DAMPER CURRENT	92
35.	QUADRATURE AXIS DAMPER CURRENT	93
36.	SPEED SYMMETRICAL SHORT CIRCUIT	94
37.	PHASE A CURRENT PHASE A SHORTED	95
38.	FIELD CURRENT PHASE A SHORTED	96
39.	DIRECT AXIS DAMPER CURRENT	97
40.	QUADRATURE AXIS DAMPER CURRENT	98
41.	SPEED PHASE A SHORTED	99
42.	PHASE A PRIMARY CURRENT	101
43.	PHASE A SECONDARY CURRENT	102
44.	PHASE A MAGNETIZING CURRENT	103
45.	SINGLE LOOP CIRCUIT WITHOUT SNUBBER	106
46.	RESULTS FOR CIRCUIT OF FIGURE 45	107
47.	SINGLE LOOP CIRCUIT WITH SNUBBER	108
48.	RESULTS FOR CIRCUIT OF FIGURE 47	109
49.	SPICE 2 TWO LOOP AC RESONANCE	110

LIST OF ILLUSTRATION (Continued)

FIGURE		PAGE
50.	PROGRAM FOR CIRCUIT OF FIGURE 49	111
51.	RESULTS FOR CIRCUIT OF FIGURE 49	112
52.	PROGRAM FOR FIGURE 49 WITH SNUBBERS	113
53.	RESULTS FOR PROGRAM OF FIGURE 52	14
54.	SPICE 2 PARALLEL SCR'S	16
55.	PROGRAM FOR FIGURE 54	
56.	RESULTS FOR FIGURE 54	118
57.	PARALLEL SCR'S WITH COMPENSATION	119
58.	RESULTS FOR PROGRAM OF FIGURE 57	120
59.	SPICE 2 SERIES SCR'S	122
60.	RESULTS FOR CIRCUIT OF FIGURE 59	123
61.	FUNCTION GENERATOR FGEN SUBPROGRAM	129
62.	PERTURBED PARAMETER SCR MODELS AND SERIES SCR'S AND DIODE	130
63.	CIRCUIT FOR PROGRAMS OF FIGURE 62	132
64.	RESULTS FOR FIGURE 62	133
65.	3 PHASE AC RESONANT CHARGING CIRCUIT	136
66.	SCEPTRE PROGRAM FOR FIGURE 65	137
67.	GATE PULSES FOR FIGURE 65	138
68.	RESULTS FOR FIGURE 65	139
69.	A DC RESONANT CHARGING SYSTEM	143
70.	GATE PULSES FOR FIGURE 69	144
71.	SCEPTRE PROGRAM FOR FIGURE 69	145
72.	RESULTS FOR FIGURE 69	146

## LIST OF ILLUSTRATIONS (Concluded)

FIGURE		PAGE
73.	THREE-PHASE GENERATOR CIRCUIT	155
74.	GENERATOR ROTOR POSITION	158
75.	VARIATION OF INDUCTANCE WITH $\theta$	160
76.	SCEPTRE CIRCUIT ELEMENTS	180
77.	SCEPTRE TABLE OF VALUES	185
78.	SCEPTRE NODE NUMBERING -TRANSFORMER	187
79.	SCEPTRE NODE NUMBERING -TRANSFORMER	211
80.	SCEPTRE 3-JUNCTION SCR NODES	217
81.	SCEPTRE SCR PROGRAM MODEL	218
82.	SUBPROGRAM FOR PX1 AND PX2	218
83.	SUBPROGRAM FOR JUNCTION CAPACITANCES	219
84.	AC RESONANT CHARGING CIRCUIT	223
85.	PROGRAM FOR FIGURE 84	224
86.	SUBPROGRAM FOR GATING IN FIGURE 84	225
87.	DC RESONANT CHARGING CIRCUIT	229
88.	PROGRAM FOR FIGURE 87	230

## LIST OF TABLES

TABLE		PAGE
1.	PARAMETERS FOR "HU-KI METHOD"	34
2.	MODEL ELEMENTS AND CRITICAL PARAMETERS	35
3.	VALUES FOR GE C602 LM SCR	37
4.	SYMBOL CONVERSION CHART	54
5.	ELEMENTS FOR 3-JUNCTION MODEL	55
6.	PROCEDURE FOR PARAMETER DETERMINATION	56
7.	PARAMETERS FOR GE C602 LM SCR	58
8.	MANUFACTURER'S SPECIFICATIONS	58
9.	ELEMENTS FOR 3-JUNCTION MODEL	68
10.	DC RESONANT CHARGIN SCALING	127
11.	SATURATION COEFFICIENTS	173
12.	PARAMETERS FOR GE C602 LM SCR	220
13.	MANUFACTURER'S SPECIFICATIONS	220
14.	ELEMENTS FOR 3-JUNCTION MODEL	221
15.	DC RESONANT CHARGING SCALING	226

SECTION I  
INTRODUCTION

This is the final report for work on the project Dynamic Simulation of Airborne High Power Systems for the period of August 15, 1979 through June 30, 1982.

Models were developed for three phase generators, three phase transformers, SCR's and resonant charging circuits. The models were developed in sufficient detail to represent operating conditions outside the range of the usual models.

The three phase ac generator model includes sufficient detail to allow inclusion of the effects of speed variation and field saturation. This allows simulations of start up and severe faults, balanced or unbalanced. Data are included for a specific machine and results are included for simulation of severe fault conditions. Methods for measuring required machine data are included.

The transformer model developed is for a three phase bank and can be used with SCEPTRE to simulate a bank of three single phase transformers or a three phase transformer. Wye-wye or delta-wye connections can be represented. The model allows inclusion of magnetic saturation and also allows inclusion of coupling between phases for the three phase transformer case.

Simulations include a composite system of generator and transformer.

The ac and dc resonant charging modeling and simulation consisted of determining an appropriate SCR model and conducting simulations using the SCR models in ac and dc resonant charging circuit configurations supplied by the Air Force.

Existing SCR models were inadequate at the specified power levels and in the resonant charging configurations. The "Hu-Ki model" was chosen as

the best existing model. Starting with the "Hu-Ki model," simulation on SPICE 2 assisted in arriving at a "modified Hu-Ki" model appropriate for this application. A SCEPTRE model was developed from the SPICE 2 model. A method of determining SCEPTRE SCR model parameters from manufacturers data is given.

The work also addresses the problems of system variable selection in nonlinear simulation, stiff differential equations and system simulation using SPICE 2 and SCEPTRE CAD programs.

## SECTION II

### THE GENERATOR MODEL

#### 2.1 OBJECTIVE

This part of the project was to develop a mathematical and computer model of a three phase ac generator. The model is to be adequate for including effects of unbalanced transient loads, startup transient, speed variation, field excitation variation and saturation of the field.

Most of the models existing in the literature (References 1,5,6) were developed for representing generators in power system stability studies. In power system applications the generator is usually connected to a large system and the generator is constrained to operation in a narrow range or it is removed from the system by protective devices. In the airborne high power system one has a single generator supplying an isolated load and the machine may be subject to more severe transients of a wider range.

Further, in a power system the concerns of the modeling for stability studies are sustained overload currents and the synchronising of the generator with the system. In this airborne high power system the operation is asynchronous and there is need to consider short duration transient pulses that may affect the operation of the electronics in the associated load.

In order to have a model sensitive to these concerns, more detail is included than is usual in power system stability studies. The model used has these additional features: direct and quadrature damping effects; variable speed; saturation effects including both variation in inductance and variation in  $\partial L/\partial i$ ; more accurate developed torque formulation; formulation in a form such that the prime mover model and the field control model may be added if these become available at some later time.

#### 2.2 GENERATOR MATHEMATICAL MODEL

Appendix A shows the generator equivalent circuit and establishes the notation and time and space references used in the modeling.

In vector and matrix form the equation for the circuit model is given either by Equation (43) or (46) and repeated here as Equations (1) or (2).

$$V = RI + \frac{d\lambda}{dt} \quad (1)$$

$$V = RI + \frac{d}{dt} (LI) \quad (2)$$

The torque equations relating electrical to mechanical variables is given by Equations (55) and (56) and here as Equations (3), (4), and (5).

$$\frac{d^2\theta}{dt^2} = \frac{1}{J} [T_m - T_e - B \frac{d\theta}{dt}] \quad (3)$$

where the  $T_e$  term represents the so called electrical torque and corresponds to the power converted from mechanical form to electrical form,  $P_e$

$$P_e = T_e \frac{d\theta}{dt} \quad (4)$$

Concordia (Reference 7) shows that the  $T_e$  is defined by

$$T_e = \frac{1}{2} [I]^T \left[ \frac{\partial L}{\partial \theta} \right] [I] \quad (5)$$

Equations (1) through (5) basically define the generator model. These equations are standard forms in the literature (References [1,3,5,6,7]). The model used in this work differs from others in the choice of system variables and in the details of defining the inductance coefficients. These points are discussed in Appendix A and in subsequent sections of this report.

### 2.3 CHOICE OF GENERATOR VARIABLES

Choices of generator state variables were made in two areas. First, the direct phase variables were chosen over the more traditional direct and quadrature axis variables. Secondly, the current variables were chosen over the flux linkage variables.

The direct phase variables were chosen over the traditional direct and quadrature variables for three reasons. First, while Parks (Reference 1) transformation does significantly simplify the generator model equations and hence aid in their solution, it is necessary at each numerical integration step to transform the variables back to direct-phase variables for compatibility

with the external load made up of electronic components and resonant charging elements. Any expected gain would be greatly diminished by this transformation.

Secondly, additional logic would need developing to represent the effect of direct-phase open and short circuits on d-q variables.

Thirdly, the application of Parks transformation and the resulting simplified equations depend on certain simplifying assumptions which don't really apply if saturation effects and  $\partial L/\partial i$  effects are significant.

The choice of the current variables over the flux linkage variables was dictated not by generator model considerations but by limitations imposed by models of the electronic components of the load (resonant charging circuit).

The developments in Section V and VI of this report indicate that for appropriate numerical integration methods, use of the  $\lambda$  variable gives less propagated error for non-linear inductances. Further, Nakra (Reference 8) and Manly (Reference 9) cite inaccuracies that may arise due to noise in the  $\partial L/\partial i$  terms which appear in the current variable formulation.

However, available data and existing models for diodes, transistors and SCR's are given in terms of current and voltage variables instead of flux linkages and charge variables. This and the need to use a program such as SPICE or SCEPTRE for the electronic component modeling dictated the use of current variables for modeling the generator. SCEPTRE normally requires that currents be the state variables in inductor elements.

#### 2.4 FORMULATION FOR NON-LINEAR INDUCTANCE

Saturation effects cause the inductance coefficients to be non-linear functions of the machine currents. The circuit model equations for direct-phase current formulation with saturation effects are now developed. The terms arising due to dependence of inductance on the currents are illustrated.

The generator circuit model equations for direct-phase current formulation and inductance as a function of current are

$$V = RI + L \frac{dI}{dt} + \left(\frac{dL}{dt}\right)(I) \quad (6)$$

In the second term on the right-hand side of the equation the inductances are those defined in the appendix by Equation (50) except that the L and M coefficients are modified by saturation. The third term involving dL/dt will be treated subsequently.

The assumptions made on the effect of saturation on the inductance terms are discussed in Appendix A. Equation (53), repeated here, illustrates how one of the inductance terms is affected by saturation.

$$\begin{aligned} L_{aas} &= C_{aa} L_s + C_{aa} L_m \cos 2\theta \\ &= C_{aa} L_{aa} \end{aligned} \quad (53)$$

Implied here is that the shape of the inductance curve as a function of rotor position is not changed by saturation, (the validity of this assumption is discussed in Appendix A). This form further implies that saturated inductance measurements can be made on the direct axis as a function of net excitation contributed by the various currents. The net excitation current in terms of equivalent main field current is

$$\begin{aligned} i_x &= i_F + N_{FD} i_D + N_{Fa} [i_a \cos(\theta) + i_b \cos(\theta - \frac{2\pi}{3}) \\ &\quad + i_c \cos(\theta + \frac{2\pi}{3})] \end{aligned} \quad (7)$$

To determine the  $C_{aa}$ , the rotor is aligned with the "a" phase axis and  $L_{aa}$  is measured as  $i_x$  is varied over an appropriate range giving a curve as shown in Figure 1.

The equation for  $L_{aa}$  as a function of  $i_x$  is obtained by appropriate polynomial curve matching techniques and results in the following form.

$$\begin{aligned} L_{aas} &= L_{ao} (1 + a_1 i_x + a_2 i_x^2 + a_3 i_x^3 + \dots) \\ &= L_{ao} C_{aa} \end{aligned} \quad (8)$$

Thus  $C_{aa}$  is the normalized polynomial of the variation of the inductance  $L_{aas}$  with  $i_x$ .

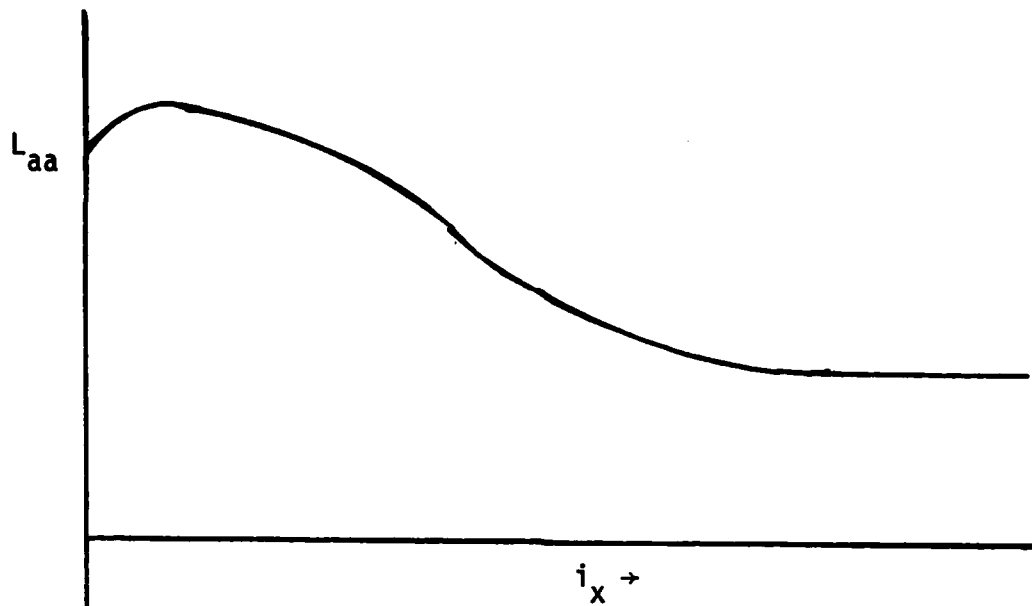


FIGURE 1. VARIATION OF  $L_{aa}$  WITH  $i_x$  (SATURATION EFFECTS)

C terms are required for each of the equations listed in Equation (50). Measurements are needed to determine the following C polynomials:  $C_{aa}$ ,  $C_{aF}$ ,  $C_{aD}$ ,  $C_{aQ}$ ,  $C_{FF}$ ,  $C_{FD}$ ,  $C_{DD}$ . These requirements are listed in more detail in a later section.

These saturation coefficients are associated with the inductance terms as shown below in Equation (9) where the s subscript is dropped

$$L_{aa} = C_{aa} (L_s + L_m \cos(2\theta))$$

$$L_{ab} = C_{aa} (-M_s + L_m \cos(2\theta - \frac{2\pi}{3})) = L_{ba}$$

$$L_{ac} = C_{aa} (-M_s + L_m \cos(2\theta + \frac{2\pi}{3})) = L_{ca}$$

$$L_{aF} = C_{aF} (M_{aF} \cos(\theta)) = L_{Fa}$$

$$L_{aD} = C_{aD} (M_{aD} \cos(\theta)) = L_{Da}$$

$$\begin{aligned}
L_{aQ} &= C_{aQ}(M_{aQ} \sin(\theta)) & = L_{Qa} \\
L_{bb} &= C_{aa}(L_s + L_m \cos(2\theta + \frac{2\pi}{3})) \\
L_{bc} &= C_{aa}(-M_s + L_m \cos(2\theta)) & = L_{cb} \\
L_{bF} &= C_{aF}(M_{aF} \cos(\theta - \frac{2\pi}{3})) & = L_{Fb} \\
L_{bD} &= C_{aD}(M_{aD} \cos(\theta - \frac{2\pi}{3})) & = L_{Db} \\
L_{bQ} &= C_{aQ}(M_{aQ} \sin(\theta - \frac{2\pi}{3})) & = L_{Qb} \\
L_{cc} &= C_{aa}(L_s + L_m \cos(2\theta - \frac{2\pi}{3})) \\
L_{cF} &= C_{aF}(M_{aF} \cos(\theta + \frac{2\pi}{3})) & = L_{Fc} \\
L_{cD} &= C_{aD}(M_{aD} \cos(\theta + \frac{2\pi}{3})) & = L_{Dc} \\
L_{cQ} &= C_{aQ}(M_{aQ} \sin(\theta + \frac{2\pi}{3})) & = L_{Qc} \\
L_{FF} &= C_{FF}L_F \\
L_{FD} &= C_{FD}M_R & = L_{DF} \\
L_{FQ} &= 0 & = L_{QF} \\
L_{DD} &= C_{DD}L_D \\
L_{DQ} &= 0 & = L_{QD} \quad (9) \\
L_{QQ} &= L_Q
\end{aligned}$$

Next consider the third term on the right hand side of Equation (6),  $(dL/dt)(I)$ .

Consider, for example, the first row of the matrix product  $(dL/dt)(I)$ .

$$\begin{aligned} & \left(\frac{d}{dt} L_{aa}\right)i_a + \left(\frac{d}{dt} L_{ab}\right)i_b + \left(\frac{d}{dt} L_{ac}\right)i_c + \left(\frac{d}{dt} L_{aF}\right)i_F \\ & + \left(\frac{d}{dt} L_{aD}\right)i_D + \left(\frac{d}{dt} L_{aQ}\right)i_Q \end{aligned} \quad (10)$$

now noting that the inductances are functions of the net excitation,  $i_x$ , and  $i_x$  is given by Equation (7), the derivative in the first term of Equation (10) expanded becomes.

$$\begin{aligned} \frac{d}{dt} L_{aa} &= \frac{\partial L_{aa}}{\partial i_x} \frac{\partial i_x}{\partial t} + \frac{\partial L_{aa}}{\partial \theta} \frac{\partial \theta}{\partial t} \quad (11) \\ &= \frac{\partial L_{aa}}{\partial i_x} \left[ \frac{\partial i_F}{\partial t} + N_{FD} \frac{\partial i_D}{\partial t} + N_{Fa} \left(\frac{\partial i_a}{\partial t}\right) \cos(\theta) - N_{Fa} i_a \sin(\theta) \frac{\partial \theta}{\partial t} \right. \\ &+ N_{Fa} \left(\frac{\partial i_b}{\partial t}\right) \cos\left(\theta - \frac{2\pi}{3}\right) - N_{Fa} i_b \sin\left(\theta - \frac{2\pi}{3}\right) \frac{\partial \theta}{\partial t} \\ &+ \left. N_{Fa} \left(\frac{\partial i_c}{\partial t}\right) \cos\left(\theta + \frac{2\pi}{3}\right) - N_{Fa} i_c \sin\left(\theta + \frac{2\pi}{3}\right) \frac{\partial \theta}{\partial t} \right] + \frac{\partial L_{aa}}{\partial \theta} \frac{\partial \theta}{\partial t} \quad (12) \end{aligned}$$

The expressions for the other terms after expanding the derivative terms of Equation (10):

$$\frac{d}{dt} L_{ab}; \frac{d}{dt} L_{ac}; \frac{d}{dt} L_{aF}; \frac{d}{dt} L_{aD}; \frac{d}{dt} L_{aQ};$$

will be the same as Equation (12) except for the quantities outside the square brackets where the inductance in question will appear. When these terms are all expanded and terms are collected, the first row of the  $L \frac{dI}{dt} + \left(\frac{dL}{dt}\right) I$  matrix becomes

$$\begin{aligned}
\frac{d\lambda_a}{dt} = & [A_a N_{Fa} \cos(\theta) + L_s C_{aa} + L_m C_{aa} \cos(2\theta)] \frac{di_a}{dt} \\
& + [A_a N_{Fa} \cos(\theta - \frac{2\pi}{3}) - M_s C_{aa} + L_m C_{aa} \cos(2\theta - \frac{2\pi}{3})] \frac{di_b}{dt} \\
& + [A_a N_{Fa} \cos(\theta + \frac{2\pi}{3}) - M_s C_{aa} + L_m C_{aa} \cos(2\theta + \frac{2\pi}{3})] \frac{di_c}{dt} \\
& + [A_a + C_{aF} M_{aF} \cos(\theta)] \frac{di_F}{dt} \\
& + [A_a N_{FD} + C_{aD} M_{aD} \cos(\theta)] \frac{di_D}{dt} \\
& + [C_{aQ} M_{aQ} \sin(\theta)] \frac{di_Q}{dt} \\
& - [A_a B + 2C_{aa} C_a L_m + (C_{aF} M_{aF} i_F + C_{aD} i_D) \sin(\theta) - C_{aQ} M_{aQ} i_Q \cos(\theta)] \frac{d\theta}{dt}
\end{aligned} \tag{13}$$

where

$$A_a = i_a \frac{\partial L_{aa}}{\partial i_x} + i_b \frac{\partial L_{ab}}{\partial i_x} + i_c \frac{\partial L_{ab}}{\partial i_x} + i_F \frac{\partial L_{aF}}{\partial i_x} + i_F \frac{\partial L_{aF}}{\partial i_x} + i_D \frac{\partial L_{aD}}{\partial i_x} + i_Q \frac{\partial L_{aQ}}{\partial i_x}$$

$$B = N_{Fa} [i_a \sin(\theta) + i_b \sin(\theta - \frac{2\pi}{3}) + i_c \sin(\theta + \frac{2\pi}{3})]$$

$$C_a = i_a \sin(2\theta) + i_b \sin(2\theta - \frac{2\pi}{3}) + i_c \sin(2\theta + \frac{2\pi}{3})$$

Similar expansions are required for each of the rows of the matrix terms corresponding to the terms

$$\frac{\partial \lambda_b}{\partial t}, \frac{\partial \lambda_c}{\partial t}, \frac{\partial \lambda_F}{\partial t}, \frac{\partial \lambda_D}{\partial t}, \text{ and } \frac{\partial \lambda_Q}{\partial t}.$$

The complete listing of these terms is included in Appendix B.

Further, one must note and include the saturation effects on the  $\frac{\partial L}{\partial i_x}$  terms. Again using phase "a" terms as example

$$L_{aa} = C_{aa} (L_s + L_m \cos(2\theta)) \tag{14}$$

and noting from Equation (8)

$$C_{aa} = 1 + a_1 i_x + a_2 i_x^2 + a_3 i_x^3 + \dots \quad (15)$$

$$\frac{\partial L_{aa}}{\partial i_x} = (L_s + L_m \cos(2\theta))(a_1 + 2a_2 i_x + 3a_3 i_x^2 + \dots) \quad (16)$$

Again the derivative of the other inductance terms with respect to  $i_x$  may be written in a similar fashion.

Finally the derivatives of the inductance terms with respect to  $\theta$  are obtained. The "a" phase terms are listed

$$\begin{aligned} \frac{\partial L_{aa}}{\partial \theta} &= -2 C_{aa} L_m \sin(2\theta) \\ \frac{\partial L_{ab}}{\partial \theta} &= -2 C_{ao} L_m \sin(2\theta - \frac{2\pi}{3}) \\ \frac{\partial L_{ac}}{\partial \theta} &= -2 C_{aa} L_m \sin(2\theta + \frac{2\pi}{3}) \\ \frac{\partial L_{aF}}{\partial \theta} &= -C_{aF} M_{aF} \sin(\theta) \\ \frac{\partial L_{aD}}{\partial \theta} &= -C_{aD} M_{aD} \sin(\theta) \\ \frac{\partial L_{aQ}}{\partial \theta} &= -C_{aQ} M_{aQ} \cos(\theta) . \end{aligned} \quad (17)$$

## 2.5 SCEPTRE EQUIVALENT CIRCUIT

The circuit model equations developed in previous sections are now in a form from which the equivalent circuit may be readily discerned. An equivalent phase "a" circuit that is easily analyzed by the SEPTRE program is shown in Figure 2. Equations for the other circuits of Figure 20 are developed in a similar manner and equivalent circuits built for them. A program in SCEPTRE can then be written. Such a program is listed in Appendix C.

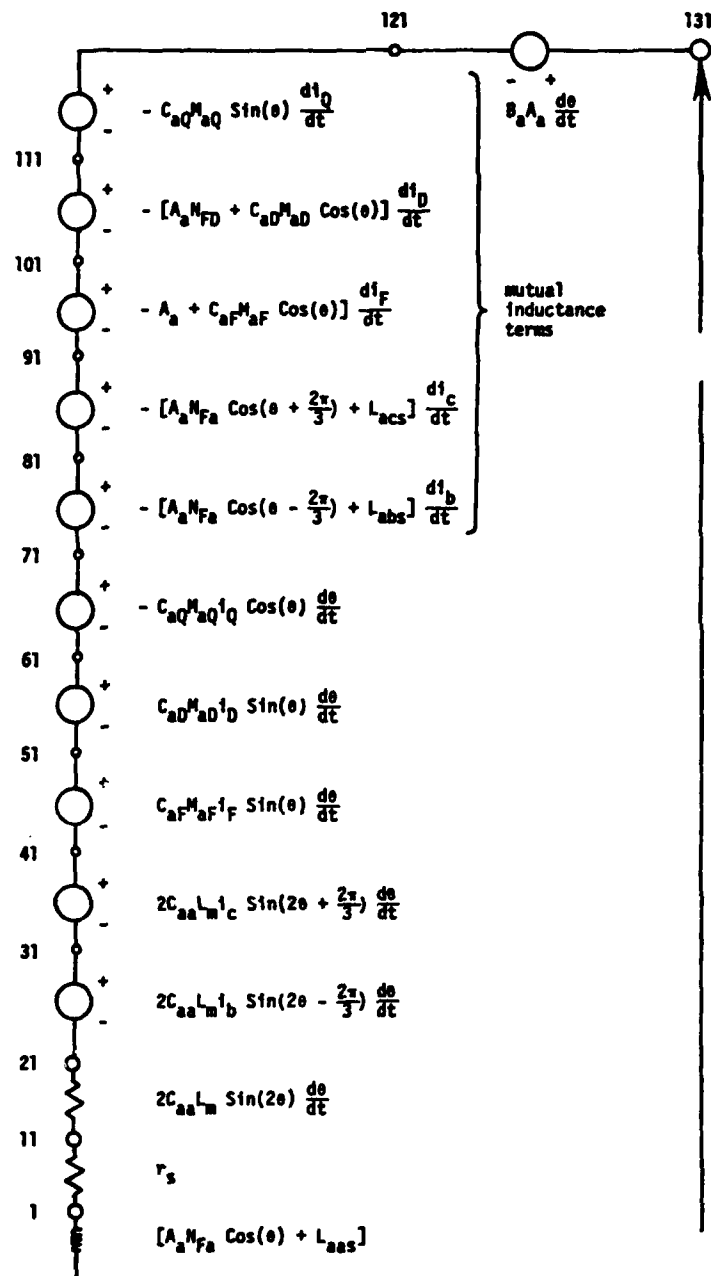


FIGURE 2. EQUIVALENT CIRCUIT FOR PHASE "a" OF SYNCHRONOUS MACHINE.

## 2.6 INCLUSION OF PRIME-MOVER AND EXCITATION CONTROL MODEL

While SCEPTRE was primarily developed to facilitate network analysis, it can be used to analyse other dynamic systems. Particularly, it has the ability to analyze systems for which transfer functions are available. SCEPTRE requires that the transfer function be converted to state equations and the state equations entered into the program. (The details of this conversion procedure are given in the manual (Reference 2).) This capability of SCEPTRE can be used to advantage in simulating the prime-mover characteristics of the system. The prime-mover model is converted to a suitable program and the output quantity of interest is the mechanical torque,  $T_m$ . This becomes an input for the synchronous machine model through Equation (3), which is the equation for rotor angle acceleration.

Similarly, excitation control system models may be added to the machine simulation. Excitation control is generally based on monitoring the terminal voltage of the generator and changing the excitation field voltage in some fashion as the response. The control system, modeled either as a transfer function or an electronic network, is easily added to the present machine model, since in the program both the terminal voltage and the excitation voltage are accessible variables. The present work has not been concerned with modeling either the prime-mover or the excitation voltage control scheme, and the above observations are offered only to show how these models can be incorporated in the present simulation.

## 2.7 AN ALTERNATIVE GENERATOR MODEL

In this report in SECTION V and SECTION VI the discussion and development lead to two conclusions. First, in solving differential equations with nonlinear inductors, the flux linkages,  $\lambda$ , should be taken as the variables and not the currents,  $i$ . Secondly, in "stiff" differential equations an

implicit integration method such as the "Backward Euler" method should be used. However, the complexity of the electronic circuit model and the desirability of using existing models from the literature for the SCR lead to the decision to use CAD programs SPICE 2 and SCEPTRE. Now, both CAD programs allow use of implicit integration but both force use of current and voltage variables.

This subsection develops a formulation for the generator model which uses flux linkages,  $\lambda$ , as the nonlinear inductor variable and is based on the "Backward Euler" implicit integration.

### 2.7.1 Nodal Analysis Approach

Since for the "Backward Euler" representation of the generator at any discrete time  $k \Delta t$  the equivalent circuit will be shown to be dc dependent voltage sources and resistors, the following paragraph establish the methods and notation for representing such as system in nodal form.

Consider the dc circuit of Figure 3

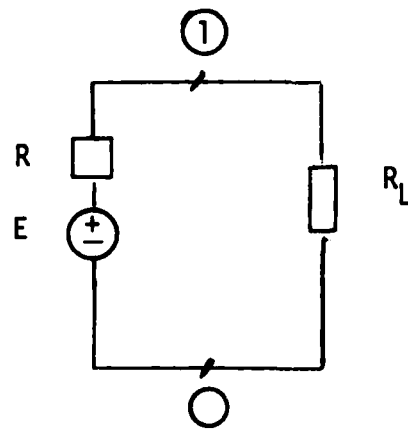


FIGURE 3. DC CIRCUIT FOR NODAL ANALYSIS

Application of Kirchhoff's current law and Norton's equivalent yields the equation

$$\left(\frac{1}{R} + \frac{1}{R_L}\right) V_1 = \frac{E}{R} \quad (18)$$

The equation solved for  $V_1$

$$V_1 = E \left(\frac{R_L}{R + R_L}\right)$$

For a constant value (dc value) of voltage source  $E$ , a resulting value of node voltage  $V_1$  may be determined.

Nodal analysis may also be applied to a circuit containing time varying voltage sources. Consider the above circuit in which  $E = E_m \cos(\omega t)$ . If time ( $t$ ) were to be considered at only discrete intervals, then the voltage source would be a constant value at each of discrete time interval. For discretized time,

$$\begin{aligned} \text{and} \quad t &= k \Delta t \\ E &= E_m \cos(k\omega\Delta t) \quad . \quad k = 0, 1, \dots \quad (19) \\ \Delta t &= \text{fixed interval} \end{aligned}$$

As is observed in this equation, for a given small value of  $\Delta t$ , the trajectory of  $E$  with time as  $k$  is increased becomes a sinusoid. A plot of  $E$ -versus-time is a sinusoid. Solution of the nodal analysis equation for each discrete value of time ( $k\omega\Delta t$ ) yields a sinusoidally varying node voltage  $V_1$ .

Since a generator can be represented by its Thevenin equivalent circuit of a voltage source in series with a resistance, one may suspect that nodal analysis is applicable to generator modeling. Since electronic circuit components can be described in terms of voltage sources, current sources, and passive circuit elements, nodal analysis may also be applied to electronic circuit modeling.

## 2.7.2 Matrix Form of DC Nodal Analysis

A composite branch defines any circuit element which can be represented in terms of a voltage source, current source, or resistor. As will be seen, later any dc circuit element may be represented in this manner.

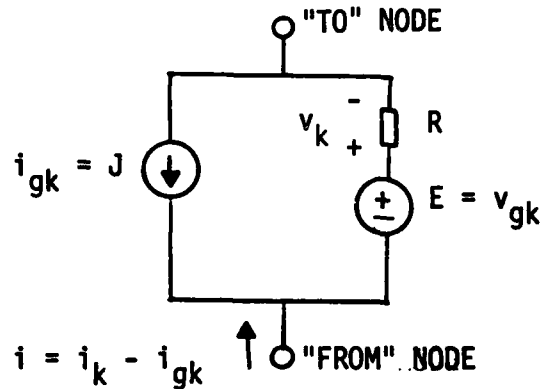


FIGURE 4. GENERAL DC NETWORK ELEMENT

Current is always assumed, by this convention, to enter the "from" node. This convention defines orientation when directed graph theory is applied to a circuit for the purpose of producing an incidence matrix. The incidence matrix (A) is a rectangular matrix whose elements have the following values:

$$\begin{aligned}
 a_{ij} &= 1 && \text{if branch } j \text{ is incident at node } i \text{ and oriented away from it} \\
 a_{ij} &= -1 && \text{if branch } j \text{ is incident at node } i \text{ and oriented toward it} \\
 a_{ij} &= 0 && \text{if branch } j \text{ is not incident at node } i.
 \end{aligned}$$

In matrix form, the Kirchhoff Current Law equation becomes

$$AI(t) = AI_g(t) \quad (20)$$

The following derivational steps are well known and offered without comment.

$$AI = AI_g \quad (21)$$

$$A(YV) = AI_g \quad (22)$$

$$(AY)(A^T V_n) = A(I_g - YV_g) \quad (23)$$

$$Y_n V_n = J_n \quad (24)$$

This derivation leads to the development of  $Y_n$  and  $J$  directly from the circuit without use of the incidence matrix.

$$(Y_n)_{ij} = \text{sum of all admittances connected to node } i \text{ when } i = j .$$

$$(Y_n)_{ij} = \text{negative sum of all admittances connected between nodes } i \text{ and } j \text{ when } i \neq j .$$

$$(J_n)_i = \text{sum of all current sources and all Norton equivalents of accompanied voltage sources connected to node } i .$$

This analysis may be extended to include non-accompanied voltage sources.

Let  $NN$  be 1 plus the number of nodes in the circuit. For an independent voltage source (no accompanying series resistance),

$$(Y_n)_{ij} = + 1 \quad \text{if branch } k \text{ is incident at node } i \text{ and oriented away from it } (j = NN)$$

$$= - 1 \quad \text{if branch } k \text{ is incident at node } i \text{ and oriented toward it } (j = NN)$$

$$= + 1 \quad \text{if branch } k \text{ is incident at node } j \text{ and oriented away from it } (i = NN)$$

$$= - 1 \quad \text{if branch } k \text{ is incident at node } j \text{ and oriented toward it } (i = NN)$$

$$(J_n)_{NN} = \text{value of independent voltage source.}$$

The introduction of an additional row and column in the matrices has created a new "node voltage". The calculated value of this "node voltage" is the value of current flow through the independent voltage source.

The current dependent voltage source requires a similar formulation. In this case, the voltage source value is  $E_j = rI_k$ , where  $I_k$  is defined to be the current flow through an independent voltage source or through another current dependent voltage source. In this case,  $I_k$  is a "node voltage" as shown above. The formulation is similar to that for the independent voltage source.

$$\begin{aligned}
(Y_n)_{ij} &= +1 \quad \text{if branch } k \text{ is incident to node } i \text{ and oriented away} \\
&\quad \text{from it (j = NN)} \\
&= -1 \quad \text{if branch } k \text{ is incident to node } i \text{ and oriented} \\
&\quad \text{toward it (j = NN)} \\
&= +1 \quad (i = \text{NN}) \\
&= -1 \quad (i = \text{NN}) \\
&= -r \quad (i = j = \text{NN}).
\end{aligned}$$

The new "node voltage" created by the addition of a row and column in the matrices is the value of current flow through the current dependent voltage source.

### 2.7.3 Application of Nodal Analysis to the Generator

As presented in the derivational work for the generator model,  $\frac{d}{dt} [\lambda]$  is a voltage source. This voltage source is composed of both independent and dependent terms. Another way of expressing  $\frac{d}{dt} [\lambda]$  is by the use of the Backward Euler integration algorithm for  $\lambda$  (flux-linkage).

$$\lambda_{n+1} = \lambda_n + h \dot{\lambda}_{n+1} \quad (25)$$

where,  $h = t_2 - t_1 = \Delta t$  the step size,  $n$  is the step number.

After rearranging the equation, we obtain

$$\frac{d}{dt} [\lambda]_{n+1} = \frac{1}{h} \lambda_{n+1} - \frac{1}{h} \lambda_n \quad (26)$$

As with all implicit integration routines,  $\lambda_{n+1}$  and  $\frac{d}{dt} [\lambda]_{n+1}$  are unknown values. An iteration technique is used to calculate these values.  $[\lambda]_{n+1}$  is approximated by a Taylor Series

$$[\lambda^{k+1}]_{n+1} = [\lambda^k]_{n+1} + [J^k]_{n+1} [\Delta I]_{n+1} \quad (27)$$

where  $J$  is the Jacobian

$$J = \frac{\partial(\lambda_a, \lambda_b, \lambda_c, \lambda_F, \lambda_D, \lambda_Q)}{\partial(i_a, i_b, i_c, i_F, i_D, i_Q)}$$

at the  $n + 1$  step and the  $k$  iteration and  $[\Delta I]_{n+1}$  is the difference between the column matrices

$$[\Delta I]_{n+1} = \left[ I_{n+1}^{k+1} - I_{n+1}^k \right] .$$

In applying the procedure to phase A quantities, the derivational steps are obtained

$$\lambda_{a_{n+1}} = \lambda_{a_n} + h \overset{\circ}{\lambda}_{a_{n+1}} \quad (28)$$

$$E_{a_{n+1}} = - \overset{\circ}{\lambda}_{a_{n+1}} = \frac{1}{h} \lambda_{a_n} - \frac{1}{h} \lambda_{a_{n+1}} \quad (29)$$

$$\begin{aligned} &= \frac{1}{h} \lambda_{a_n} - \frac{1}{h} \lambda_{a_{n+1}}^k \\ &\quad - \frac{1}{h} \left. \frac{\partial \lambda_a^k}{\partial i_a^k} \right|_{n+1} \left( i_{a_{n+1}}^{k+1} - i_{a_{n+1}}^k \right) \\ &\quad - \frac{1}{h} \left. \frac{\partial \lambda_a^k}{\partial i_b^k} \right|_{n+1} \left( i_{b_{n+1}}^{k+1} - i_{b_{n+1}}^k \right) \\ &\quad - \frac{1}{h} \left. \frac{\partial \lambda_a^k}{\partial i_c^k} \right|_{n+1} \left( i_{c_{n+1}}^{k+1} - i_{c_{n+1}}^k \right) \\ &\quad - \frac{1}{h} \left. \frac{\partial \lambda_a^k}{\partial i_F^k} \right|_{n+1} \left( i_{F_{n+1}}^{k+1} - i_{F_{n+1}}^k \right) \\ &\quad - \frac{1}{h} \left. \frac{\partial \lambda_a^k}{\partial i_D^k} \right|_{n+1} \left( i_{D_{n+1}}^{k+1} - i_{D_{n+1}}^k \right) \\ &\quad - \frac{1}{h} \left. \frac{\partial \lambda_a^k}{\partial i_Q^k} \right|_{n+1} \left( i_{Q_{n+1}}^{k+1} - i_{Q_{n+1}}^k \right) \quad (30) \end{aligned}$$

This equation may be realized into circuit elements represented by composite branches, independent voltage sources and current dependent voltage sources.

This phase A circuit is shown in Figure 5.

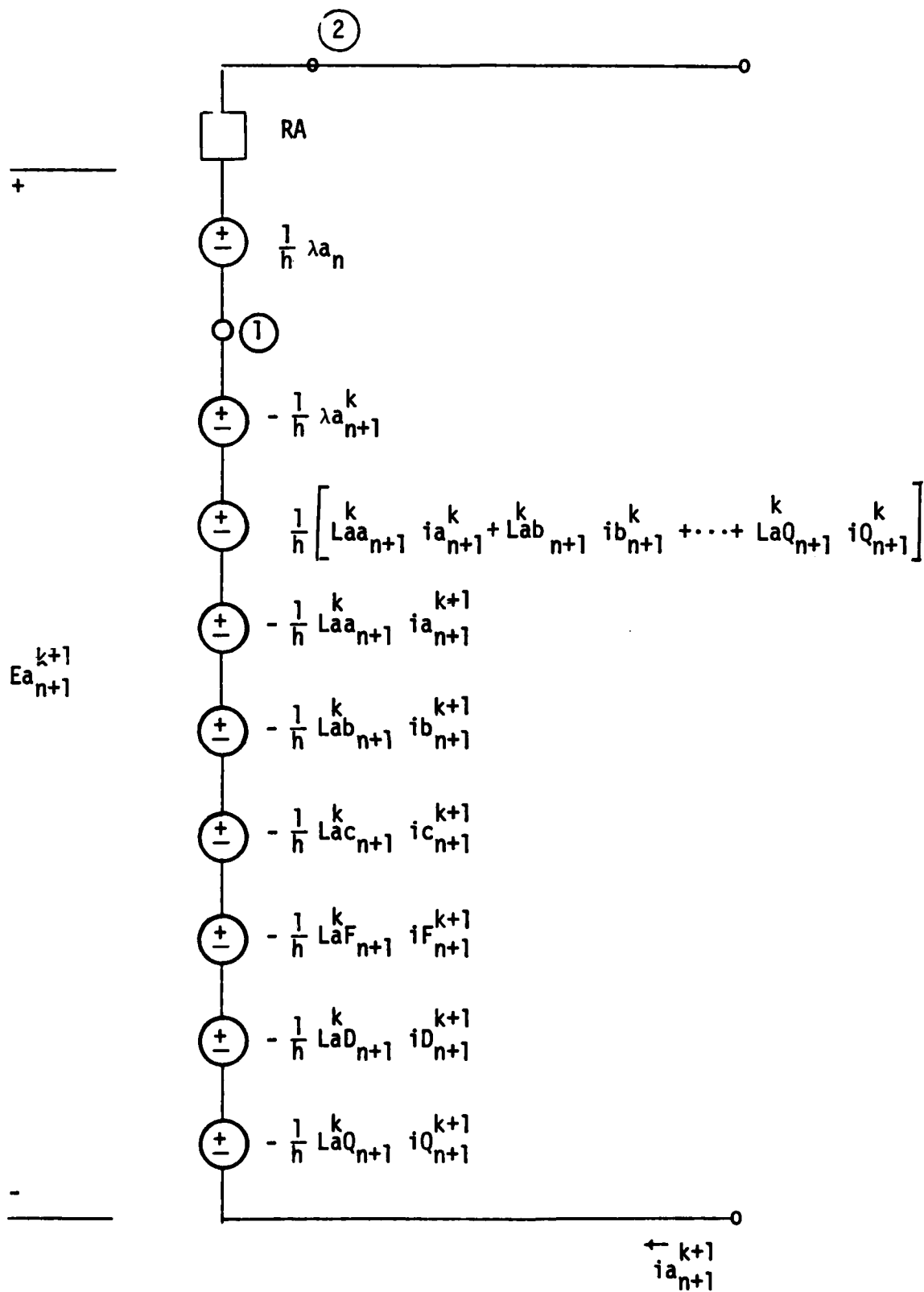


FIGURE 5. PHASE A BACKWARD EULER NODAL CIRCUIT

One realizes from the circuit, that  $-\lambda a_{n+1}^{k+1}$  is equivalent to node voltage  $v_n(1)$ . The value of  $\lambda a_{n+1}^{k+1}$  is obtained by solving the set of node equations evaluated in terms of values determined during the  $k^{\text{th}}$  iteration. All terms are updated at the end of each iteration until no change in node voltage (or current, or  $\lambda$ ) is observed.

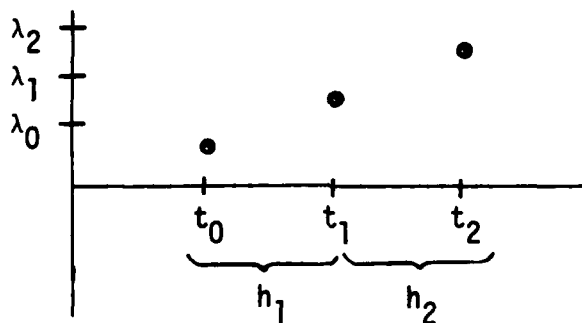
#### 2.7.4 Step Size Selection

All terms in the equation for  $\frac{d}{dt} [\lambda]$  are dependent upon step size. The Backward Euler formula approximates the true solution but introduces a local error

$$O(h^2) = \frac{1}{2} \frac{d^2}{dt^2} (\lambda(t^*)) h^2 \quad (31)$$

where  $t_1 \leq t^* \leq t_1 + h = t_2$  and where  $t^*$  represents the value of time within the interval which results in the largest error.  $\frac{d^2}{dt^2} [\lambda(t)]$  is approximated numerically by

$$\frac{d^2}{dt^2} [\lambda_2] = \frac{1}{h_2^2} \lambda_2 + \frac{1}{h_1 h_2} \lambda_0 - \frac{(h_1 + h_2)}{h_1 h_2^2} \lambda \quad (32)$$



Total error is derived to be

$$E_{rr} = \frac{1}{2} h_2^2 \left[ \frac{d^2}{dt^2} [\lambda] \right] = \frac{1}{2} \lambda_2 - \left( \frac{h_1 + h_2}{2h_1} \right) \lambda_1 + \left( \frac{h_2}{2h_1} \right) \lambda_0 \quad (33)$$

During the integration process, step size is determined based upon previously determined values.

- a) Accept step size ( $h_2$ ) if  $\text{Err} \leq \text{maximum error}$
- b) reject step size ( $h_2 = \frac{1}{2} h_2$ ) if  $\text{Err} > \text{maximum error}$
- c) increase step size ( $h_2 = 2h_2$ ) if  $\text{Err} \leq \frac{1}{4} \text{maximum error}$ .

Results of all calculations are saved for plotting, by a digital plotting routine.

This program has been written and is in the "debugging" stage. No results are as yet available for publication.

SECTION III  
THE TRANSFORMER MODEL

3.1 OBJECTIVE

A model was developed and tested which will represent a three phase transformation. The transformation may be made using three single phase transformers in a three phase array or may be made using a three phase transformer. The use of SCEPTRE allows consideration of the wye-wye and delta-wye systems of the ac and dc charging systems.

Further the model developed allows for operation of the transformer in the non-linear range of the magnetization curve and/or variation in coupling between phases of the three phase transformer during unbalanced operation.

Allowance for hysteresis effects are not included in the model.

3.2 THE TRANSFORMER MODEL

The equation which defines the electric-magnetic circuit relationship for the transformer is:

$$[V] = [R][I] + \frac{d}{dt} [\lambda] \quad (34)$$

where  $V$  = the set of six terminal voltages

$R$  = a matrix containing the six winding resistance

$I$  = the set of six phase currents

$\lambda$  = the set of six flux-linkages

and

$$[\lambda] = [L][I].$$

Equation 34 expanded becomes

$$\begin{bmatrix} V_{a_1} \\ V_{b_1} \\ V_{c_1} \\ V_{a_2} \\ V_{b_2} \\ V_{c_2} \end{bmatrix} = \begin{bmatrix} R_{a_1} & 0 & 0 & 0 & 0 & 0 \\ 0 & R_{b_1} & 0 & 0 & 0 & 0 \\ 0 & 0 & R_{c_1} & 0 & 0 & 0 \\ 0 & 0 & 0 & R_{a_2} & 0 & 0 \\ 0 & 0 & 0 & 0 & R_{b_2} & 0 \\ 0 & 0 & 0 & 0 & 0 & R_{c_2} \end{bmatrix} \begin{bmatrix} i_{a_1} \\ i_{b_1} \\ i_{c_1} \\ i_{a_2} \\ i_{b_2} \\ i_{c_2} \end{bmatrix} + \frac{d}{dt} \begin{bmatrix} \lambda_{a_1} \\ \lambda_{b_1} \\ \lambda_{c_1} \\ \lambda_{a_2} \\ \lambda_{b_2} \\ \lambda_{c_2} \end{bmatrix} \quad (35)$$

$$\begin{bmatrix} \lambda_{a_1} \\ \lambda_{b_1} \\ \lambda_{c_1} \\ \lambda_{a_2} \\ \lambda_{b_2} \\ \lambda_{c_2} \end{bmatrix} = \begin{bmatrix} \frac{\partial \lambda_{a_1}}{\partial i_{a_1}} & \frac{\partial \lambda_{a_1}}{\partial i_{b_1}} & \frac{\partial \lambda_{a_1}}{\partial i_{c_1}} & \frac{\partial \lambda_{a_1}}{\partial i_{a_2}} & \frac{\partial \lambda_{a_1}}{\partial i_{b_2}} & \frac{\partial \lambda_{a_1}}{\partial i_{c_2}} \\ \frac{\partial \lambda_{b_1}}{\partial i_{a_1}} & \frac{\partial \lambda_{b_1}}{\partial i_{b_1}} & \frac{\partial \lambda_{b_1}}{\partial i_{c_1}} & \frac{\partial \lambda_{b_1}}{\partial i_{a_2}} & \frac{\partial \lambda_{b_1}}{\partial i_{b_2}} & \frac{\partial \lambda_{b_1}}{\partial i_{c_2}} \\ \frac{\partial \lambda_{c_1}}{\partial i_{a_1}} & \frac{\partial \lambda_{c_1}}{\partial i_{b_1}} & \frac{\partial \lambda_{c_1}}{\partial i_{c_1}} & \frac{\partial \lambda_{c_1}}{\partial i_{a_2}} & \frac{\partial \lambda_{c_1}}{\partial i_{b_2}} & \frac{\partial \lambda_{c_1}}{\partial i_{c_2}} \\ \frac{\partial \lambda_{a_2}}{\partial i_{a_1}} & \frac{\partial \lambda_{a_2}}{\partial i_{b_1}} & \frac{\partial \lambda_{a_2}}{\partial i_{c_1}} & \frac{\partial \lambda_{a_2}}{\partial i_{a_2}} & \frac{\partial \lambda_{a_2}}{\partial i_{b_2}} & \frac{\partial \lambda_{a_2}}{\partial i_{c_2}} \\ \frac{\partial \lambda_{b_2}}{\partial i_{a_1}} & \frac{\partial \lambda_{b_2}}{\partial i_{b_1}} & \frac{\partial \lambda_{b_2}}{\partial i_{c_1}} & \frac{\partial \lambda_{b_2}}{\partial i_{a_2}} & \frac{\partial \lambda_{b_2}}{\partial i_{b_2}} & \frac{\partial \lambda_{b_2}}{\partial i_{c_2}} \\ \frac{\partial \lambda_{c_2}}{\partial i_{a_1}} & \frac{\partial \lambda_{c_2}}{\partial i_{b_1}} & \frac{\partial \lambda_{c_2}}{\partial i_{c_1}} & \frac{\partial \lambda_{c_2}}{\partial i_{a_2}} & \frac{\partial \lambda_{c_2}}{\partial i_{b_2}} & \frac{\partial \lambda_{c_2}}{\partial i_{c_2}} \end{bmatrix} \begin{bmatrix} i_{a_1} \\ i_{b_1} \\ i_{c_1} \\ i_{a_2} \\ i_{b_2} \\ i_{c_2} \end{bmatrix} \quad (36)$$

The inductance matrix  $[L]$  is composed of a set of partial derivative terms of the general form

$$L_{jk} = \frac{\partial \lambda_j}{\partial i_k} \quad \left( \text{e.g., } L_{a_1 c_2} = \frac{\partial \lambda_{a_1}}{\partial i_{c_2}} \right) \quad (37)$$

The inductance matrix terms are defined as incremental inductances.

A sketch illustrating winding and current relationships is shown in Figure 6.

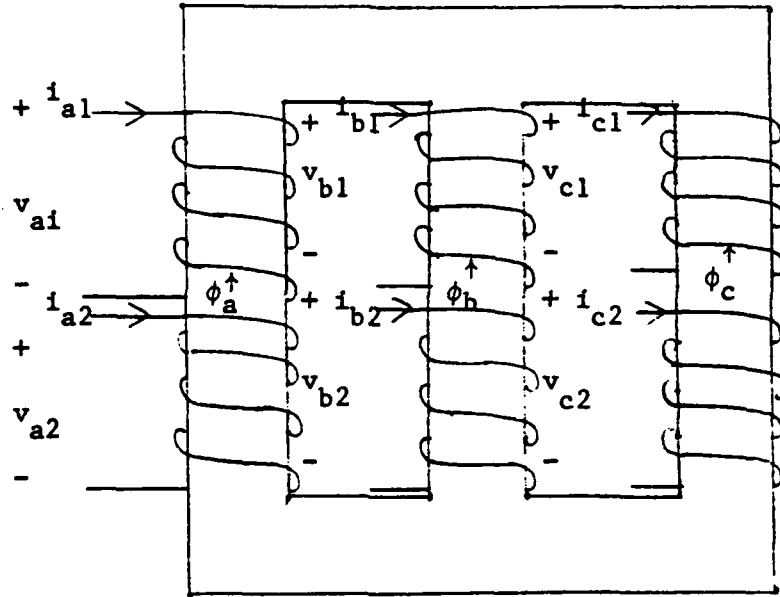


FIGURE 6. THREE LEG THREE PHASE TRANSFORMER CORE CURRENTS AND VOLTAGES

In general, flux linkage of any winding is a non-linear function of all the winding currents.

$$\lambda_j = \lambda_j(i_{a1}, i_{a2}, i_{b1}, i_{b2}, i_{c1}, i_{c2}) \quad (38)$$

This nonlinear relationship is further complicated by the presence of hysteresis. Allowance for hysteresis effects is not included in the model developed here. Hysteresis effects may be neglected without significant error for low core loss grades of transformer core steel. Unreasonable amounts of data and a cumbersome model would be required to include these effects.

The magnetization curve can be measured by standard means. The effect of this nonlinear curve is not considered to be negligible. The partial derivative of the magnetization curve,  $L_{jk}$ , is also a non-linear function of current. Each inductance can be expressed as a function of six currents.

$$\begin{aligned}
L_{jk} &= L (ia_1, ib_1, ic_1, ia_2, ib_2, ic_2) \\
L_{jk} &= L \left[ a_0 + a_{11} ia_1 + a_{12} ia_1^2 + a_{13} ia_1^3 \right. \\
&\quad + a_{21} ib_1 + a_{22} ib_1^2 + a_{23} ib_1^3 \\
&\quad + a_{31} ic_1 + a_{32} ic_1^2 + a_{33} ic_1^3 \\
&\quad + a_{41} ia_2 + a_{42} ia_2^2 + a_{43} ia_2^3 \\
&\quad + a_{51} ib_2 + a_{52} ib_2^2 + a_{53} ib_2^3 \\
&\quad \left. + a_{61} ic_2 + a_{62} ic_2^2 + a_{63} ic_2^3 \right]
\end{aligned} \tag{39}$$

This expression requires a different set of constants ( $a_{ij}$ ) for each of the 36 inductance terms. By assumption of constant turns ratio, the expression can be simplified.

$$\begin{aligned}
i_x &= ia_1 + N ia_2 \\
i_y &= ib_1 + N ib_2 \\
i_z &= ic_1 + N ic_2
\end{aligned}$$

$$\begin{aligned}
\frac{\partial \lambda_j}{\partial i_k} = L_{jk} &= L \left[ b_0 + b_{11} i_x + b_{12} i_x^2 + b_{13} i_x^3 \right. \\
&\quad + b_{21} i_y + b_{22} i_y^2 + b_{23} i_y^3 \\
&\quad \left. + b_{3k} i_z + b_{32} i_z^2 + b_{33} i_z^3 \right]
\end{aligned} \tag{40}$$

Equation (40) is the form used in the SCEPTRE model.

Nakra and Barton (Reference 8) computed inductance coefficients for each  $i_{jk}$  state using a simplified magnetic circuit calculation.

The inductance coefficients could be determined by using "finite element" analysis of the transformer electrical and magnetic circuit.

However, the assumption in the model used here is that with modern digital instrumentation and an existing transformer, the required data would be measured. A multiple regression analysis then would be used to determine the  $a_{ij}$  coefficients for storage.

Since

$$\begin{aligned} [\lambda] &= \left[ \frac{\partial \lambda}{\partial I} \right] [I] \\ &= [L] [I] \end{aligned} \quad (41)$$

and

$$\begin{aligned} \frac{d}{dt} [\lambda] &= \left[ \frac{\partial \lambda}{\partial I} \right] \left[ \frac{\partial I}{\partial t} \right] \\ &= [L] \left[ \frac{dI}{dt} \right] \end{aligned} \quad (42)$$

The  $[L]$  matrix is considered constant incremental inductance evaluated at each  $[I]$  state. Expanded Equation 34 becomes

$$\begin{aligned} \begin{bmatrix} V_{a_1} \\ V_{b_1} \\ V_{c_1} \\ V_{a_2} \\ V_{b_2} \\ V_{c_2} \end{bmatrix} &= \begin{bmatrix} R_{a_1} & 0 & 0 & 0 & 0 & 0 \\ 0 & R_{b_1} & 0 & 0 & 0 & 0 \\ 0 & 0 & R_{c_1} & 0 & 0 & 0 \\ 0 & 0 & 0 & R_{a_2} & 0 & 0 \\ 0 & 0 & 0 & 0 & R_{b_2} & 0 \\ 0 & 0 & 0 & 0 & 0 & R_{c_2} \end{bmatrix} \begin{bmatrix} i_{a_1} \\ i_{b_1} \\ i_{c_1} \\ i_{a_2} \\ i_{b_2} \\ i_{c_2} \end{bmatrix} \\ &+ \begin{bmatrix} L_{a_1 a_1} & L_{a_1 b_1} & L_{a_1 c_1} & L_{a_1 a_2} & L_{a_1 b_2} & L_{a_1 c_2} \\ L_{b_1 a_1} & L_{b_1 b_1} & L_{b_1 c_1} & L_{b_1 a_2} & L_{b_1 b_2} & L_{b_1 c_2} \\ L_{c_1 a_1} & L_{c_1 b_1} & L_{c_1 c_1} & L_{c_1 a_2} & L_{c_1 b_2} & L_{c_1 c_2} \\ L_{a_2 a_1} & L_{a_2 b_1} & L_{a_2 c_1} & L_{a_2 a_2} & L_{a_2 b_2} & L_{a_2 c_2} \\ L_{b_2 a_1} & L_{b_2 b_1} & L_{b_2 c_1} & L_{b_2 a_2} & L_{b_2 b_2} & L_{b_2 c_2} \\ L_{c_2 a_1} & L_{c_2 b_1} & L_{c_2 c_1} & L_{c_2 a_2} & L_{c_2 b_2} & L_{c_2 c_2} \end{bmatrix} \frac{d}{dt} \begin{bmatrix} i_{a_1} \\ i_{b_1} \\ i_{c_1} \\ i_{a_2} \\ i_{b_2} \\ i_{c_2} \end{bmatrix} \end{aligned} \quad (43)$$

### 3.3 SCEPTRE MODELING

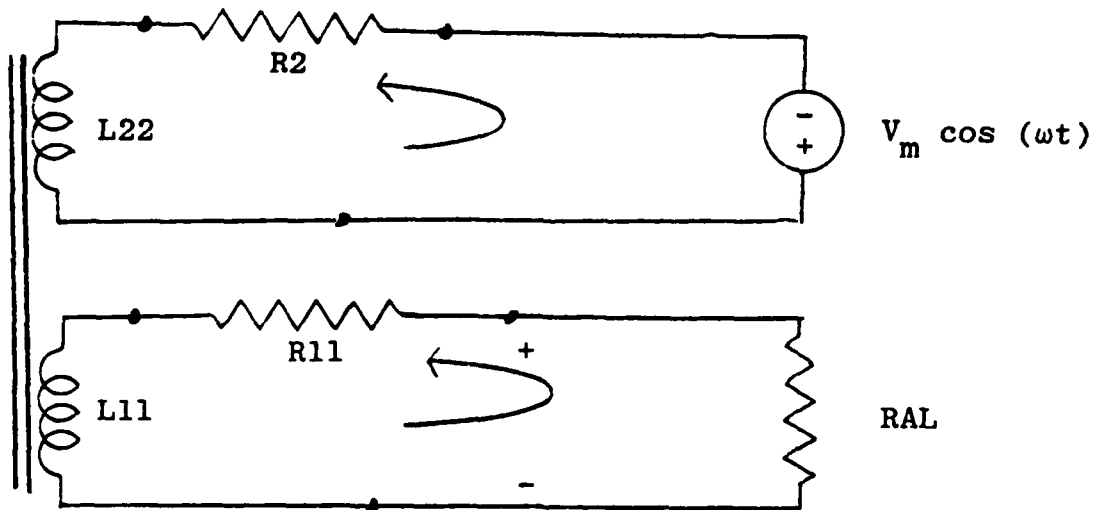


FIGURE 7. SCEPTRE EQUIVALENT CIRCUIT FOR PHASE A

Implementation of the three phase transformer requires the use of all 36 terms of the inductance matrix. These are computed in a FORTRAN subroutine for each current state in terms of stored  $a_{ij}$  data. Implementation of a bank of three single phase transformers requires the exclusion of all mutual inductance (off-diagonal) terms with the exception of mutual inductances between primary and secondary windings of each transformer.

A listing of a SCEPTRE program in which a three phase transformer is modeled is included in Appendix (D). This model has been successfully developed and implemented for the data used. This data does not represent any known transformer. In the generator and transformer results section plots of several parameters are shown as an illustration of operating characteristics of the model.

The generator and transformer models have been successfully linked to form a small isolated power system. A listing of the SCEPTRE program for

this system is shown in Appendix (D). It should be noted that this transformer does not match the generator terminal characteristics. In addition, the transformer data do not represent a known transformer.

No attempt has been made to model the generator, transformer, and electronic circuit since compatible data were not available.

## SECTION IV

### THE RESONANT CHARGING CIRCUITS

#### 4.1 OBJECTIVE

This part of the project was the development of computer program models of the ac and the dc resonant charging circuit which are to be the possible alternative loads on the generator and transformer discussed in earlier sections. The characteristics of the series RLC resonant circuit are well known (Reference 22) and the sequence of switching events are defined by prior knowledge of the particular application. Thus, the work reported here involved developing an SCR model that would adequately represent turn on and turn off characteristics in resonant charging circuits, using the SCR models in both ac and dc charging circuits and extending the range of the models using compensation and series and/or parallel operation of the device models.

The final model is in SCEPTRE since it must be compatible with the generator and transformer models. Further, the practical feature of obtaining model parameters from manufacturers' data sheets is maintained.

The developments are based on previous work done in SPICE 2 with necessary modifications and conversions to SCEPTRE. Much of the preliminary development work was done in SPICE 2 since it is more efficient in electronic circuit applications. It was necessary to modify existing SCR models and to include snubber circuits to assure proper model performance in this high power resonant charging application.

#### 4.2 THE SCR MODEL IN SPICE 2

The SCR model was developed starting with the SPICE 2 model shown in Figure 8. Figure 9 shows the SPICE 2 SCR model equivalent circuit. Some parameters not shown are given SPICE 2 built in default values.

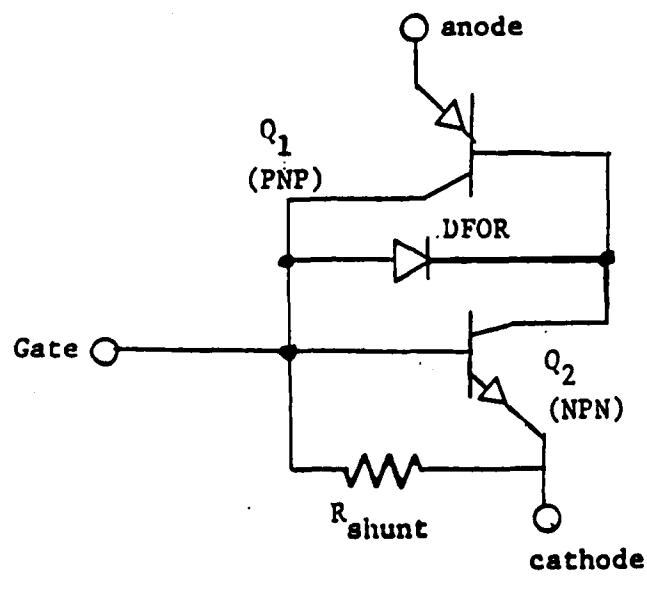


FIGURE 8. A SPICE 2 SCR MODEL BASED ON THE TWO BJT MODEL

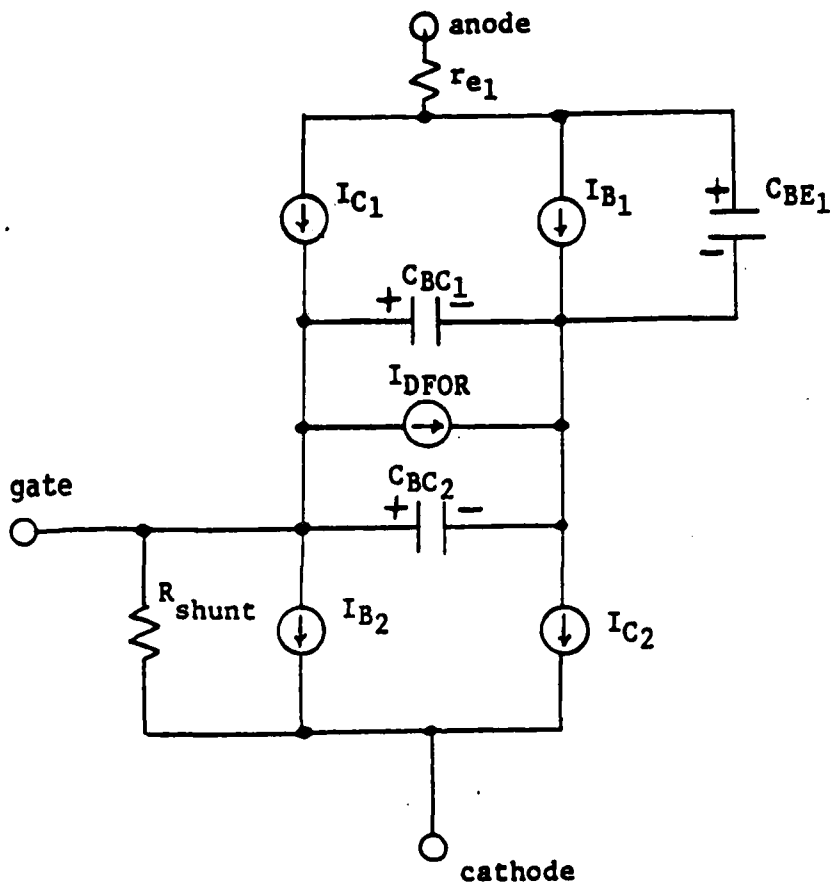


FIGURE 9. THE SPICE 2 SCR MODEL EQUIVALENT CKT

When using the SPICE 2 BJT and DIODE MODELS, there are a large number of parameters that may be specified (28 for the BJT, 14 for the Diode).

W. Ki and C. Hu have developed a method of determining 11 of these parameters from SCR specification sheet data (Reference 34). A summary of this method is given later along with modifications to the method of Ki and Hu.

The 10 circuit components of Figure 9 are described by the following equations in which any SPICE 2 default values used in the model have been applied to the equations. ( $\theta$  = Einstein's Relation = 0.925° V at 300°K)

$$r_{e_1} = r_{e_1} \quad (44)$$

$$I_{C_1} = I_{S_1} \left( e^{V_{EB_1}/\theta} - e^{V_{CB_1}/\theta} \right) - \frac{I_{S_1}}{\beta_{R_1}} \left( e^{V_{CB_1}/\theta} - 1 \right) \quad (45)$$

$$I_{B_1} = \frac{I_{S_1}}{\beta_{F_1}} \left( e^{V_{EB_1}/\theta} - 1 \right) + \frac{I_{S_1}}{\beta_{R_1}} \left( e^{V_{CB_1}/\theta} - 1 \right) \quad (46)$$

$$C_{BE_1} = \frac{\tau_{f_1} I_{S_1}}{\theta} e^{V_{EB_1}/\theta} \quad (47)$$

$$C_{BC_1} = \frac{\tau_{R_1} I_{S_1}}{\theta} e^{V_{CB_1}/\theta} \quad (48)$$

$$I_{DFOR} = \frac{I_{S_{diode}} \left( e^{V_{CB_1}/\theta} - 1 \right)}{1 + \left[ \frac{V_{CB_1}}{V_{BO}} \right]^6} = \frac{I_{S_{diode}} \left( e^{V_{BC_2}/\theta} - 1 \right)}{1 + \left[ \frac{V_{BC_2}}{V_{BO}} \right]^6} \quad (49)$$

$$I_{C_2} = I_{S_2} \left( e^{V_{BE_2}/\theta} - 2 e^{V_{BC_2}/\theta} + 1 \right) \quad (50)$$

$$I_{B_2} = \frac{I_{S_2}}{\beta_{f_2}} \left( e^{V_{BE_2}/\theta} - 1 \right) + I_{S_2} \left( e^{V_{BC_2}/\theta} - 1 \right) \quad (51)$$

$$C_{BC_2} = C_{jC_2} (1 - V_{BC_2})^{-.5} \quad (52)$$

$$R_{shunt} = R_{shunt} \quad (53)$$

From these 10 equations, one develops the following list of parameters that must be provided in order for the SPICE 2 model to function. These are shown in Table 1

1.  $r_{e_1}$
2.  $I_{S_1}$
3.  $\beta_{f_1}$
4.  $\beta_{R_1}$
5.  $\tau_{f_1}$
6.  $\tau_{R_1}$
7.  $I_{S_{diode}}$
8.  $V_{B0}$
9.  $I_{S_2}$
10.  $\beta_{f_2}$
11.  $C_{jC_2}$
12.  $R_{shunt}$

TABLE 1. Parameters to be determined for the "Hu-Ki Method" in implementing the two transistor SCR Model in SPICE 2.

Table 2 lists the model elements, the critical model parameters required by Equations (44-53), and the manufacturers specifications from which these can be calculated. Table 3 lists numerical values for a particular SCR.

Model Element	Critical Model Parameters	Obtainable From								
		$I_H$	$I_{GT}$	$t_r$	$(t_{on})$	$V_T$	$R_{on}$	$V_{BO}$	$\frac{dv}{dt}$	$t_q$
R	$R = R_{shunt}$		x							
D	$BV = V_{BO}$							x		
$Q_1$	$\alpha_1 = \alpha_{R1}$	x	x							
	$\tau_{F1}$			x						
	$I_{S1}$	x	x			x				
	$R_{E1}$						x			
$Q_2$	$\tau_{R1}$									x
	$I_{S2}$	x	x			x				
	$C_{jc2}$ $\alpha_2 = 0.9$	x			(x)				x	

TABLE 2. Model Elements and Critical Parameters for the "Hu-Ki Model"

Note:  $\beta = \frac{\alpha}{1-\alpha}$   $I_{S_{diode}} \gg I_{S1} = I_{S2}$

Each of the critical model parameters may be calculated from one or a combination of the thyristor specifications as shown. All other model parameters may be left unspecified.  $I_H$ : holding current,  $I_{GT}$ : gate trigger current,  $t_r$ : rise time,  $t_{on}$ : turn-on time,  $V_T$  and  $R_{on}$  are from the on-state I-V characteristics:  $V = V_T + IR_{on}$ ,  $V_{BO}$ : forward break-over voltage,  $\alpha_1$ : current gain of transistor 1,  $R_{E1}$ : emitter resistance of transistor,  $\tau_F$ : forward transit time,  $C_{jc}$ : collector junction capacitance,  $I_S$ :  $I_C = I_S e^{qV_{BE}/kT}$ , etc. (Table 2 is taken from Reference 35 p. 175).

From the same reference the "Hu-Ki" nine step procedure for calculating these parameters not defaulted is given below

Part I: "normal model" characteristics:

Step 1. Given  $I_{GT}$ , find R from  $R = 0.75(V)/I_{GT}$

Step 2. Set  $\alpha_2 = 0.9$  or  $0.95$

Step 3. Given  $I_H$  and  $I_{GT}$ , find  $\alpha_1$  from

$$\alpha_1 = 1 - \alpha_2 + \frac{I_{GT}}{\alpha_2 I_H}$$

If  $\alpha_1 > 0.9$ , set  $\alpha_1 = 0.9$ . Find  $\alpha_{R1}$  from  $\alpha_{R1} = \alpha_1$ .

Step 4. Given  $t_r$  and  $\alpha_1, \alpha_2$  from Steps 1, 3, find  $\tau_{F1}$  from

$$\tau_{F1} = (\beta_1 \beta_2 - 1)t_r / (1.8 \beta_1)$$

Step 5. Given  $V_T$ , find  $I_{S1}, I_{S2}$  from

$$I_{S1} = I_{S2} = 10^{-\frac{(V_T + 0.74)}{0.11}} \text{ (A)}$$

Step 6. Given  $R_{on}$ , find  $R_{E1}$  from  $R_{E1} = R_{on}$

Part II. "failure mode" characteristics:

Step 7. Given  $t_q$ , find  $\tau_{R1}$  from  $\tau_{R1} = 9t_q$

Step 8. Given  $I_H, dv/dt, t_{on}$  (if only  $t_r$  given, assume

$t_{on} = 3t_r/2$ ) find  $C_{jc2}$  from

$$C_{jc2}(f) = 0.4I_H(A) \sqrt{t_{on} \frac{dV}{dt}}$$

Step 9. Given  $V_{B0}$ , find diode BV from  $BV = V_{B0}$ .

<u>Data sheet specifications</u>		<u>Model parameters</u>
$I_H = 100 \text{ mA}$		$R = 9.375\Omega$
$I_{GT} = 80 \text{ mA}$	following proposed procedure	$\alpha_2 = 0.9$
$t_r = 3.6 \mu\text{s}$		$\alpha_1 = \alpha_{1R} = 0.9$
$V_T = 1.1\text{V}$		$\tau_{F1} = 17.8 \mu\text{s}$
$R_{on} = 0.005\Omega$		$I_{S1} = I_{S2} = 10^{-16.65}\text{A}$
$V_{BO} = 2700\text{V}$	—————→	$R_{E1} = 0.005\Omega$
$\frac{dV}{dt} = 500\text{V}/\mu\text{s}$		$\tau_{R1} = 1125 \mu\text{s}$
$t_q = 125 \mu\text{s}$		$C_{jc2} = 4000 \text{ pF}$
		$BV = 2700\text{V}$

TABLE 3. Values for the GE C602 LM SCR Model Using the "Hu-Ki Method".

#### 4.3 THE MODIFIED HU-KI MODEL OF THE SCR FOR SPICE 2

Using the "Hu-Ki Model" for SPICE 2 a simulation of an ac resonant charging simulation was run using parameters for a GE C602 LM SCR. The circuit of Figure 10 was used and the results are shown in Figure 12. The results show a proper triggering and normal operation until the turn off or commutation interval. Here erratic high amplitude oscillations are noted in the SCR current instead of the expected low amplitude oscillations which are quickly damped out. Further noted is the enormously high base-emitter voltage of the NPN transistor. This voltage was also erratic in behavior indicating that nearly all the primary current was being carried by  $R_{SHUNT}$  during periods of reverse current.

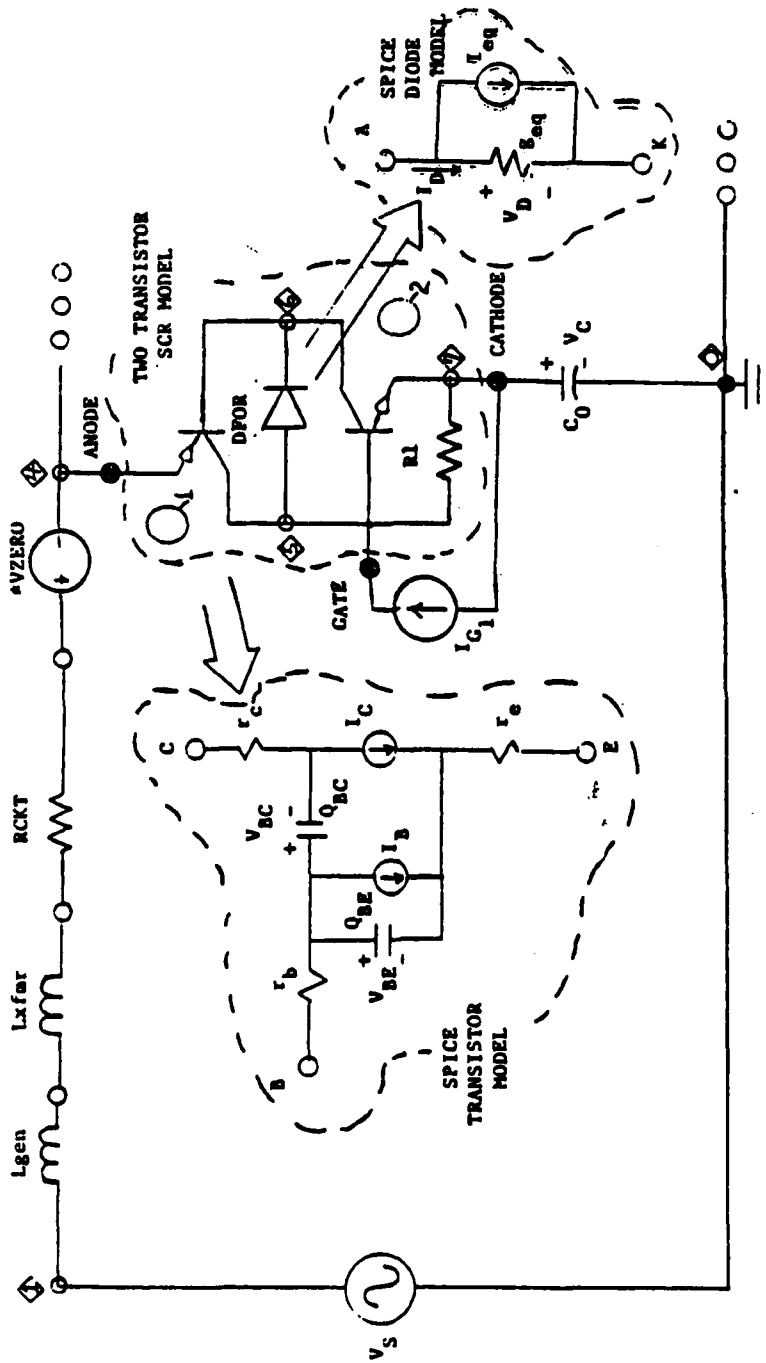


FIGURE 10. SPICE CIRCUIT DIAGRAM FOR THE SINGLE LOOP AC RESONANT CHARGING SYSTEM.

\*VZERO is a zero value voltage source which provides a test point in SPICE2

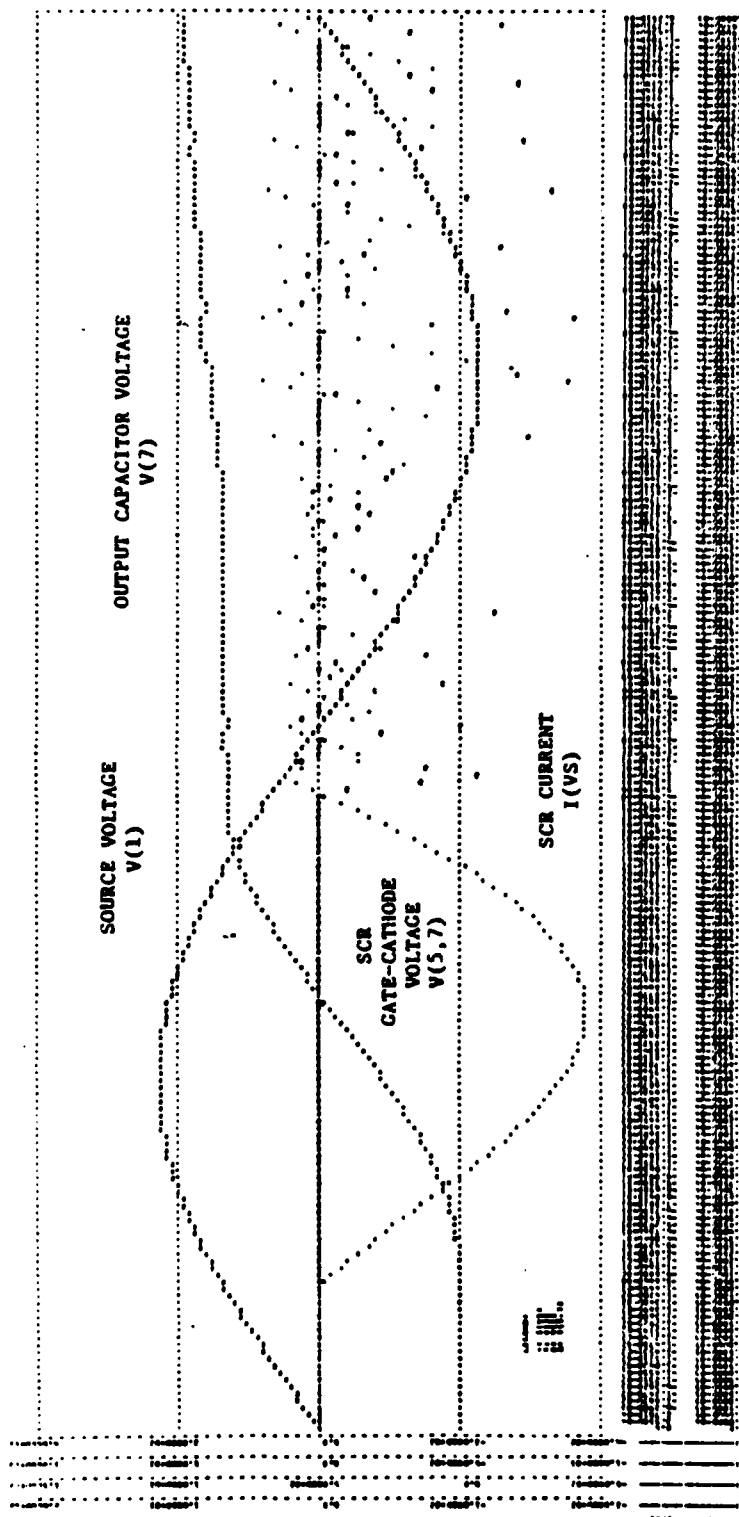


FIGURE 11. SPICE 2 SIMULATION OF THE AC RESONANT CHARGING CIRCUIT OF FIGURE 10.

The problems noted in this simulation appeared centered on the "Hu-Ki Method" SCR model's ability to simulate the SCR's turn-off transient behavior. This conclusion was supported by the results given by Hu (Reference 35) which noted the models SCR turn-off transient simulation required additional development.

Modifications to the Hu-Ki model were made to provide better simulation of the reverse transient behavior. Modifications were limited to those necessary to simulate gross behavior of the device with minor effects unsimulated. The modified model is shown in Figure 12 and the following paragraphs define the required changes. Also refer to Figure 13 for identifying particular junctions. Since SPICE 2 has no capability to simulate a junction breakdown in its transistor model, then a diode (for which breakdown is modeled in SPICE 2) must be added in parallel with  $J_3$ .  $J_3$  is the base-emitter junction of  $Q_2$  in the "Hu-Ki Model". Addition of this diode is illustrated in Figure 12 as DJCTN1.

SCR specification sheet data frequently specifies a maximum reverse gate voltage. This limitation of  $-V_G$  gives an indication of the  $J_3$  breakdown voltage. If this specification is given, then set the breakdown voltage of DJCTN1 ( $V_{BO}$ ) equal to  $1.1 \times \max\{-V_G\}$  otherwise use  $V_{BO} = 5V$ .

$$V_{BO_{DJCTN1}} = \begin{cases} 1.1 \times \max\{-V_G\} \\ \text{or } 5V \end{cases} \quad (54)$$

[Reference 36, p. 87]

To minimize influence of the diode on forward biasing of the  $Q_2$  base-emitter junction, set the saturation current of the diode ( $I_{S_{DJCTN1}}$ ) to less than 10% of the  $Q_2$  saturation current ( $I_{S_2}$  of Table 2)

$$I_{S_{DJCTN1}} \leq 0.1 I_{S_2} \quad (55)$$

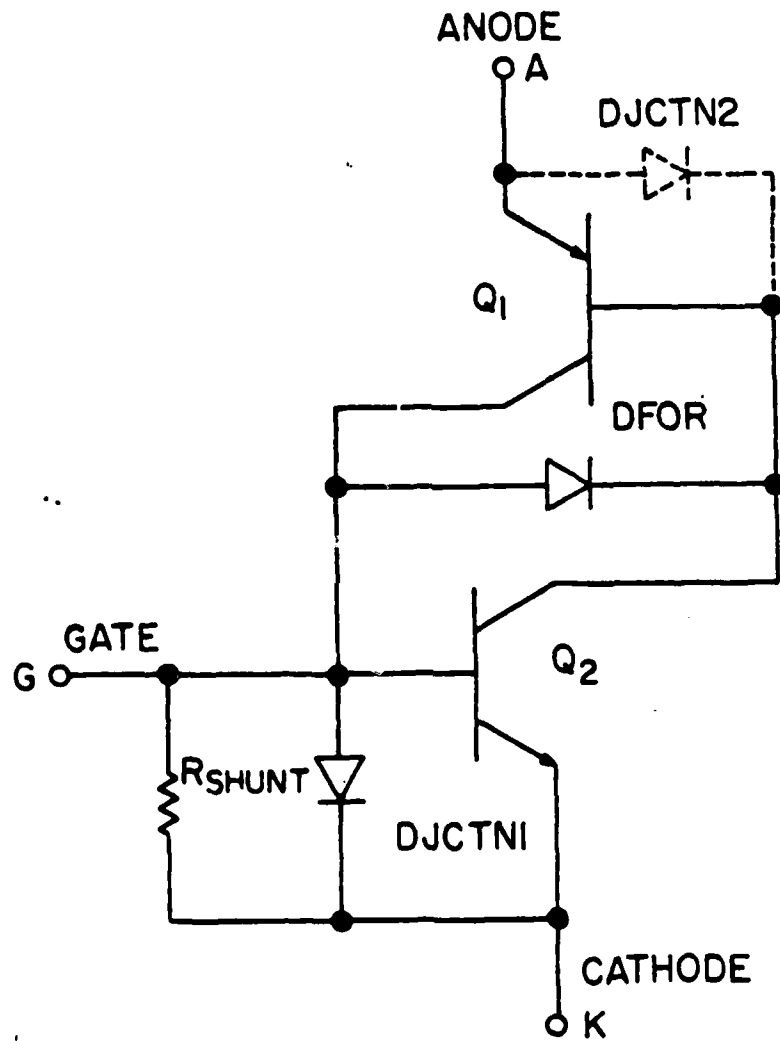


FIGURE 12. "MODIFIED HU-KI MODEL" OF THE SCR FOR SPICE2.

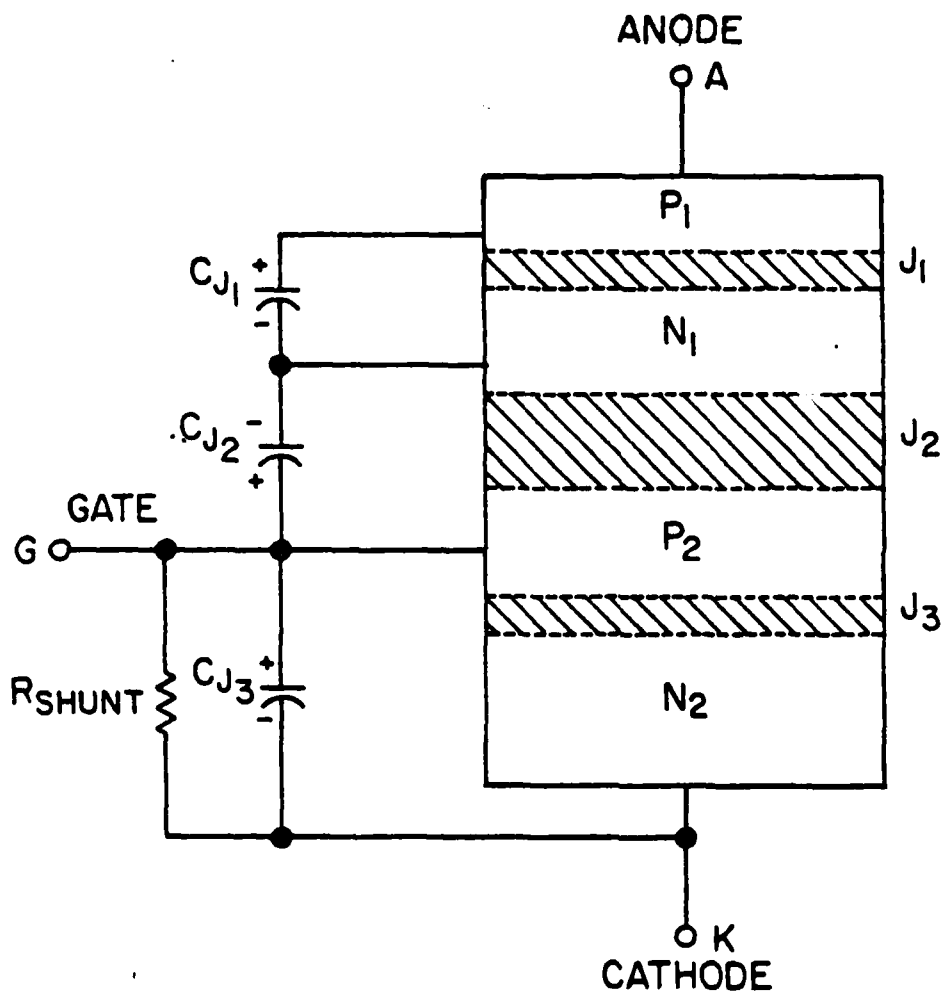


FIGURE 13. SCR REPRESENTATION SHOWING JUNCTION CAPACITANCES AND POLARITY OF CHARGE DURING SCR ON STATE.

Two further corrections are needed in the model. Adding a depletion layer capacitance term to Equation (47) will allow the inductive energy to be stored in  $J_1$  without reaching excessive reverse  $V_{AK}$  in a properly designed circuit. Equation (47) becomes:

$$C_{EB_1} = \frac{\tau_{f_1} I_{S_1}}{\theta} \left( e^{V_{EB_1}/\theta} - 1 \right) + C_{JE_1} (1 - V_{EB_1})^{-1/2} \quad (56)$$

depletion  
layer term

In the event that junction breakdown voltage should be exceeded, then a diode ((DJCTN2) in Figure 12) may be added in parallel with the emitter-base junction of  $Q_1$ .

With this result, three more parameters must be supplied to the model.

$$C_{JE_1} \left\{ \begin{array}{l} \geq 0.5 C_{JC_2} \\ \leq C_{JC_2} \end{array} \right\} \quad (57)$$

where  $C_{JC_2}$  is that determined in Step 8 of the "Hu-Ki Method". Since  $J_1$  and  $J_2$  are typically reasonably similar junctions [Reference 37]

$$I_{S_{DJCTN2}} \leq 0.1 I_{S_1} \quad (I_{S_1} \text{ from Step 5 of the "Hu-Ki Method"}) \quad (58)$$

$$V_{BO_{DJCTN2}} \approx V_{B0} \quad (V_{B0} \text{ from Step 9 of the "Hu-Ki Method"}). \quad (59)$$

As with DJCTN1 discussed earlier, care must be taken to avoid the diode influencing the forward characteristics of the  $Q_1$  emitter-base junction.

Note: The addition of DJCTN2 is purely optional in that it only models a failure of the SCR during a reverse transient.

For the final modification the saturation current through diode DFOR must be adjusted. This diode provided in the "Hu-Ki Model" to simulate the high

voltage turn-on of an SCR is conveniently in position to allow control of the recombination interval of the commutation time while maintaining low values of principal current. To do this, the saturation current of DFOR,  $I_{S_{DFOR}}$ , must be made much greater than the saturation currents of  $Q_1$  and  $Q_2$  ( $I_{S_1}$  and  $I_{S_2}$  respectively).

$$I_{S_{DFOR}} \gg I_{S_1} = I_{S_2} \quad (60)$$

The "Hu-Ki Model" uses the SPICE 2 default value of  $10^{-14}$  for  $I_{S_{DFOR}}$ . Since Step 5 of the "Hu-Ki Method" is used to determine  $I_{S_1}$  and  $I_{S_2}$ , it is evident that the condition of Equation (60) may not always hold by the "Hu-Ki Method".

One way of improving the model would be to assign  $I_{S_{DFOR}}$  some arbitrarily greater value than  $I_{S_1}$  and  $I_{S_2}$ . For example, let  $I_{S_{DFOR}} = 10^3 \times I_{S_1}$ . Then adjust the diffusion capacitance term (via  $\tau_{R_1}$  of Equation 48) to meet the commutation time criteria. An alternative method is to preset the diffusion capacitance term then determine some method of selecting an appropriate  $I_{S_{DFOR}}$ . Since the "Hu-Ki Method" provides the diffusion capacitance term (i.e.  $\tau_{R_1}$ ), then the latter approach is selected here.

Using Figure 14 for illustration, the following discussion presents an analytic method of determining an appropriate value for  $I_{S_{DFOR}}$  using two network constraints as apply to Figure 14.

$$V_{AK} = V_{J_1} + V_{J_2} + V_{J_3} = V_{EB_1} + V_{BC_1} + V_{BE_2} \quad (61)$$

$$I_{DFOR} = \alpha_1 I_A - (1 - \alpha_2)(I_A - I_R) \quad (62)$$

Noting that  $I_{S_1} = I_{S_2}$ ,  $\theta \approx 0.0259V @ 300^\circ K$  then:

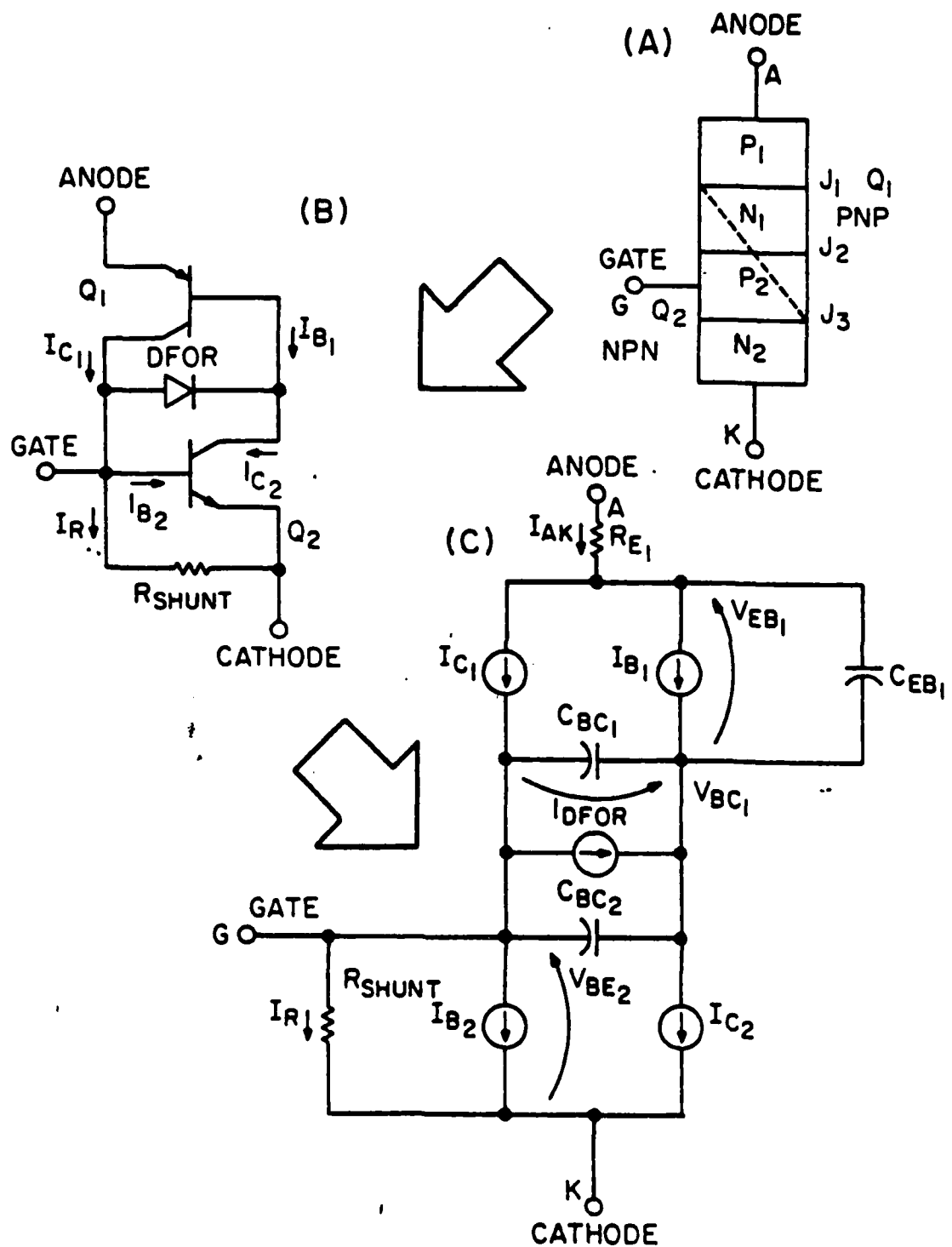


FIGURE 14. SPICE2 SCR MODEL BASED ON "HU-KI METHOD".

$$I_A = I_S \left( e^{\frac{V_{EB_1}}{\theta}} - 1 \right) \approx I_S e^{\frac{V_{EB_1}}{\theta}} \quad (63)$$

gives:

$$V_{EB_1} \approx \theta \ln \left[ \frac{I_A}{I_S} \right] \quad (64)$$

Also:

$$(I_A - I_R) = I_S \left( e^{\frac{V_{BE_2}}{\theta}} - 1 \right) \approx I_S e^{\frac{V_{BE_2}}{\theta}} \quad (65)$$

gives:

$$V_{BE_2} \approx \theta \ln \left[ \frac{I_A - I_R}{I_S} \right] \quad (66)$$

Now:

$$I_{DFOR} = I_{S_{DFOR}} \left( e^{\frac{-V_{BC_1}}{\theta}} - 1 \right) \approx I_{S_{DFOR}} e^{\frac{-V_{BC_1}}{\theta}} \quad (67)$$

and Equation (62) gives

$$V_{BC_1} \approx \theta \ln \left[ \frac{I_{S_{DFOR}}}{\alpha_1 I_A - (1 - \alpha_2)(I_A - I_R)} \right] \quad (68)$$

Referring to Figure 15 which gives the V-I characteristic of a SCR, the known point  $(I_H, V_H)$  available from the specification sheet data may be used to develop the relation between  $I_{S_{DFOR}}$  AND  $I_S$ .

Using Equations (61), (64), (66), (68),

$$V_{AK} = V_H \approx \theta \ln \left[ \frac{I_H}{I_S} \right] + \theta \ln \left[ \frac{I_{S_{DFOR}}}{\alpha_1 I_H - (1 - \alpha_2)(I_H - I_R)} \right] + \theta \ln \left[ \frac{I_H - I_R}{I_S} \right] \quad (69)$$

Now at  $I_A = I_H$ ,  $I_R \approx I_{GT}$  a specification sheet value.

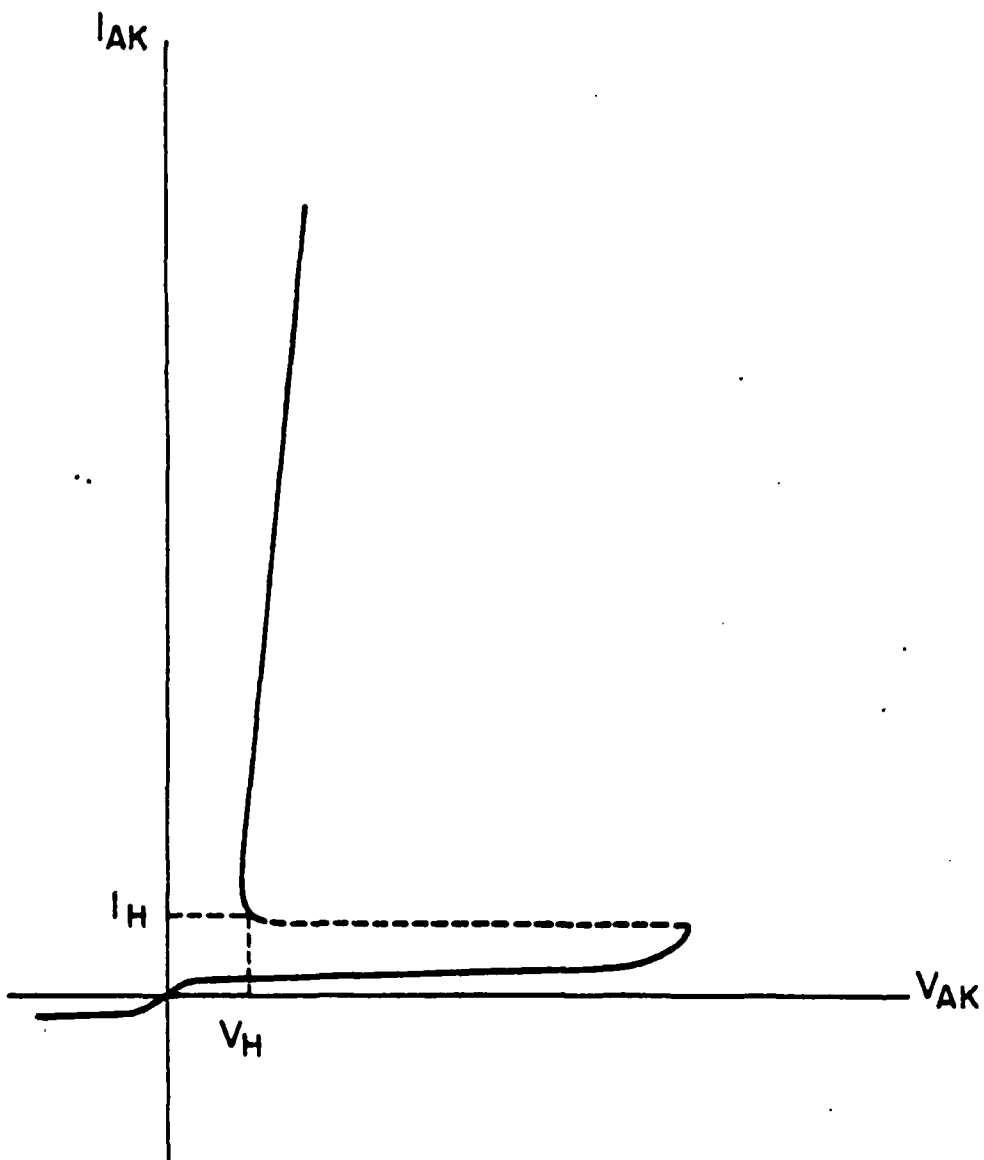


FIGURE 15. SCR V-I CHARACTERISTIC CURVE.

Substitution into Equation (69) gives

$$I_{S_{DFOR}} \approx \exp \frac{V_H}{\theta} - \ln \left[ \frac{I_H}{I_S} \right] - \ln \left[ \frac{I_H - I_{GT}}{I_S} \right] + \ln(\alpha_1 I_H - (1 - \alpha_2)(I_H - I_{GT})) \quad (70)$$

With the development of Equation (70) the parameters  $I_{S_{DFOR}}$  may now be provided to the SPICE 2 SCR model bringing the total to 17 parameters (15 if DJCTN 2 is omitted).

This modified Hu-Ki model is used in the SPICE 2 simulations that follow in later sections.

#### 4.4 THE SCR MODEL IN SCEPTRE

SPICE 2 is a fast, efficient, user oriented circuit analysis program; however, SCEPTRE provides additional versatility for non-linear network simulation through its subprogram capabilities. Also, SPICE 2 has built in models for transistors and diodes. The SCR model in SPICE 2 was constructed to the constraints of those models. SCEPTRE does not have built in models, but it does have programming constraints which should be observed to effect good efficient modeling. To achieve the expanded versatility of SCEPTRE, the SPICE 2 SCR model is reconfigured to a SCEPTRE SCR Model. The "modified Hu-ki" parameter determination technique for SPICE 2 is adapted for use with this SCEPTRE SCR Model.

##### 4.4.1 Reconfiguration of the SPICE 2 SCR Model into a SCEPTRE SCR Model

As mentioned previously SCEPTRE, while having no built in model constraints, does have programming constraints to which modeling must adhere. The constraints of particular importance in converting the SPICE 2 SCR Model configuration to a SCEPTRE SCR Model configuration are as follows.

1. Semiconductor PN junctions should be modeled as primary dependent current sources using the DIODE EQUATION special value expression of the SCEPTRE input format.

2. Primary dependent current sources should have a capacitor in parallel so that the independent variable, capacitor voltage, will be a state variable.
3. All capacitors inserted in the model to satisfy 2 should be as large as possible to avoid unnecessarily small time steps.
4. Injected, collected, or breakdown currents should be modeled as secondary dependent current sources as defined in the SCEPTRE input format.

Constraints 1 through 4 result in a substantially larger equivalent circuit network for the SCR Model in SCEPTRE than for the model in SPICE 2. Two transistor models, a PNP and a NPN, are connected in a regenerative feedback configuration to effect the SCR switching action. In order to satisfy the programming constraints 1 through 4, the transistor model is the injection configuration of the modified Ebers-Moll model [Reference 37,38] and the  $C_{BE}$  of the NPN transistor may not be neglected as it was for SPICE 2. Figure 16 shows the SCEPTRE equivalent circuit for the SCR.  $I_{DFOR}$  which reflects the diode DFOR's (of the SPICE 2 Model) forward conducting characteristics, but provides no reverse breakdown simulation capability. Therefore, to simulate SCR high-voltage break-over in SCEPTRE, the secondary dependent current source  $I_{BD_C}$  is added to the model. To simulate the reverse breakdown of the gate to cathode junction during turn-off,  $I_{BD_K}$  is used instead of  $D_{JCTN1}$  of the SPICE 2 SCR Model. The SCEPTRE SCR Model is functionally complete at this point; however, to avoid computational delays, RA and RC are high value resistors added to meet SCEPTRE programming requirements.

Figure 16 give the SCEPTRE SCR equivalent circuit. Figure 17 and Figure 18 put this circuit in SCEPTRE format and terminology and at the same time reduces the number of elements required. Table 4 summarizes the

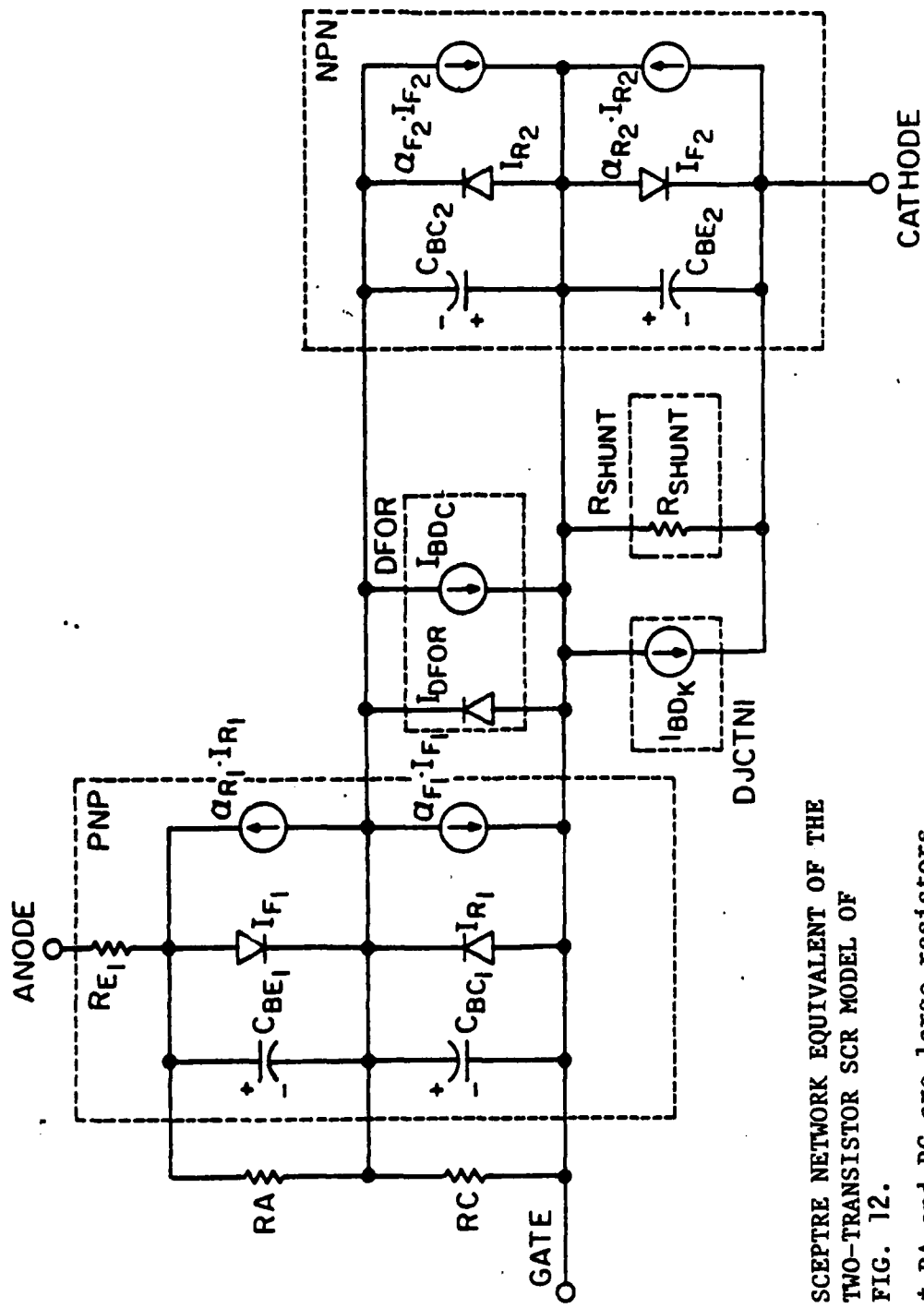


FIGURE 16. SCEPTRE NETWORK EQUIVALENT OF THE TWO-TRANSISTOR SCR MODEL OF FIG. 12.

\* RA and RC are large resistors added to meet programming requirements only.

relationships in the three figures. The reduction in the number of elements is achieved by parallel combinations of capacitors and parallel combinations of current sources. The identities of the primary dependent current sources are retained.

Note Figure 18 also includes a snubber circuit usually included to protect SCR's from transients.

Table 5 lists all the elements of the SCEPTRE 3-Junction SCR Model of Figure 18 with optional snubber. The elements are listed in appropriate SCEPTRE input format, and are defined in generalized parameters. The method of computing these generalized parameters is discussed in Section 4.4.2.

#### 4.4.2 Determination of Parameters For The SCEPTRE 3-Junction SCR Model.

The procedure for determining parameters for the SCEPTRE 3-Junction SCR Model of Figure 18 is an adaptation of the "Modified Hu-Ki" procedure used for determining parameters for the SPICE 2 2-Transistor SCR Model discussed in Section 4.2, 4.3 of this report. The adaptation consists primarily of adjusting SPICE 2 model parameters to reflect the reconfiguration of the SPICE 2 2-Transistor SCR Model into the SCEPTRE 3-Junction SCR Model.

Table 6 summarizes the entire procedure for determining parameters for the SCEPTRE 3-Junction SCR Model of Figure 18.

Using the procedure described in Table 6, the parameters for the GE C602 LM SCR are calculated and tabulated in Table 7.

The model description as entered in a SCEPTRE input deck is listed in Figure 19. In order for the model to function properly as listed, two special subroutines, FCJ and FBD must be provided in the input deck. These subroutines are listed in Figure 20 and Figure 21 respectively.

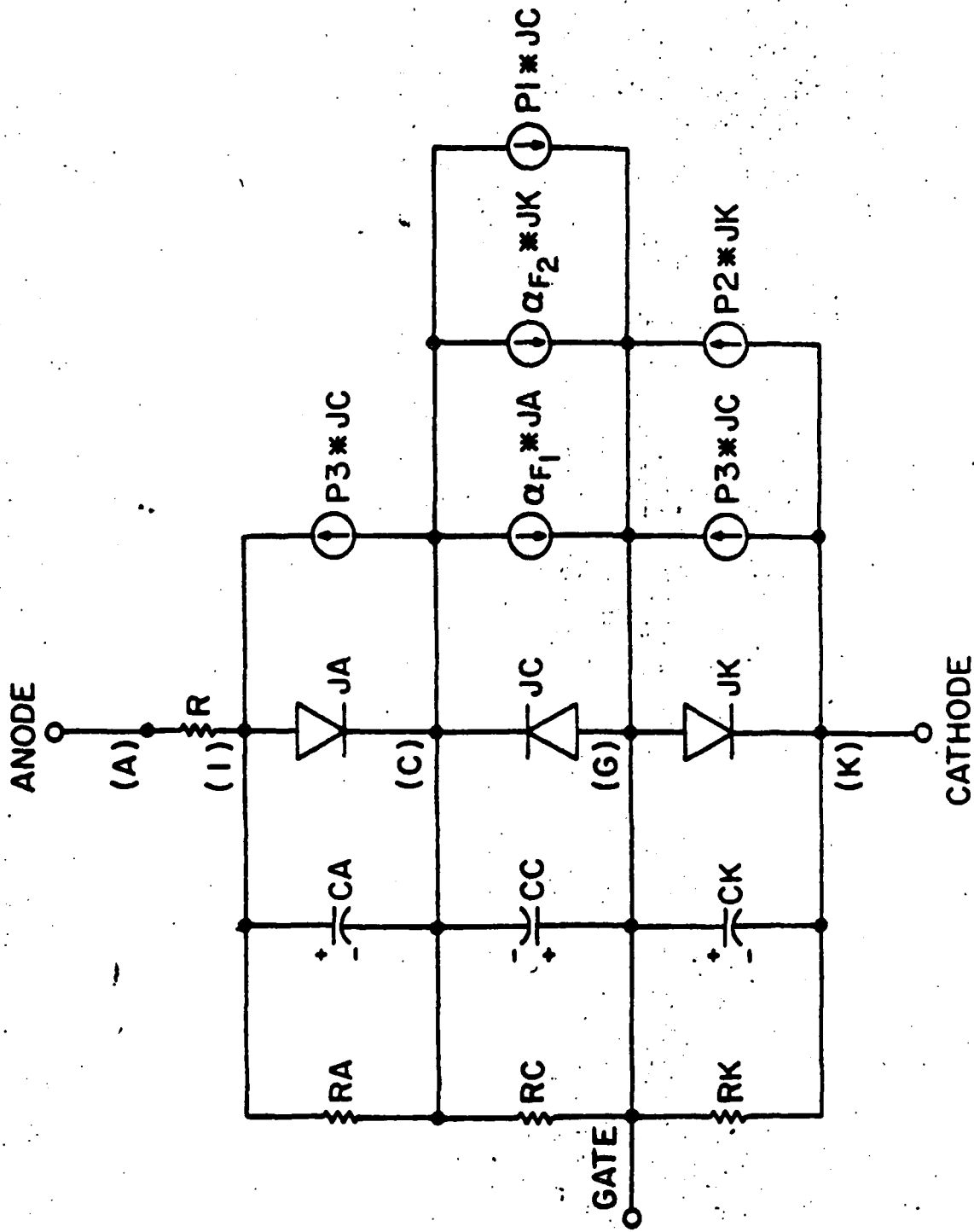


FIGURE 17. THE SCEPTRE 3-JUNCTION SCR MODEL NETWORK REPRESENTATION with elements defined according to SCEPTRE element name.

\* (x) denotes network node designation assigned for SCEPTRE INPUT DATA.

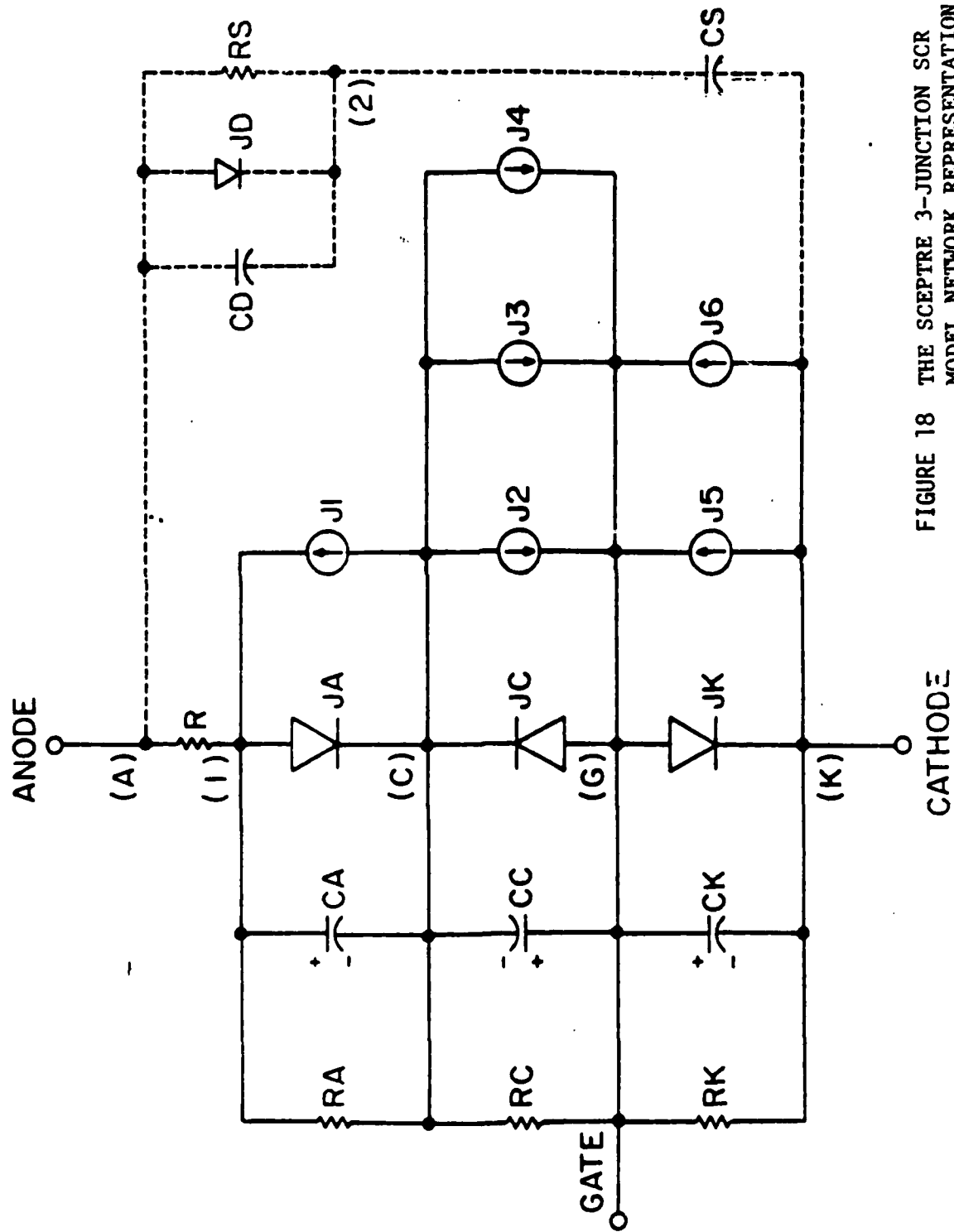


FIGURE 18 THE SCEPTRE 3-JUNCTION SCR MODEL NETWORK REPRESENTATION (—) WITH OPTIONAL SNUBBER (----).

TABLE 4. Symbol Conversion Chart

<u>Fig. 16</u>	<u>Fig. 17</u>	<u>Fig. 18</u>
$R_{E_1}$	R	R
$\alpha_{R_1} I_{R_1}$	P3 * JC	J1
$I_{f_1}$	JA	JA
$C_{BE_1}$	CA	CA
RA	RA	RA
$\alpha_{f_1} I_{f_1}$	$\alpha_{f_1} * JA$	J2
$I_{R_1} + I_{DFOR} + I_{R_2}$	JC	JC
$C_{BC_1} + C_{BC_2}$	CC	CC
$\alpha_{f_2} I_{f_2}$	$\alpha_{f_2} * JK$	J3
$I_{BDC}$	P1 * JC	J4
RC	RC	RC
$R_{Shunt}$	RK	RK
$C_{BE_2}$	CK	CK
$I_{f_2}$	JK	JK
$\alpha_{R_2} I_{R_2}$	P3 * JC	J5
$I_{BDK}$	P2 * JK	J6

TABLE 5. SCEPTRE SCR Model Circuit Element Description For The 3-Junction Model of Figure 18.

RESISTORS

R,A-1 = R  
 RA,1-C = 1.D6  
 RC,C-6 = 1.D6  
 RK,G-K = RK

PRIMARY DEPENDENT SOURCES (PN JUNCTIONS)

JA ,1-C = DIODE Q(IAS,  $\theta$ )  
 JC ,G-C = DIODE Q(ICS,  $\theta$ )  
 JK ,G-K = DIODE Q(IKS,  $\theta$ )

SECONDARY DEPENDENT SOURCES (COLLECTED CURRENTS & REVERSE BREAKDOWN CURRENTS)

J1 ,C-1 = P3 \* JC  
 J2 ,C-G =  $\alpha f_1$  \* JA  
 J3 ,C-G =  $\alpha f_2$  \* JK  
 J4 ,C-G = P1 \* JC  
 J5 ,K-G = P3 \* JC  
 J6 ,K-G = P2 \* JK

CAPACITANCES (JUNCTION DEPLETION LAYER AND NEUTRAL REGION EXCESS CHARGE STORAGE [DIFFUSION])

CA,1-C = FCJ( $\tau_{f1}$ , IAS,  $\theta$ , JA, VCA, CJAO, CMIN)  
 CC,G-C = FCJ( $\tau_{r1}$ , ICS,  $\theta$ , JC, VCC, CJCO, CMIN)  
 CK,G-K = CK

DEFINED PARAMETERS (REVERSE BREAKDOWN MULTIPLIERS)

P1 = FBD(VCC, VBOC)  
 P2 = FBD(VCK, VBOK)

SNUBBER ELEMENTS (OPTIONAL)

RS ,A-2 = VALUE IN OHMS  
 CS ,2-K = VALUE IN FARADS

ALSO IF USING DIODE SNUBBER:

JD ,A-2 = DIODE Q(DIODE SAT. CURRENT, THERMAL VOLTAGE)  
 CD ,A-2 = VALUE IN FARADS

TABLE 6. Procedure For Determining Parameters For The SCEPTRE 3-Junction SCR Model of Figure 18.

STEP 1. Obtain the following nine parameters from manufacturer's specifications data sheets. [22]

- $I_H$  - Holding current.
- $I_{GT}$  - Gate trigger current.
- $t_r(t_{on})$  -  $t_r$ ; rise time:  $t_{on}$ ; turn-on time.
- $V_T$  - Minimum on-state voltage.
- $R_{on}$  - On-state resistance (use inverse slope of  $i_{AK}$  vs.  $v_{AR}$  curve).
- $V_{BD}$  - Break-over voltage.
- $dv/dt$  - Maximum rate of rise of forward blocking voltage.
- $t_q$  - Circuit commutated turn-off time.
- $V_{GRM}$  - Maximum reverse gate voltage.

STEP 2.

$$R_K = .75V/I_{GT} \text{ ohms.}$$

STEP 3.

$$\alpha_{R2} = .5$$

$$\alpha_{f2} = .9 \text{ or } .95$$

$$\alpha_{f1} = \min \left\{ .9 \text{ or } 1 - \alpha_{f2} + \frac{I_{GT}}{\alpha_{f2} I_H} \right\}$$

$$\alpha_{R1} = \alpha_{f1}$$

STEP 4.

$$\tau_{f1} = (\beta_1 \beta_2 - 1) t_r / 1.8 \beta_1 \text{ seconds.}$$

$$\text{where: } \beta_1 = \frac{\alpha_{f1}}{1 - \alpha_{f1}}, \quad \beta_2 = \frac{\alpha_{f2}}{1 - \alpha_{f2}}$$

STEP 5.

$$\theta = q/KT \approx 38.61 \text{ V}^{-1} \text{ at } 300^\circ\text{K}$$

TABLE 6. (Continued)

$$I_S = 10^{-(V_T + .74)/.11} \text{ Amps.}$$

$$I_{AS} = I_S/\alpha f_1 \text{ Amps.}$$

$$I_{KS} = I_S/\alpha f_2 \text{ Amps.}$$

$$I_{CS} = I_S/R_1 + I_S/R_2 + \exp\left[\frac{V_H}{e}\right] - \ln\left[\frac{I_H}{I_S}\right] \\ - \ln\left[\frac{I_H - I_{GT}}{I_S}\right] + \ln[\alpha f_1 I_H - (1 - \alpha f_2)(I_H - I_G)] \text{ Amps.}$$

$$P_3 = I_S/I_{CS}$$

STEP 6.

$$R = R_{on} \text{ ohms.}$$

STEP 7.

$$\tau_{R1} = 9t_q P_3 \text{ seconds.}$$

STEP 8.

$$C_{JC0} = .4I_H(t_{on}/(dV/dt))^{1/2} \text{ farads.}$$

$$\text{where: } t_{on} = 1.5 t_r$$

dV/dt is volts/second.

$$C_{JA0} = \{ .5C_{JC0} \leq C_{JA0} \leq C_{JC0} \} \text{ farads.}$$

$$C_K \leq C_{JC0} \text{ farads.}$$

STEP 9.

$$V_{BOC} = V_{BO} \text{ volts.}$$

$$V_{BOK} = V_{GRM} \text{ (or 5V if not given) volts.}$$

STEP 10.

$$C_{MIN} = C_{JC0}/(V_{BO})^{1/2} \text{ farads.}$$

or: 1.0-10

Note: This procedure adapted from that presented by Hu and Ki in [Reference 34].

TABLE 7. SCEPTRE 3-Junction SCR Model Parameters Obtained Using The Procedure of Table 6 For a GE C602 LM SCR.

$RK = 9.375 \Omega$	$I_{CS} = 5.65D-15 A$
$\alpha_{R_2} = 0.5$	$P3 = 4.4D-3$
$\alpha_{f_2} = 0.9$	$R = 5.D-4 \Omega$
$\alpha_{f_1} = 0.9$	$\tau_{R_1} = 4.95D-6 S$
$\alpha_{R_1} = 0.9$	$C_{JC_0} = 4.D-9 F$
$\tau_{f_1} = 1.780-5 S$	$C_{JA_0} = 4.D-9 F$
$\theta = 38.61 V^{-1}$	$CK = 1.D-9 F$
$I_S = 2.239D-17 A$	$V_{BOC} = 2.7D3$
$I_{AS} = 2.488D-17 A$	$V_{BOK} = 5.$
$I_{KS} = 2.488D-17 A$	$C_{MIN} = 1.D-10$

TABLE 8. Manufacturer's Specifications For a GE C602 LM SCR And SCEPTRE Computer Simulation Specification Predictions.

<u>Quantity</u>	<u>Manufacturer's specifications</u>	<u>SCEPTRE simulation value</u>
$I_H$	100 ma	100 ma
$I_{GT}$	80 ma	87 ma
$t_r(t_{on})$	3.6 $\mu s$ (5.4 $\mu s$ )	4 $\mu s$ (7 $\mu s$ )
$V_T$	1.1V	1.1V
$V_{BO}$	2700V	2700V
dv/dt	G.T. 500V/ $\mu s$	G.T. 500V/ $\mu s$
$t_q$	L.T. 125 $\mu s$	L.T. 125 $\mu s$

MODEL DESCRIPTION

MODEL SCR(A-G-K)

THIS MODEL IS CALLED THE 3-JUNCTION SCR MODEL FOR SCEPTRE. IT IS DEVELOPED TO UTILIZE A PARAMETER DETERMINATION PROCEEDURE WHICH IS BASED ON THE MODIFIED HU-KI PROCEEDURE OF PARAMETER DETERMINATION FOR THE 2-TRANSISTOR SCR MODEL FOR SPICE2.

THIS MODEL IS REFERED TO AS THE THREE JUNCTION MODEL SINCE ALL SECONDARY DEPENDENT CURRENT SOURCES ARE REFERENCED TO THREE PRIMARY DEPENDENT CURRENT SOURCES (PN JUNCTIONS).

UNITS: OHMS, FARADS, HENRIES, SECONDS, AMPS, VOLTS  
ELEMENTS

R, A-1=5.0-3

RA, 1-C=1.06

RC, C-G=1.06

RK, G-K=9.375

JA, 1-C=DIODE Q(2.4880-17, 38.61)

JC, G-C=DIODE Q(5.650-15, 38.61)

JK, G-K=DIODE Q(2.4880-17, 38.61)

J1, C-1=4.40-3\*JC

J2, C-G=.9\*JA

J3, C-G=.9\*JK

J4, C-G=P1\*JC

J5, K-G=4.40-3\*JC

J6, K-G=P2\*JK

CA, 1-C=FCJ(1.780-5, 2.4880-17, 38.61, JA, VCA, 4.0-9, 1.0-9)

CC, G-C=FCJ(4.950-6, 5.650-15, 38.61, JC, VCC, 4.0-9, 1.0-9)

CK, G-K=4.0-9

RS, A-2=10.

CS, 2-K=.10-6

DEFINED PARAMETERS

P1=FBD(VCC, 2.703, 5.650-15)

P2=FBD(VCK, 5., 2.4880-17)

OUTPUTS

VCA, VCC, VCK, PLOT

FIGURE 19. SCEPTRE INPUT LISTING FOR A GE C602 LM SCR MODEL USING THE PARAMETERS OF TABLE 7 IN THE MODEL NETWORK OF FIGURE 18.

```

DOUBLE PRECISION FUNCTION FCJ(TAU,IS,THT,J,VC,CJO,CMIN)
C SUBROUTINE FCJ CALCULATES THE NON-LINEAR INCREMENTAL CAPACITANCE ASSOCIATED
C WITH THE CHARGE STORAGE OCCURRING ABOUT A PN JUNCTION. IF THE JUNCTION IS
C FORWARD BIASED THE DEPLETION LAYER TERM IS HELD CONSTANT WHILE THE DIFFUSION
C CALCULATED. CONVERSELY IF THE JUNCTION IS REVERSE BIASED ONLY A DEPLETION
C TERM IS CALCULATED. FOR A REVERSED BIASED JUNCTION THE CAPACITANCE IS LIMITED
C TO A MINIMUM VALUE, CMIN, TO AVOID UNREASONABLY SMALL TIME CONSTANTS IN THE
C CIRCUIT SIMULATION. PARAMETERS ARE; TAU = THE EXCESS CARRIER LIFETIME IN THE
C NEUTRAL REGIONS ABOUT THE JUNCTION, IS = JUNCTION SATURATION CURRENT, THT =
C EINSTEIN'S CONSTANT (Q/KT = 38.61 @ 300 DEG K.), J = CURRENT SOURCE SIMULATING
C THE PN JUNCTION FOR WHICH CAPACITANCE IS BEING CALCULATED, VC = VOLTAGE ACROSS
C CAPACITOR WHOSE VALUE IS BEING CALCULATED, CJO = ZERO BIAS VALUE OF THE
C DEPLETION LAYER CAPACITANCE, CMIN = MINIMUM VALUE OF JUNCTION CAPACITANCE TO
C BE ALLOWED.
      IMPLICIT REAL*8(A-Z)
      IF(VC.GT.0.) GO TO 10
      FCJ=CJO/(1.-VC)**.5
      IF(FCJ.GE.CMIN) RETURN
      FCJ=CMIN
      RETURN
10 FCJ=TAU*THT*(J+IS)+CJO
      RETURN
      END

```

FIGURE 20. SPECIAL SUBROUTINE FCJ USED TO CALCULATE NON-LINEAR JUNCTION CAPACITANCES OF THE SCEPTRE 3-JUNCTION SCR MODEL.

```

DOUBLE PRECISION FUNCTION FBD(VJ,VBD,IS)
C FBD IS A SUBROUTINE TO DETERMINE IF THE REVERSE BREAKDOWN VOLTAGE OF A PN
C JUNCTION HAS BEEN EXCEEDED AND IF SO TO CALCULATE A MULTIPLIER TO REFLECT
C AVALANCHE CURRENTS IN THE PN JUNCTION. THIS MULTIPLIER IS USED AS THE
C COEFFICIENT OF A SECONDARY DEPENDENT CURRENT SOURCE IN PARALLEL WITH THE
C PRIMARY DEPENDENT CURRENT SOURCE WHICH SIMULATES THE PN JUNCTION. PARAMETERS
C ARE; VJ = THE VOLTAGE ACROSS THE JUNCTION, VBD = THE BREAKDOWN VOLTAGE
C OF THE JUNCTION, IS = JUNCTION SATURATION CURRENT.
C THE JUNCTION AVALANCHE BREAKDOWN MULTIPLIER IS THEORETICALLY EXPRESSED AS
C (-1/(1-(VJ/VBD)**6)); HOWEVER, TO ACHIEVE SHORTER RUN TIMES, AN EXPONENTIAL
C MULTIPLIER, -DEXP(100.*(-VBD-VJ)), IS USED IN THIS CASE.
      IMPLICIT REAL*8(A-Z)
      IF(VJ.GT.(-VBD))GO TO 10
      A=100.*(-VBD-VJ)
      IF(A.LE.40.) GO TO 30.
      A=40.
30 FBD=-DEXP(A)
      GO TO 20
10 FBD=0.0
20 RETURN
      END

```

FIGURE 21. SPECIAL SUBROUTINE FBD USED TO CALCULATE JUNCTION BREAK-DOWN CURRENTS FOR THE SCEPTRE 3-JUNCTION SCR MODEL.

Computer simulation test verification of the model for a GE C602 LM SCR is presented in Table 8. The parameters to be verified are listed in the table along with the manufacturer's specified value and SCEPTRE simulation results.

#### NOTE

Default accuracy requirements of SCEPTRE may not always be adequate to insure proper simulation results. Erroneous results are most likely to occur in simulating circuits with high  $dv/dt$  (either forward or reversed) without a snubber circuit. Reducing error tolerance under Run Controls will solve the problem; however, longer run times are to be expected for greater accuracy criterion.

#### 4.4.3 A SCEPTRE 3-Junction SCR Model With a Reduced Number of Current Sources In The Model

Sections 4.4.1 and 4.4.2 presented the development of an SCR model for use in SCEPTRE which is functionally equivalent to the SPICE 2 SCR Model is, however, quite imposing with respect to the number of elements contained in the network representation of the model as given by Figure 18.

A major objective of the research of this project was to simulate high voltage resonant charging pulse power circuits. Since typical high power SCR's have maximum blocking voltage ratings on the order of 3000V, high voltage circuits are developed using a number of SCR's in series to meet the voltage blocking requirements.

Also, pulse power circuits may have a number of parallel or anti-parallel branches each having several SCR's. The basic controlled 3- $\phi$  rectifier circuit is an example. In order to provide controlled rectification of a 700V, 3- $\phi$  source, typically 18 SCR's of 3000V blocking capability might be employed.

The problem presented to simulation of this type of circuit using the SCR model of Figure 18 is that SCEPTRE internal limitations on the number of sources the program can accommodate may be exceeded.

This problem required some experimentation with SCEPTRE capabilities before a satisfactory solution was achieved. Initially, attempts were made to formulate each of the three junction currents as a mathematical equivalent to the total of the sources in parallel representing each junction. This approach was in violation of the SCEPTRE suggested programming constraints listed in Section 4.4.1. Not only was the mathematical formulation rather imposing, but, the end result was that an exact formulation of the model of Figure 18 as three current sources resulted in the following.

1. Run times for identical problems increased in some cases as much as 200% to 300%.
2. The failure to adhere to constraints 1 through 4 of Section 4.4.1 made initial conditions solutions available only through the transient approach, i.e. using RUN IC VIA IMPLICIT. Without special operator input, the effects of this on CPU time to calculate initial conditions was drastic. Even small networks were observed to require as much as 15 mins. CPU time to complete initial conditions solutions. Long CPU times resulted due to the extremely small time step required (less than  $10^{-30}$  sec.) to handle the steep transients of the nonlinear circuit elements such as junction capacitances and due to the large number of multiple operations necessary in each iteration necessary to calculate values of the junction current sources described by the long and complex match expressions defining the sources.

The primary and secondary dependent current source approach to defining junction relationships as shown in Figure 18 is inherently more efficient. The reason being that a relatively simple non-linear expression defines the primary dependent current source thereby minimizing the number of multiply operations by the computer. Secondary dependent current sources are either linear or simple non-linear multiples of the primary dependent current sources. In the case of non-linear secondary dependence, SCEPTRE offers the use of subroutines. Through this device, logic statements may be used to test the need for non-linear versus linear secondary dependence before initiating the calculation. For these reasons, the model of Figure 18 having a larger network was judged superior to a three current source model using a mathematical equivalent formulation to the nine current source model of Figure 18.

A second approach was then conceived to effect the goal of a reduced number of sources in the model. This second approach was judged successful and is summarized as follows:

1. The secondary dependent current sources, J1 and J5 are equivalent to  $\alpha_{R_1} \cdot I_{R_1}$  and  $\alpha_{R_2} \cdot I_{R_2}$  of Figure 16. It is most easily visualized through the 2-transistor basis of the model of Figure 16 that these two current sources model third quadrant operation of the PNP and NPN transistor respectively. Since even at high currents, the SCR center junction (JC of Figure 18) and  $I_{R_1} + I_{DFOR} + I_{R_2}$  of Figure 16 reaches a substantially lower forward biased state than do the outer junctions JA and JK, then it is reasonable to neglect the J1 and J5 secondary dependent current sources.

2. The two secondary dependent current sources, J2 and J3, are linearly dependent upon the primary dependent current sources JA and JK respectively. Since the calculation of both JA and JK must precede the calculation of J1 and J3 due to the SCEPTRE calculation procedure, then a simple summation of J1 and J2 into a single source seemed reasonable although SCEPTRE literature seemed to exclude this possibility [Reference 41 p.13] the approach seemed feasible, however.
3. The secondary dependent current sources J4 and J6 used to model junction breakdown were handled by a more novel approach. Considering the DIODE EQUATION (X1, X2) special value expression used in SCEPTRE to define primary dependent current sources modeling PN junctions, the parameters X1 and X2 are presented in SCEPTRE users literature to be constants. X1 represents the diode reverse saturation current, and X2 represents the junction thermal voltage. Since classical PN junction theory expresses the PN junction reverse saturation current as a function of the junction voltage, then it was deemed desirable to express X1 as a function of the junction voltage.

Again SCEPTRE's calculation heirarchy was used to effect this result. Defined parameters are the first quantities calculated at the beginning of each time step and are then provided to the network as constants. Also defined parameters may be evaluated through the subroutine capability, thereby allowing a logical test to be made before consuming CPU time to evaluate functions.

With this approach, J4 and J6 were eliminated from the model and the PN Junction breakdown capability was developed by developing a function relationship for X1 through the defined parameter technique.

It is noted that the success of this approach will also admit the possibility of semiconductor thermal behavior studies through developing a functional relationship for the thermal voltage parameter X2. Also a functional relationship for X2 would permit distinction between high level and low level injection and  $\beta$  variations.

The result of the modifications just summarized is the model network illustrated in Figure 22. It has four dependent current sources versus the nine dependent sources of the model network shown in Figure 18.

Table 9 gives a generalized listing of the element descriptions in SCEPTRE input format for the SCR model of Figure 22.

The parameters for the reduced 3-Junction SCR model of Figure 22 are determined by the procedure of TABLE 6 in exactly the same manner as the parameters for the 3-Junction SCR Model of Figure 18. The only difference being that the  $\alpha_{R_1}$  and  $\alpha_{R_2}$  parameters of step 3 and the P3 parameter of step 5 are not required for the reduced 3-Junction model of Figure 22.

A SCEPTRE model description for a GE C602 LM SCR model is given in Figure 23, a special subroutine FIS required to evaluate defined parameters PX1 and PX3 of the reduced 3-Junction SCR Model is shown in Figure 24.

Model validation tests were done to verify computer prediction of manufacturers specification data used to determine model parameters. Computer simulation values for the reduced 3-Junction model were not distinguishable from those predicted for the 3-Junction model and tabulated in Table 8.

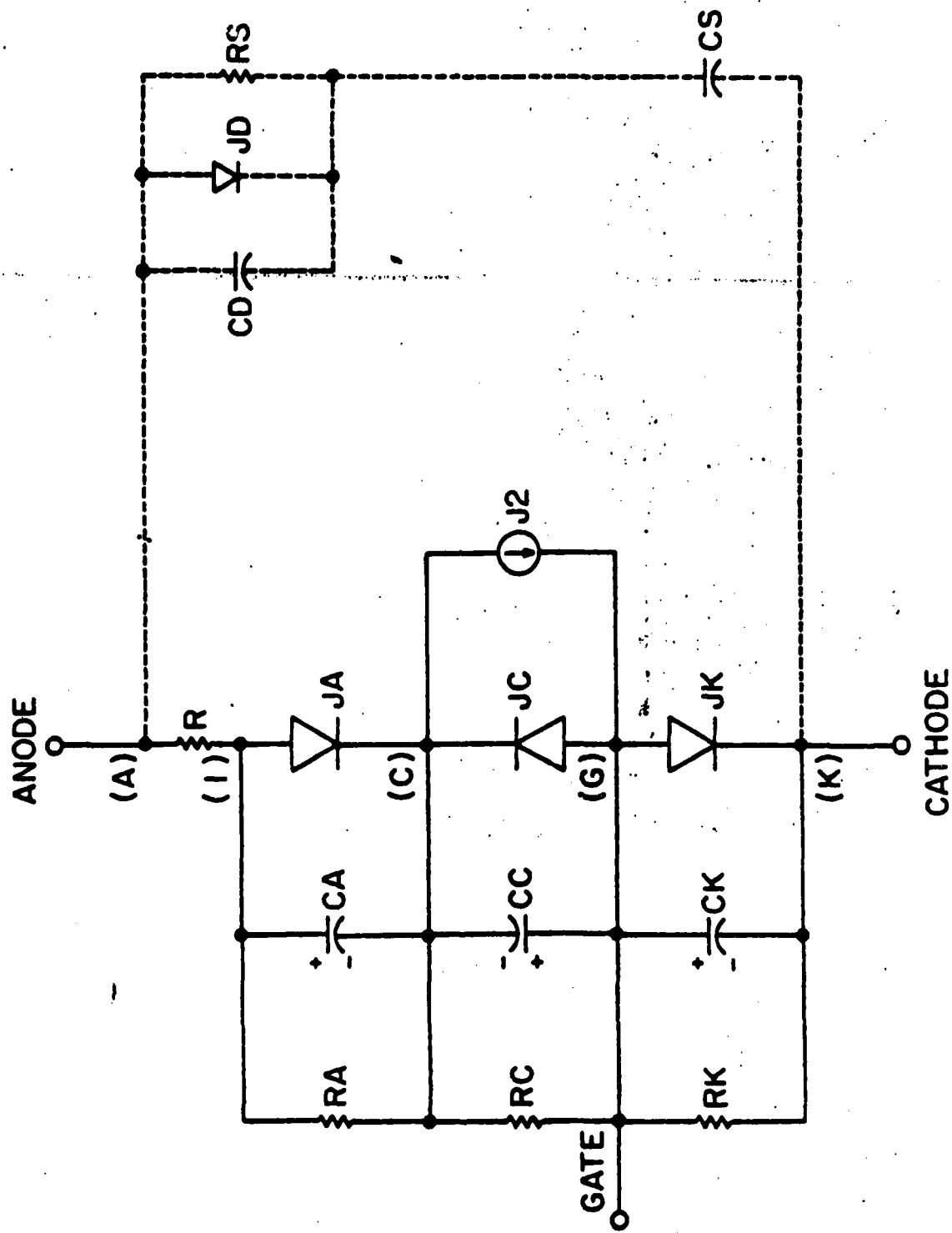


FIGURE 22. THE SCEPTRE REDUCED 3-JUNCTION SCR MODEL WITH A REDUCED NUMBER OF CURRENT SOURCES IN THE MODEL. (—) model. (---) optional snubber.

MODEL DESCRIPTION

MODEL SCR(A-G-K)

THIS IS A REDUCED ELEMENT VERSION OF THE 3-JUNCTION SCR MODEL DEVELOPED FOR USE WITH SCEPTRE. THE PARAMETER DETERMINATION PROCEEDURE FOR THIS MODEL IS THE SAME AS FOR THE 3-JUNCTION MODEL.

UNITS: OHMS, FARADS, HENRIES, SECONDS, AMPS, VOLTS  
ELEMENTS

R, A-1=5. D-3

RA, 1-C=1. D6

RC, C-G=1. D6

RK, G-K=9. 375

JA, 1-C=DIODE Q(2.488D-17, 38.61)

JC, G-C=DIODE Q(PX1, PX2)

JK, G-K=DIODE Q(PX3, PX2)

J2, C-G=X1(.9\*JA+.9\*JK)

CA, 1-C=FCJ(1.78D-5, 2.488D-17, 38.61, JA, VCA, 4. D-9, 1. D-10)

CC, G-C=FCJ(4.95D-6, 5.65D-15, 38.61, JC, VCC, 4. D-9, 1. D-10)

CK, G-K=1. D-9

RS, A-2=100.

CS, 2-K=. 1D-6

DEFINED PARAMETERS

PX1=FIS(5.65D-15, VCC, 2.7D3)

PX2=38.61

PX3=FIS(2.488D-17, VCK, 5.)

OUTPUTS

VCA, VCC, VCK, PLOT

FIGURE 23. SCEPTRE MODEL DESCRIPTION  
INPUT FOR A GE C602 LM

DOUBLE PRECISION FUNCTION FIS(IS, VJ, VBD)  
C SUBROUTINE FIS IS USSD TO SIMULATE JUNCTION BREAKDOWN BY VARYING THE  
C SATURATION CURRENT, IS, INPUT TO THE DIODE EQUATION FOR PRIMARY DEPENDENT  
C CURRENT SOURCES. IS = JUNCTION REVERSE SATURATION CURRENT: VJ =  
C CAPACITOR STATE VARIABLE VOLTAGE FOR JUNCTION: VBD = BREAKDOWN VOLTAGE:  
IMPLICIT REAL\*8(A-K, O-Z)  
FIS=IS  
IF(VJ.GE.-VBD) RETURN  
A=100.\*(-VBD-VJ)  
IF(A.LE.40.) GO TO 10  
A=40.  
10 FIS=IS\*DEXP(A)  
RETURN  
END

FIGURE 24. SUBROUTINE FIS USED TO  
CALCULATE PX1 & PX2 OF  
TABLE 9.

TABLE 9. SCEPTRE SCR Model Circuit Element Description For The 3-Junction Model of Figure 24.

RESISTORS

R,A-1 = R  
 RA,1-C = 1.D6  
 RC,C-6 = 1.D6  
 RK,G-K = RK

PRIMARY DEPENDENT SOURCES (PN JUNCTIONS)

JA ,1-C = DIODE Q(I<sub>AS</sub>, θ)  
 JC ,G-C = DIODE Q(PX1, PX2)  
 JK ,G-K = DIODE Q(PX3, PX2)

SECONDARY DEPENDENT SOURCES (COLLECTED CURRENTS & REVERSE BREAKDOWN CURRENTS)

J2 = X1(α<sub>f1</sub>\*JA + α<sub>f2</sub>\*JK)

CAPACITANCES (JUNCTION DEPLETION LAYER AND NEUTRAL REGION EXCESS CHARGE STORAGE [DIFFUSION])

CA,1-C = FCJ(τ<sub>f1</sub>, I<sub>AS</sub>, θ, JA, VCA, C<sub>JAO</sub>, C<sub>MIN</sub>)  
 CC,G-C = FCJ(τ<sub>r1</sub>, I<sub>CS</sub>, θ, JC, VCC, C<sub>JCO</sub>, C<sub>MIN</sub>)  
 CK,G-K = CK

DEFINED PARAMETERS (REVERSE BREAKDOWN MULTIPLIERS)

PX1 = FIS(I<sub>CS</sub>, VCC, VBOC)  
 PX2 = θ  
 PX3 = FIS(I<sub>KS</sub>, VCK, VBOK)

SNUBBER ELEMENTS (OPTIONAL)

RS ,A-2 = VALUE IN OHMS  
 CS ,2-K = VALUE IN FARADS

ALSO IF USING DIODE SNUBBER:

- - - - -

JD ,A-2 = DIODE Q(DIODE SAT. CURRENT, THERMAL VOLTAGE)  
 CD ,A-2 = VALUE IN FARADS

The run times for the reduced 3-Junction model of Figure 22 were observed to be approximately 5% to 10% shorter than those of the 3-Junction model of Figure 18.

## SECTION V

### CHOICE OF VARIABLES

#### 5.1 OBJECTIVE

When solving systems of equations using numerical methods and in particular when the equations are non-linear, the choice of system variables may have significant effect on the computation time and or the reliability of the results. In this section the nature of these effects are examined even though the decision to use CAD programs such as SPICE 2 and SCEPTRE may preclude such considerations.

#### 5.2 CHOICE OF VARIABLES

Chua and Lin (Reference 11) have shown that the selection of a certain set of state variables depends on the nature of the nonlinear elements. For a nonlinear capacitor characterized by a nonmonotonic voltage-controlled  $q-v$  curve, for example, the capacitor voltage must be chosen as the state-variable. Similarly, inductor current must be chosen as the state variable for a nonlinear inductor characterized by a nonmonotonic current-controlled  $\lambda-i$  curve. However, if the capacitor and inductor characteristic curves are strictly monotonic, then either capacitor voltage or charge may be chosen as the capacitor state variable, and for the inductor, the state variable may be chosen as either inductor flux linkage or current.

However, it is shown (Reference 12) that it is advantageous to choose capacitor charge and inductor flux linkage as the state variables when a numerical integration algorithm is used because this particular choice of state variables reduces the global error. Global error is the error accrued over the finite time interval during which the numerical integration is performed.

To see why this is so, consider a nonlinear system (Reference 12) modeled by the equations

$$\dot{\underline{x}} = \underline{f}(\underline{x}, t) \quad \underline{x}(0) = \underline{x}_0 \quad (71)$$

where the bar implies the use of vectors or matrices.

To estimate the growth of errors over some time interval, say time  $t = 0$  to  $t = t_f$  when solving Equation (71) numerically, consider the differential equation which results when the initial condition is perturbed so that  $\underline{x}(0) \rightarrow \underline{x}_0 + \delta\underline{x}(0) = \underline{x}_0 + \underline{\delta}_0$ . Then from Equation (34) the perturbed equations become

$$\frac{d}{dt} (\underline{x}(t) + \delta\underline{x}(t)) = \underline{f}(\underline{x}(t) + \delta\underline{x}(t), t) \quad (72)$$

$$\delta\underline{x}(0) = \underline{\delta}_0$$

Assuming  $\delta\underline{x}(t)$  is small and expanding the right side of Equation (72) by a Taylor series gives

$$\frac{d}{dt} (\underline{x}(t) + \delta\underline{x}(t)) = \underline{f}(\underline{x}, t) + \frac{\partial \underline{f}}{\partial \underline{x}} \delta\underline{x}(t) \quad (73)$$

$$\delta\underline{x}(0) = \underline{\delta}_0$$

Subtracting Equation (73) from Equation (71) gives

$$\dot{\delta\underline{x}} = \left( \frac{\partial \underline{f}}{\partial \underline{x}} \right) \delta\underline{x} \quad \delta\underline{x}(0) = \underline{\delta}_0 \quad (74)$$

where the matrix  $(\partial \underline{f} / \partial \underline{x})$  is a time-varying Jacobian matrix  $J_x(t)$ . Equation (74) represents a linear time-varying system; thus no simple solution exists. In the case where  $\underline{x}$  and  $\underline{f}$  are scalar quantities, the solution to Equation (74) is

$$\delta x(t) = \delta_0 e^{\int_0^t J_x(\tau) d\tau} \quad (75)$$

Equation (75) indicates that whenever  $J_x(\tau) > 0$ , the error (accumulated at time  $t$  in the exact solution to the scalar version of Equation (71), due to an error  $\delta_0$  in the initial condition) actually decreases exponentially with time. Since the concern is the accrued effects of errors made at all time steps (and not just that due to an error in the initial condition), proceed to determine the accrued error  $E_{0,t_f}$ , i.e., the sum of errors from time  $t = 0$  to time  $t = t_f$ . To this end it is assumed that the error per

unit time (which is denoted by  $\epsilon_t$ ) is constant. Then the error made in an interval of time  $dt$ , is  $\epsilon_t dt$ . From Equation (75), the growth of error for  $t_1 < t$  is given by

$$\epsilon_{t_1, t} = \epsilon_t dt_1 e^{\int_{t_1}^t J_X(\tau) d\tau} \quad (76)$$

so that the accrued error  $E^{0, t_f}$  at time  $t_f$  is the sum of the error originating for all times  $t_1 < t_f$ , so that

$$E^{0, t_f} = \left( \epsilon_t \int_0^{t_f} e^{\int_{t_1}^{t_f} J_X(\tau) d\tau} dt_1 \right) \quad (77)$$

To demonstrate error growth, Calahan (Reference 11) used the circuit of Figure 25, where the nonlinear capacitance is strictly monotonic. If the state equation is written in terms of the capacitor voltage we have

$$(C_T + C_d^0 e^{\lambda v}) \frac{dv}{dt} = -\frac{v}{R} + \frac{v_s}{R} - I_s(e^{\lambda v} - 1); \quad \lambda = 40 \quad (78)$$

The Jacobian is given by

$$J_V = \frac{\lambda C_d^0 e^{\lambda v} \left( \frac{v - v_s}{R} \right) + I_s(e^{\lambda v} - 1)}{(C_T + C_d^0 e^{\lambda v})^2} - \frac{\left( \frac{1}{R} + \lambda I_s e^{\lambda v} \right)}{(C_T + C_d^0 e^{\lambda v})} \quad (79)$$

where  $\lambda = 40$ .

During switching, when  $v_s < 0$  and  $v > 0$ , the first term shifts the eigenvalue  $J_V$  toward the right half plane. Indeed if  $v_s$  is made sufficiently negative, the eigenvalue  $J_V$  can be made as positive as desired. Thus, during this time when  $J_V$  is positive, truncation errors introduced by

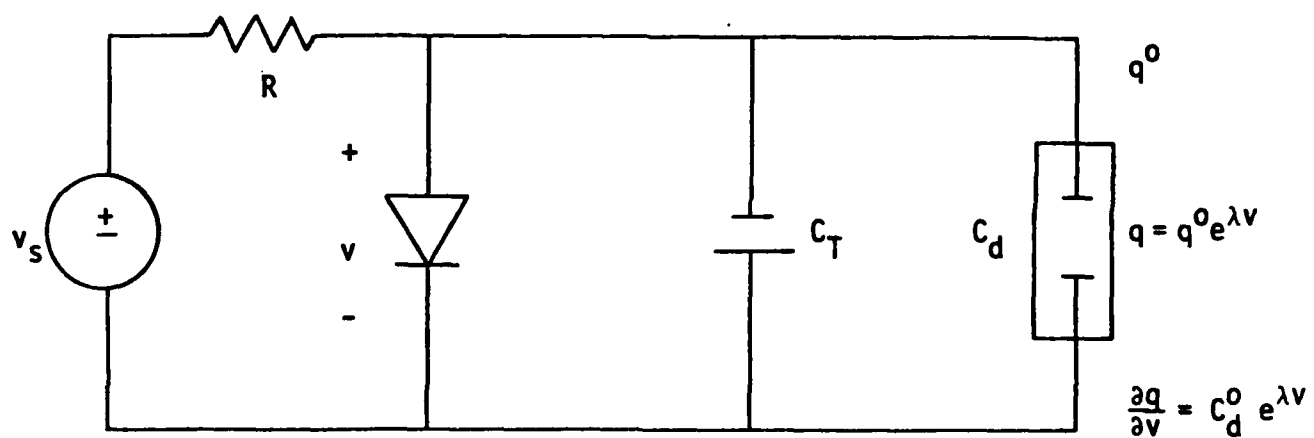


FIGURE 25. CALAHAN'S EXAMPLE CIRCUIT

the integration formula used will be amplified according to Equation (40). By choosing charge as the state variable, the resulting eigenvalue  $J_F$  can be shown to lie in the left half plane during switching, so that truncation errors will decay according to Equation (40). Finally, it should be noted that in the case of linear capacitors or inductors, either  $q$  or  $v$  for a capacitor, or  $\lambda$  or  $i$  for an inductor may be chosen as the state variable (Reference 11).

### 5.3 SCEPTRE VARIABLES

In Section VII the decision to use the CAD system called SCEPTRE is discussed. Whether SCEPTRE or the other system considered SPICE 2, is used, the system variables are capacitor voltages, inductor currents or other variables determined by the CAD system. Thus, the decision to use a CAD system represents a trade-off between ease of system formulation and some control of integration error by judicious choice of system variables.

The state-variables used in SCEPTRE are capacitor voltage and inductor current. Both nonlinear capacitors and nonlinear inductors are present in the integrated system. The nonlinear inductors arise naturally in the generator and transformer models, the nonlinear capacitors in the SCR model. Further, the nonlinear capacitors in the SCR model are strictly monotonic so that computationally the choice of capacitor voltage as the state variable is desirable. Also, the nonlinear inductors in the transformer and generator model are strictly monotonic so that inductor flux linkages are the preferred state variables.

While it has been rigorously proven that for nonlinear dynamic networks containing passive elements and independent sources it is desirable to choose capacitor charges and inductor flux linkages as state variables, no one has been yet able to prove that the same criterion applies for networks containing active elements and controlled sources, although it would seem to apply (Reference 11). In a system as complex as the one in this project it is not clear what the trade-off may have cost in terms of integration error.

## SECTION VI

### NUMERICAL METHODS FOR STIFF DIFFERENTIAL EQUATIONS

#### 6.1 INTRODUCTION

In this section suitable numerical methods for solving stiff differential equations are investigated. Stiff means that the magnitude of the largest eigenvalue to the smallest eigenvalue of the system differs by many orders of magnitude. Most standard methods, such as the Runga Kutta method, or the forward Euler method, are not well suited for solving stiff differential equations (Reference 15). This is because the step size in the forward Euler method, for example, is determined by the smallest time constant, but the number of iterations required to reach the steady state is determined by the largest time constant. Thus, if the time constants are widely separated a small step size would necessarily be employed and a great deal of computer time would be spent on determining the steady-state solution (Reference 16).

#### 6.2 INTEGRATION METHODS

It has been shown (Reference 16) that the widely separated time constant problem can be eased by using implicit integration algorithms, such as the backward Euler and trapezoidal algorithms. Typically, the use of the trapezoidal algorithm is avoided because of the "ringing behavior" it exhibits when implemented with a large step size. This is undesirable since it may erroneously lead the designer to conclude the solution to the system is oscillatory (Reference 16).

Gear (Reference 17) has proposed a family of methods of order  $p+1$  which have been shown to be extremely useful for solving stiff differential equations. These methods are based on the implicit formula

$$y_{n+1} = \sum_{i=0}^p c_i y_{n-1} + d \dot{y}_{n+1} \quad (80)$$

For  $p = 0$  the backward Euler method is obtained. The Gear methods possess the property that  $\text{Re}\{h\lambda\} < -a$  for some small positive  $a$ ; that is, the

method is stable where stability is the prime consideration. In addition, when  $\text{Re}(h\lambda) > a$  they are accurate (Reference 17, 18). In general there is a tradeoff between accuracy and stability for any numerical integration method. Choosing a high-order Gear method, for example, increases the accuracy (ie, reduces truncation error) at the expense of decreasing the stability (Reference 17). The maximum order must be limited to  $p+1=5$  because of stability considerations (Reference 17).

Gear's methods can be implemented in a fixed or variable step size mode, or in a variable step size and variable-order mode. While the latter is difficult to implement there are several reasons why it is well worth the effort. First of all, since the computation is started with a low-order rule and small step size the method is self-starting. The order and the step size are adaptive in the sense that they are modified at each time step so that the optimal order and step size are chosen, subject to certain constraints. This leads to a very efficient and accurate solution over the integration interval of interest. At the present time, stability theory in variable step size, variable-order methods is not fully comprehended so that decisions for determining step size are based on experimental evidence (Reference 18).

Another advantage of using Gear's method is that it has an outstanding error control feature (Reference 19). Calahan was the first to discuss how to implement Gear's method in a nodal-based analysis program (Reference 20).

Gear's method is a vast improvement over previous techniques because it is not troubled by the minimum time constant problem. However, if step size is changed very rapidly, Gear's method could become numerically unstable. To overcome this deficiency in Gear's method, Brayton, Gustafson and Hachtel (Reference 21) have proposed yet another method which is less likely to become unstable when the step-size changes rapidly, as demonstrated by numerical experiments. In the case where the step size is fixed, the method of Brayton et al. can be shown to be equivalent to Gear's method (Reference 21).

### 6.3 INTEGRATION METHODS OF SCEPTRE

SCEPTRE offers several options for integration methods including Gear's (Reference 17) method in variable step size. SCEPTRE should be appropriate for this project. The generator, transformer and SCR models in a composite system with its stiff differential equations require the implicit integration capability. The program also allows specification of maximum and minimum step size and error limits can be specified control the variable step size feature.

However, even though implicit integration allows larger step size than non-implicit methods there is no doubt that a step size appropriate for the short time constants of the SCR model will still require long computer times for the representation of the periodic swings of the electromechanical equations of the generator.

## SECTION VII

### SYSTEM INTEGRATION

In making the decision to use SCEPTRE as a modeling and simulation program, system integration problems are solved.

The original plan was to model the system by components and form the system by integrating the components. This is in contrast to modeling the system by elements (R, L, C and sources) and integration of the system with network equation formulation.

As work began in the study of methods for solving "stiff" differential equations several problems became apparent. First, small step sizes and long computation times would be required to account for the effects of both long and short time constants. Secondly, while implicit integration methods for "stiff" differential equations allow larger step sizes, iteration is required for convergence to a solution at each step. Finally, any further iterations that may be required to find the equilibrium point for the component interface variables make the component approach less attractive.

Three alternatives were considered.

1. write a network solving program
2. use CAD program SPICE 2
3. use CAD program SCEPTRE

The first alternative has the advantages of a much simpler and smaller program than SPICE 2 or SCEPTRE since they were written to do much more than a simple transient network analysis. Also, system variables could be used which would enhance the accuracy of the nonlinear systems. (Note Section V) SPICE 2 and SCEPTRE normally use voltage and current as variables.

The disadvantage is an unpredictable amount of time in writing and debugging such a program.

While SPICE 2 is well recognized as a good computer aided design program for electronic components, it has limited capability in representing nonlinear time varying coefficients such as the inductance of the generator model. SCEPTRE allows definition of such elements through functions and FORTRAN function subprograms.

SPICE 2 has the capability of defining dependent sources as polynomial functions of current variables, thus, some nonlinearities can be represented. Possibly the time varying nonlinear generator inductances could be represented in SPICE 2 but SCEPTRE is preferred since such manipulation is not required.

Both SPICE 2 and SCEPTRE have implicit integration options for "stiff" differential equations. Both have variable step size with some external control through error limit specifications. Also, both have the capability of storing electronic component models.

In SPICE 2 the system elements are supplied to the program and the program integrates the elements into a system using a nodal formulation. In SCEPTRE the system elements are supplied to the program in much the same format as for the SPICE 2 program. SCEPTRE then integrates the elements into a system by formulating state equations. It is well known that the nodal formulation is generally more efficient.

The overriding features that resulted in the selection of SCEPTRE over SPICE 2 was the limited capability of SPICE 2 in representing nonlinear elements. Both generator and transformer model components not only have nonlinear elements but these elements are subject to saturation effects. SCEPTRE's ability to define elements in more general terms and to use FORTRAN function subprograms for further flexibility were necessary in the generator and transformer model.

## SECTION VIII

### GENERATOR AND TRANSFORMER SIMULATION RESULTS

#### 8.1 INTRODUCTION

Appendix D lists the SCEPTRE program models for the generator and the transformers. Appendix C lists the data used in test and simulation runs to illustrate the operation of the models. In this section the various test runs which were made are listed and some of the plotted results are given to demonstrate that the models are working properly.

Three generator models are included in the general model listed in Appendix D. The appropriate model is selected by assigning appropriate parameters in the SCEPTRE program.

First, the generator model without variation of the inductance due to saturation (the unsaturated model) is obtained by setting terms of the form of  $A_a$  equal to zero and terms of the form of  $C_{aa}$ ,  $C_{aF}$ ,  $C_{aD}$  and  $C_{aQ}$  equal to unity. Secondly, the  $A_a$  type terms are set equal to zero and the  $C_{aa}$ ,  $C_{aF}$ ,  $C_{aD}$  and  $C_{aQ}$  terms are computed by a subroutine for the "partially saturated" case.

The third model is obtained when the  $A_a$  type terms are included. Note that this includes the  $\frac{\partial L}{\partial i}$  effects.

The transformer model also listed in Appendix D is for a wye-wye connection. The delta-wye connection can be simulated by the proper listing of circuit elements in the SCEPTRE program. No data were available to represent a particular transformer or to include the effects of saturation and coupling between phases. However, with proper data entered, the subroutine FINDI computes altered inductance coefficients as effected by saturation.

## 8.2 THE SIMULATION RUNS

Computer simulation runs were made on the generator alone, on the transformer alone and on the combination of the transformer and generator. These runs were made after all test runs assured all programs and models were working properly. The results of all these runs are on file but only selected results are presented here. The simulations runs are

- I.       Unsaturated Generator Model
  1.   determine steady state initial conditions
  2.   apply a symmetric three phase short circuit
  3.   apply an unsymmetric three phase short circuit.
- II.      Partially Saturated Model
  1.   determine steady state initial conditions
  2.   apply a symmetric three phase short circuit
  3.   apply an unsymmetric three phase short circuit. Three runs were made. A run was made as each of the phases were shorted to neutral separately.
- III.     Fully Saturated Model
  1.   determine steady state initial conditions
  2.   apply a symmetrical short circuit.
- IV.      The Transformer Model (linear)
  1.   balanced three phase operation.
- V.       The Transformer Model (interphase coupling and saturation)

Note: no valid saturation or coupling data were supplied.
- VI.      The Partially Saturated Generator and the Transformer Combined Model
  1.   steady state load run.

### 8.3 RESULTS

The first three figures of this section Figures 26, 27 and 28 are the phase A current, the direct axis damper current and the rotor speed. These are for balanced steady state operation of the linear model. Since the computer model is different from the steady state phasor diagram model of the generator, a preliminary computer run is necessary to determine appropriate initial conditions for the various state variables. These runs were made and initial conditions used in runs for the above mentioned figure. The results show that correct initial conditions were used since phase A current is immediately in steady state, the speed is constant and the direct axis damper current is essentially zero.

Figures 29, 30 and 31 illustrate that previous runs have determined appropriate initial conditions for the partially saturated model. For constant load steady state runs the phase A current is immediately in steady state, the speed is constant and the direct axis damper current is essentially zero.

The next five figures illustrate the operation of the generator and model with a symmetrical three phase short circuit applied when the generator is supplying 80% load. The generator is operated at steady state for three cycles, the short is applied for three cycles then the fault is removed and the load resistor restored to the pre fault value. The results include Phase A current, the main field current the direct axis damper current, the quadrature axis damper current and the speed during the above defined sequence of events.

The results are classical, indicating that the model and program are working properly. Data were not supplied by the Air Force for a particular machine operating under conditions that would have tested the details of the model.

Computer simulation runs were made with single phase short circuit on each phase. Some of the results for a line to ground fault on phase A are included here to verify the operation of the model under severe unbalanced conditions.

The computer simulation runs were made for 10 cycles of a 60 Hz frequency. The longest CPU time was approximately 60 seconds for these ten cycles and the most severe fault.

No results are given for the model which includes the  $A_a$  type terms. For the particular machine saturation data used the sum of all of these terms per phase was of the order of magnitude of 60 volts maximum compared with 15,000 volts rating. SCEPTRE step size routine had trouble finding an appropriate step size with this term included and long runs were encountered. A different machine with more severe saturation problems may need these  $A_a$  terms.

AD-A123 730

DYNAMIC SIMULATION OF AIRBORNE HIGH POWER SYSTEMS(U)  
CLEMSON UNIV SC DEPT OF ELECTRICAL AND COMPUTER  
ENGINEERING R W GILCHRIST ET AL NOV 82

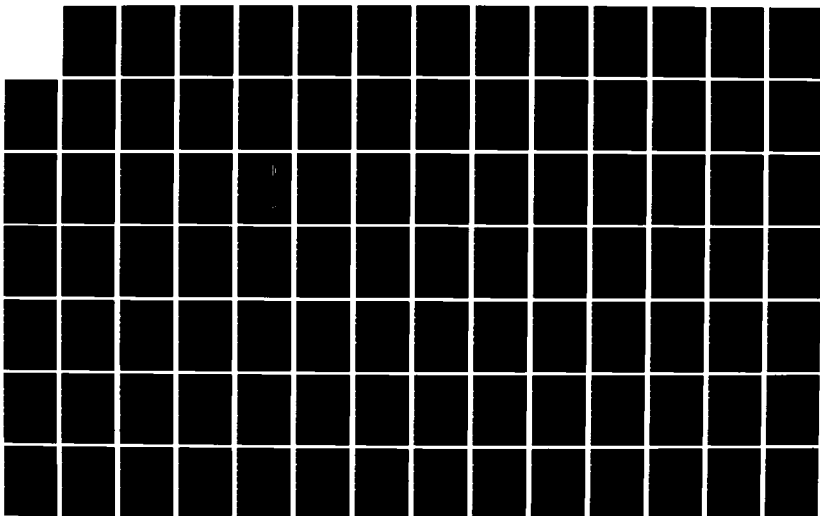
2/3

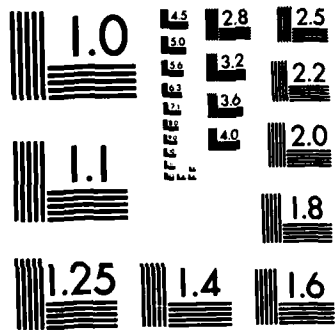
UNCLASSIFIED

AFWAL-TR-82-2092 F33615-79-C-2047

F/G 10/2

NL





MICROCOPY RESOLUTION TEST CHART  
NATIONAL BUREAU OF STANDARDS-1963-A

IL11

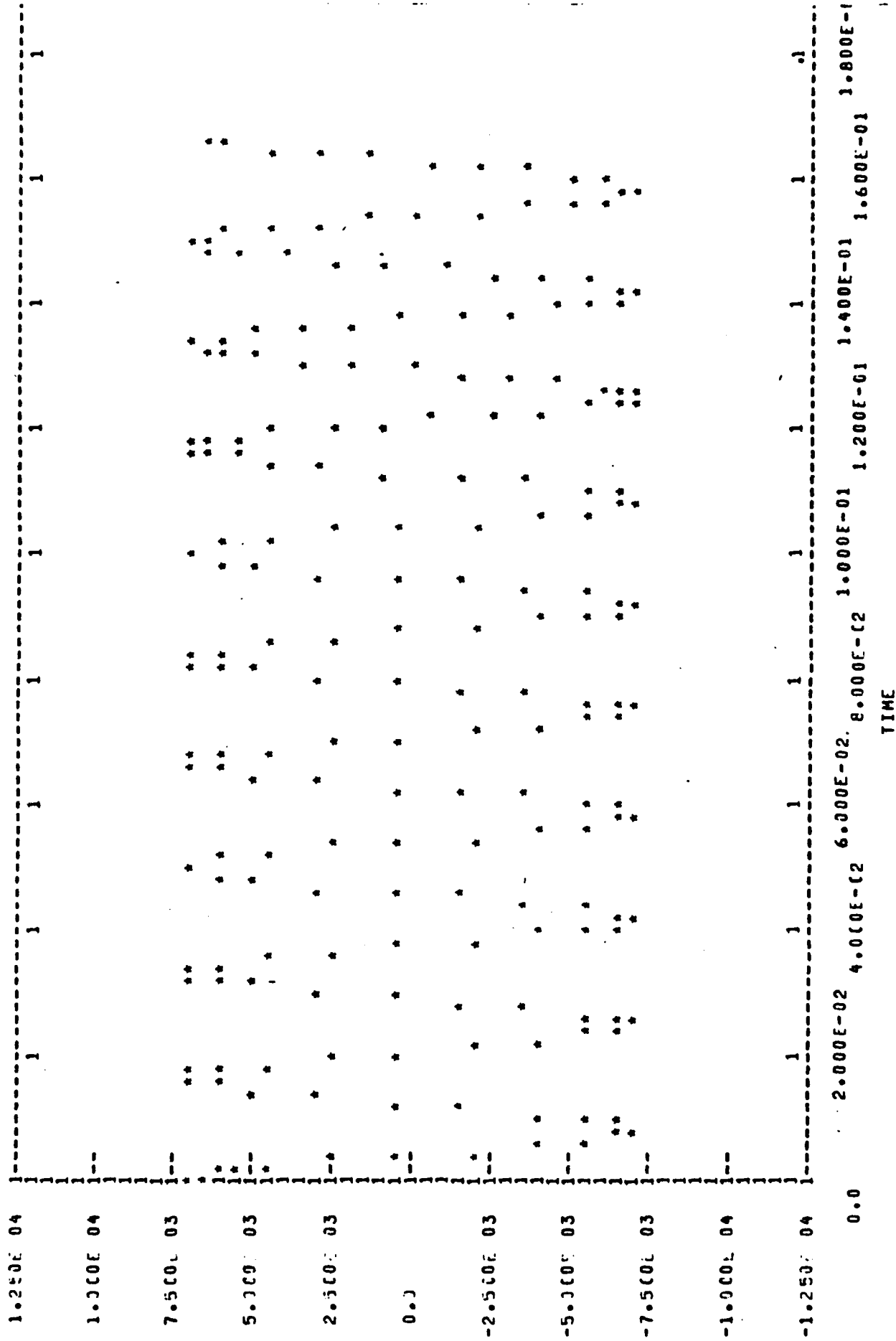


FIGURE 26. PHASE A LINE CURRENT LINEAR MODEL STEADY STATE

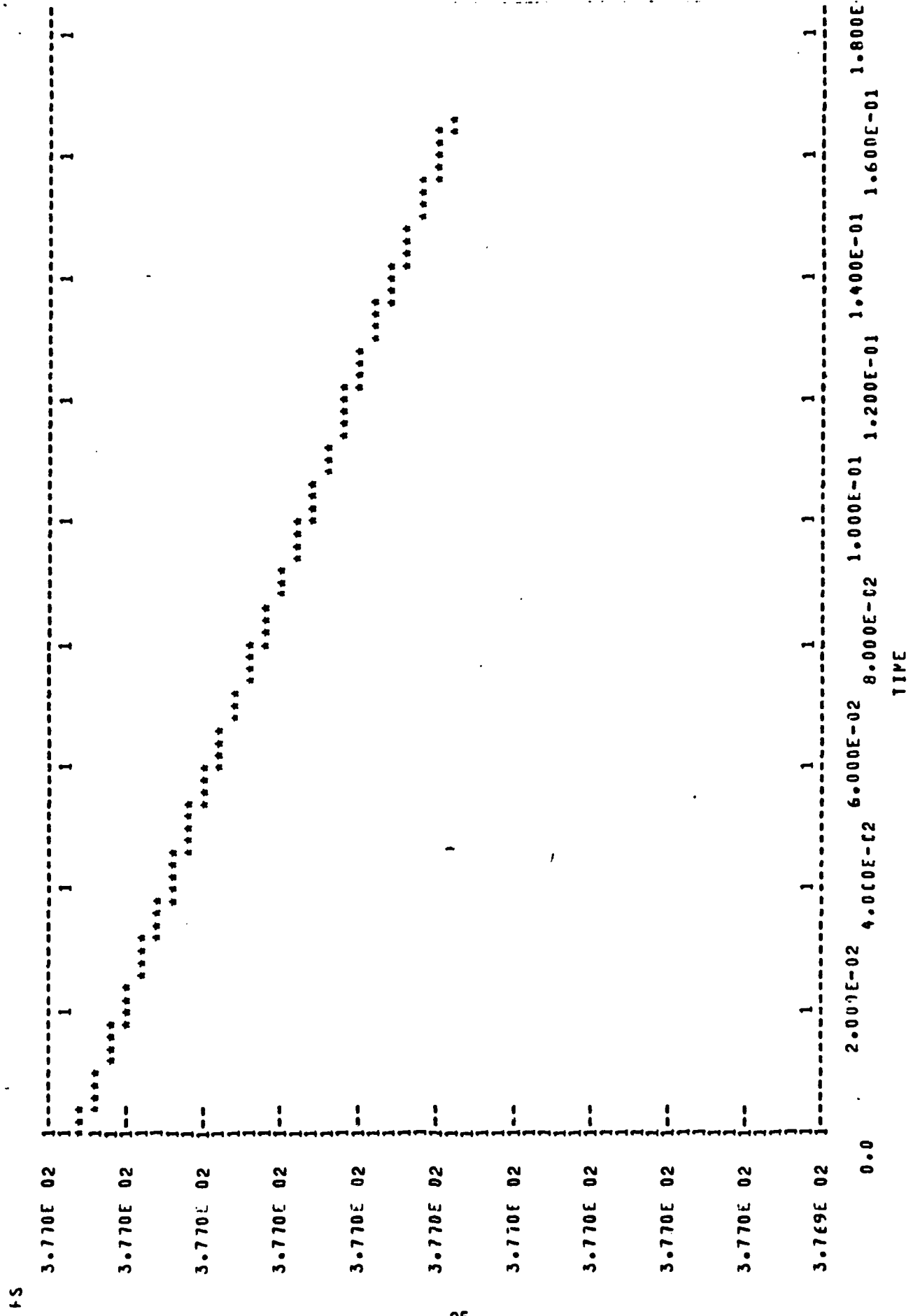


FIGURE 27. SPEED VS TIME LINEAR MODEL STEADY STATE

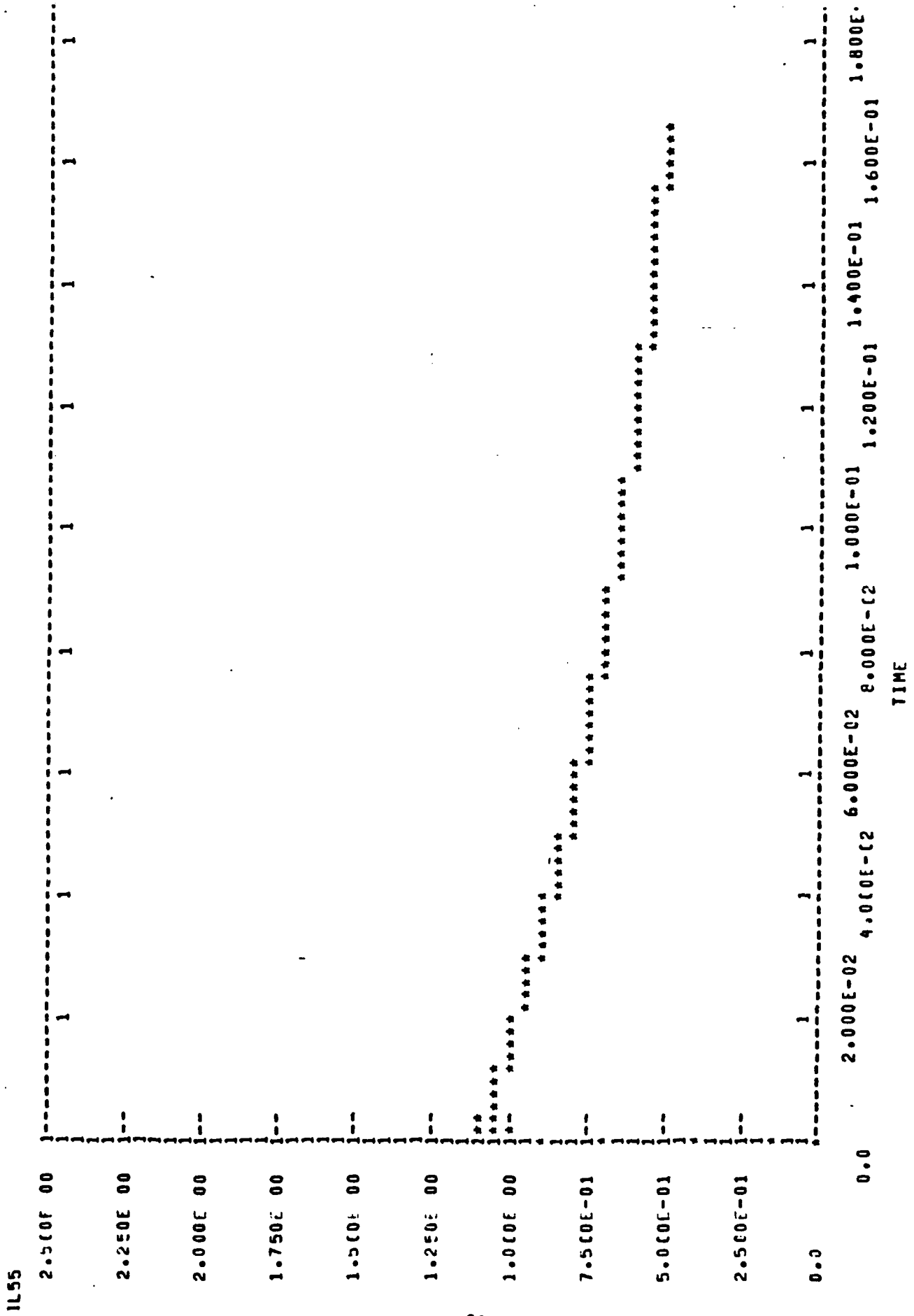


FIGURE 28. DIRECT AXIS DAMPER CURRENT LINEAR MODEL STEADY STATE

IL11

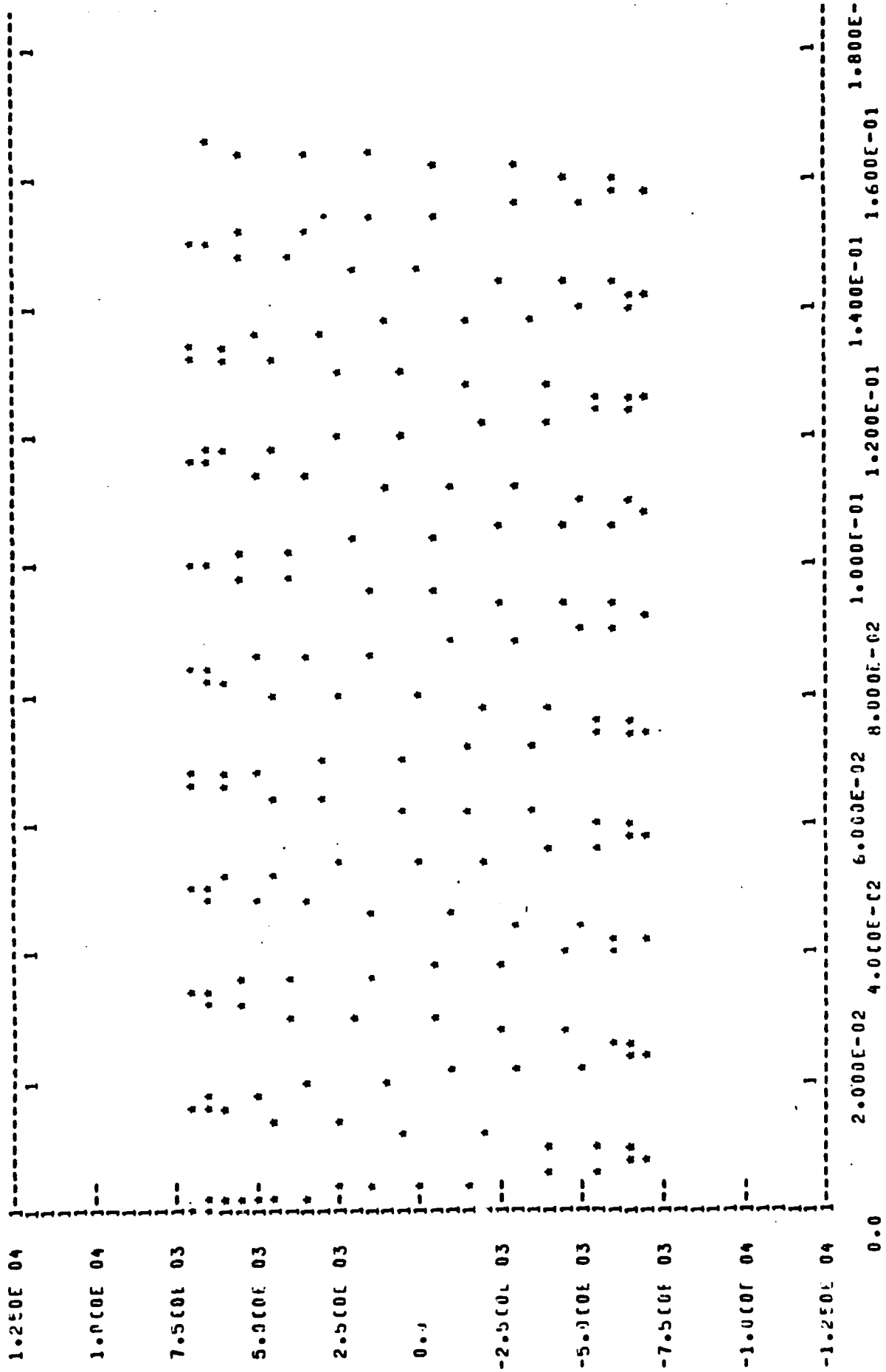


FIGURE 29. PHASE A LINE CURRENT PARTIALLY SATURATED MODEL STEADY STATE





IL11

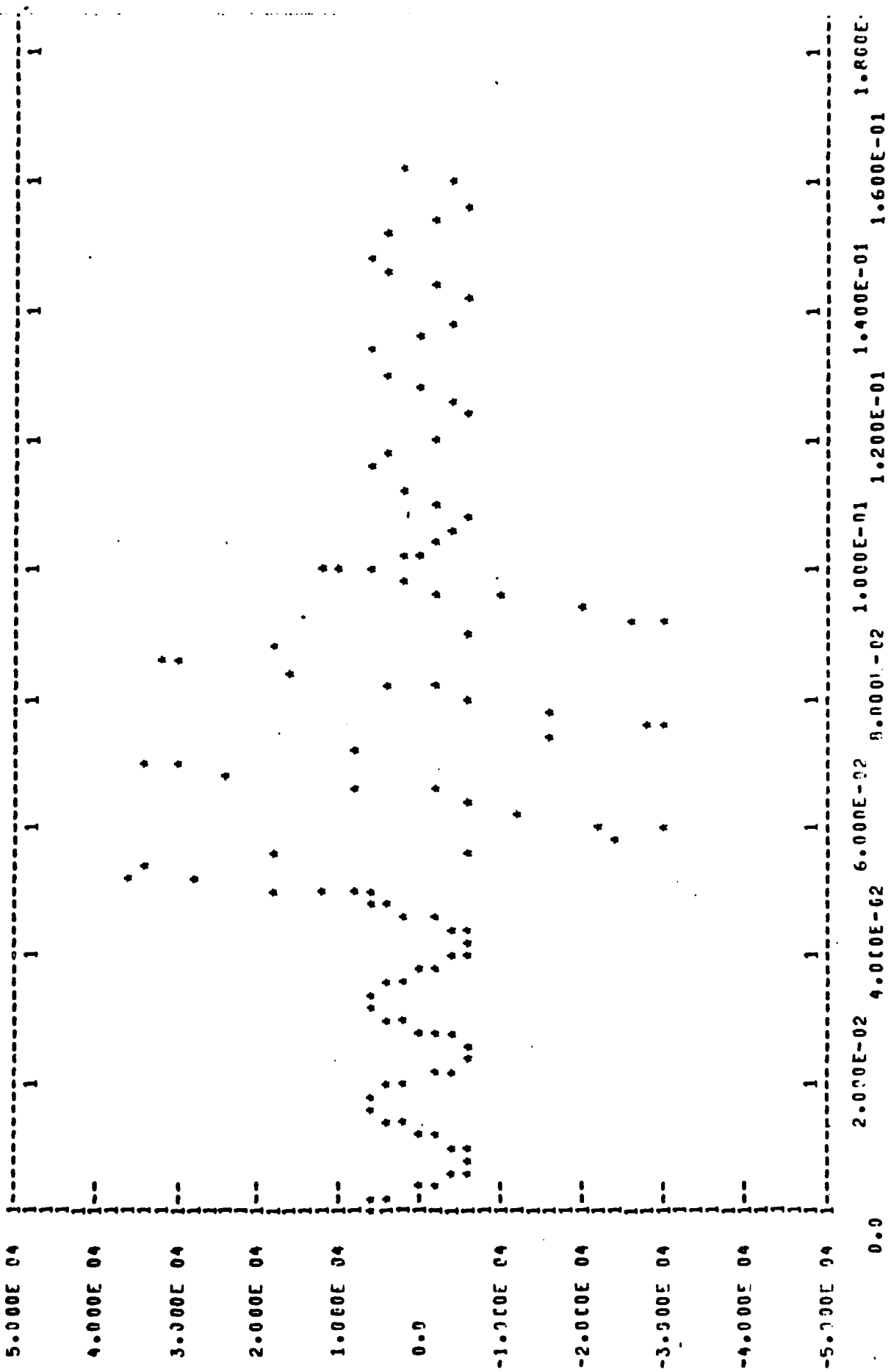


FIGURE 32. PHASE A CURRENT SYMMETRICAL SHORT CIRCUIT PARTIALLY SATURATED MODEL

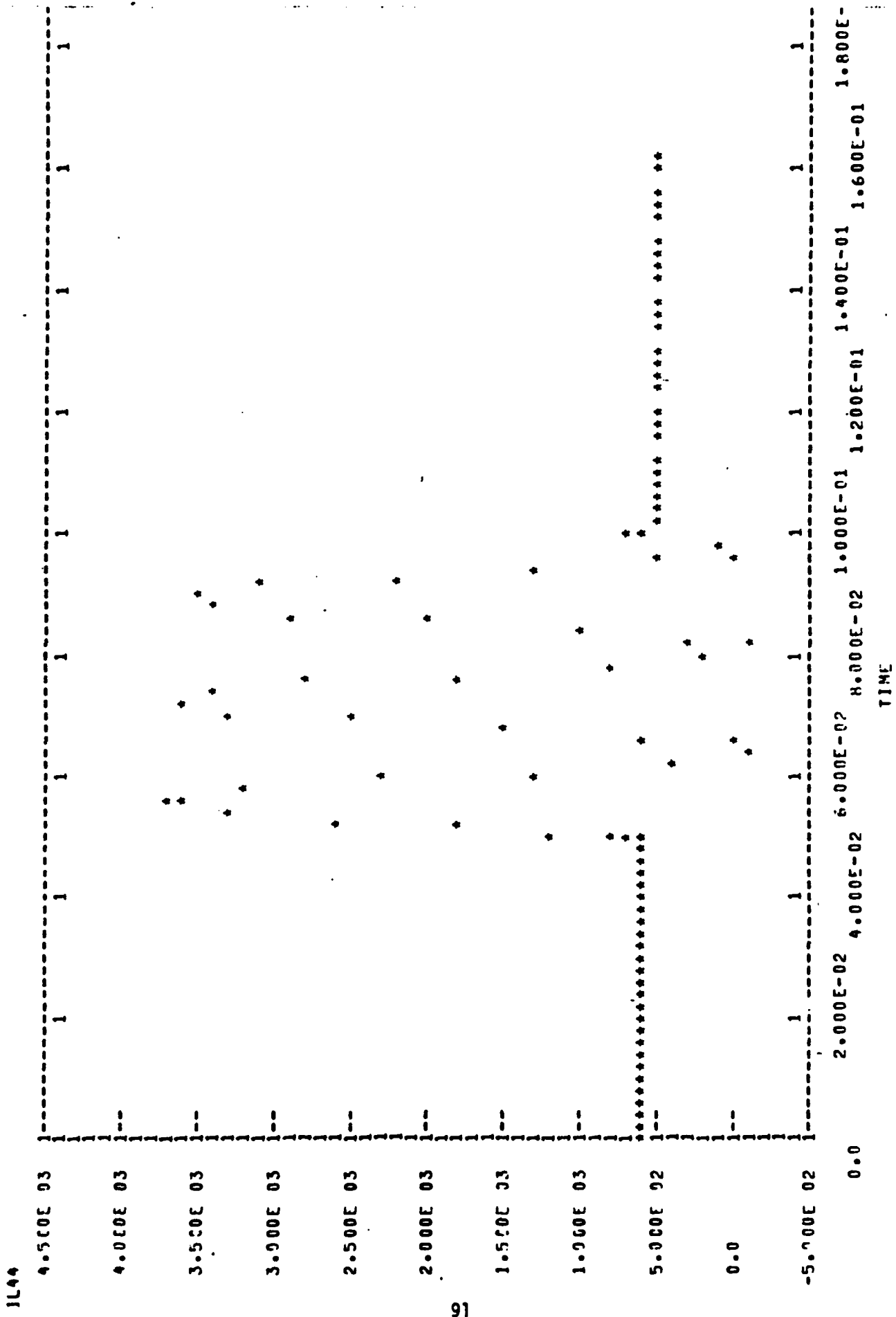


FIGURE 33. FIELD CURRENT SYMMETRICAL SHORT CIRCUIT PARTIALLY SATURATED MODEL

1L55

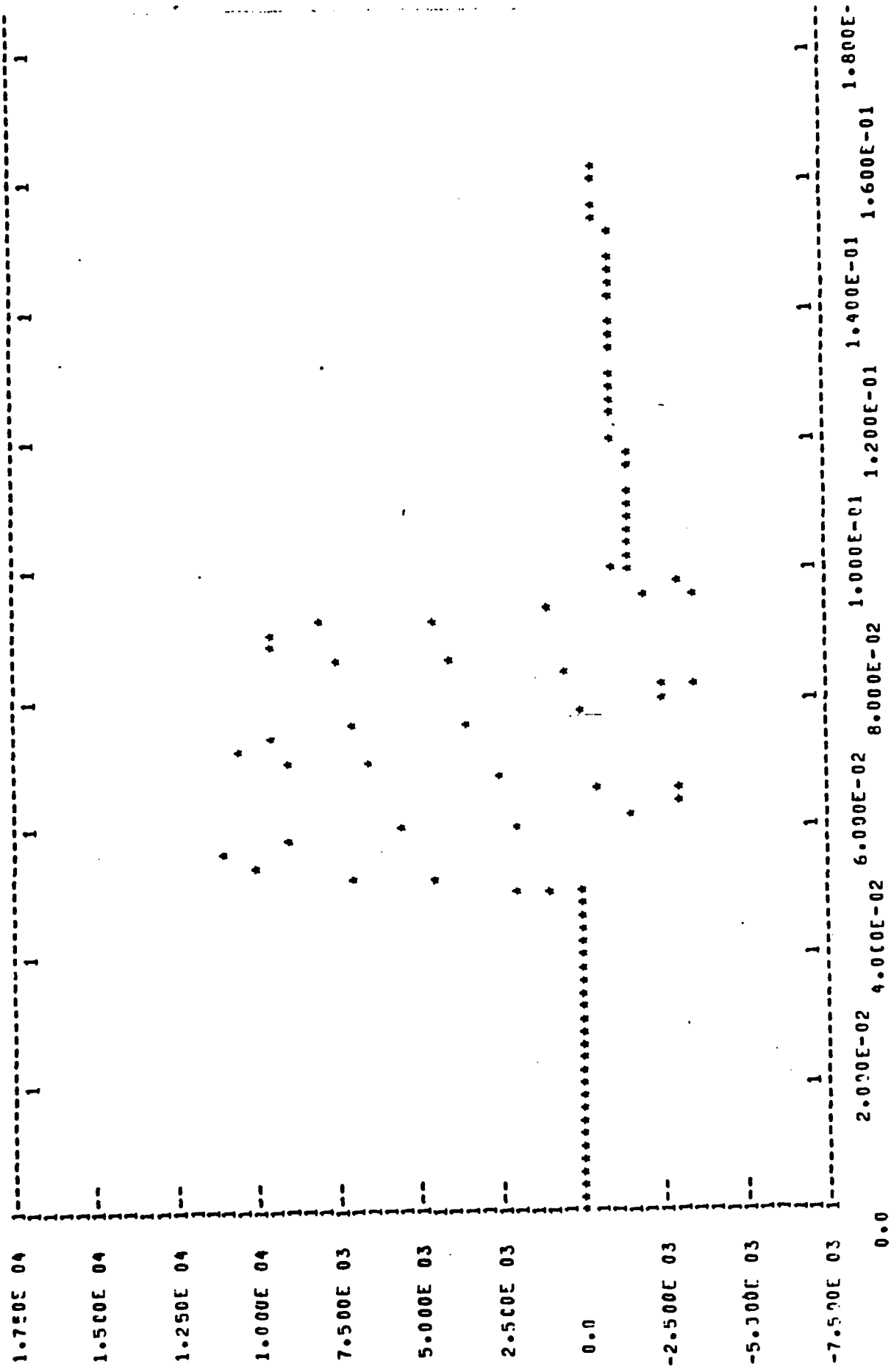


FIGURE 34. DIRECT AXIS DAMPER CURRENT SYMMETRICAL SHORT CIRCUIT PARTIALLY SATURATED MODEL

IL66

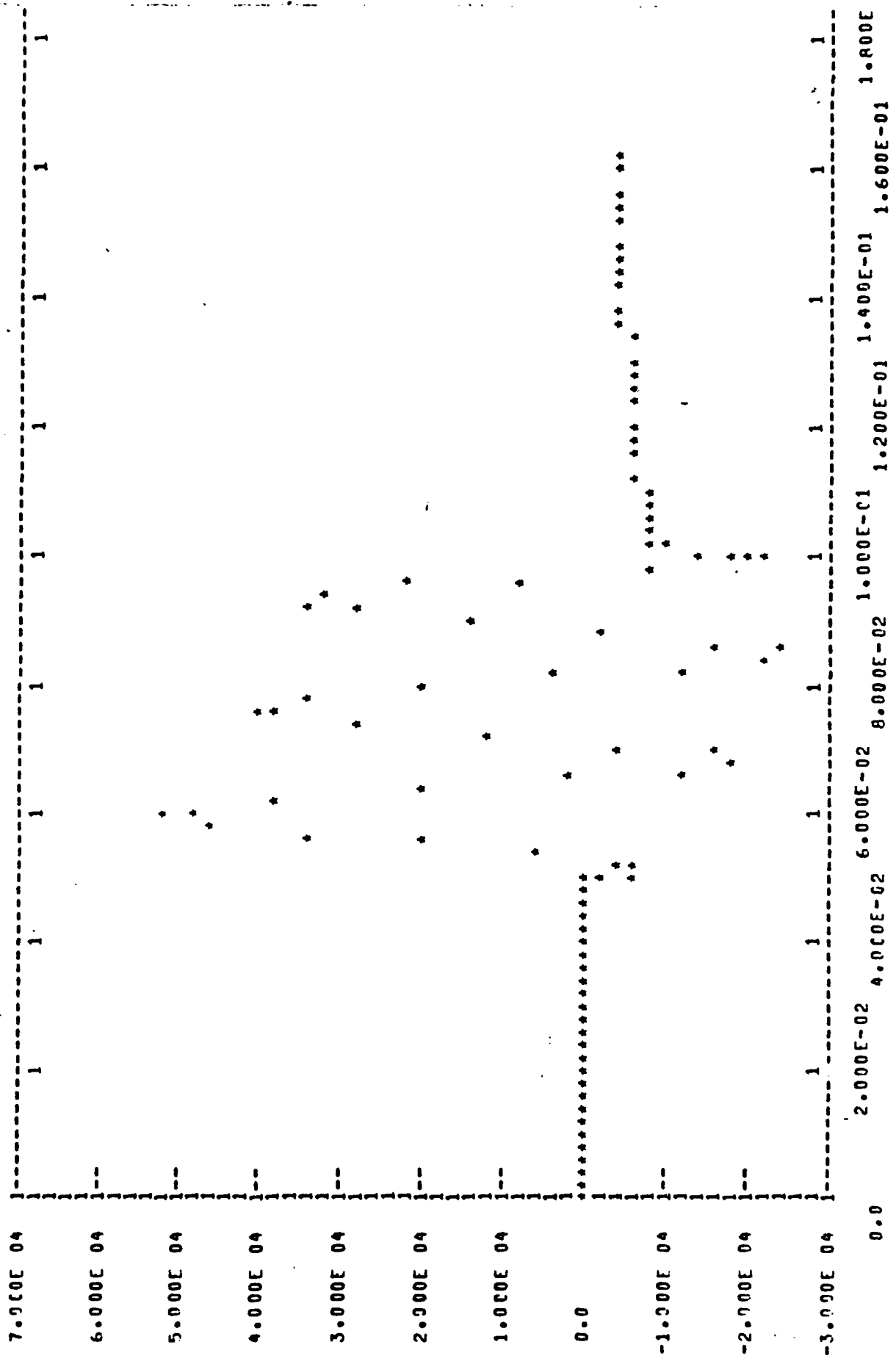


FIGURE 35. QUADRATURE AXIS DAMPER CURRENT SYMMETRICAL SHORT CIRCUIT PARTIALLY SATURATED MODEL



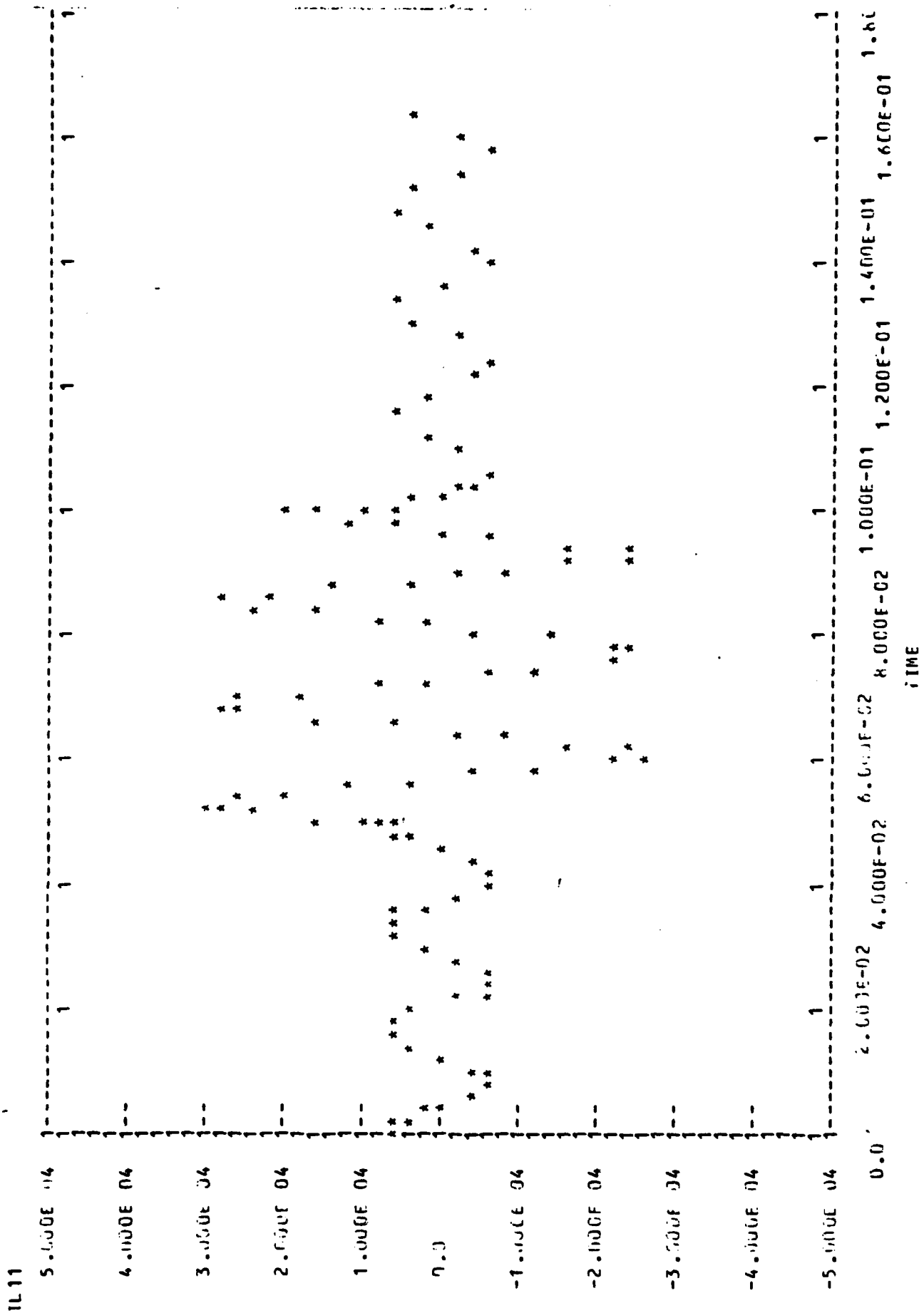


FIGURE 37. PHASE A CURRENT PHASE A SHORTED PARTIALLY SATURATED MODEL

IL44

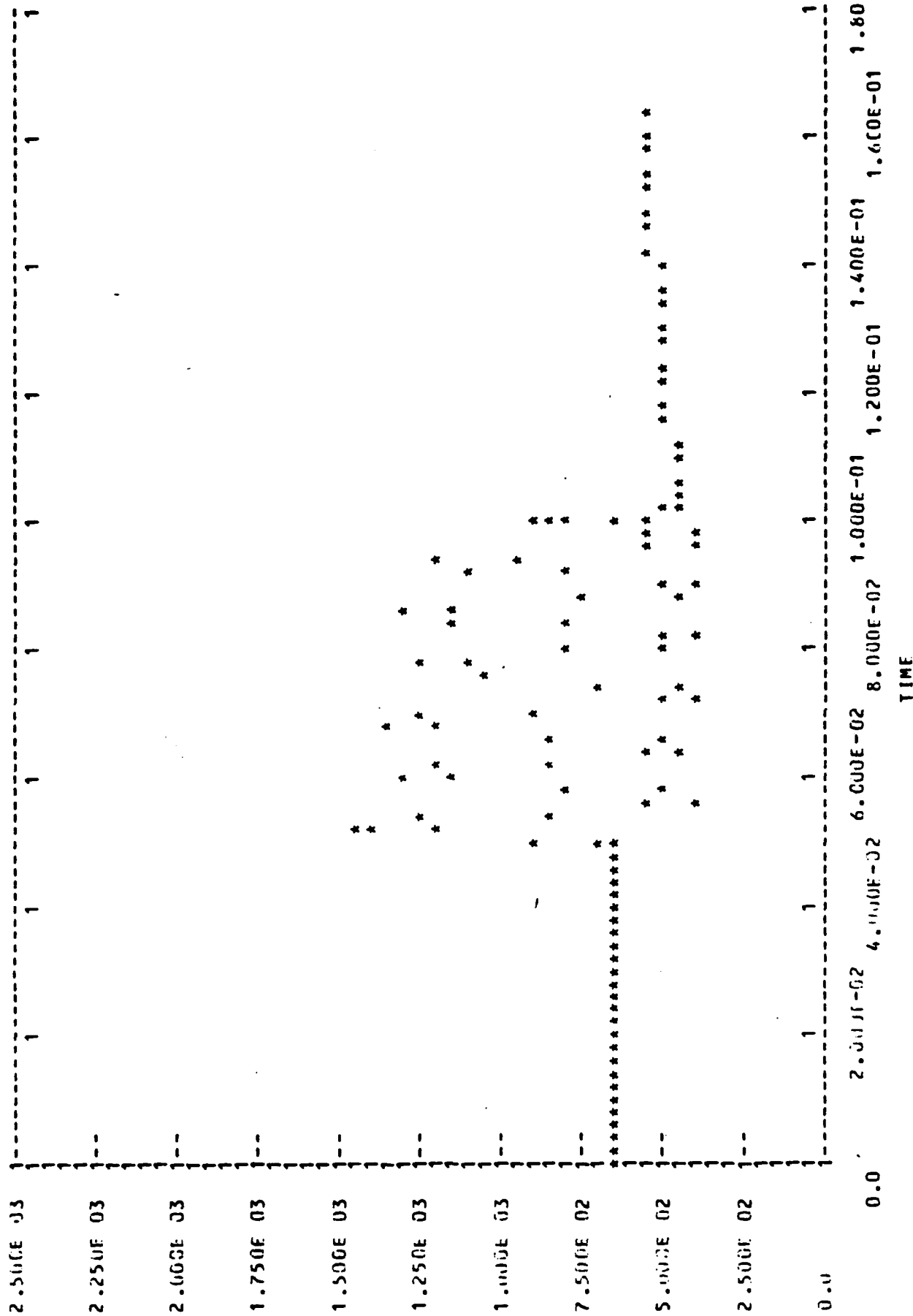


FIGURE 38. FIELD CURRENT PHASE A SHORTED PARTIALLY SATURATED MODEL

IL55

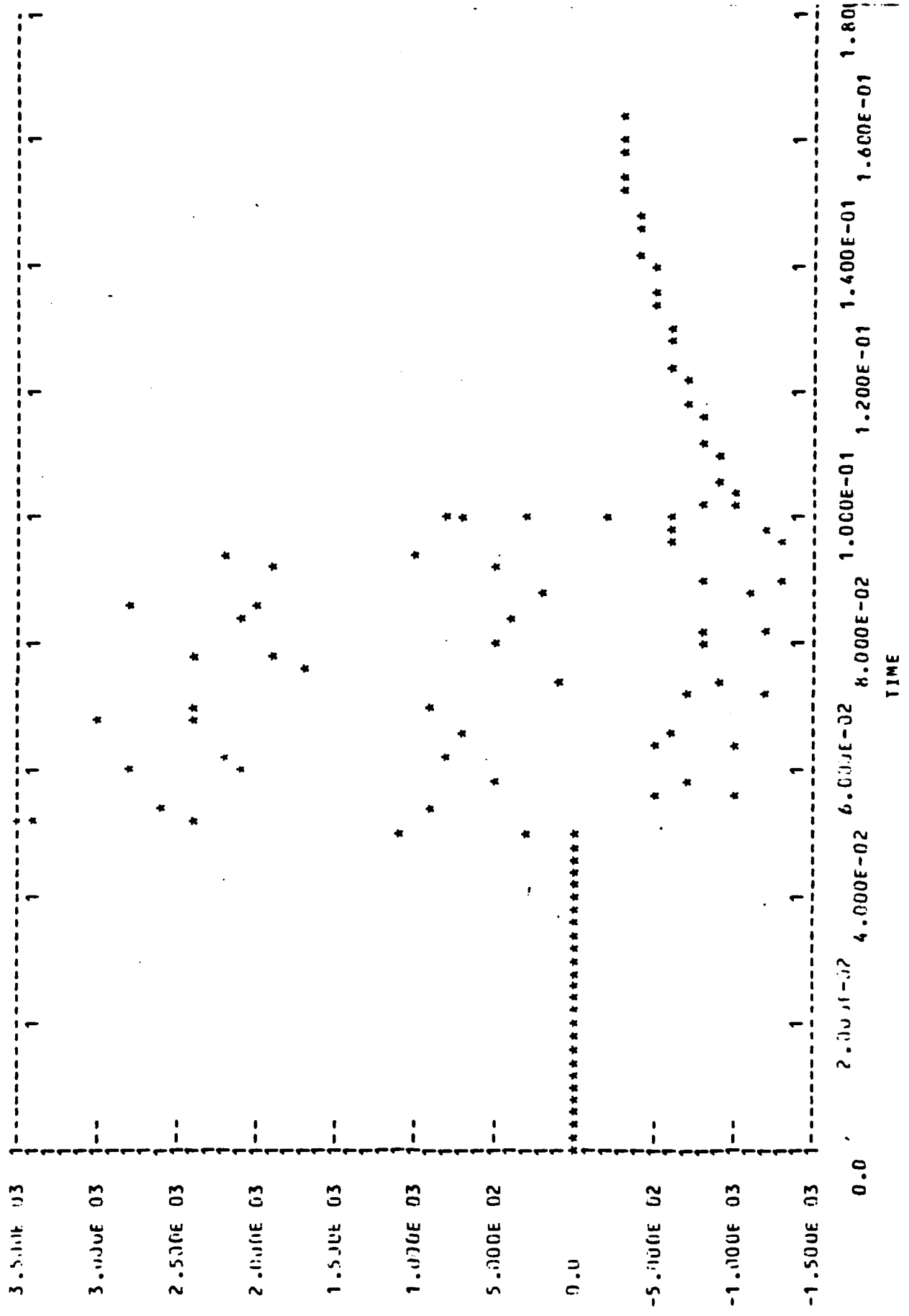


FIGURE 39. DIRECT AXIS DAMPER CURRENT PHASE A SHORTED PARTIALLY SATURATED MODEL

1L66

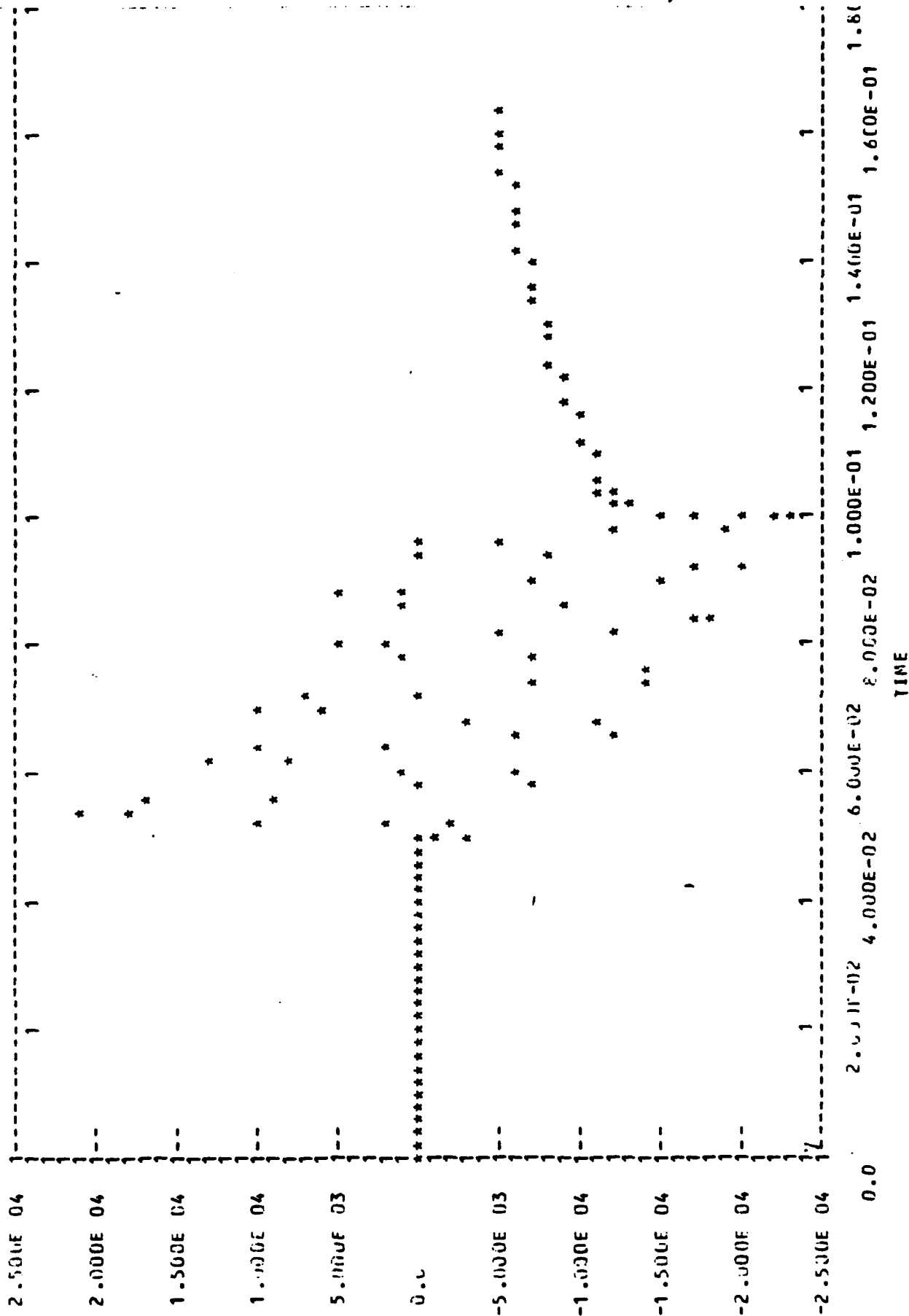


FIGURE 40. QUADRATURE AXIS DAMPER CURRENT PHASE A SHORTED PARTIALLY SATURATED MODEL



The transformer simulation results are illustrated by Figures 42, 43 and 44. These curves give the secondary current of phase A,  $IL_{11}$ , the primary current of phase A,  $IL_{22}$ , and the magnetizing current of phase A, due to  $IL_{11}$  and  $IL_{22}$ , PIX.

The simulation was for wye-wye connection of three single phase transformers. The data used was not for any specific transformer but does represent transformers with high leakage reactances.

A reordering of the circuit elements in SCEPTRE readily models the delta-wye transformer connection.

Saturation and coupling between phases of the delta-wye connected, three leg core, three phase transformer can be accounted for by supplying the appropriate transformer data to the subroutine FINDI. These data were to be supplied by the Air Force but no valid data were available at the end of the contract time.

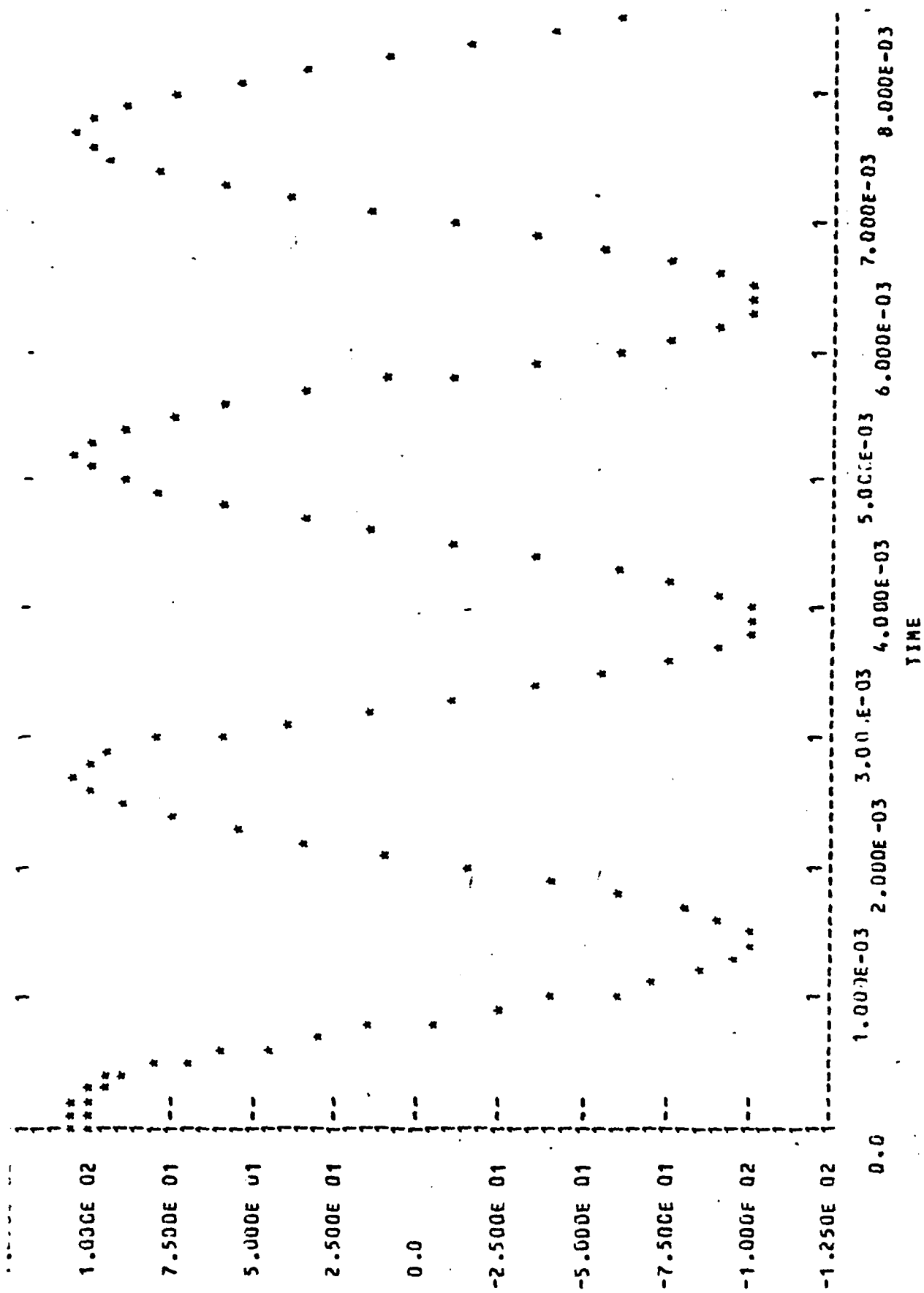


FIGURE 42. PHASE A PRIMARY CURRENT IL<sub>22</sub>

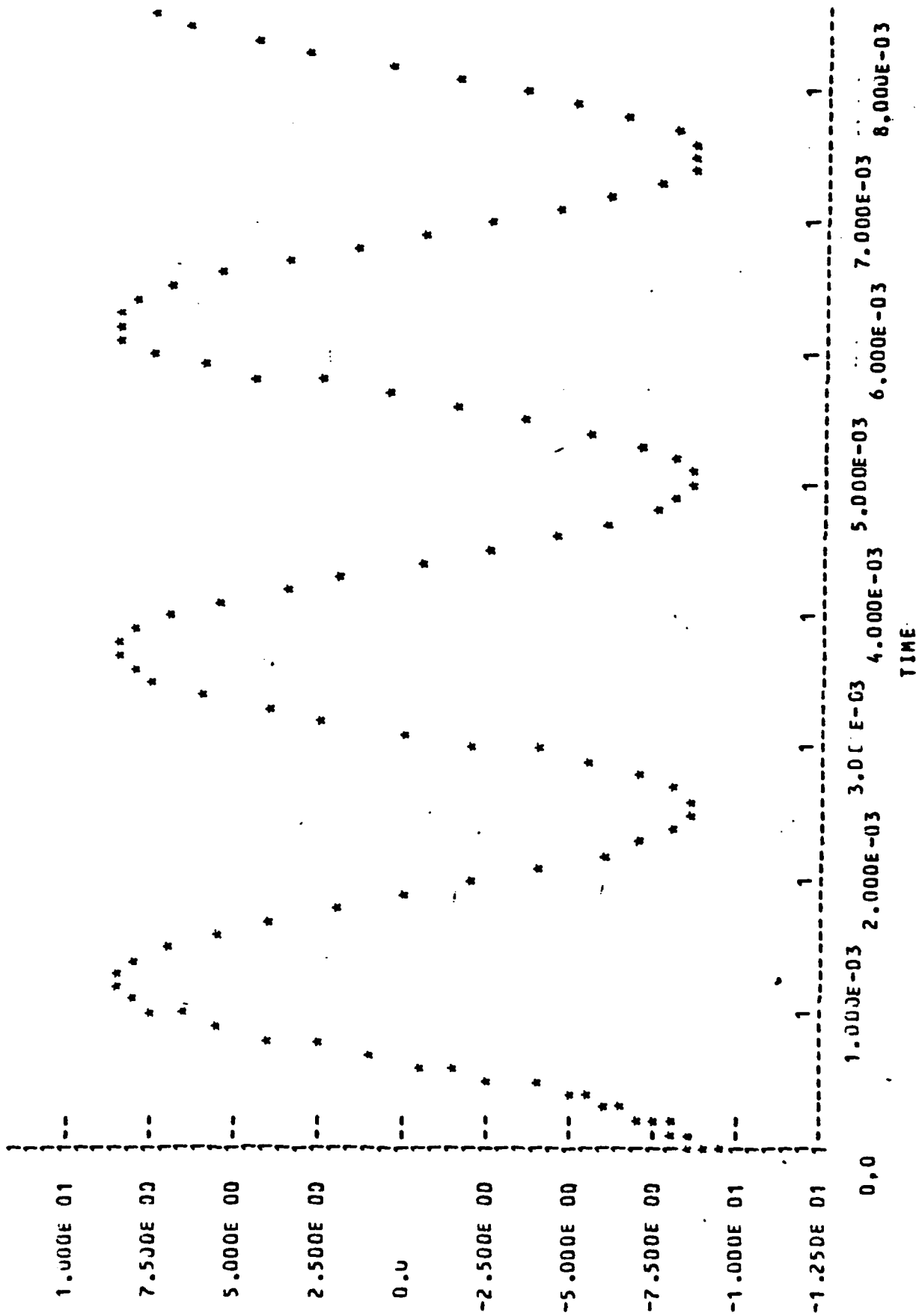


FIGURE 43. PHASE A SECONDARY CURRENT IL<sub>1</sub>

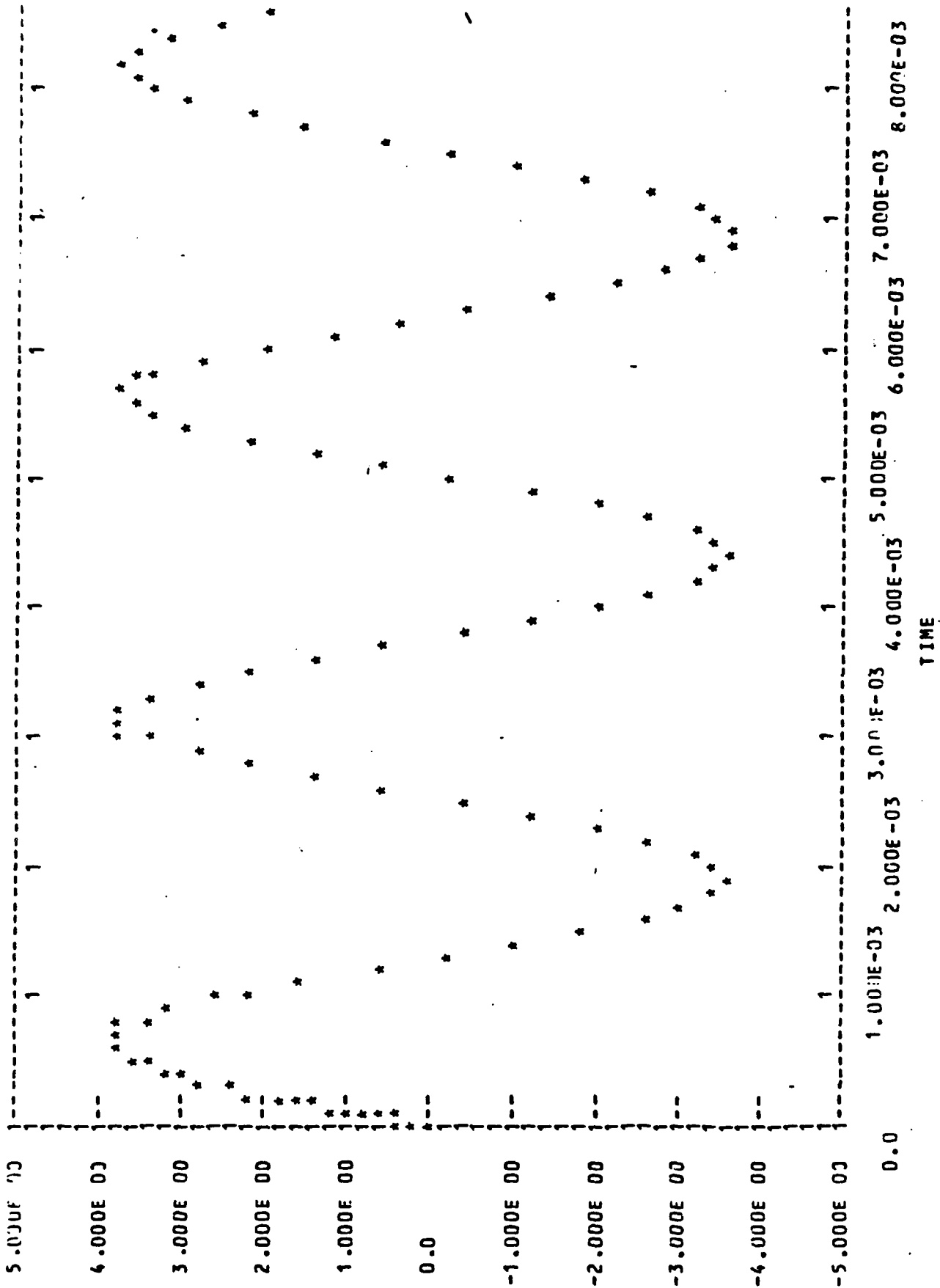


FIGURE 44. PHASE A MAGNETIZING CURRENT PIX

## SECTION IX

### AC AND DC CHARGING CIRCUIT SIMULATION RESULTS

#### 9.1 INTRODUCTION

Two types of simulations were conducted. Simulations were conducted using SPICE 2 to test the "Modified Hu-Ki Model" in various circuit configurations that may be encountered in ac and dc resonant charging applications. Next the SCEPTRE model of the SCR was used in SCEPTRE programs simulating ac and dc resonant charging.

The SPICE 2 simulations runs included: (all using "modified Hu-Ki Model").

1. Single Loop AC Resonant Charging.
  - a. Without snubber.
  - b. With snubber.
2. Resonant Charging on Both Positive and Negative Half Loops.
  - a. Without snubber.
  - b. With snubber.
3. Single Loop Resonant Charging With Two Parallel SCR's.
  - a. Without balancing resistors.
  - b. With balancing resistors.
4. Single Loop Resonant Charging With Two Series SCR's.
  - a. With balancing resistors.

The SCEPTRE simulation runs using the "Reduced 3-Junction Model" included:

1. Single Phase Single Loop With 3 SCR's and a Diode in Series For 6465.85 Volts at 400 Hertz.
2. Three Phase AC Resonant Charging Scaled to 1000 Volts and 1000 Hertz.

### 3. DC Resonant Charging Scaled to 1000 Volts and 1000 Hertz on the Three Phase AC Side.

#### 9.2 SPICE 2 SINGLE LOOP SIMULATION

Section 4.3 presented the results of a simulation of an AC Resonant Charging Circuit using the unmodified "Hu-Ki Model" Figure 10. A comparative example is given in Figure 46 which illustrates the results of simulating the circuit of Figure 45 using the "Modified Hu-Ki Model" developed in SECTION IV. Striking improvement is noted in the turn-off simulation results during the period following start of SCR commutation at approximately 500  $\mu$ s.

The circuit of Figure 47 (corresponding results are in Figure 48) has a snubber added to demonstrate a means of suppressing the damped oscillatory behavior following SCR commutation.

#### 9.3 SPICE 2 SIMULATION OF A TWO LOOP AC RESONANT CHARGING CIRCUIT

A two loop AC Resonant Charging Circuit is shown in Figure 49. The results of simulating this circuit without snubbers is shown in Figure 51. As was indicated in Section 9.2, the oscillatory behavior of the SCR turn-off transient in an inductive circuit can cause undesirable operation of some circuits. The two loop circuit is such a circuit. The second branch SCR is programmed (Figure 50) to receive a gate trigger pulse from IG1 at 600  $\mu$ s. SCR 2 begins conduction at 505  $\mu$ s (95  $\mu$ s prematurely). This occurs because the  $J_1$  junction of SCR1 is supporting a rapidly rising reverse voltage which is seen by SCR 2 as a rapidly rising forward voltage and therefore causes a  $dv/dt$  turn-on of SCR 2.

The problem is corrected by adding snubber circuits. The desired operation is then obtained as is illustrated in Figure 53.

GL C602 LM SLC - ONE BRANCH AC RES CHG'NG CKT - DESCNTE - NO SNUBBER

TEMPERATURE = 27.000 DEG C

INPUT LISTING

```

*****
V2 1 0 SIMIO 500 1K 1
VZERO 2 4 SINIC U 01
IG1 7 5 PULSEIC .5 100US U U 10US 1
LXFMR 1 2 5MH
RCKT 2 3 5.O
U1 5 6 4 QMOD1 OFF
U4 6 5 7 QMOD2 OFF
DFUN 3 6 QMOD1 OFF
DJLIM 5 7 QMOD2
KSMI 1 5 7 4.375
CUI 7 0 5.CUF
.MODEL LMCO1 U1BV=760.1S=5.20E-15)
.MODEL DMOD2 U1EV=5.1S=1.0E-16)
.MODEL QMOD1 MPPIBF=5.0PK=9.1S=1.0E-10.05 PLEZ.(C5,1F=17.0US,TR=112>US,CJE=400GPF)
.MODEL QMOD2 MPPIBF=5.1S=1.0E-16.05,CJC=400GPF)
.TKAN >US 100US
.PRINT IKAN I(VZERU) V(7,0) V(1,6) V(5,6) V(5,7)
.PLOT IKAN I(VZERU) V(7,0) V(1,6)
*PULUNS NUMOD NUPAGE LVLTIM=1 ITLS=10000 LIMPTS=10000
*END

```

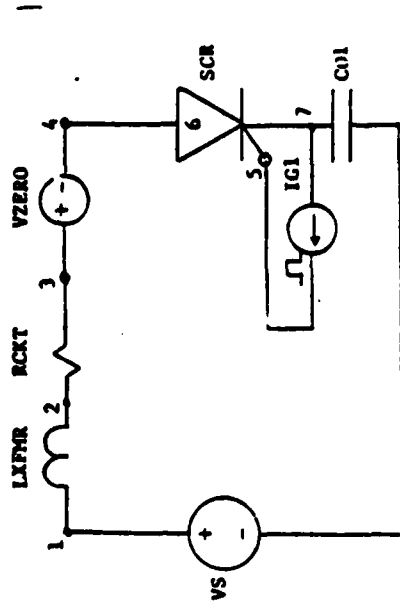


FIGURE 45. SINGLE LOOP CIRCUIT WITHOUT SNUBBER

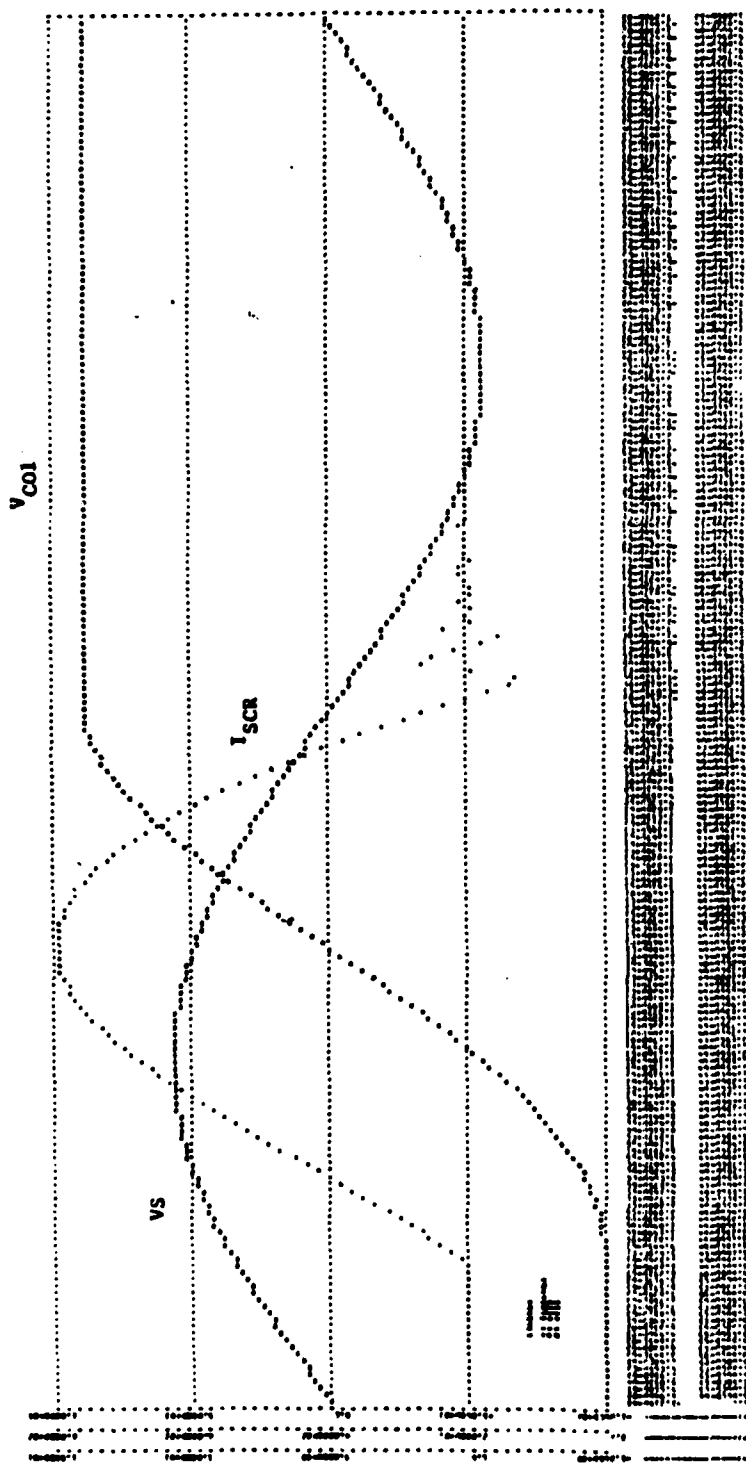


FIGURE 46. SPICE 2 SIMULATION OF A SINGLE LOOP AC RESONANT CHARGING CIRCUIT (FIG. 45) USING THE "MODIFIED HU-KI MODEL" OF A SCR.

UC 602 LM SCR - LINE BRANCH AL RES CHONG CNT - DESKRETE - WITH SNUBBER

TEMPERATURE = 27.000 DEG C

INPUT LISTING

```

V2 1 0 5 INIO 500 IK 1
VZRO 3 4 SINIC 0 C 1
Y2 7 3 PULSE 1.0 100US 0 0 5US 1
LXPMR 1 2 500
RCKT 2 3 5 C
Y1 2 6 5 UM001 OFF
Y2 6 5 7 CM002 OFF
Y3 5 6 0 UM001 OFF
Y4 5 7 0 JUF
Y5 5 7 1 CC
Y6 5 7 0 UM001 OFF
Y7 5 7 4.375
L 1 1 2 50F
MODEL UM001 LIB=2700 IS=5 SEE=15)
MODEL CM001 PAPE=5 TR=9 IS=1E-16 OS=RE=1000 TF=17.0US TR=1125US (LJE=4000PF)
MODEL CM002 NPATE=5 IS=1E-16 OS=RE=1000 TF=4000PF)
TRAN 5US 1000US
.PRINT TRAN IV(ZLKM) V(I) V(I) V(I)
.PLOT TRAN IV(ZLKM) V(I) V(I)
.OPTIONS NUMD HOPAGE LVLTIM=1 I115=10000 LIMP13=10000
.END

```

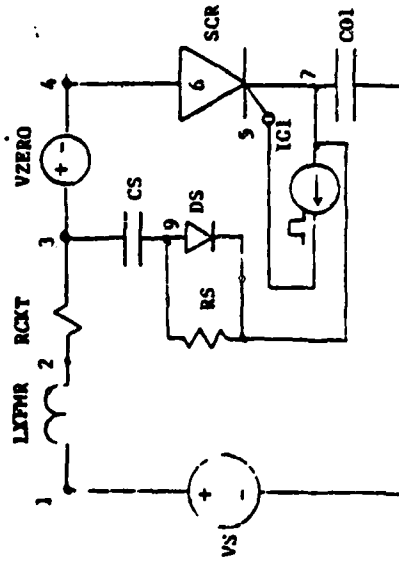


FIGURE 47. SINGLE LOOP CIRCUIT WITH SNUBBER

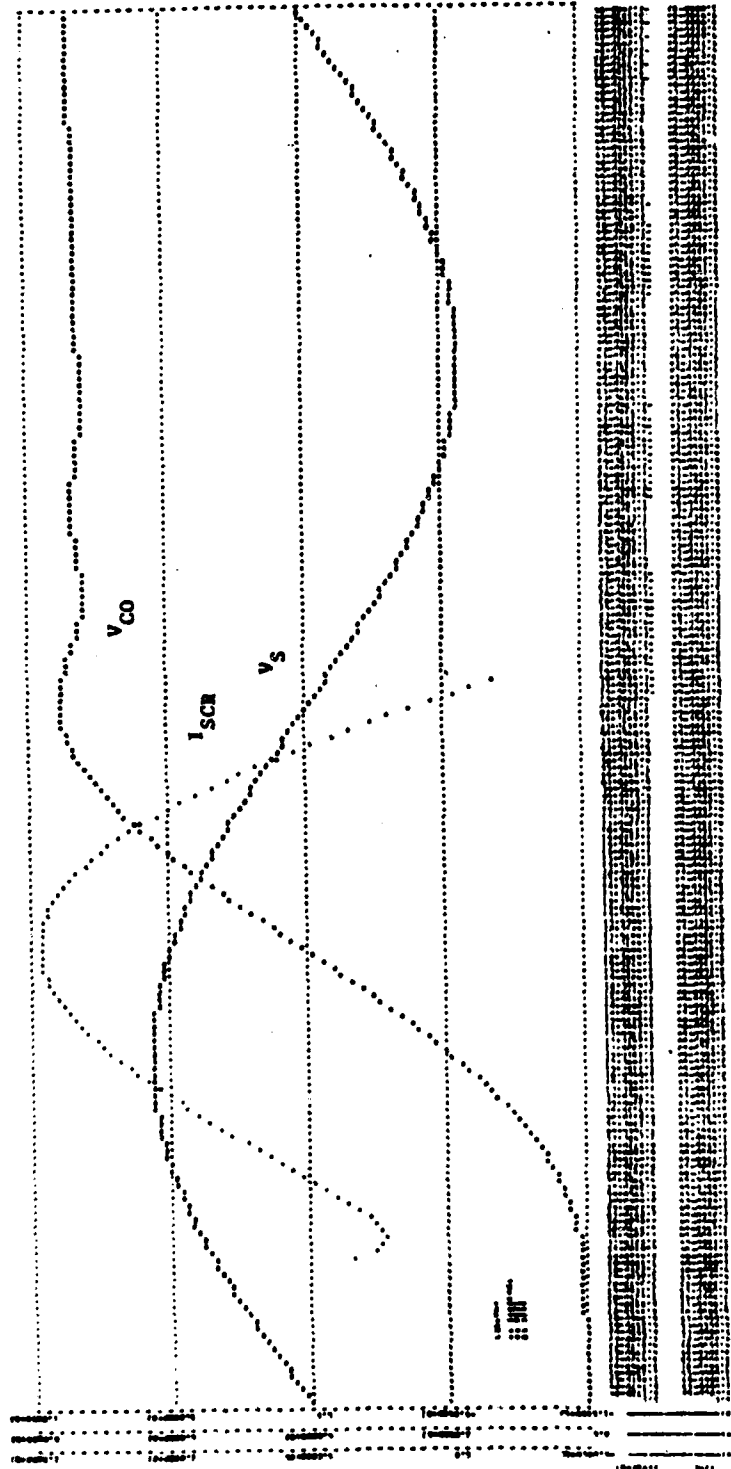
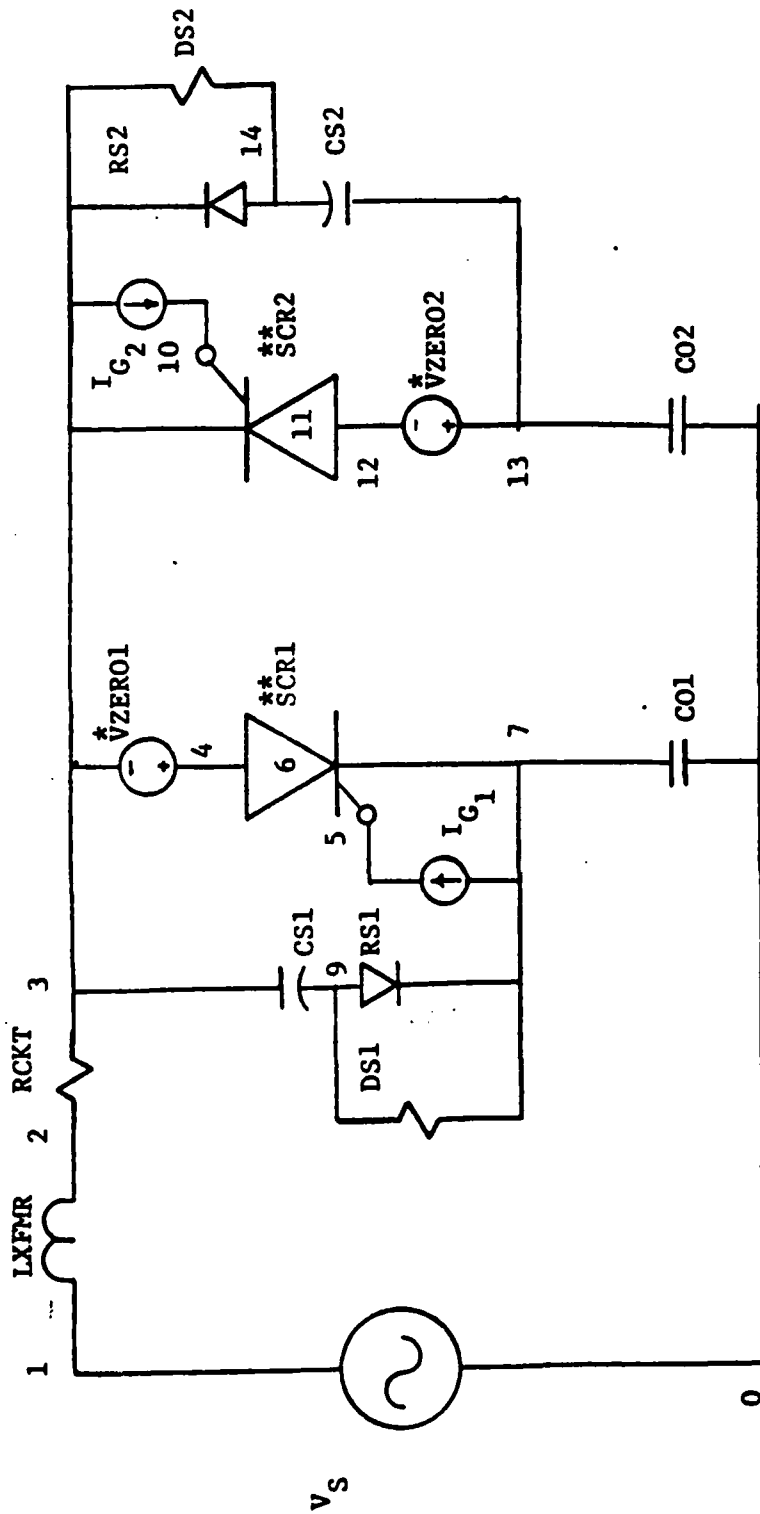


FIGURE 48. SPICE 2 SIMULATION OF SINGLE LOOP AC RESONANT CIRCUIT WITH A SNUBBER (FIG. 47). THE "MODIFIED HU-KI MODEL" WAS USED.



\*\*REF. FIG. 2.5 FOR SPICE2  
SCR MODEL CKT.

\*VZERO - A ZERO VOLTAGE SOURCE  
USED AS CURRENT MONITOR IN  
SPICE2 PROGRAMS.

FIGURE 49. THE SPICE2 CIRCUIT DIAGRAM FOR THE TWO LOOP AC RESONANT CHARGING SYSTEM

GE C602 LM SCR - TWO BRANCH AC RES CHG'NG CKT - DESCRETE - NO SNUBBER

INPUT LISTING TEMPERATURE = 27.000 DEG C

\*\*\*\*\*

```
VS 1 0 SIN(0 566 1K )
IG1 7 5 PULSE(0 1.0 100US 0 0 5US )
IG2 3 10 PULSE(0 1.0 600US 0 0 5US )
VZER01 3 4 SIN(0 0 0 )
VZER02 13 12 SIN(0 0 0 )
LXFMR 1 2 5MH
KCKT 2 3 5.0
Q1 5 6 4 QMOD1 OFF
Q2 6 5 7 QMOD2 OFF
Q3 10 11 12 QMOD1 OFF
Q4 11 10 3 QMOD2 OFF
UFOR1 5 6 DMOD1 OFF
DFOR2 10 11 DMOD1 UFF
DJCIN1 5 7 DMOD2 UFF
DJCIN2 10 3 DMOD2 OFF
RSH11 5 7 9.375
RSH12 10 3 9.375
C01 7 0 4UF
C02 0 13 4UF
.MODEL DMOD1 D(BV=2700,IS=5.58E-15)
.MODEL DMOD2 D(BV=5,IS=1.E-16)
.MODEL QMOD1 PNP(BF=9,BR=9,IS=1.0E-16.65,RE=.005,TF=17.8US,TR=1125US,CJE=4000PF)
.MODEL QMOD2 NPN(BF=9,IS=1.0E-16.65,CJC=4000PF)
.TRAN 5US 1000US
.PRINT TRAN I(VS) V(1) V(5,7) V(7,0) V(10,8) V(0,13) I(VZER01) I(VZER02)
.PLOT TRAN V(1) I(VZER01) I(VZER02)
.OPTIONS NOMOD NOPAGE LVLTIM=1 IITL5=10000 LIMPTS=10000
.END
```

FIGURE 50. SPICE PROGRAM LISTING FOR CIRCUIT OF FIGURE 49. WITHOUT THE SNUBBER CIRCUITS. SIMULATION RESULTS ARE GIVEN IN FIG. 51.

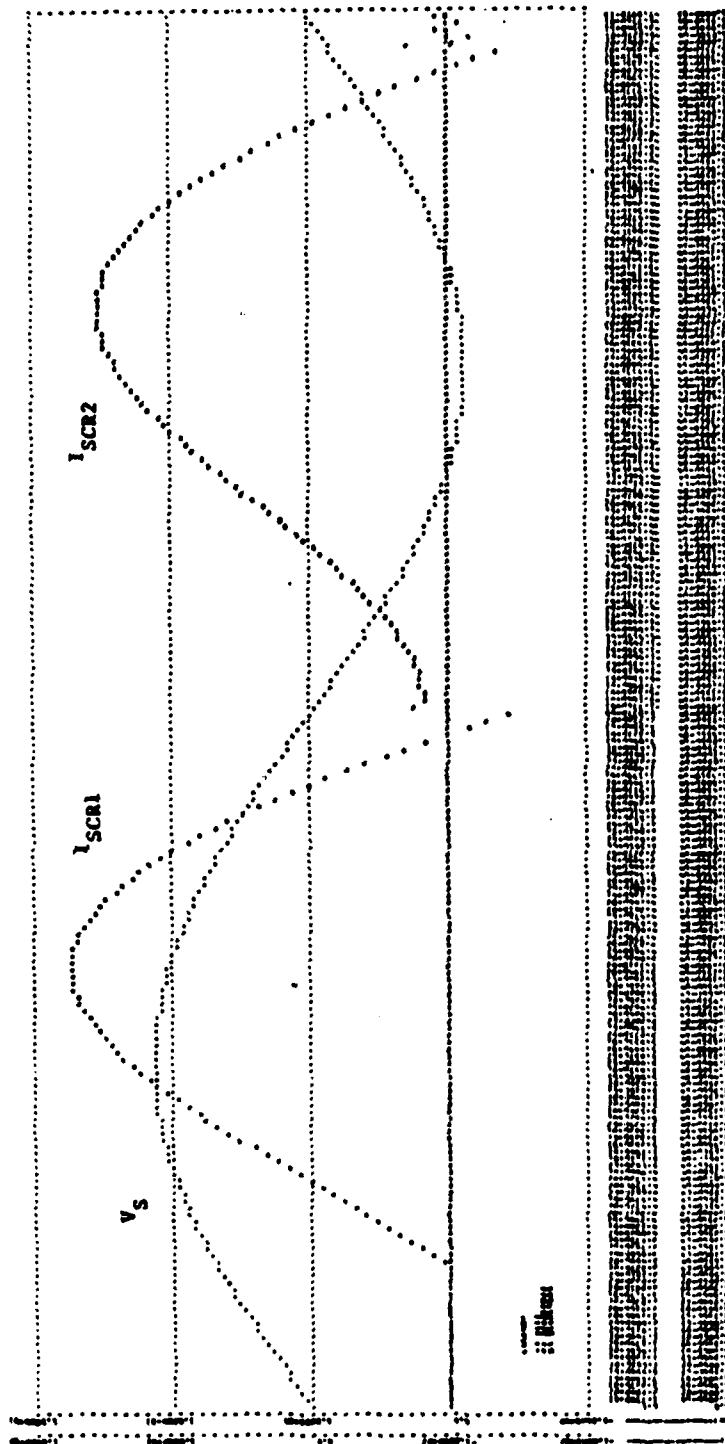


FIGURE 51. SPICE 2 SIMULATION OF A TWO LOOP AC RESONANT CHARGING CIRCUIT WITHOUT SNUBBER (FIG. 49). NOTE, CONDUCTION OF SCR2 STARTING AT 505  $\mu s$ . GATE SIGNAL IS NOT APPLIED UNTIL 600  $\mu s$ .

GE C602 LM SCR - TWO BRANCH AC RES CHG'NG CKT - DESCRETE - WITH SNUBBER

TEMPERATURE = 27.000 DEG C

INPUT LISTING

\*\*\*\*\*

```

VS 1 0 SIN(0 566 1K 1)
IG1 7 5 PULSE(0 1.0 100US 0 0 5US )
IG2 3 10 PULSE(0 1.0 600US 0 0 5US )
VZERO1 3 4 SIN(0 0 0)
VZERO2 13 12 SIN(0 0 0)
LXFMR 1 2 5MH
RCKT 2 3 5.0
Q1 5 6 4 QMOD1 OFF
Q2 6 5 7 QMOD2 OFF
Q3 10 11 12 QMOD1 OFF
Q4 11 10 3 QMOD2 OFF
DFOR1 5 6 DMOD1 OFF
DFOR2 10 11 DMOD1 OFF
RSHT1 5 7 9.375
RSHT2 10 3 9.375
DJCTN1 5 7 DMOD2 OFF
DJCTN2 10 3 DMOD2 OFF
C01 7 0 5UF
C02 0 13 5UF
CS1 9 3 0.1UF
RS1 7 9 15.
DS1 9 7 DMOD1
CS2 13 14 0.1UF
RS2 14 3 15
DS2 14 3 DMOD1
.MODEL DMOD1 D(BV=2700,IS=58E-15)
.MODEL DMOD2 D(BV=5,IS=1E-18)
.MODEL QMOD1 PNP(BF=9,BR=9,IS=1E-16,RE=.005,TF=17.8US,TR=1125US,CJE=4000PF)
.MODEL QMOD2 NPN(BF=9,IS=1E-16,RE=.005,CJC=4000PF)
.TRAN 5US 1000US
.PRINT TRAN V(1) I(VZERO1) I(VZERO2)
.PLOT TRAN V(1) I(VZERO1) I(VZERO2)
.OPTIONS NOMOD NOPAGE LVLTIM=1 ITL5=10000 LIMPTS=10000
.END

```

FIGURE 52. SPICE2 PROGRAM LISTING FOR CIRCUIT OF FIG. 49 WITH SNUBBERS. SIMULATION RESULTS ARE SHOWN IN FIG. 53.

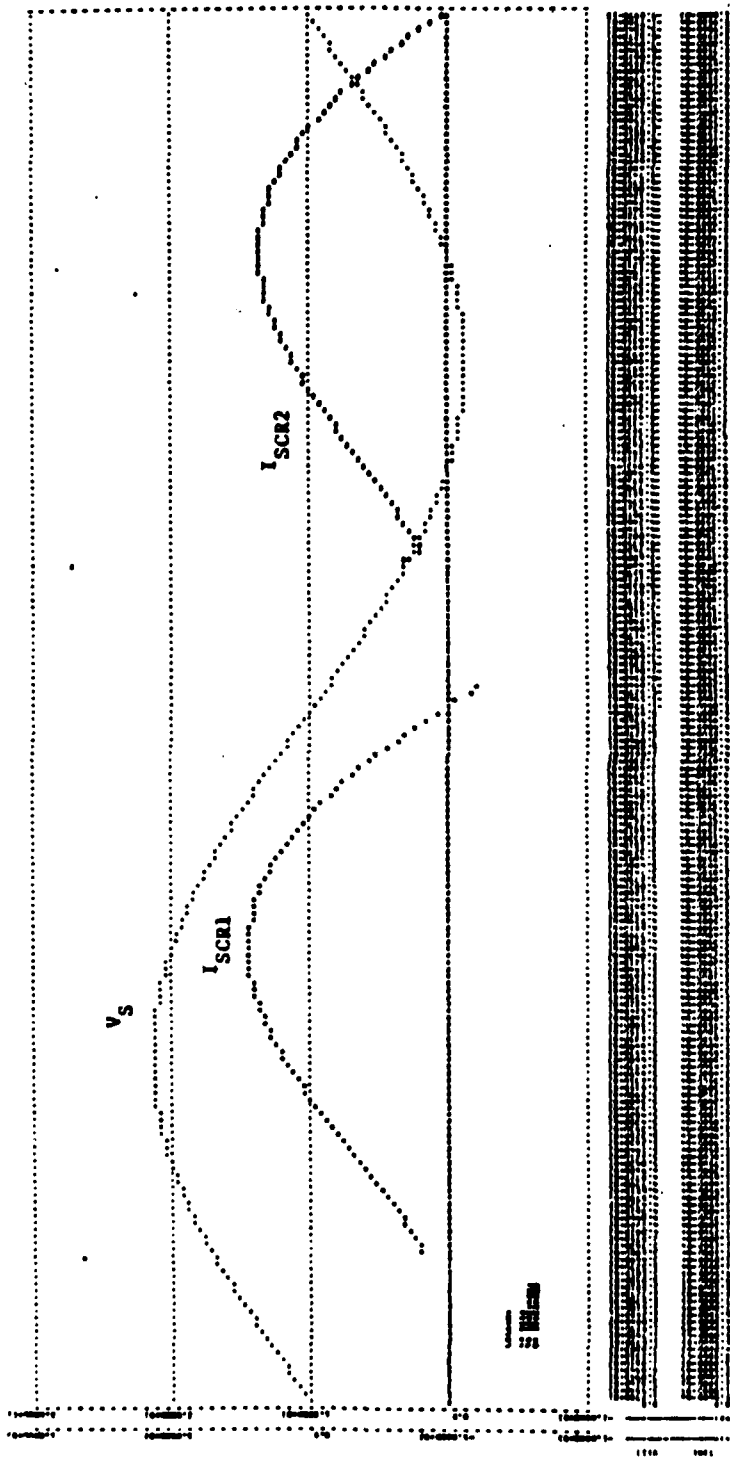


FIGURE 53. SPICE 2 SIMULATION RESULTS OF A TWO LOOP AC RESONANT CHARGING CIRCUIT WITH SNUBBERS (FIG. 49). NOTE, CONDUCTION OF SCR 2 STARTS AT 600  $\mu$ s AT THE TIME THE GATE PULSE IS APPLIED.

#### 9.4 SPICE 2 SIMULATION OF A SINGLE LOOP AC RESONANT CHARGING CIRCUIT USING TWO SCR'S IN PARALLEL

Figure 54 illustrates a basic circuit application of two SCR's in parallel. Such circuit applications occur when load current requirements exceed the current rating of the chosen SCR type.

Problems with using SCR's in parallel occur mainly due to slight differences in device characteristics among SCR's of the same type. This can result in one SCR turning on faster than the other. The corresponding principal voltage drop may then result in insufficient  $V_{AK}$  of the other device to insure turn on. This situation is illustrated in Figure 56 for which SCR 1 and SCR 2 have been programmed (Figure 55) to have slightly different parameters. In Figure 56, it is seen that SCR 2 ( $I(VZERO\ 2)$ ) begins to conduct more quickly than SCR 1 ( $I(VZERO\ 1)$ ). Since the series balancing resistance ( $R_{SER}$ ) is essentially zero (actually 0.0001 ohms) then  $V_{AK}$  for SCR 1 drops in correspondence with  $V_{AK}$  for SCR 2.  $V_{AK}$  for SCR 1 falls below the required value for turn on before SCR 1 primary current reaches the holding current and therefore, the SCR 1 does not turn on.

This situation may be prevented (although at a loss of efficiency) by inserting sufficient balancing resistance ( $R_{SER}$ ) in series with each SCR. This was done (Figure 57 -  $R_{SER1} = R_{SER2} = 0.5$  ohms) and the results are given in Figure 58. Both SCR's turn on since an increase in the current of one SCR causes an increase in the voltage drop across the other and a subsequent increase in its current.

#### 9.5 SPICE 2 SIMULATION OF A SINGLE LOOP AC RESONANT CHARGING CIRCUIT USING TWO SCR'S IN SERIES

Sometimes circuit applications call for SCR's to block voltages which exceed the blocking voltage rating of the device (either forward or reverse).

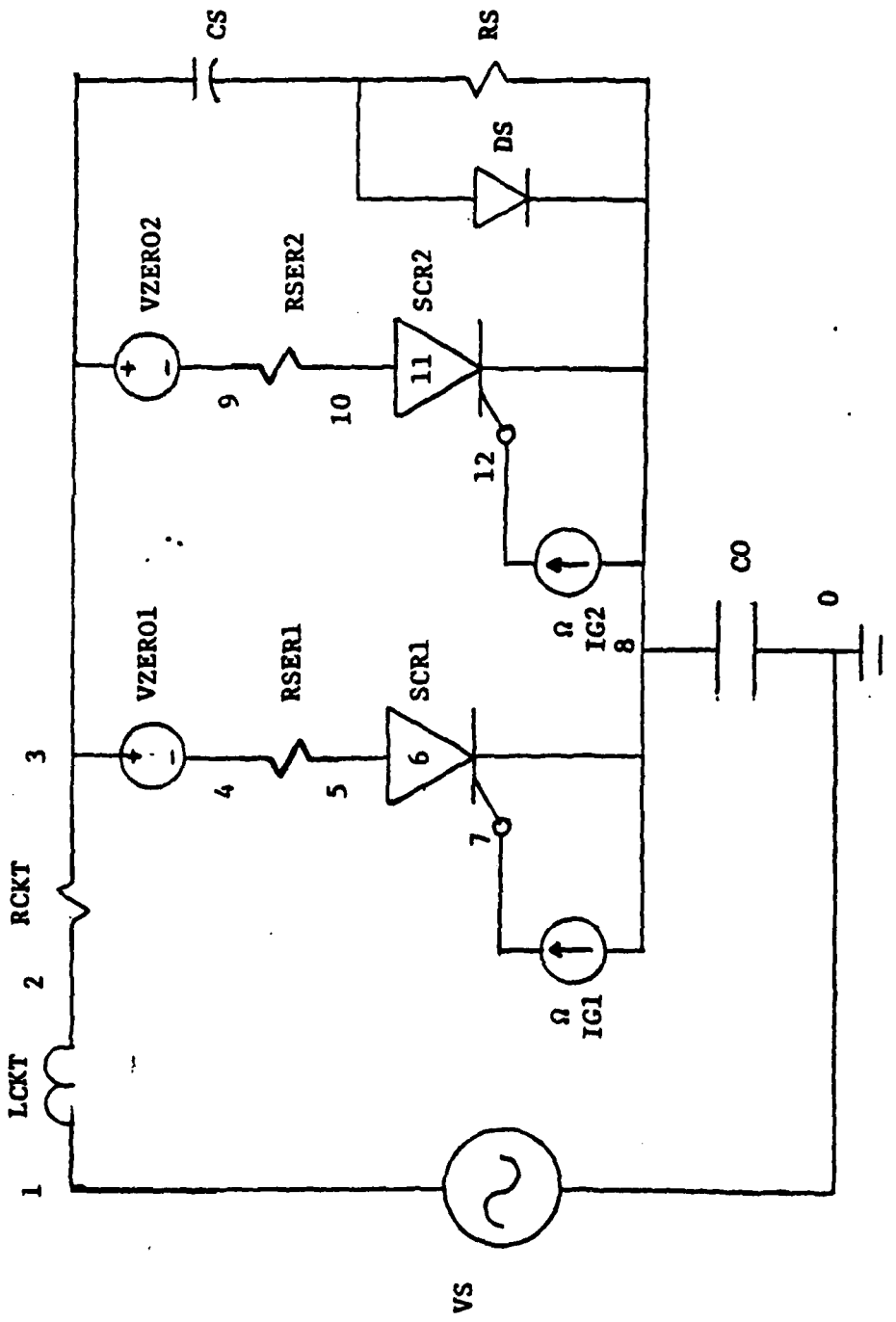


FIGURE 54. SPICE2 CIRCUIT DIAGRAM FOR TWO SCR'S IN PARALLEL IN A SINGLE LOOP AC RESONANT CHARGING CIRCUIT.



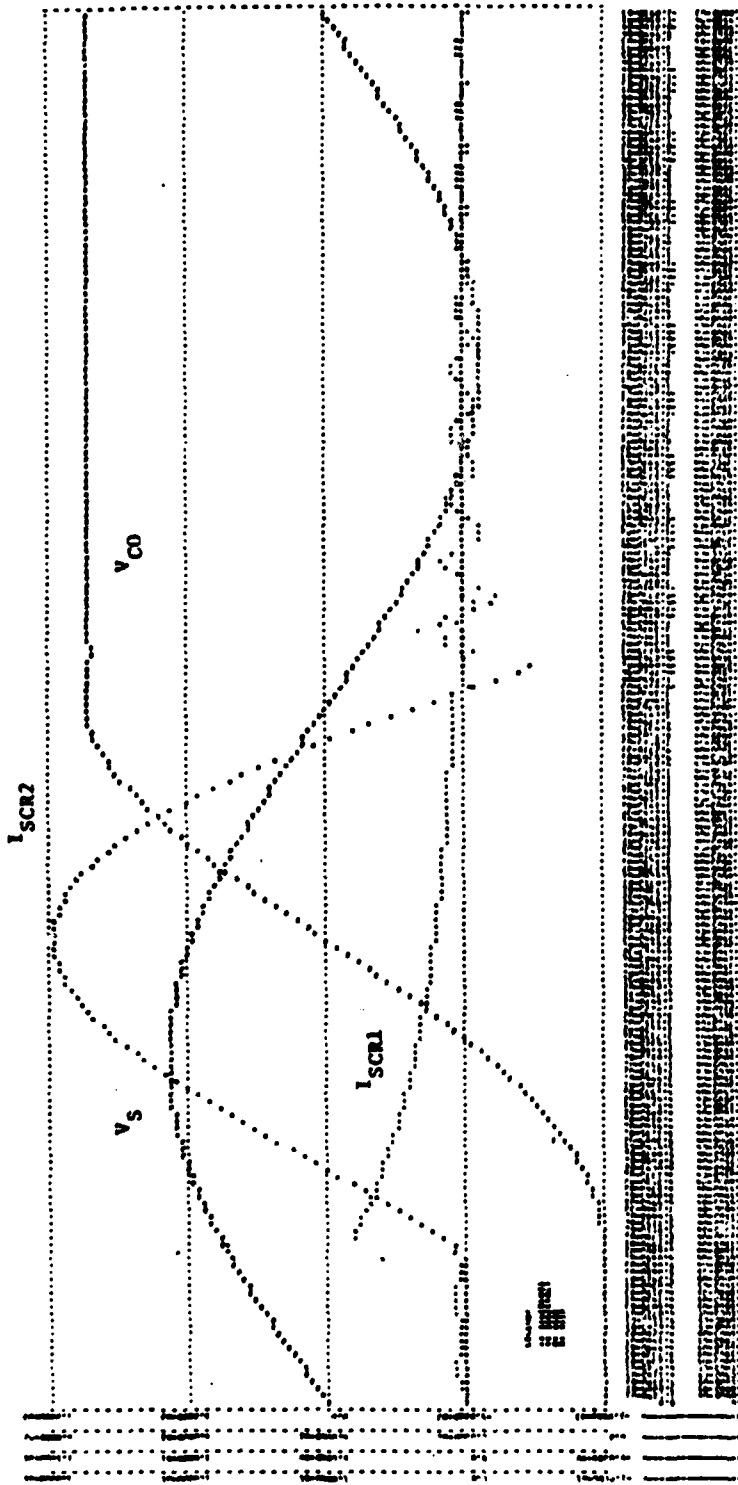


FIGURE 56. SPICE 2 SIMULATION OF A SINGLE LOOP AC RESONANT CHARGING CIRCUIT USING TWO PARALLEL SCR'S (FIG. 54). NOTE, FOR INSUFFICIENT SERIES BALANCING RESISTANCE (RSER) ONE SCR2 TURNS ON FASTER WITH THE RESULT THAT SCR 1 FAILS TO TURN ON.





Such an application is illustrated in the AC Resonant Charging Circuit of Figure 59 where the reverse voltage to be blocked may be as high as three times the forward voltage of 1000V peak. The GE C602 LM SCR which has a blocking voltage rating of only 2700V may not be able to block the peak reverse voltage of this circuit which might reach 3000V. To insure adequate blocking, two GE C602 LM SCR's are connected in series as shown in Figure 59.

As in the case of parallel SCR's, slight variations in device characteristics may cause problems in circuit operation. In this case primary concern is to insure sharing of the voltage to be blocked in such a manner as to avoid exceeding the rating of either SCR. For this purpose, the balancing network composed of RBAL 1 , RBAL 2 , for forward balancing and CS 1, CS 2 , RS 1, and RS 2, for reverse balancing is provided. Notice that the reverse balancing network provides a snubber system in the forward direction.

Simulation results for the circuit of Figure 59 are shown in Figure 60. Prior to application of the gate trigger at 100  $\mu$ s both SCR's carry very nearly equal voltages ( $V(4,7)$  and  $V(9,12)$  in Figure 60). During the on period (100  $\mu$ s to 505  $\mu$ s),  $V_{AK}$  for both SCR's is a very low forward value. At the start of commutation (505  $\mu$ s) the charge stored in each SCR differs due to slight parameter variations. As a result, the charge transferred to the two equal valued capacitors in the reverse voltage balancing network is different. The resulting unbalance in the reverse voltages is seen in the  $V_{SCR_1}$  and  $V_{SCR_2}$  curves in Figure 60.

## 9.6 AC RESONANT CHARGING CIRCUIT SIMULATIONS IN SCEPTRE

An SCR model for use with SCEPTRE was presented in Section IV. Two versions of the model were developed, one called the 3-Junction model and



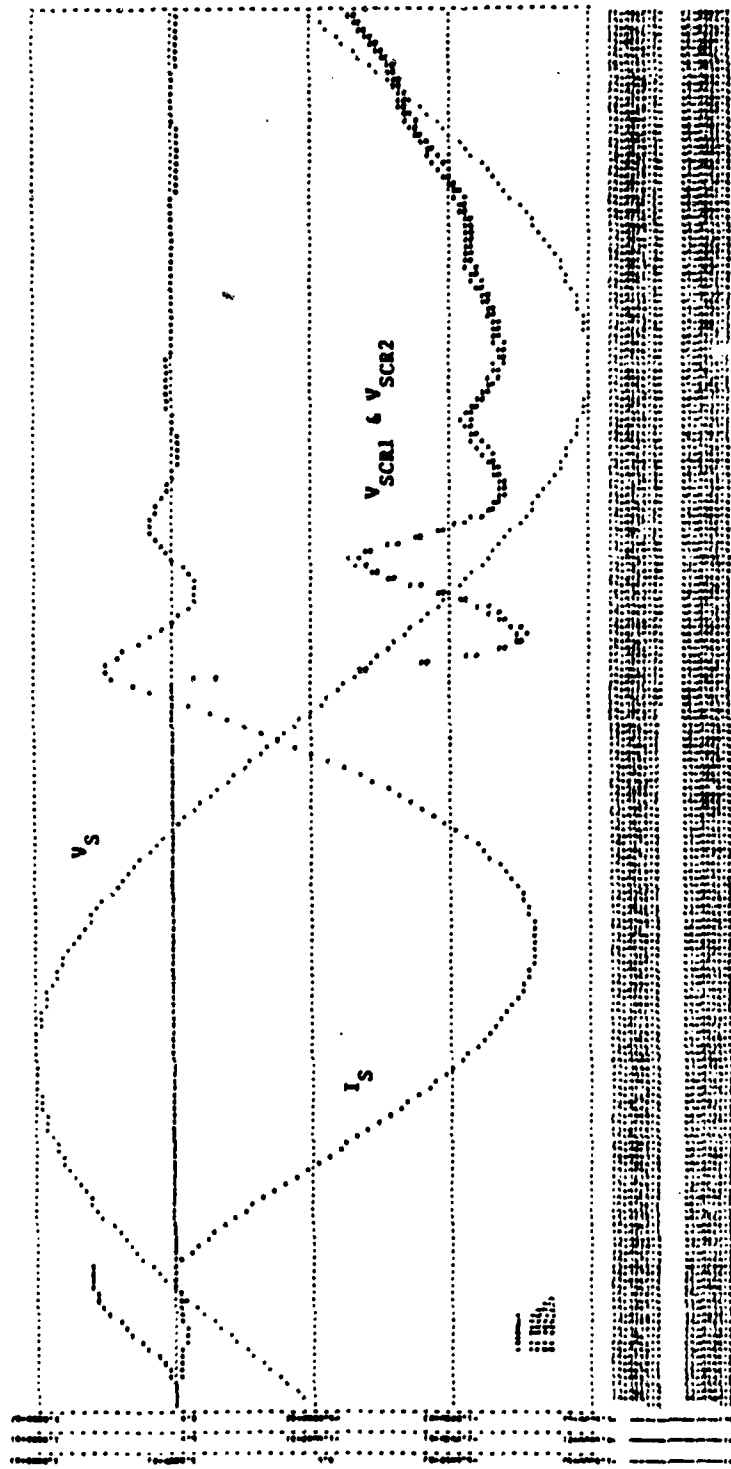


FIGURE 60. SPICE 2 SIMULATION RESULTS FOR SINGLE LOOP AC RESONANT CIRCUIT WITH TWO SCR'S IN SERIES (FIG. 59).

the other called the Reduced 3-Junction model. The simulation performance of the two models was shown to be virtually identical through model verifications runs. Since the run times using the reduced 3-Junction model were observed to be slightly shorter than those for the 3-Junction model, and since the likelihood of exceeding a SCEPTRE capacity limit is less with the reduced model it is selected for use in doing SCEPTRE simulations of resonant charging circuits.

Circuits to be simulated in this research are adaptations of the AC and DC resonant charging circuits developed by Lt. J. Silva at AFIT and reported in Reference 42. Silva developed his circuits using diodes as rectifier switches, however, the goal of this research is to develop a computer simulation capability to simulate controlled rectifier (SCR) circuits. This simulation capability will then serve as a design aid in development of the actual resonant charging circuits using SCRs. This report presents the development of the computer simulation capability for simulating the controlled rectifiers (SCRs) and other electronics of such circuits.

Magnetics are treated as linear elements in this report, however concurrent research is being conducted by Clemson University to enable treatment of the non-linearities of the magnetics.

In order to do controlled rectifier (SCR) circuit simulations, facsimile circuits substituting SCR's for some of the diodes in Silva's circuits were devised. The plan being to compare simulation data of the facsimile circuits to Silva's charging system data. The considerable differences between SCR circuits and Silva's diode circuits makes direct substitution of SCR rectifiers for diode rectifiers impossible. For this reason, careful consideration had to be given to construction of proper facsimile circuits. Significant considerations are summarized as follows:

1. The line voltages in Silva's circuit greatly exceed any single SCR's blocking voltage rating. Actual SCR circuits performing at the voltage levels of Silva's circuits would require a large number of SCR's to simulate a full three phase system.

Simulation of sufficient SCR's in series (seven) to provide the needed values of blocking voltages was confronted by SCEPTRE network programming limits (on the total number of sources present in the network) when considering the total 3- $\phi$  system (42 SCR's). While the SCR circuits may have been simulated, review with Clemson revealed that the combined system simulation would exceed SCEPTRE limits.

A prospect to assign arbitrarily high (and unrealistic) values for device blocking voltage ratings was considered but was deemed to limit the value of the research results in the end result.

The solution was to design facsimile circuits having the minimum number of SCR's necessary to obtain controlled rectification in Silva's resonant charging circuits. This concept involved use of SCR's to provide forward blocking prior to triggering and Diodes to provide reverse blocking capability in series with the SCR's reverse blocking to sustain the substantially higher voltages in the reverse direction presented by the resonantly charged load capacitor voltages in series with the negative half-cycle source voltages.

Since magnetic elements are treated as linear, simulation of more than one phase bank array in the AC system is merely redundant, therefore a single phase system having a resonant

charging load on one-half cycle of the source is presented in Section 9.7.

2. The high cost of complete transient simulations of full scale facsimiles of Silva's circuits made design and debug operations cost prohibitive. The solution to this problem required development of scaled circuits. Since the research objective was to develop and validate a simulation capacity, then scaling is both a valid and desirable approach. While a rigorous approach to scaling [Reference 43] may be performed, absolute rigor is not required in this case since the simulation is not to validate or analyze an actual circuit, but to demonstrate a simulation capability. The validity of the simulation is established by the reasonableness of results as compared to the results obtained in circuits of a similar nature. The circuits of similar nature being Silva's diode switched resonant charging circuits. In the case of ac resonant charging circuits, Silva did not obtain final results for his circuits and therefore the validity of ac resonant charging circuit simulations is established only by the consistency of results with explanation of phenomena by engineering analysis.

A scaled 3-phase ac resonant charging circuit simulation is presented in Section 9.7. Scaled elements were as follows in Table 10.

#### 9.7 AN AC RESONANT CHARGING CIRCUIT WITH THREE SCRS AND A DIODE IN SERIES

A single phase single loop AC resonant charging circuit is shown in Figure 63. The circuit has 3-SCRs and a diode in series. Silva's circuits used transformer secondary phase voltages of 6500V peak at 400 Hz. Simulation of the required forty-two SCRs to develop a totally SCR 3 $\phi$  circuit of

TABLE 10. DC Resonant Charging Scaling

Quality	Silva's Diode Circuits (unscaled)	SCR Facsimile Circuits (scaled)
3-Phase AC System (section 6.2)		
Source Voltage	6465.85V per phase	1000V per phase
Source Frequency	400 hertz	1000 hertz.
Resonant load inductance	0.327 henries	0.05897 henries
Resonant load capacitance	0.43 micro-farads	0.43 micro-farads
DC Resonant Load on 3-phase Source (section 7.1)		
Source voltage	6465.85V per phase	1000V
Source frequency	400 hertz.	1000 hertz.
Resonant load inductance	2.58 henries	0.173 henries
Resonant load capacitance	2.58 micro-farads	0.586 micro-farads

this nature exceeds SCEPTRE capacity, therefore a single phase simulation is presented to illustrate the series SCR configuration.

Seven GE C602 L<sup>1</sup> SCR's with reverse blocking voltages of 2700 voltage are required in a totally SCR circuit in order to block the reverse voltages following resonant commutation of the SCR's. However, only three SCR's are needed to block the forward voltages. As a result, the design was simplified to SCR's to provide forward blocking and controller rectification and one diode (actual circuit may use several diodes) to provide additional reverse blocking needed. Figure 64 gives simulation results for the circuit of Figure 63. The extended oscillatory behavior following commutation is due to snubber circuit resonant behavior with the large series inductor. CAD can be a useful tool in optimizing snubber design in this type of circuit.

The SCR's, S1, S2, and S3 of Figure 63 had simulation parameters perturbed varying amounts within a 25% limit of deviation. Simulation results clearly showed the results of the perturbations. This provides a design aid to the balancing network requirements. CPU time for the simulation was 41.28 seconds for the 2.5 ms transient simulation of one complete cycle of the 400 Hz source. It was observed that the 3-SCR series configuration required only slightly more CPU time than that for a single SCR in the same circuit configuration. This suggests that time step and not circuit size is the dominant factor in CPU time for a simulation.

## 9.8 A THREE PHASE AC RESONANT CHARGING CIRCUIT

As mentioned previously, simulating Silva's circuit design requiring 42 SCR's in a 3-phase system exceeds SCEPTRE capacities using the reduced SCR model of Section IV. Even an SCR/Diode combination such as that of

```

      DOUBLE PRECISION FUNCTION FGEN(HIGH,LOW,TD,TON,TP,TIME,MNEG)
C FGEN IS A PULSE GENERATOR SUBROUTINE. THE PARAMETERS ARE AS FOLLOWS;
C HIGH = MAXIMUM VALUE OF FUNCTION , LOW = MINIMUM VALUE OF FUNC-
C TD = TIME DELAY UNTIL START OF FIRST PULSE, TON = TIME OF PULSE DURA-
C TION , TP = TIME OF PULSE CYCLE PERIOD, TIME = TIME POINT OF CIR-
C CUIT BEING SIMULATED. PULSE VALUE IS SET TO LOW FOR TIME LESS THAN
C OR EQUAL TO ZERO IF MNEG IS NOT EQUAL TO 1. MNEG = 1 IF PULSE MAY HAVE
C NON-ZERO VALUE AT OR PRIOR TO TIME EQUAL ZERO.
      IMPLICIT REAL*8(A-L,N-Z)
      FGEN=LOW
      IF(TIME.LE.0..AND.MNEG.NE.1) GO TO 20
      N=(TIME-TD)/TP
      IF(N.LT.0.0) GO TO 20
      M=IDINT(N)
      P=(N-M)*TP
      IF(P.GT.TON) GO TO 10
      FGEN=HIGH
      GO TO 20
10 FGEN=LOW
20 RETURN
   END

```

FIGURE 61. SUBROUTINE FGEN IS A PULSE GENERATOR SUBROUTINE USED IN CIRCUIT SIMULATIONS TO SIMULATE GATE DRIVES AND CAPACITOR DISCHARGE SWITCHES.

MODELSCR1(A-G-K)  
 THIS IS A REDUCED ELEMENT VERSION OF THE 3-JUNCTION SCR MODEL DEVELOPE  
 FOR USE WITH SCEPTRE. THE PARAMETERS DETERMINED FOR THIS MODEL BY THE  
 SCEPTRE 3-JCTNSCR MODEL PARAMETER DETERMINATION PROCEDURE HAVE BEEN  
 PERTURBED SLIGHTLY TO SIMULATE BATCH PARAMETER VARIATION.  
 UNITS: OHMS, FARADS, HENRIES, SECONDS, AMPS, VOLTS  
 ELEMENTS  
 R, A-1=5.0-3  
 RA, 1-C=1.06  
 RC, C-G=1.06  
 RK, G-K=9.375  
 JA, 1-C=DIODEQ(2.488D-17, 38.61)  
 JC, G-C=DIODEQ(PX1, PX2)  
 JK, G-K=DIODEQ(PX3, PX2)  
 J2, C-G=X1(.9\*JA+.9\*JK)  
 (a) CA, 1-C=FCJ(1.78D-5, 2.488D-17, 38.61, JA, VCA, 4.0-9, 1.0-10)  
 CC, G-C=FCJ(4.95D-6, 5.65D-15, 38.61, JC, VCC, 4.0-9, 1.0-10)  
 CK, G-K=1.0-9  
 RS, A-2=100.  
 CS, 2-K=.1D-6  
 DEFINED PARAMETERS  
 PX1=FIS(5.65D-15, VCC, 2.7D3)  
 PX2=38.61  
 PX3=FIS(2.488D-17, VCK, 5.)  
 OUTPUTS  
 VCC, VCK, PLOT

MODELSCR3(A-G-K)  
 THIS IS A REDUCED ELEMENT VERSION OF THE 3-JUNCTION SCR MODEL DEVELOPE  
 FOR USE WITH SCEPTRE. THE PARAMETERS DETERMINED FOR THIS MODEL BY THE  
 SCEPTRE 3-JCTNSCR MODEL PARAMETER DETERMINATION PROCEDURE HAVE BEEN  
 PERTURBED SLIGHTLY TO SIMULATE BATCH PARAMETER VARIATION.  
 UNITS: OHMS, FARADS, HENRIES, SECONDS, AMPS, VOLTS  
 ELEMENTS  
 R, A-1=5.0-3  
 RA, 1-C=1.06  
 RC, C-G=1.06  
 RK, G-K=9.375  
 JA, 1-C=DIODEQ(2.388D-17, 38.61)  
 JC, G-C=DIODEQ(PX1, PX2)  
 JK, G-K=DIODEQ(PX3, PX2)  
 J2, C-G=X1(.9\*JA+.9\*JK)  
 (b) CA, 1-C=FCJ(1.88D-5, 2.388D-17, 38.61, JA, VCA, 5.0-9, 1.0-10)  
 CC, G-C=FCJ(4.85D-6, 5.65D-15, 38.61, JC, VCC, 4.5D-9, 1.0-10)  
 CK, G-K=1.0-9  
 RS, A-2=100.  
 CS, 2-K=.1D-6  
 DEFINED PARAMETERS  
 PX1=FIS(5.65D-15, VCC, 2.7D3)  
 PX2=38.61  
 PX3=FIS(2.488D-17, VCK, 5.)  
 OUTPUTS  
 VCC, VCK, PLOT

FIGURE 62. INPUT LISTING FOR FIGURE 63. (2-PAGES)  
 (a), (b), (c) ARE PERTURBED SCR MODELS  
 (d) CIRCUIT ELEMENT LISTING.

FIGURE 62 (CONTINUED)

```

MODELSCR2(A-G-K)
THIS IS A REDUCED ELEMENT VERSION OF THE 3-JUNCTION SCR MODEL DEVELOPE
FOR USE WITH SCEPTRE. THE PARAMETERS DETERMINED FOR THIS MODEL BY THE
SCEPTRE 3-JUNCTION SCR MODEL PARAMETER DETERMINATION PROCEDURE HAVE BEEN
PERTURBED SLIGHTLY TO SIMULATE BATCH PARAMETER VARIATION.
UNITS: OHMS, FARADS, HENRIES, SECONDS, AMPS, VOLTS
ELEMENTS
R, A-1=5. D-3
RA, 1-C=1. D6
RC, C-G=1. D6
RK, G-K=9. 375
JA, 1-C=DIODEQ(2. 588D-17, 38. 61)
(c) JC, G-C=DIODEQ(PX1, PX2)
JK, G-K=DIODEQ(PX3, PX2)
J2, C-G=X1(. 9*JA+. 91*JK)
CA, 1-C=FCJ(1. 68D-5, 2. 588D-17, 38. 61, JA, VCA, 3. D-9, 1. D-10)
CC, G-C=FCJ(4. 90D-6, 5. 65D-15, 38. 61, JC, VCC, 3. 5D-9, 1. D-10)
CK, G-K=1. D-9
RS, A-2=100.
CS, 2-K=. 1D-6
DEFINED PARAMETERS
PX1=FIS(5. 65D-15, VCC, 2. 7D3)
PX2=38. 61
PX3=FIS(2. 488D-17, VCK, 5. )
OUTPUTS
VCC, VCK, PLOT

```

```

CIRCUIT DESCRIPTION
THIS CIRCUIT IS A SINGLE PHASE AC CIRCUIT HAVING 3 SCR'S AND A DIODE
IN SERIES.
ELEMENTS
EAN, 0-1=X1(6465. 85*DSIN(2513. 2*TIME))
RA, 1-2=1.
LA, 2-3=. 327
S1, 3-4-5=MODEL SCR1
S2, 5-6-7=MODEL SCR2
S3, 7-8-9=MODEL SCR3
JD1, 9-10=DIODE Q(1. D-6, 38. 61)
CD1, 9-10=1. D-8
CO, 10-0=. 43D-6
RB1, 3-5=17. 5D3
RB2, 5-7=17. 5D3
RB3, 7-9=17. 5D3
RB4, 9-10=1. D5
(d) JG1, 5-4=FGEN(. 2, 0. , 1. D-4, 5. D-5, 2. 5D-3, TIME, 0)
JG2, 7-6=FGEN(. 2, 0. , 1. D-4, 5. D-5, 2. 5D-3, TIME, 0)
JG3, 9-8=FGEN(. 2, 0. , 1. D-4, 5. D-5, 2. 5D-3, TIME, 0)
OUTPUTS
EAN, VRB1, ILA, VCO, PLOT1
VCAS1, VCAS2, VCAS3, VCD1, PLOT2
VCCS1, VCCS2, VCCS3, PLOT3
RUN CONTROLS
COMPUTER TIME LIMIT = 10.
INTEGRATION ROUTINE = IMPLICIT
PLOT INTERVAL = 1. 5D-5
MAXIMUM PRINT POINTS=0
STOP TIME=2. 5E-3
MINIMUM STEP SIZE = 1. E-30
END

```

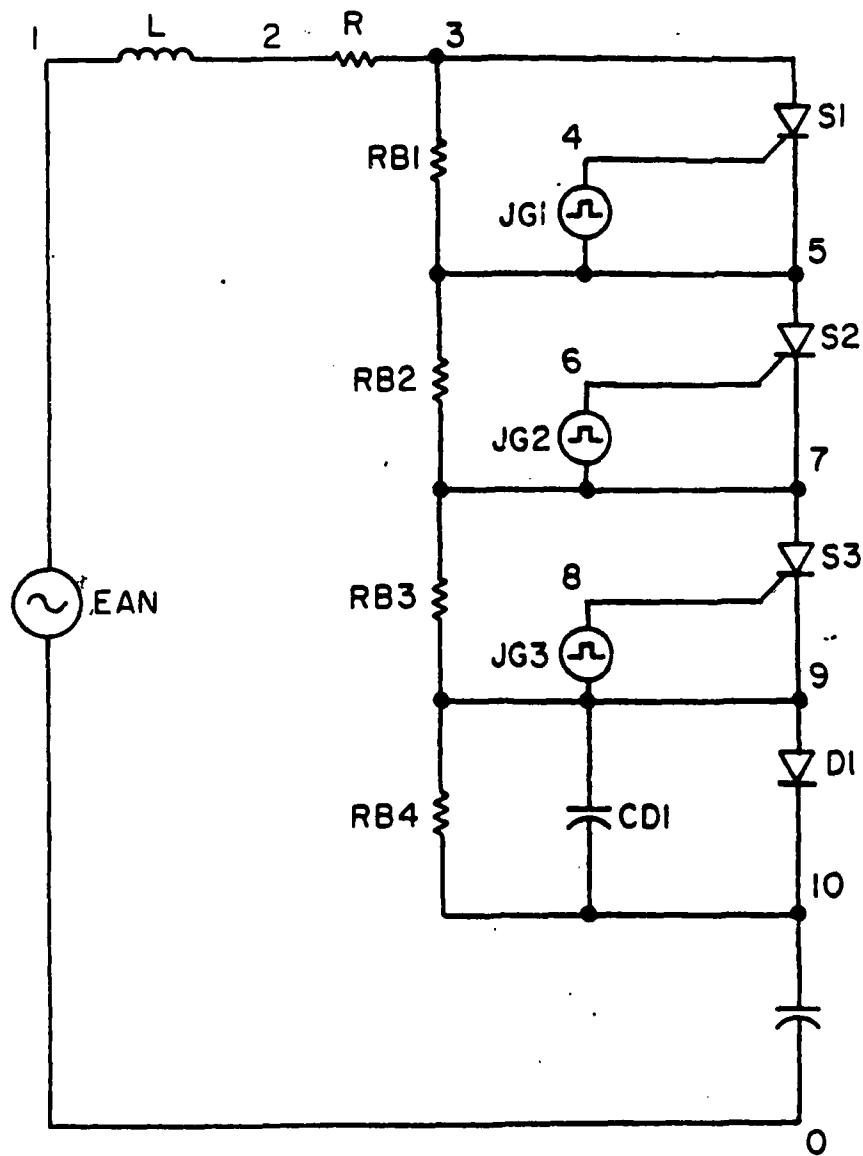


FIGURE 63. 3-SCRs AND A DIODE IN SERIES.





Figure 63 would require 18 SCR's which would again approach some SCEPTRE capacity limits. For this reason, a 3-phase ac resonant charging circuit was simulated using only six SCR's. This circuit is shown in Figure 65. Phase voltages were changed to 1000V - 1000 Hz to accommodate the reduced number of SCR's and to have a shorter transient CPU time for one complete cycle of the source.

Figure 65 shows two branches of each phase bank charging array. The capacitors are discharged by the switches during alternate half-cycles of the phase sources. The actual circuit used thyatron discharge switches, but a non-linear resistor was simulated via subroutine FGEN. (Figure 61) for this report.

Preliminary circuit design revealed that the conducting half-cycle SCR would turn-off during discharge of the alternate half-cycle capacitor in each phase bank array. CAD revealed that the problem was the discharge current limiting resistors, R1A, R2A, ..., etc. These resistors were originally inserted in series with the charging capacitors, C1A, C2A, ..., between RSW1A, RSW2A, ..., . When fired, the line to neutral voltage dropped suddenly causing the conducting SCR to commutate.

The solution was to move the current limiting resistors to be in series with the switches and neutral (as in Figure 65).

Simulation results are presented in Figure 68 for each phase bank array. The usefulness of CAD is emphasized in the simulations of phases B and C.

The charging array is brought on line at time  $t = 0$ , but SCR firing is synchronized to phase voltage zero crossing. Consequently, phase inductance/snubber capacitor resonant behavior results in non-zero phase inductor currents at the time of firing of the appropriate SCR.

CPU time for one cycle of the 1K Hz sources was 16 min., 8.9 seconds.

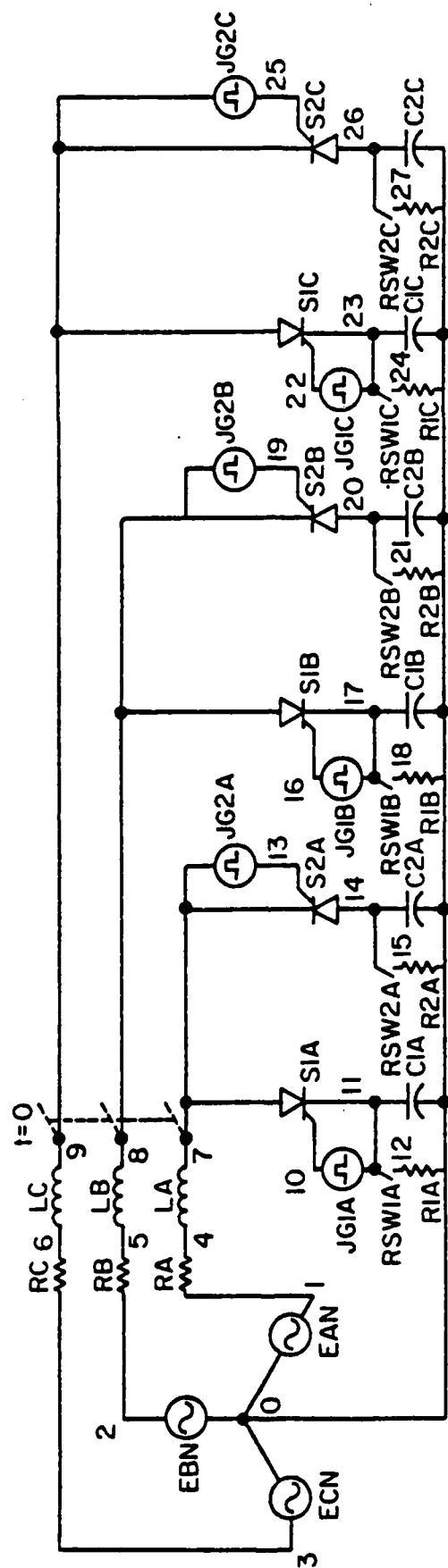


FIGURE 65. 3- $\phi$  AC RESONANT CHARGING CIRCUIT.

```

CIRCUIT DESCRIPTION
ELEMENTS
EAN,0-1=X1(1.D3*DSIN(6285.18*TIME))
RA,1-4=1.
LA,4-7=5.897E-2
EBN,0-2=X2(1.D3*DSIN(6285.18*TIME-2.094))
RB,2-5=1.
LB,5-8=5.897E-2
ECN,0-3=X3(1.D3*DSIN(6285.18*TIME+2.094))
RC,3-6=1.
LC,6-9=5.897E-2
S1A,7-10-11=MODEL SCR
S2A,14-13-7=MODEL SCR
C1A,11-0=.43D-6
C2A,0-14=.43D-6
R1A,12-0=11.
R2A,15-0=11.
JG1A,11-10=FGEN(.2,0.,0.,1.D-4,1.D-3,TIME,0)
JG2A,7-13=FGEN(.2,0.,5.D-4,1.D-4,1.D-3,TIME,0)
RSW1A,11-12=FGEN(1.D7,0.,-2.25D-4,9.75D-4,1.D-3,TIME,1)
RSW2A,14-15=FGEN(1.D7,0.,-7.25D-4,9.75D-4,1.D-3,TIME,1)
S1B,8-16-17=MODEL SCR
S2B,20-19-8=MODEL SCR
C1B,17-0=.43D-6
C2B,0-20=.43D-6
R1B,18-0=11.
R2B,21-0=11.
JG1B,17-16=FGEN(.2,0.,3.33D-4,1.D-4,1.D-3,TIME,0)
JG2B,8-19=FGEN(.2,0.,-1.67D-4,1.D-4,1.D-3,TIME,0)
RSW1B,17-18=FGEN(1.D7,0.,-8.92D-4,9.75D-4,1.D-3,TIME,1)
RSW2B,20-21=FGEN(1.D7,0.,-3.92D-4,9.75D-4,1.D-3,TIME,1)
S1C,9-22-23=MODEL SCR
S2C,26-25-9=MODEL SCR
C1C,23-0=.43D-6
C2C,0-26=.43D-6
R1C,24-0=11.
R2C,27-0=11.
JG1C,23-22=FGEN(.2,0.,6.67D-4,1.D-4,1.D-3,TIME,0)
JG2C,9-25=FGEN(.2,0.,1.67D-4,1.D-4,1.D-3,TIME,0)
RSW1C,23-24=FGEN(1.D7,0.,-5.58D-4,9.75D-4,1.D-3,TIME,1)
RSW2C,26-27=FGEN(1.D7,0.,-5.58D-4,9.75D-4,1.D-3,TIME,1)
OUTPUTS
EAN,VC1A,VC2A,ILA,PLOT1
EBN,VC1B,VC2B,ILB,PLOT2
ECN,VC1C,VC2C,ILC,PLOT3
RUN CONTROLS
INTEGRATION ROUTINE = IMPLICIT
PLOT INTERVAL = 1.E-5
MAXIMUM PRINT POINTS=0
STOP TIME=1.E-3
MINIMUM STEP SIZE = 1.E-30
END

```

FIGURE 66. SCEPTRE INPUT CIRCUIT DESCRIPTION FOR THE CIRCUIT OF FIGURE 65.

# AC RESONANT CHARGING SYSTEM TIMING DIAGRAM

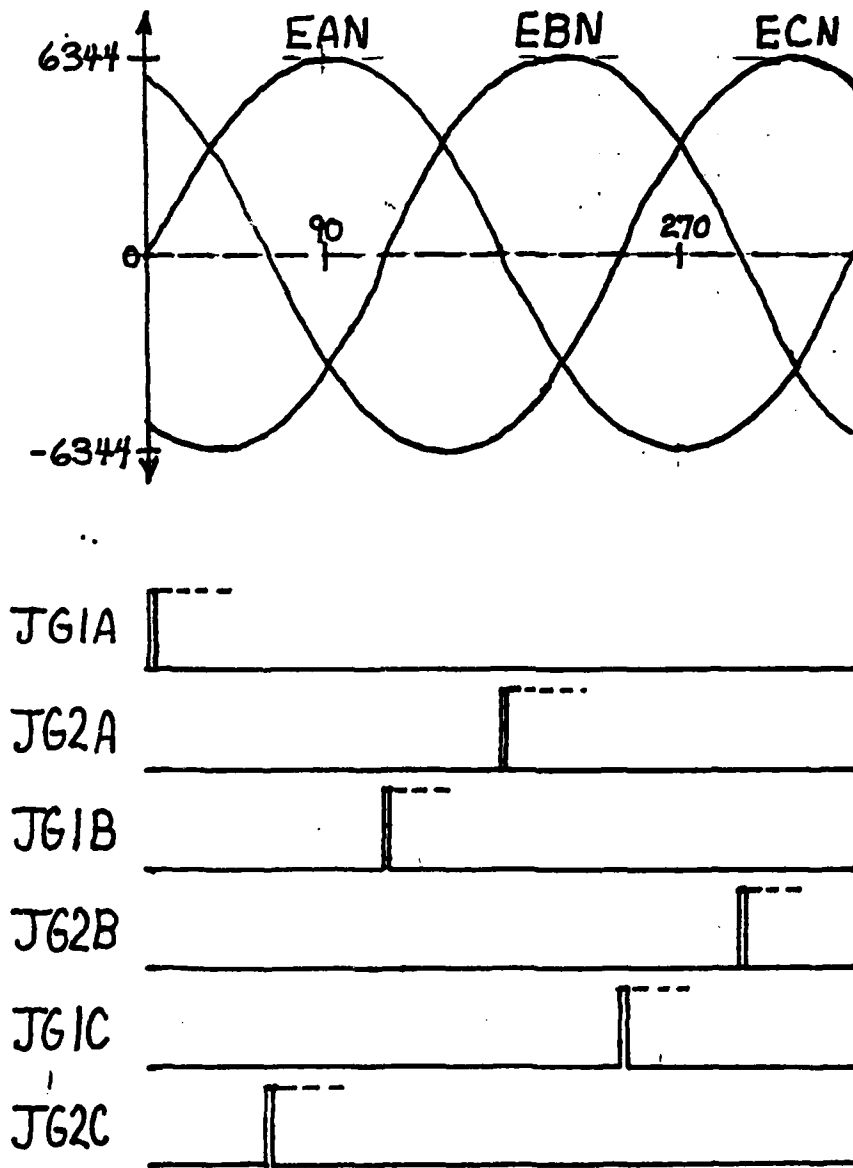


FIGURE 67. TIMING DIAGRAM FOR GATE SOURCES OF FIG. 65.

PLOT - 1

EAM CHARACTER - A  
 VC1A CHARACTER - B  
 VC2A CHARACTER - C  
 ILA CHARACTER - D

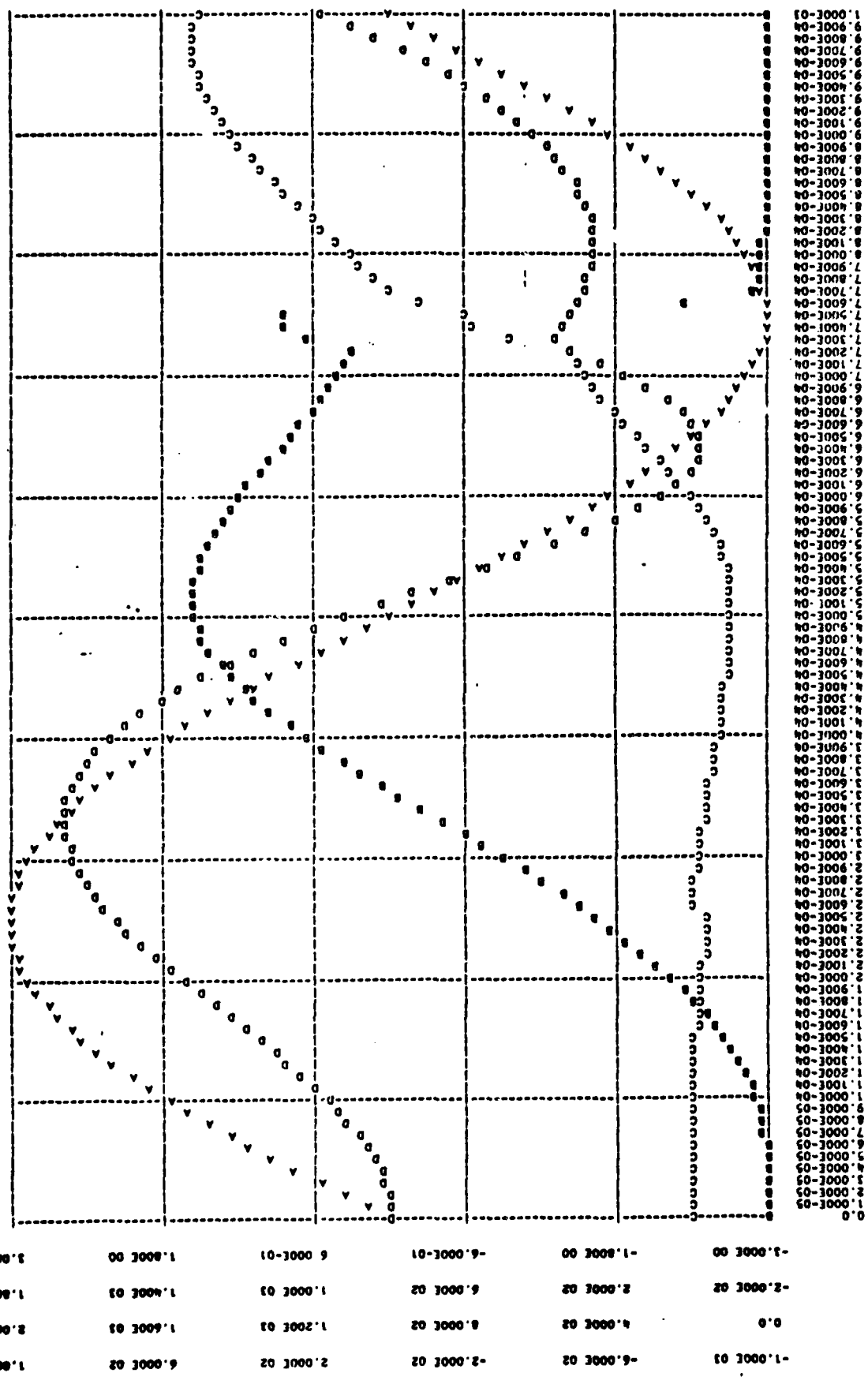
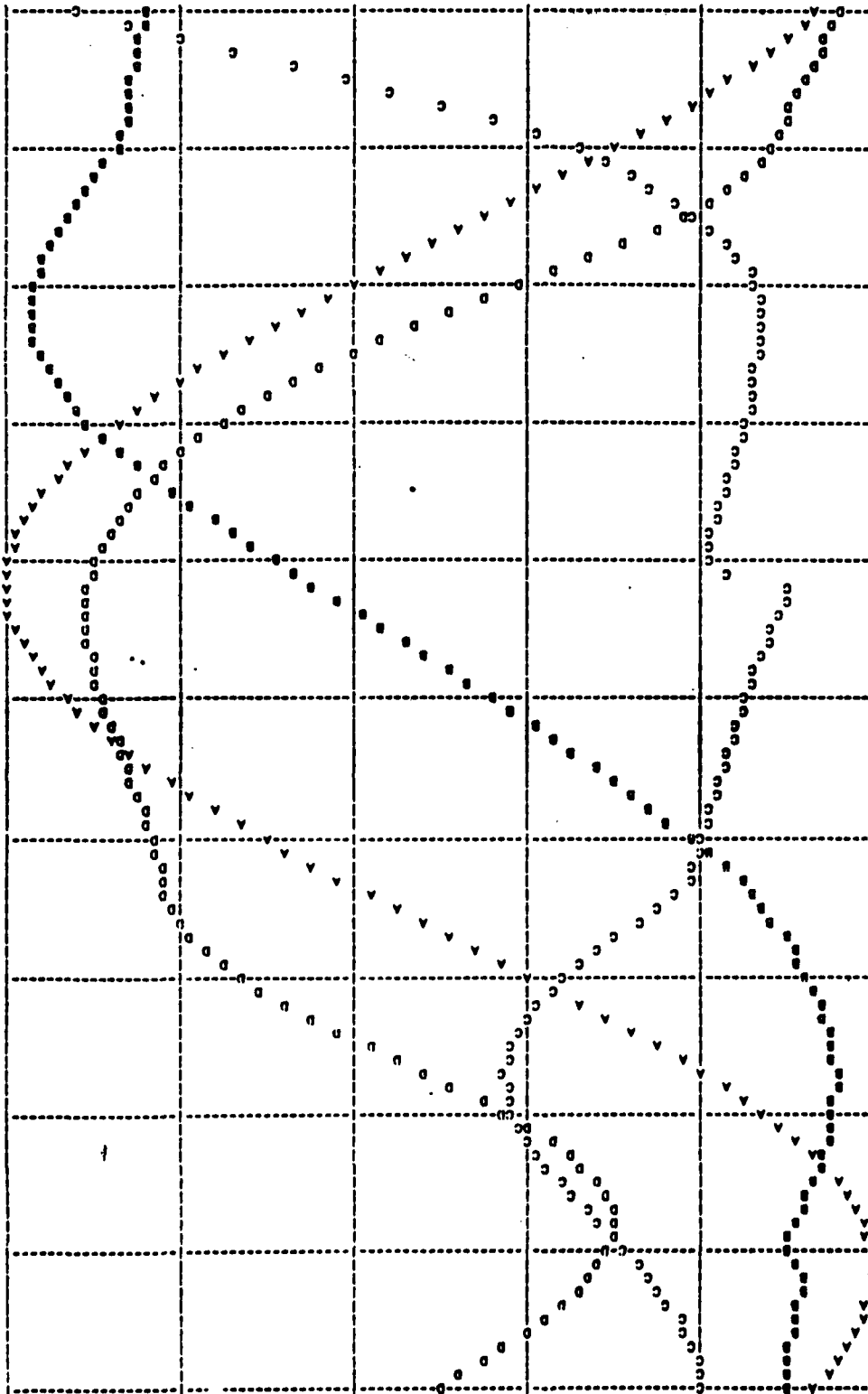


FIGURE 68. SCEPTRE SIMULATION RESULTS FOR THE 3- $\phi$  AC RESONANT CHARGING CIRCUIT OF FIG. 65 (PAGE 1 OF 3) PHASE A.

PIOT - 2

CBM ..... CHARACTER - A  
 VC1B ..... CHARACTER - B  
 VC2B ..... CHARACTER - C  
 ILB ..... CHARACTER - D

1.000E 01	6.000E 02	2.000E 02	-2.000E 02	-6.000E 02	-1.000E 01	CBM
1.000E 01	1.400E 01	1.000E 01	6.000E 02	2.000E 02	-8.000E 02	VC1B
7.200E 02	5.400E 02	3.600E 02	1.000E 02	1.000E 02	-1.000E 02	VC2B
3.000E 00	1.000E 00	6.000E 01	10-3000 9	-6.000E 01	20 3000 00	ILB

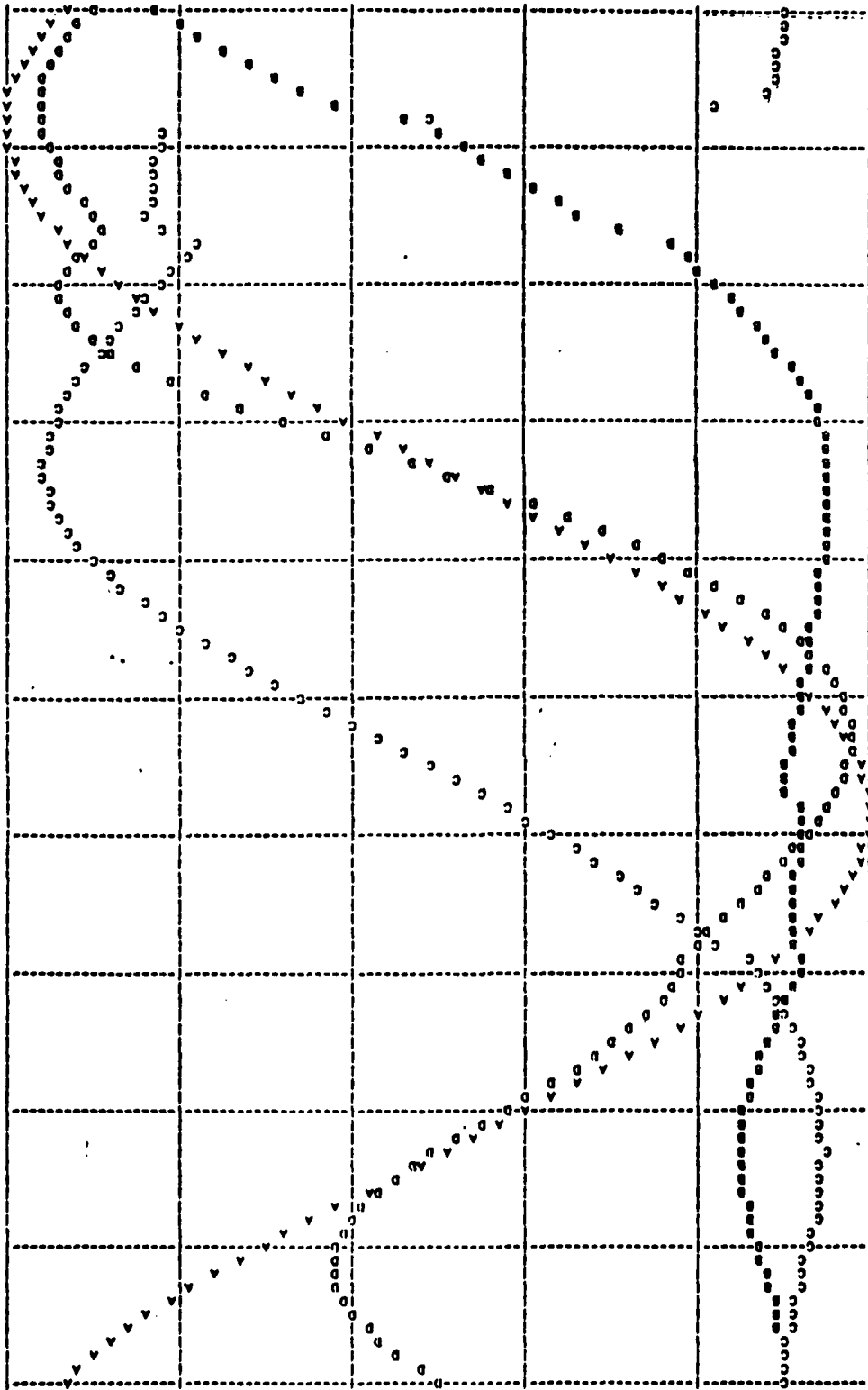


1.000E 01  
 2.000E 01  
 3.000E 01  
 4.000E 01  
 5.000E 01  
 6.000E 01  
 7.000E 01  
 8.000E 01  
 9.000E 01  
 1.000E 02  
 2.000E 02  
 3.000E 02  
 4.000E 02  
 5.000E 02  
 6.000E 02  
 7.000E 02  
 8.000E 02  
 9.000E 02  
 1.000E 03  
 2.000E 03  
 3.000E 03  
 4.000E 03  
 5.000E 03  
 6.000E 03  
 7.000E 03  
 8.000E 03  
 9.000E 03  
 1.000E 04  
 2.000E 04  
 3.000E 04  
 4.000E 04  
 5.000E 04  
 6.000E 04  
 7.000E 04  
 8.000E 04  
 9.000E 04  
 1.000E 05  
 2.000E 05  
 3.000E 05  
 4.000E 05  
 5.000E 05  
 6.000E 05  
 7.000E 05  
 8.000E 05  
 9.000E 05

FIGURE 68. (PAGE 2 OF 3) PHASE B.

PLOT - 3

ECR ..... CHARACTER - A  
 VC1C ..... CHARACTER - B  
 VC2C ..... CHARACTER - C  
 ILC ..... CHARACTER - D



1.000E-05  
 2.000E-05  
 3.000E-05  
 4.000E-05  
 5.000E-05  
 6.000E-05  
 7.000E-05  
 8.000E-05  
 9.000E-05  
 1.000E-04  
 2.000E-04  
 3.000E-04  
 4.000E-04  
 5.000E-04  
 6.000E-04  
 7.000E-04  
 8.000E-04  
 9.000E-04  
 1.000E-03  
 2.000E-03  
 3.000E-03  
 4.000E-03  
 5.000E-03  
 6.000E-03  
 7.000E-03  
 8.000E-03  
 9.000E-03  
 1.000E-02  
 2.000E-02  
 3.000E-02  
 4.000E-02  
 5.000E-02  
 6.000E-02  
 7.000E-02  
 8.000E-02  
 9.000E-02  
 1.000E-01  
 2.000E-01  
 3.000E-01  
 4.000E-01  
 5.000E-01  
 6.000E-01  
 7.000E-01  
 8.000E-01  
 9.000E-01  
 1.000E-00

1.000E-05	1.000E-05	2.000E-05	2.000E-05	2.000E-05	2.000E-05	2.000E-05	ILC
1.000E-05	VC2C						
1.000E-05	VC1C						
1.000E-05	ECR						

FIGURE 68. (PAGE 3 OF 3) PHASE C.

## 9.9 A DC RESONANT CHARGING SYSTEM

Figure 69 shows a DC resonant charging system. A full-bridge controlled rectifier circuit provides DC voltage to a resonant charging load circuit. As for the 3 $\phi$  AC system discussed previously, Silva's circuit source was 6465V/400 Hz whereas the simulation circuit is 1000V/1000 Hz. The switch SW1 simulates a thyatron discharge switch.

One cycle of the source is simulated to demonstrate each rectifier switch firing, then the charging capacitor is discharged. Simulation results are shown in Figure 72.

CPU time for the simulation was 17 min., 33.84 seconds.

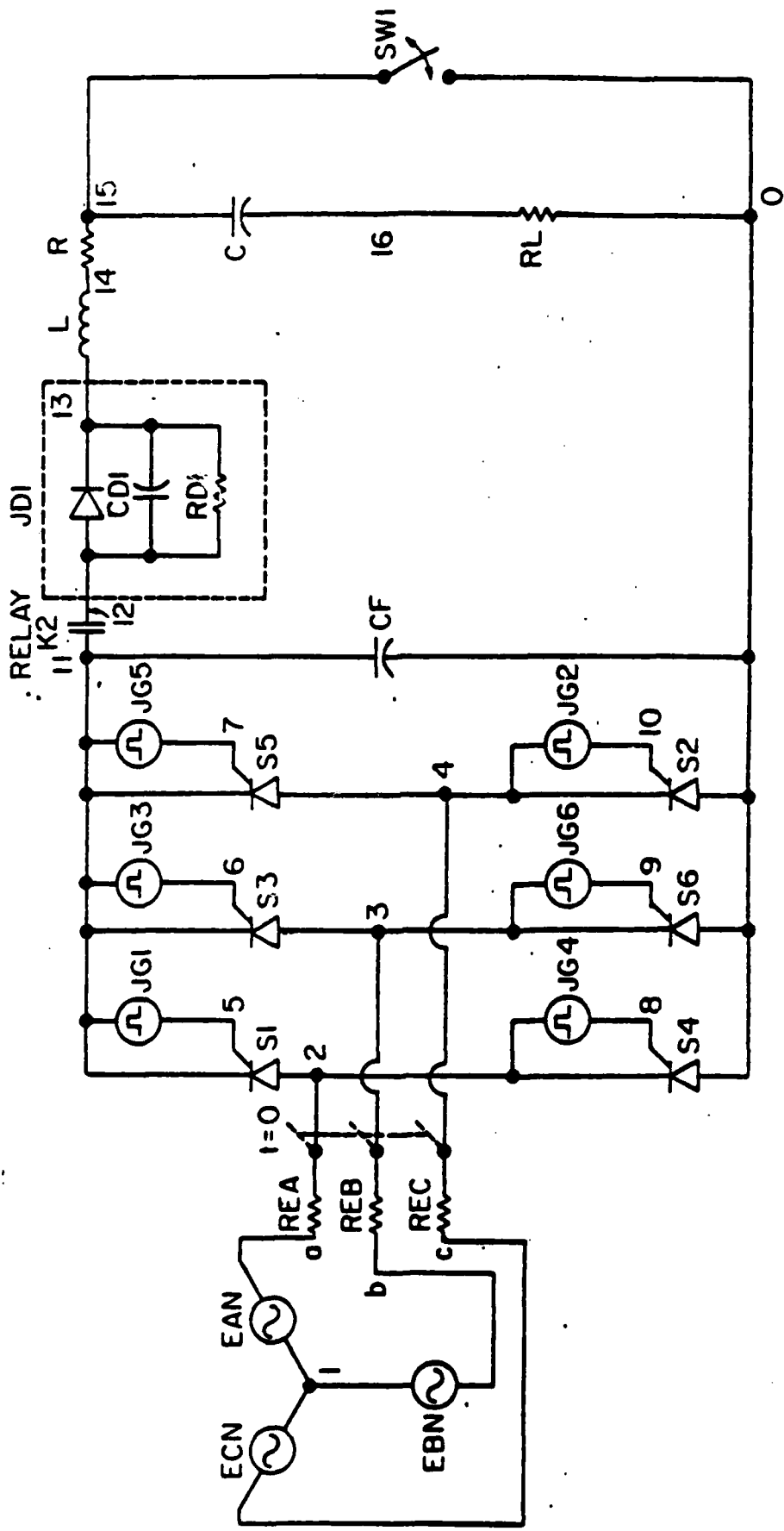


FIGURE 69. A DC RESONANT CHARGING SYSTEM.

# DC RESONANT CHARGING SYSTEM TIMING DIAGRAM

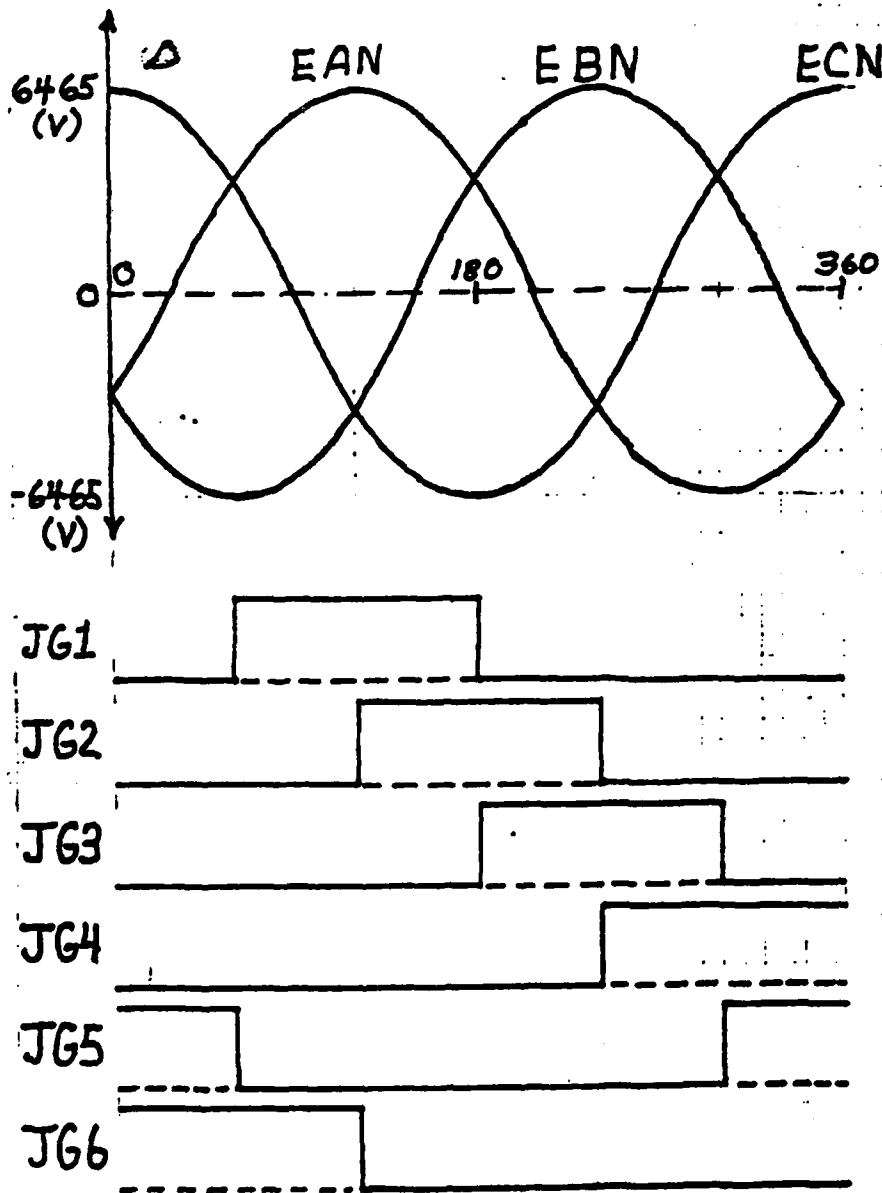


FIGURE 70. GATE TRIGGER DIAGRAM FOR FIG. 69.

```

MODEL DESCRIPTION
MODEL RLY1(1-2)
THIS MODEL REPRESENTS RELAY K2 IN JAMIE SILVA'S CIRCUIT
ELEMENTS
R, 1-2=TABLE 1
FUNCTIONS
TABLE 1
0., 1.E8, 2.5E-5, 1.E8, 2.5E-5, 0., 2.E-3, 0.
MODEL DESCRIPTION
MODEL RLY2(1-2)
THIS MODEL REPRESENTS SWITCH SW1 IN JAMIE SILVA'S CIRCUIT
ELEMENTS
R, 1-2=TABLE 1
FUNCTIONS
TABLE 1
0., 0., 2.0E-5, 0., 2.5E-5, 1.E8, 1.E-3, 1.E8, 1.E-3, 0., 1.02E-3, 0., 1.02E-3,
1.E8, 2.E-3, 1.E8
CIRCUIT DESCRIPTION
THIS CIRCUIT SIMULATES A 1000V/1KHZ RESONANT CHARGING PULSE POWER
SYSTEM.
ELEMENTS
EAN, 1-A=X1(1.D3*DSIN(6285.18*TIME-5.236D-1))
REA, A-2=1.
EBN, 1-B=X2(1.D3*DSIN(6285.18*TIME-2.618))
REB, B-3=1.
ECN, 1-C=X3(1.D3*DSIN(6285.18*TIME+1.5708))
REC, C-4=1.
S1, 2-5-11=MODEL SCR
S2, 0-10-4=MODEL SCR
S3, 3-6-11=MODEL SCR
S4, 0-8-2=MODEL SCR
S5, 4-7-11=MODEL SCR
S6, 0-9-3=MODEL SCR
JG1, 11-5=FGEN(.2, 0., 1.67E-4, 3.33E-4, 1.E-3, TIME, 1)
JG2, 4-10=FGEN(.2, 0., 3.33E-4, 3.33E-4, 1.E-3, TIME, 1)
JG3, 11-6=FGEN(.2, 0., 5.00E-4, 3.33E-4, 1.E-3, TIME, 1)
JG4, 2-8=FGEN(.2, 0., 6.67E-4, 3.33E-4, 1.E-3, TIME, 1)
JG5, 11-7=FGEN(.2, 0., -1.67E-4, 3.33E-4, 1.E-3, TIME, 1)
JG6, 3-9=FGEN(.2, 0., 0., 3.33E-4, 1.E-3, TIME, 1)
CF, 11-0=7.5E-9
K2, 11-12=MODEL RLY1
JD1, 12-13=DIODE Q(1.D-8, 38.61)
CD1, 12-13=5.D-9
RD1, 12-13=1.D4
L, 13-14=.173
R, 14-15=1.E-2
SW1, 15-0=MODEL RLY2
CO, 15-16=.586E-6
RL, 16-0=1.82
OUTPUTS
EAN, VCF, IRL, VCO, PLOT1
IREA, IREB, IREC, PLOT2
RUN CONTROLS
RUN INITIAL CONDITIONS
INTEGRATION ROUTINE = IMPLICIT
PLOT INTERVAL = 1.E-5
MAXIMUM PRINT POINTS=0
STOP TIME=1.02E-3
MINIMUM STEP SIZE = 1.E-30
END

```

FIGURE 71. SCEPTRE INPUT LISTING FOR THE DC RESONANT CHARGING SYSTEM OF FIG. 69.

THIS CIRCUIT SIMULATES A 1000V/100HZ RESONANT CHARGING PULSE POWER SYSTEM.

..... CHARACTER - A  
 ..... CHARACTER - B  
 ..... CHARACTER - C  
 ..... CHARACTER - D  
 CAN  
 VCT  
 INL  
 VCS

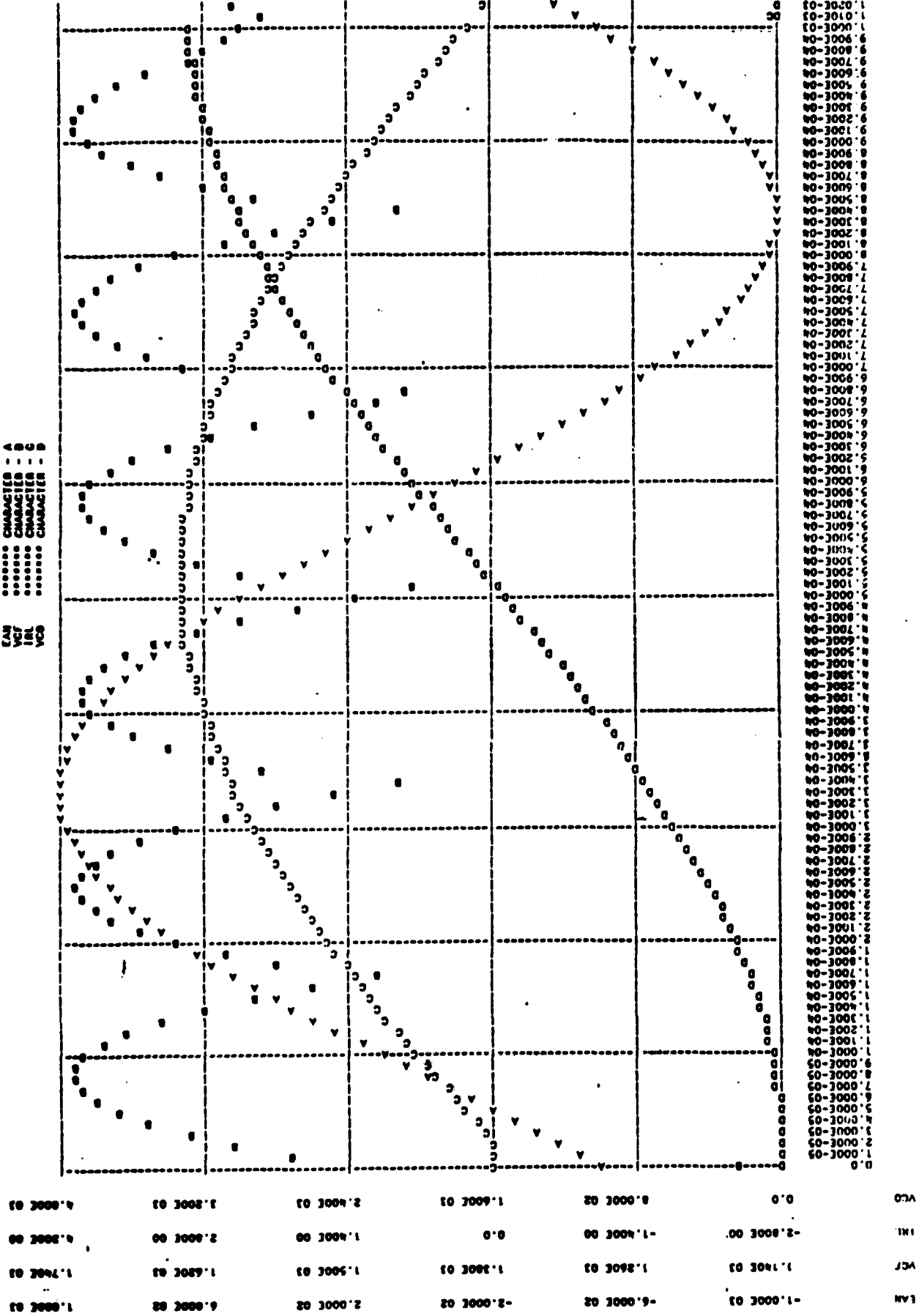


FIGURE 72. SIMULATION RESULTS FOR THE DC RESONANT CHARGING SYSTEM OF FIG. 69 (PAGE 1 OF 2) OUTPUT VOLTAGE.



## SECTION X

### CONCLUSIONS AND RECOMMENDATIONS

#### 10.1 INTRODUCTION

In airborne high power systems, in order to achieve an optimum energy to weight ratio, it may be necessary to design and operate system components in variable ranges and under conditions not covered by available models. For this reason more detailed models were developed for three phase AC generator, three phase transformers and SCR's.

Circuit models and computer program models were developed and the models tested by simulation of typical operating conditions and severe faults.

Consideration was given to the problems of the simulation of the composite system of short time constant electronic components and the long time constants of the generator and transformer.

#### 10.2 SYSTEM VARIABLES

Section V shows that for nonlinear inductors the flux linkages,  $\lambda$ , should be chosen as variables instead of the inductor currents. Similarly for nonlinear capacitors the charges,  $q$ , should be chosen as variables instead of the capacitor voltages. However, in order to use the large body of BJT and SCR modeling work already documented in the literature the decision was made to use the CAD programs SPICE 2 and SCEPTRE.

The use of SPICE 2 and SCEPTRE dictate the use of network currents and voltages as mode or state variables. This choice of variables either

implicitly or explicitly involves terms of the type  $\partial L/\partial i$  or  $\partial c/\partial v$ . Including the terms of the type  $\partial L/\partial i$  in the nonlinear inductors caused problems in the generator model simulations by giving excessive run times. In the generator simulation results reported the  $\partial L/\partial i$  type terms were left out. The total of all  $\partial L/\partial i$  terms was only on the order of 60 volts compared with 15,000 volts rating for the example machine used. However, the large percentage variation of the  $\partial L/\partial i$  terms caused the variable step size program in SCEPTRE to spend excessive time hunting for an appropriate step size. In a different machine this effect may need to be included.

### 10.3 NUMERICAL METHODS FOR STIFF DIFFERENTIAL EQUATIONS

In Section VI integration methods best suited for systems of "stiff differential equations" are considered. It was generally concluded in the references cited therein that implicit integration methods are required. Both SPICE 2 and SCEPTRE offer implicit methods as options.

Even with the larger step size permitted with implicit integration, long run times are required when the step size is determined by the SCR model and the run time is determined by the resonant charging circuit period.

### 10.4 THE GENERATOR MODEL

The generator model developed uses "phase variables" in contrast to "direct and quadrature axis variables."

The model includes direct and quadrature axis damper circuits which may be important with the rapid fluctuation of the load in AC and DC resonant charging applications. In the results section very large damper currents were experienced during balanced and unbalanced faults which were simulated.

The model will allow for consideration of saturation. In the generator simulation runs made, no striking differences were evident in the runs with and without saturation. However, the machine data used was for a typical electric power system generator and it is probable that in an airborne system the equipment will be driven to more extreme limits and saturation effects will be more significant.

No data were available on the prime mover or the field control apparatus, however the form of the model and the SCEPTRE CAD program allow for adding these additional components.

For the results reported reasonable run times were required even for severe faults on the unsaturated and partially saturated cases.

No compatible parameter data were received for generator, transformer and AC and DC charging circuits so a simulation of the composite system was not run. Data and results supplied were not in sufficient detail to test the intricacies of the modeling work done.

#### 10.5 THE TRANSFORMER MODEL

The transformer model is dependent on SCEPTRE to take into account the transformer connections. Thus, the wye-wye or the delta-wye of the AC and DC charging systems pose no problems. The coupling between primary and secondary of a given phase or the coupling between phases are accounted for by expressing the inductances as functions of magnetizing currents. These inductances are computed in a subroutine which must contain measurement or computed data relating inductance to currents.

Thus, a three phase bank of single phase transformers or a three phase three leg core transformer can be represented.

## 10.6 AC AND DC RESONANT CHARGING CIRCUITS

This report has presented research to develop SCR modeling techniques for use with the CAD programs SPICE2 and SCEPTRE. The modeling techniques were employed in simulation of AC and DC resonant charging system load banks.

Research using SPICE2 has examined a method of determining parameters for the two transistor SCR model from SCR specification sheet data. The method is that developed by C. Hu and W. Ki at the University of California at Berkeley. This "Hu-Ki Model" was developed for use with the CAD program SPICE2 also developed at Berkeley by L. W. Nagel. The conclusions resulting from this examination of the "Hu-Ki Model" are as follows.

1. The "Hu-Ki Model" for the SCR provides good simulation of most SCR terminal characteristics with one exception being the SCR turn-off transient behavior. This model requires improvement to be useful in computer simulation of AC Resonant Charging Circuits during commutation.
2. An improved SCR model denoted as the "modified Hu-Ki Model" has been developed in this report. It has been demonstrated to perform satisfactorily through simulation of AC Resonant Charging Circuits having one and two SCR's.
3. SPICE2 computer simulation of power electronic circuits such as AC Resonant Charging Circuits may be performed with sufficient accuracy to serve as a design aid when using the "modified Hu-Ki model". The accuracy of such simulation has been demonstrated through simulation of circuits using two GE C602 LM SCR's which have parameters differing within the normal model mix range of variation. These simulations are accurate enough to show the distinct activity of each SCR and its effect on overall circuit performance.

While it is felt that an advance has been made in SCR modeling to facilitate computer simulation of AC Resonant Charging Circuits, important areas of research remain to be explored. Some regions of interest surfaced during the work of this research. The "modified Hu-Ki model" provides only a functional representation of the terminal characteristics of an SCR. There are several deviations from the true physical activity within an SCR. One of the more gross examples is the use of constant forward current transfer ratio's ( $\alpha$ ) in the transistor models. Another is the use of a constant and extremely small saturation current for the transistors. This latter leads to forward voltage drops in excess of 1V for the J1 and J3 junctions: a substantial deviation from reality for a pn junction. Still other examples exist but are left to the interested to explore.

The SCR model developed for use with SCEPTRE is called the 3-Junction model. The method of parameter determination for this SCEPTRE SCR model is an adaptation of the "modified Hu-Ki model" method used with SPICE2. As modified for SCEPTRE, the procedure of parameter determination is an easy to use ten-step procedure which requires only manufacturer's specification sheet data from which to calculate model parameters. The following conclusions are made as a result of the research with SCEPTRE.

1. The SPICE2 two-transistor SCR model and the associated "modified Hu-Ki" parameter determination procedure is adaptable for use with a similar parameter determination procedure.
2. The three-junction SCR model and the associated parameter determination procedure provides an excellent CAD tool for simulating resonant charging circuits for pulse power applications.

3. The SCEPTRE 3-Junction SCR model may be functional in a variety of network configurations because of the flexibility of SCEPTRE input format. This report presents two configurations called the 3-Junction model and the reduced element count 3-Junction model. The latter of these two was preferred in this research; however, an optimal configuration was not determined.
4. The 3-Junction SCR model is an effective simulation tool for SCEPTRE simulation of AC and DC resonant charging circuits.
5. SCEPTRE computer simulation CPU times are typically larger than with SPICE2. One reason is that SCEPTRE internal subroutines do not have overflow/underflow protection. Consequently, on IBM machines using Fortran G1, traceback routines may be activated excessively.
6. Large signal circuit design such as resonant charging circuits is difficult to say the least and typically requires a great deal of experimenting to achieve the right combination of snubber elements, gate drive times, etc. The work reported in this paper provides a basis for use of the highly cost effective CAD for preliminary design and debug of such circuits.

Excessive underflow and overflow has been determined to occur frequently in SCEPTRE internal subroutines. The problem is therefore not solvable through control of input network description. A solution would entail writing alternative subroutines and incorporating overflow and underflow protection in the subroutines.

The most direct approach would seem to be to take the actual SCEPTRE subroutines, copy them, develop overflow/underflow protection and then input them as user subroutines. The actual Fortran coding of the subroutines is available only from the SCEPTRE program tape as received from the Air Force.

APPENDIX A  
THE GENERATOR MODEL

The purpose of this appendix is to establish the notation and address the approximations and assumptions in the generator model.

A.1 EQUIVALENT CIRCUIT EQUATIONS

Figure 73 shows the three phase generator equivalent circuit. The vector circuit equations are

$$V = RI + \frac{d\lambda}{dt} \quad (82)$$

where

$$V = [v_a, v_b, v_c, v_F, v_D, v_Q]^T \quad (83)$$

$$I = [i_a, i_b, i_c, i_F, i_D, i_Q]^T \quad (84)$$

$$\lambda = [\lambda_a, \lambda_b, \lambda_c, \lambda_F, \lambda_D, \lambda_Q]^T \quad (85)$$

$$R = \begin{bmatrix} r_a & & & & & \\ & r_b & & & & \\ & & r_c & & & \\ & & & r_F & & \\ & & & & r_D & \\ & & & & & r_Q \end{bmatrix} \quad (86)$$

and

$v_a, v_b, v_c$  are the stator phase terminal voltages

$v_F$  is the rotor field terminal voltage

$v_D$  and  $v_Q$  are the damper winding terminal voltages

$i_a, i_b, i_c$  are the stator phase currents

$i_F$  is the rotor field current

$i_D$  and  $i_Q$  are the direct and quadrature damper field currents

$\lambda_a, \lambda_b, \lambda_c, \lambda_F, \lambda_D, \lambda_Q$  are the circuit flux linkages with the subscripts

a, b, c, F, D, Q referring to the same circuits as for V and I.

Generator Model

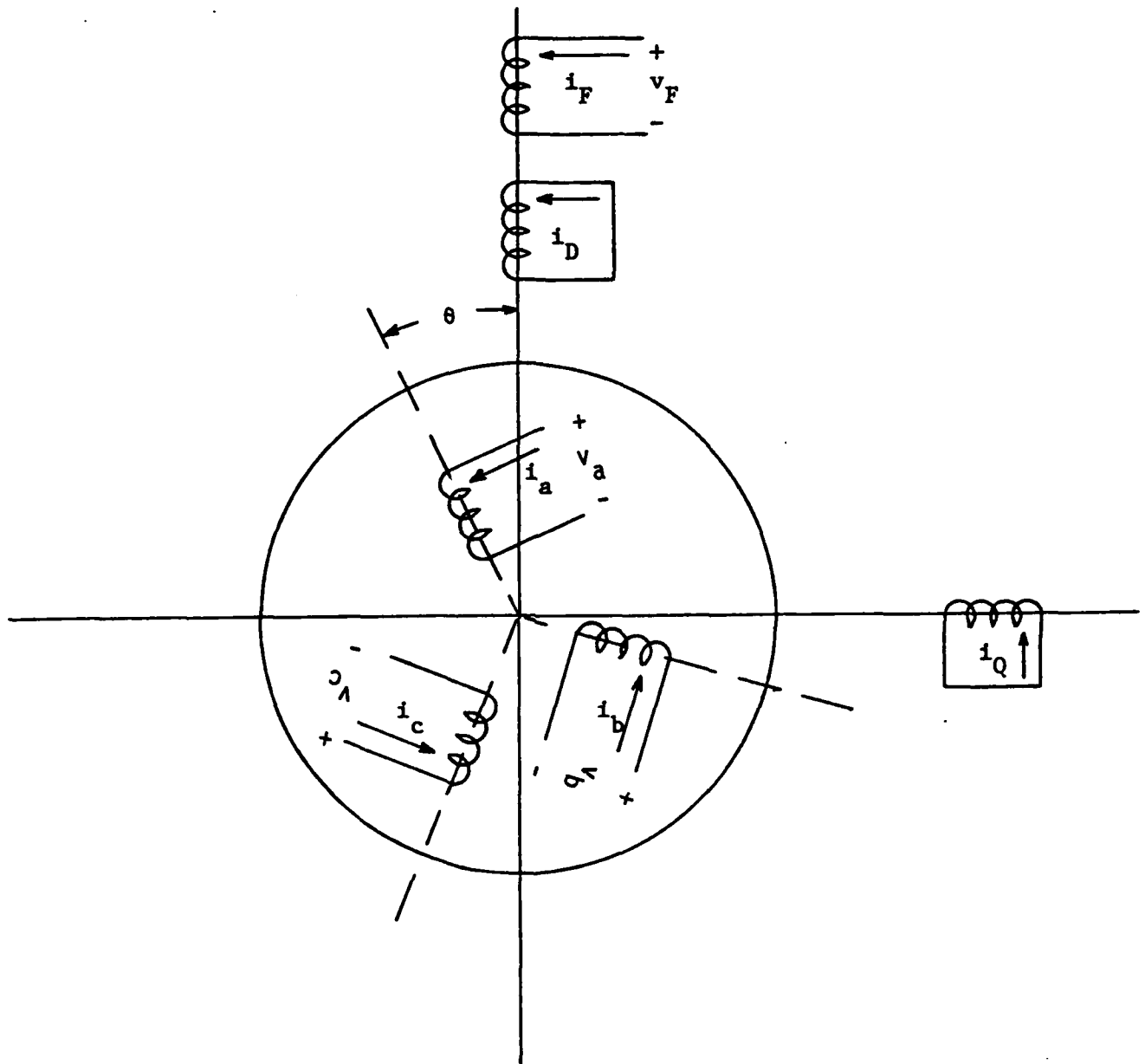


FIGURE 73. IDEALIZED CIRCUIT MODEL OF A THREE-PHASE GENERATOR

In terms of inductances Equation (82) can be written

$$V = RI + \frac{d}{dt} (LI) \quad (87)$$

with the flux linkages defined by

$$\begin{bmatrix} \lambda_a \\ \lambda_b \\ \lambda_c \\ \lambda_F \\ \lambda_D \\ \lambda_Q \end{bmatrix} = \begin{bmatrix} L_{aa} & L_{ab} & L_{ac} & L_{aF} & L_{aD} & L_{aQ} \\ L_{ba} & L_{bb} & L_{bc} & L_{bF} & L_{bD} & L_{bQ} \\ L_{ca} & L_{cb} & L_{cc} & L_{cF} & L_{cD} & L_{cQ} \\ L_{Fa} & L_{Fb} & L_{Fc} & L_{FF} & L_{FD} & L_{FQ} \\ L_{Da} & L_{Db} & L_{Dc} & L_{DF} & L_{DD} & L_{DQ} \\ L_{Qa} & L_{Qb} & L_{Qc} & L_{QF} & L_{QD} & L_{QQ} \end{bmatrix} \begin{bmatrix} i_a \\ i_b \\ i_c \\ i_F \\ i_D \\ i_Q \end{bmatrix} \quad (88)$$

Some approximations and assumptions are implied in the choice of the inductance terms used. These involve the space distribution of the air gap flux and the resulting variation of inductance with rotor position. The inductances are given by the following:

$$L_{aa} = L_s + L_m \cos(2\theta)$$

$$L_{bb} = L_s + L_m \cos 2\left(\theta - \frac{2\pi}{3}\right)$$

$$L_{cc} = L_s + L_m \cos 2\left(\theta + \frac{2\pi}{3}\right)$$

$$L_{ab} = -M_s - L_m \cos 2\left(\theta + \frac{\pi}{3}\right) = L_{ba}$$

$$L_{bc} = -M_s - L_m \cos 2\left(\theta - \frac{\pi}{3}\right) = L_{cb}$$

$$L_{ca} = -M_s - L_m \cos 2\left(\theta + \frac{5\pi}{3}\right) = L_{ac}$$

$$\begin{aligned}
L_{aF} &= M_F \cos(\theta) &= L_{Fa} \\
L_{bF} &= M_F \cos\left(\theta - \frac{2\pi}{3}\right) &= L_{Fb} \\
L_{cF} &= M_F \cos\left(\theta + \frac{2\pi}{3}\right) &= L_{Fc} \\
L_{aD} &= M_D \cos(\theta) &= L_{Da} \\
L_{bD} &= M_D \cos\left(\theta - \frac{2\pi}{3}\right) &= L_{Db} \\
L_{cD} &= M_D \cos\left(\theta + \frac{2\pi}{3}\right) &= L_{Dc} \\
L_{aQ} &= M_Q \sin(\theta) &= L_{Qa} \\
L_{bQ} &= M_Q \sin\left(\theta - \frac{2\pi}{3}\right) &= L_{Qb} \\
L_{cQ} &= M_Q \sin\left(\theta + \frac{2\pi}{3}\right) &= L_{Qc} \\
L_{FF} &= L_F \\
L_{DD} &= L_D \\
L_{QQ} &= L_Q \\
L_{FD} &= M_R = L_{DF} \\
L_{FQ} &= 0 = L_{QF} \\
L_{DQ} &= 0 = L_{QD}
\end{aligned} \tag{89}$$

Figure 74 defines the rotor angle,  $\theta$  used in the inductance expressions  
 $\theta(t) = \omega t$  (90)

## A.2 SATURATION EFFECTS

References 3, 5, 6 show curves of the inductance variation with rotor position,  $\theta$ , similar to the curves of Figure 75. Kimbark (Reference 5) and Anderson (Reference 6) use the same equation form as used here in Equation (89). Smith (Reference 3) uses an  $L_{aa}$  of the form

$$L_{aa} = L_s + L_{m2} \cos(2\theta) + C_{m4} \cos(4\theta) \tag{91}$$

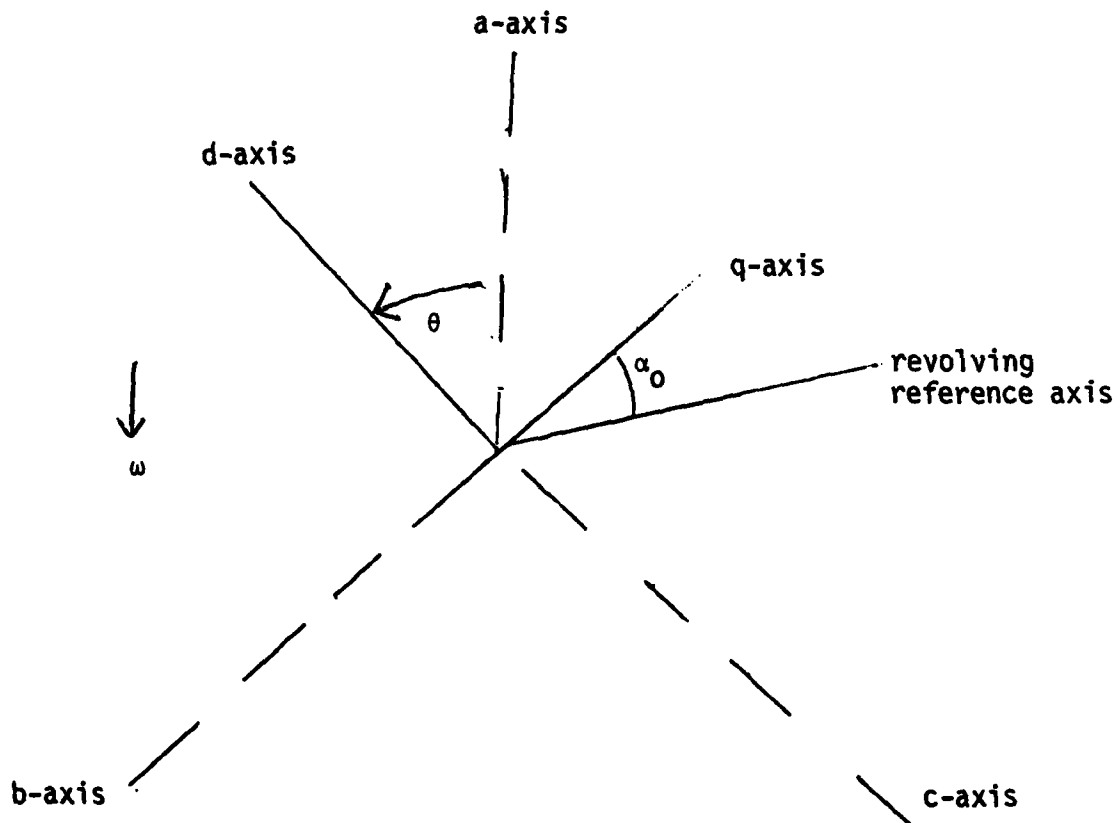


FIGURE 74. CONVENTION FOR DEFINING ROTOR POSITION

the fourth harmonic being due to a third harmonic in the space distribution of the air gap flux. Smith further states that this fourth harmonic is the highest significant harmonic observed over many tests.

The simpler model of Equations (89) was used here for various reasons. First, the inductance model of Equations (89) is a generally accepted model and it is simpler than Smith (Reference 4). This becomes significant when the non-linear terms of  $\frac{\partial L}{\partial I}$  are expanded.

Secondly, the third harmonic in the flux space distribution is evidence of the peaks of the wave being flattened. This effect is due to saturation effects or is at least analogous to saturation effects and saturation effects in our model are being accounted for by direct measurements.

In this work saturation is taken into account by assuming the shape of the curve of inductance variation with  $\theta$  will not change but the inductance coefficients in the equation change. For example the saturated  $L_{aa}$  becomes  $L_{aas}$

$$\begin{aligned} L_{aas} &= C_{aa} L_{aa} = \\ &= C_{aa} L_s + C_{aa} L_m \cos(2\theta) \end{aligned} \quad (92)$$

Where the  $C_{aa}$  is obtained from a measured curve showing the variation of  $L_{aa}$  as a function of a net excitation,  $i_x$ , of the magnetic circuit.

It is clear that more saturation gives a larger third harmonic in the flux space distribution and hence also changes the shape of the inductance curves of Figure 75. According to Smith (Reference 4) this changes the relative amplitude of the fourth harmonic compared to the second. Smith computes his saturated  $L_{aas}$  as follows.

$$L_{aas} = L_{s1} + (1 + \frac{K}{3}) \frac{L_d C_{aa} - L_q}{2} \cos(2\theta) + \frac{K}{3} \frac{L_d C_{aa} + L_q}{2} \cos(4\theta) \quad (93)$$

where

$L_d$  is the direct axis inductance

$L_q$  is the quadrature axis inductance

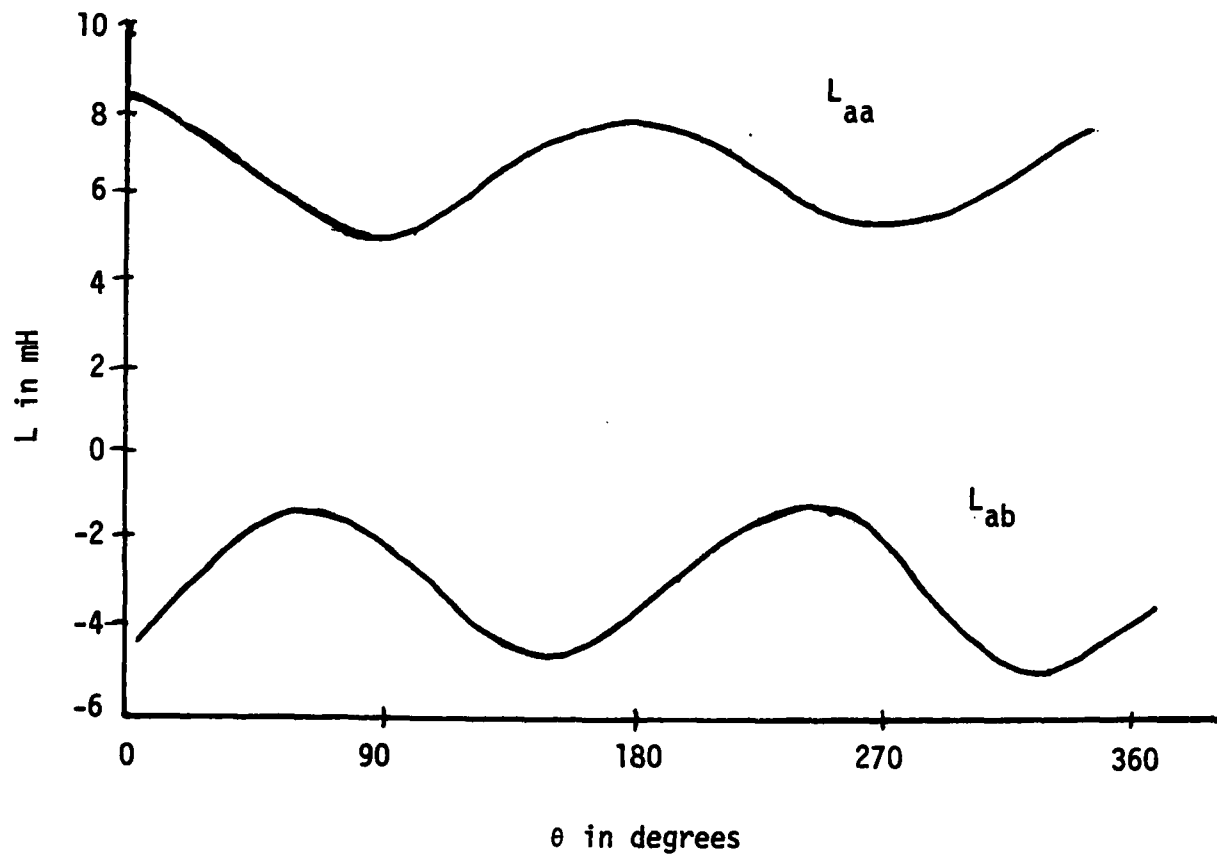


FIGURE 75. VARIATION OF INDUCTANCE WITH  $\theta$

K is the decimal fraction of third harmonic to fundamental flux

$$L_{s1} = \frac{L_d C_{aa} + L_q}{2} \quad (94)$$

Equation (93) assumes saturation effects on the direct axis and no saturative effects on the quadrature axis which seems reasonable for a salient pole machine. Smith does not refer to the fact that K is a function of saturation.

While the Smith formulation Equation (93) does address the fact that saturation would affect the shape of the  $L_{aa}(\theta)$  curve it is quite complex and it is not clear that it would give better results than Equation (92) with measured  $C_{aa}$  since it does include several assumptions and approximations.

This is an area that may be worthy of further investigation if the computer simulation results do not match observations adequately.

### A.3 THE TORQUE EQUATION

The equation relating electrical circuit quantities to mechanical rotation quantities is

$$\frac{d^2\theta}{dt^2} = \frac{1}{J} [T_m - T_e - B \frac{d\theta}{dt}] \quad (95)$$

where

J is the polar moment of inertia of the rotating parts

B represents rotational losses and may include viscous damping and possibly core losses related to rotational speed.

$T_m$  is the mechanical torque input at the shaft

$T_e$  is the so called electric torque developed.

The electrical torque developed is given by the expression

$$T_e = \frac{1}{2} [I]^T \left[ \frac{\partial L}{\partial \theta} \right] [I] \quad (96)$$

The circuit model and Equations (95) and (96) do not include any eddy current or hysteresis loss effects.

These losses are sometimes considered as rotational losses and the B in Equation (95) is adjusted to include them. It is quite common to neglect both the core losses and the viscous damping and omit the B term.

APPENDIX B  
SATURATED GENERATOR MODEL

B.1 SATURATED GENERATOR EQUATIONS

Section II of this report discusses the effects of saturation on the network model. Equations (12) and (13) illustrate the phase "a" equation development. This section shows more detail in the phase "a" equation and also lists the equations for the other phases.

This development is based on the expansion of Equation (32) and (87) of Appendix A. From these we write

$$\frac{d\lambda}{dt} = \frac{d}{dt} (LI) \quad (97)$$

or

$$\frac{d\lambda}{dt} = L \frac{dI}{dt} + \left(\frac{dL}{dt}\right) I \quad (98)$$

The expansion of the matrix products gives as the first row of Equation (98)

$$\begin{aligned} \frac{d\lambda_a}{dt} = & L_{aa} \frac{di_a}{dt} + L_{ab} \frac{di_b}{dt} + L_{ac} \frac{di_c}{dt} + L_{aF} \frac{di_F}{dt} + L_{aD} \frac{di_D}{dt} \\ & + L_{aQ} \frac{di_Q}{dt} + \frac{dL_{aa}}{dt} i_a + \frac{dL_{ab}}{dt} i_b + \frac{dL_{ac}}{dt} i_c + \frac{dL_{aF}}{dt} i_F \\ & + \frac{dL_{aD}}{dt} i_D + \frac{dL_{aQ}}{dt} i_Q \end{aligned} \quad (99)$$

Saturation effects on the first six terms on the right hand side of Equation (99) are as shown in Appendix A Equation (92).

The development of the one derivative term  $\frac{dL_{aa}}{dt}$  is shown in Equation (12) The complete set of terms for  $\frac{d\lambda_a}{dt}$  is now listed

$$\begin{aligned} \frac{d\lambda_a}{dt} = & \left[ N_{Fa} \cos(\theta) i_a \frac{\partial L_{aa}}{\partial i_x} \right] \frac{\partial i_a}{\partial t} + \left[ N_{Fa} \cos(\theta - \frac{2\pi}{3}) i_a \frac{\partial L_{aa}}{\partial i_x} \right] \frac{\partial i_b}{\partial t} \\ & + \left[ N_{Fa} \cos(\theta + \frac{2\pi}{3}) i_a \frac{\partial L_{aa}}{\partial i_x} \right] \frac{\partial i_c}{\partial t} + \left[ i_a \frac{\partial L_{aa}}{\partial i_x} \right] \frac{\partial i_F}{\partial t} + \left[ N_{FD} i_a \frac{\partial L_{aa}}{\partial i_x} \right] \frac{\partial i_D}{\partial t} \end{aligned}$$

$$\begin{aligned}
& - \left[ N_{Fa} i_a \frac{\partial L_{aa}}{\partial i_x} (i_a \sin(\theta) + i_b \sin(\theta - \frac{2\pi}{3}) + i_c \sin(\theta + \frac{2\pi}{3})) \right. \\
& \quad \left. + i_a 2C_{aa}L_m \sin 2\theta \right] \frac{\partial \theta}{\partial t} \\
& + \left[ N_{Fa} \cos(\theta) i_b \frac{\partial L_{ab}}{\partial i_x} \right] \frac{\partial i_a}{\partial t} + \left[ N_{Fa} \cos(\theta - \frac{2\pi}{3}) i_b \frac{\partial L_{ab}}{\partial i_x} \right] \frac{\partial i_b}{\partial t} \\
& + \left[ N_{Fa} \cos(\theta + \frac{2\pi}{3}) i_b \frac{\partial L_{ab}}{\partial i_x} \right] \frac{\partial i_c}{\partial t} + \left[ i_b \frac{\partial L_{ab}}{\partial i_x} \right] \frac{\partial i_F}{\partial t} + \left[ N_{FD} i_b \frac{\partial L_{ab}}{\partial i_x} \right] \frac{\partial i_D}{\partial t} \\
& - \left[ N_{Fa} i_b \frac{\partial L_{ab}}{\partial i_x} (i_a \sin(\theta) + i_b \sin(\theta - \frac{2\pi}{3}) + i_c \sin(\theta + \frac{2\pi}{3})) \right. \\
& \quad \left. + i_b 2C_{aa}L_m \sin(2\theta - \frac{2\pi}{3}) \right] \frac{\partial \theta}{\partial t} \\
& + \left[ N_{Fa} \cos(\theta) i_c \frac{\partial L_{ac}}{\partial i_x} \right] \frac{\partial i_a}{\partial t} + \left[ N_{Fa} \cos(\theta - \frac{2\pi}{3}) i_c \frac{\partial L_{ac}}{\partial i_x} \right] \frac{\partial i_b}{\partial t} \\
& + \left[ N_{Fa} \cos(\theta + \frac{2\pi}{3}) i_c \frac{\partial L_{ac}}{\partial i_x} \right] \frac{\partial i_c}{\partial t} + \left[ i_c \frac{\partial L_{ac}}{\partial i_x} \right] \frac{\partial i_F}{\partial t} + \left[ N_{FD} i_c \frac{\partial L_{ac}}{\partial i_x} \right] \frac{\partial i_D}{\partial t} \\
& - \left[ N_{Fa} i_c \frac{\partial L_{ac}}{\partial i_x} (i_a \sin(\theta) + i_b \sin(\theta - \frac{2\pi}{3}) + i_c \sin(\theta + \frac{2\pi}{3})) \right. \\
& \quad \left. + i_c 2C_{aa}L_m \sin(2\theta - \frac{2\pi}{3}) \right] \frac{\partial \theta}{\partial t} \\
& + \left[ N_{Fa} \cos(\theta) i_F \frac{\partial L_{aF}}{\partial i_x} \right] \frac{\partial i_a}{\partial t} + \left[ N_{Fa} \cos(\theta - \frac{2\pi}{3}) i_F \frac{\partial L_{aF}}{\partial i_x} \right] \frac{\partial i_b}{\partial t} \\
& + \left[ N_{Fa} \cos(\theta + \frac{2\pi}{3}) i_F \frac{\partial L_{aF}}{\partial i_x} \right] \frac{\partial i_c}{\partial t} + \left[ i_F \frac{\partial L_{aF}}{\partial i_x} \right] \frac{\partial i_F}{\partial t} + \left[ N_{FD} i_F \frac{\partial L_{aF}}{\partial i_x} \right] \frac{\partial i_D}{\partial t} \\
& - \left[ N_{Fa} i_F \frac{\partial L_{aF}}{\partial i_x} (i_a \sin(\theta) + i_b \sin(\theta - \frac{2\pi}{3}) + i_c \sin(\theta + \frac{2\pi}{3})) \right. \\
& \quad \left. + i_F C_{aF}M_{aF} \sin(\theta) \right] \frac{\partial \theta}{\partial t}
\end{aligned}$$

$$\begin{aligned}
& + \left[ N_{Fa} \cos(\theta) i_D \frac{\partial L_{aD}}{\partial i_x} \right] \frac{\partial i_a}{\partial t} + \left[ N_{Fa} \left( \cos \theta - \frac{2\pi}{3} \right) i_D \frac{\partial L_{aD}}{\partial i_x} \right] \frac{\partial i_b}{\partial t} \\
& + \left[ N_{Fa} \cos\left(\theta + \frac{2\pi}{3}\right) i_D \frac{\partial L_{aD}}{\partial i_x} \right] \frac{\partial i_c}{\partial t} + \left[ i_D \frac{\partial L_{aD}}{\partial i_x} \right] \frac{\partial i_F}{\partial t} + \left[ N_{FD} i_D \frac{\partial L_{aD}}{\partial i_x} \right] \frac{\partial i_D}{\partial t} \\
& - \left[ N_{Fa} i_D \frac{\partial L_{aD}}{\partial i_x} (i_a \sin(\theta) + i_b \sin(\theta - \frac{2\pi}{3}) + i_c \sin(\theta + \frac{2\pi}{3})) \right. \\
& \quad \left. + i_D C_{aD} M_{aD} \sin \theta \right] \frac{\partial \theta}{\partial t} \\
& + \left[ N_{Fa} \cos(\theta) i_Q \frac{\partial L_{aQ}}{\partial i_x} \right] \frac{\partial i_a}{\partial t} + \left[ N_{Fa} \cos\left(\theta - \frac{2\pi}{3}\right) i_Q \frac{\partial L_{aQ}}{\partial i_x} \right] \frac{\partial i_b}{\partial t} \\
& + \left[ N_{Fa} \left( \cos \theta + \frac{2\pi}{3} \right) i_Q \frac{\partial L_{aQ}}{\partial i_x} \right] \frac{\partial i_c}{\partial t} + \left[ i_Q \frac{\partial L_{aQ}}{\partial i_x} \right] \frac{\partial i_F}{\partial t} + \left[ N_{FD} i_Q \frac{\partial L_{aQ}}{\partial i_x} \right] \frac{\partial i_D}{\partial t} \\
& - \left[ N_{Fa} i_Q \frac{\partial L_{aQ}}{\partial i_x} (i_a \sin(\theta) + i_b \sin(\theta - \frac{2\pi}{3}) + i_c \sin(\theta + \frac{2\pi}{3})) \right. \\
& \quad \left. - i_Q C_{aQ} M_{aQ} \cos(\theta) \right] \frac{\partial \theta}{\partial t} \\
& + L_{aa} \frac{di_a}{dt} + L_{ab} \frac{di_b}{dt} + L_{ac} \frac{di_c}{dt} + L_{aF} \frac{di_F}{dt} + L_{aD} \frac{di_D}{dt} + L_{aQ} \frac{di_Q}{dt} \quad (100)
\end{aligned}$$

To make the expression appear less formidable the following terms are defined,

$$A_a = i_a \frac{\partial L_{aa}}{\partial i_x} + i_b \frac{\partial L_{ab}}{\partial i_x} + i_c \frac{\partial L_{ac}}{\partial i_x} + i_F \frac{\partial L_{aF}}{\partial i_x} + i_D \frac{\partial L_{aD}}{\partial i_x} + i_Q \frac{\partial L_{aQ}}{\partial i_x} \quad (101)$$

$$B_a = N_{Fa} \left[ i_a \sin(\theta) + i_b \sin\left(\theta - \frac{2\pi}{3}\right) + i_c \sin\left(\theta + \frac{2\pi}{3}\right) \right], \quad (102)$$

and 
$$C_a = 2C_{aa} L_m \left[ i_a \sin(2\theta) + i_b \sin\left(2\theta - \frac{2\pi}{3}\right) + i_c \sin\left(\theta + \frac{2\pi}{3}\right) \right] \quad (103)$$

The voltage generated in phase "a" can now be written more compactly as

$$\begin{aligned}
 \frac{d\lambda_a}{dt} = & \left[ A_a N_{Fa} \cos(\theta) + C_{aa} (L_s + L_m \cos(2\theta)) \right] \frac{di_a}{dt} \\
 & + \left[ A_a N_{Fa} \cos\left(\theta - \frac{2\pi}{3}\right) + C_{aa} (-M_s + L_m \cos(2\theta - \frac{2\pi}{3})) \right] \frac{di_b}{dt} \\
 & + \left[ A_a N_{Fa} \cos\left(\theta + \frac{2\pi}{3}\right) + C_{aa} (-M_s + L_m \cos(2\theta + \frac{2\pi}{3})) \right] \frac{di_c}{dt} \\
 & + \left[ A_a + C_{aF} M_{aF} \cos(\theta) \right] \frac{di_F}{dt} + \left[ A_a N_{FD} + C_{aD} M_{aD} \cos(\theta) \right] \frac{di_D}{dt} \\
 & + C_{aQ} M_{aQ} \sin(\theta) \frac{di_Q}{dt} \\
 & - \left[ B_a A_a + C_a + (i_F C_{aF} M_{aF} + i_D C_{aD} M_{aD}) \sin(\theta) - i_Q C_{aQ} M_{aQ} \cos(\theta) \right] \frac{d\theta}{dt} \quad (104)
 \end{aligned}$$

For the other generator circuits the results are now listed

$$\begin{aligned}
 \frac{d\lambda_b}{dt} = & \left[ A_b N_{Fa} \cos(\theta) - C_{aa} M_s + C_{aa} L_m \cos(2\theta - \frac{2\pi}{3}) \right] \frac{di_a}{dt} \\
 & + \left[ A_b N_{Fa} \cos\left(\theta - \frac{2\pi}{3}\right) + C_{aa} L_s + C_{aa} L_m \cos(2\theta + \frac{2\pi}{3}) \right] \frac{di_b}{dt} \\
 & + \left[ A_b N_{Fa} \cos\left(\theta + \frac{2\pi}{3}\right) - C_{aa} M_s - C_{aa} L_m \cos(2\theta) \right] \frac{di_c}{dt} \\
 & + \left[ A_b + C_{aF} M_{aF} \cos\left(\theta - \frac{2\pi}{3}\right) \right] \frac{di_F}{dt} \\
 & + \left[ A_b N_{FD} + C_{aD} M_{aD} \cos\left(\theta - \frac{2\pi}{3}\right) \right] \frac{di_D}{dt} \\
 & + \left[ C_{aQ} M_{aQ} \sin\left(\theta - \frac{2\pi}{3}\right) \right] \frac{di_Q}{dt} \\
 & - \left[ A_b B_a + 2C_b C_{aa} L_m + (C_{aF} M_{aF} i_F + C_{aD} M_{aD} i_D) \sin\left(\theta - \frac{2\pi}{3}\right) \right. \\
 & \quad \left. - C_{aQ} M_{aQ} i_Q \cos\left(\theta - \frac{2\pi}{3}\right) \right] \frac{d\theta}{dt} \quad (105)
 \end{aligned}$$

where

$$A_b = i_a \frac{\partial L_{ba}}{\partial i_x} + i_b \frac{\partial L_{bb}}{\partial i_x} + i_c \frac{\partial L_{bc}}{\partial i_x} + i_F \frac{\partial L_{bF}}{\partial i_x} + i_D \frac{\partial L_{bD}}{\partial i_x} + i_Q \frac{\partial L_{bQ}}{\partial i_x} \quad (106)$$

$$C_b = i_a \sin(2\theta - \frac{2\pi}{3}) + i_b \sin(2\theta + \frac{2\pi}{3}) + i_c \sin(2\theta) \quad (107)$$

$$\begin{aligned} \frac{d\lambda_c}{dt} = & \left[ A_{cN_{Fa}} \cos(\theta) - C_{aa}M_s + C_{aa}L_m \cos(2\theta + 120) \right] \frac{di_a}{dt} \\ & + \left[ A_{cN_{Fa}} \cos(\theta - 120) - C_{aa}M_s + C_{aa}L_m \cos(2\theta) \right] \frac{di_b}{dt} \\ & + \left[ A_{cN_{Fa}} \cos(\theta + 120) - C_{aa}L_s + C_{aa}L_m \cos(2\theta - 120) \right] \frac{di_c}{dt} \\ & + \left[ A_c + C_{aF}M_{aF} \cos(\theta + 120) \right] \frac{di_F}{dt} \\ & + \left[ A_{cN_{FD}} + C_{aD}M_{aD} \cos(\theta + 120) \right] \frac{di_D}{dt} \\ & + \left[ C_{aQ}M_{aQ} + \sin(\theta + 120) \right] \frac{di_Q}{dt} \\ & - \left[ A_{cB_a} + 2 C_c C_{aa}L_m + (C_{aF}M_{aF} i_F + C_{aD}M_{aD} i_D) \sin(\theta + 120) \right. \\ & \quad \left. - M_{aQ} i_Q \cos(\theta + 120) \right] \frac{d\theta}{dt} \quad (108) \end{aligned}$$

Where 
$$A_c = i_a \frac{\partial L_{ca}}{\partial i_x} + i_b \frac{\partial L_{cb}}{\partial i_x} + i_c \frac{\partial L_{cc}}{\partial i_x} + i_F \frac{\partial L_{cF}}{\partial i_x} + i_D \frac{\partial L_{cD}}{\partial i_x} + L_Q \frac{\partial L_{cQ}}{\partial i_x} \quad (109)$$

$$C_c = i_a \sin(2\theta + 120) + i_b \sin(2\theta) + i_c \sin(2\theta - 120) \quad (110)$$

$$\begin{aligned} \frac{d\lambda_F}{dt} = & \left[ A_{FN_{Fa}} \cos(\theta) + C_{aF}M_{aF} \cos(\theta) \right] \frac{\partial i_a}{\partial t} \\ & + \left[ A_{FN_{Fa}} \cos(\theta - 120) + C_{aF}M_{aF} \cos(\theta - 120) \right] \frac{\partial i_b}{\partial t} \end{aligned}$$

$$\begin{aligned}
& + \left[ A_F N_{Fa} \cos(\theta + 120) + C_{aF} M_{aF} \cos(\theta + 120) \right] \frac{\partial i_c}{\partial t} \\
& + \left[ A_F + C_{FF} L_F \right] \frac{\partial i_F}{\partial t} \\
& + \left[ A_F N_{FD} + C_{FD} M_R \right] \frac{\partial i_D}{\partial t} \\
& - \left[ B_a A_F - C_F C_{aF} M_{aF} \right] \frac{\partial \theta}{\partial t} \tag{111}
\end{aligned}$$

where

$$A_F = i_a \frac{\partial L_{Fa}}{\partial i_x} + i_b \frac{\partial L_{Fb}}{\partial i_x} + i_c \frac{\partial L_{Fc}}{\partial i_x} + i_F \frac{\partial L_{FF}}{\partial i_x} + i_D \frac{\partial L_{FD}}{\partial i_x} \tag{112}$$

$$C_F = i_a \sin(\theta) + i_b \sin(\theta - 120) + i_c \sin(\theta + 120) \tag{113}$$

$$\begin{aligned}
\frac{d\lambda_D}{dt} &= \left[ A_D N_{Fa} \cos \theta + C_{aD} M_{aD} \cos(\theta) \right] \frac{di_a}{dt} \\
& + \left[ A_D N_{Fa} \cos(\theta - 120) + C_{aD} M_{aD} \cos(\theta - 120) \right] \frac{di_b}{dt} \\
& + \left[ A_D N_{Fa} \cos(\theta + 120) + C_{aD} M_{aD} \cos(\theta + 120) \right] \frac{di_c}{dt} \\
& + \left[ A_D + C_{FD} M_R \right] \frac{di_F}{dt} \\
& + \left[ N_{FD} A_D + C_{DD} L_D \right] \frac{di_D}{dt} \\
& - \left[ B_a A_D + C_{aD} M_{aD} C_D \right] \frac{d\theta}{dt} \tag{114}
\end{aligned}$$

where

$$A_D = i_a \frac{\partial L_{Da}}{\partial i_x} + i_b \frac{\partial L_{Db}}{\partial i_x} + i_c \frac{\partial L_{Dc}}{\partial i_x} + i_F \frac{\partial L_{DF}}{\partial i_x} + i_D \frac{\partial L_{DD}}{\partial i_x} \tag{115}$$

$$C_D = i_a \sin(\theta) + i_b \sin(\theta - 120) + i_c \sin(\theta + 120) \tag{116}$$

$$\begin{aligned}
\frac{d\lambda_Q}{dt} = & \left[ C_{aQ} M_{aQ} \sin(\theta) \right] \frac{\partial i_a}{\partial t} \\
& + \left[ C_{aQ} M_{aQ} \sin(\theta - 120) \right] \frac{\partial i_b}{\partial t} \\
& + \left[ C_{aQ} M_{aQ} \sin(\theta + 120) \right] \frac{\partial i_c}{\partial t} \\
& + \left[ L_Q \right] \frac{\partial i_Q}{\partial t} \\
& + \left[ C_Q M_{aQ} \right] \frac{\partial \theta}{\partial t}
\end{aligned} \tag{117}$$

where  $C_Q = i_a \cos(\theta) + i_b \cos(\theta - 120) + i_c \cos(\theta + 120)$  (118)

## APPENDIX C

### GENERATOR DATA USED

Considerable difficulty was encountered in obtaining data for the machine model. Data were needed to test the model performance. Some data were supplied by the Air Force through technical publications AFAPL-TR-75-87 and AFAPL-TR-77-31. In both publications the data were incomplete even for a fairly standard model. In one of the publications the data purported to have been used was inconsistent in the sense that it gave mutual inductance with coefficients of coupling that were greater than unity. This problem was identified after spending considerable time and effort and having several unsuccessful computer runs. Further, neither of the above reports contained any useful saturation data. The needed data is not available currently.

#### C.1 UNSATURATED GENERATOR DATA

In order to have data for a real machine and move forward with the simulation, data were taken for a machine from Reference 6. No usable saturation data were available from this reference. Saturation conditions were simulated using trend curves from Reference 3.

The machine data used are listed below. These are unsaturated values.

Balanced three phase 60 Hz Generator

$$L_s = 4.152 \text{ mH}$$

$$L_m = 0.074 \text{ mH}$$

$$L_F = 2.189 \text{ H}$$

$$L_D = 5.989 \text{ mH}$$

$$L_Q = 1.423 \text{ mH}$$

$$M_s = 2.076 \text{ mH}$$

$$M_F = 89.006 \text{ mH}$$

$$M_D = 4.721 \text{ mH}$$

$$M_Q = 2.269 \text{ mH}$$

$$M_R = 0.108994 \text{ H}$$

Rated Power 160 MVA

Rated Voltage 15 KV (line to line)

Inertia Constant H = 2.37 sec.

$$R_a = 0.001542 \ \Omega$$

$$R_F = 0.371 \ \Omega$$

$$R_D = 0.018421 \ \Omega$$

$$R_Q = 0.018969 \ \Omega$$

rated field excitation voltage = 375 volts

## C.2 SATURATION DATA

The additional data required for the model are saturation data. It will be necessary to measure or determine in some other manner this saturation data for the specific machine being modeled. Measurement methods are discussed briefly in subsequent paragraphs.

For the purpose of obtaining numbers for the machine model used to test the computer model, curve data were used from Smith and Snider (Reference 3,4). These curves were normalized and applied to the above machine data. The premise in measurement of this saturation data is that saturation is dependent on some net equivalent field excitation

$$i_x = i_F + N_{FD} i_D + N_{Fa} \left[ i_a \cos(\theta) + i_b \cos\left(\theta - \frac{2\pi}{3}\right) + i_c \cos\left(\theta + \frac{2\pi}{3}\right) \right] \quad (119)$$

The excitation level can be obtained by varying only  $i_F$ . The incremental inductances are obtained by perturbing the various other currents, say  $\Delta i_a$ , for incremental  $L_{aa}$ . Integrated incremental inductances give saturated inductances. Thus a plot of  $L_{aa}$  versus  $i_F$  with  $\theta = 0$  gives appropriate saturation data for the "a" phase self inductance. Data for the plot of  $L_{aa}$  vs  $i_F$  is normalized and put into an algebraic equation form using a least square regression analysis. The following form is obtained from the  $L_{aa}$  versus  $i_F$  data

$$C_{aa} = a_{10} + a_{11} i_x + a_{12} i_x^2 + a_{13} i_x^3 \quad (120)$$

Saturation data must be determined for  $L_{aa}$ ,  $L_{aF}$ ,  $L_{DD}$ ,  $L_{aD}$ ,  $L_{FD}$ . From these the regression coefficients for the C's are found:  $C_{aa}$ ,  $C_{FF}$ ,  $L_{DD}$ ,  $C_{aF}$ ,  $C_{AD}$ ,  $C_{aQ}$ ,  $C_{FD}$ .

Table 11 lists the coefficients used in the simulation. These were obtained by reading data from curves given by Smith and Snider (Reference 3) and are not necessarily correct or typical for the machine used here. The ballistic method described in Snider and Smith (Reference 3,4) permits the measurement of saturated incremental inductances. These are integrated into the saturated inductance curves.

### C.3 MEASUREMENT OF THE UNSATURATED INDUCTANCES

#### 1. $L_s$ and $L_m$

With the rotor locked into position ( $\theta = 0^\circ$ ), measure the inductance of phase A of the stator. The measured inductance is  $L_s + L_m$ . Rotate the rotor and lock into position ( $\theta = 45^\circ$ ). Measure the inductance of phase A of the stator. The measured inductance is  $L_s$ .

Rotate the rotor and lock into position ( $\theta = 90^\circ$ ). Measure the inductance of phase A of the stator. The measured value is  $L_s - L_m$ . Compare all measured values.

TABLE II. SATURATION COEFFICIENTS

	$a_{j0}$	$a_{j1}$	$a_{j2}$	$a_{j3}$
aa	0.98367	$-2.9246 \times 10^{-5}$	$-1.0771 \times 10^{-7}$	$2.0394 \times 10^{-11}$
FF	1.0088	$-2.9867 \times 10^{-5}$	$-1.0519 \times 10^{-7}$	$1.8699 \times 10^{-11}$
DD	0.97827	$-2.1569 \times 10^{-5}$	$-7.9586 \times 10^{-8}$	$1.5930 \times 10^{-11}$
AF	1.0000	$-6.9202 \times 10^{-5}$	$-8.4819 \times 10^{-8}$	$1.6303 \times 10^{-11}$
AD	0.9886	$-8.0120 \times 10^{-5}$	$-6.1443 \times 10^{-8}$	$1.2983 \times 10^{-11}$
AQ	0.99419	$-2.6322 \times 10^{-5}$	$-5.5511 \times 10^{-8}$	$1.0182 \times 10^{-11}$
DF	1.0007	$-6.9355 \times 10^{-5}$	$-6.6663 \times 10^{-8}$	$1.3054 \times 10^{-11}$

$$C_{xx} = a_{j0} + a_{j1} i_x + a_{j2} i_x^2 + a_{j3} i_x^3$$

2.  $\underline{L}_S$  and  $\underline{M}_S$

With the rotor locked into position ( $\theta = 105^\circ$ ), connect a sinusoidal voltage source between phase A and neutral of the stator. Measure the RMS current flow in phase A. Measure the resultant RMS voltage induced between phase B and neutral. The mutual inductance between phase A and Phase B is computed as

$$-M_S = \frac{V_{b-N}(\text{RMS})}{\omega I_a(\text{RMS})} ,$$

where  $\omega$  is the radian frequency of the phase A current. The quantity  $M_S$  should be positive and should be smaller than  $L_S$ .

With the rotor locked into position ( $\theta = 60^\circ$ ), measure  $V_{b-N}$  and  $I_a$  as before. The result yields  $L_m - M_S$ . With the rotor locked into position ( $\theta = 150^\circ$ ), measure  $V_{b-N}$  and  $I_a$  as before. Calculation results in  $-M_S - L_m$ . Compare values of  $M_S$ .

3.  $\underline{L}_F$

Measure the field coil inductance directly.

4.  $\underline{M}_{aF}$

With the rotor locked into position ( $\theta = 0^\circ$ ), connect a sinusoidal voltage source between the field terminal connections. Measure the RMS current flow in the field coil. Measure the RMS voltage induced between phase A and neutral of the stator. Calculate  $M_{aF}$ .

$$M_{aF} = \frac{V_{a-N}(\text{RMS})}{\omega I_F(\text{RMS})} .$$

5.  $\underline{L}_D$ ,  $\underline{M}_R$ ,  $\underline{R}_F$ ,  $\underline{R}_D$

As measured from the field coil terminals,

$$Z_F = \frac{V_F(\text{RMS})}{I_F(\text{RMS})} = R + j\omega L$$

$$\begin{aligned}
Z_F &= R_F + j\omega L_F + \frac{\omega^2 M_{DF}^2}{R_D + j\omega L_D} \\
&= \left( R_F + \frac{\omega^2 R_D M_{DF}^2}{R_D^2 + \omega^2 L_D^2} \right) - j \left( \frac{\omega^3 M_{DF}^2 L_D}{R_D^2 + \omega^2 L_D^2} \right) \\
&= R_F + R_e + j\omega(L_F + L_e)
\end{aligned}$$

Measure the field coil resistance directly.

$$R_e = R - R_F$$

$$L_e = L - L_F$$

Assume a value of damper resistance  $R_D$

$$M_{DF}^2 = \frac{R_e(R_D^2 + \omega^2 L_D^2)}{\omega^2 R_D^2}$$

$$L_D = -\frac{L_e R_D}{R_e}$$

Note that  $M_R$  and  $M_{FD}$  are the same parameter.

6.  $M_{aQ}$ ,  $L_Q$ ,  $R_A$

As measured from phase A terminals,

$$Z_a = \frac{V_a(\text{RMS})}{I_a(\text{RMS})} = R + j\omega L, \quad Z_a = R_a + j\omega L_a + \frac{\omega^2 M_{aQ}^2}{R_Q + j\omega L_Q},$$

All measurements are taken with the rotor locked into position ( $\theta = 90^\circ$ )

$$\begin{aligned}
Z_a &= \left( R_a + \frac{\omega^2 R_Q M_{aQ}^2}{R_Q^2 + \omega^2 L_Q^2} \right) - j \left( \frac{\omega^3 M_{aQ}^2 L_Q}{R_Q^2 + \omega^2 L_Q^2} \right) \\
&= R_a + R_e + j\omega(L_a + L_e)
\end{aligned}$$

Measure the phase A resistance directly.

$$R_e = R - R_a$$

$$L_e = L - L_a$$

Assume a value of quadrature damper resistance  $R_Q$  (Reference 4)

$$L_Q = -\frac{L_e R_Q}{R_e}$$

$$M_{aQ}^2 = \frac{R_e (R_Q^2 + \omega^2 L_Q^2)}{\omega^2 R_Q^2}$$

7.  $M_{aD}$

With the rotor locked into position ( $\theta = 0^\circ$ ) and the field coil open,

$$Z_a = \frac{V_a (\text{RMS})}{I_a (\text{RMS})} = R + j\omega L$$

$$Z_a = R_a + j\omega L_a + \frac{\omega^2 M_{aD}^2}{R_D + j\omega L_D}$$

$$Z_a = \left( R_a + \frac{\omega^2 R_D M_{aD}^2}{R_D^2 + \omega^2 L_D^2} \right) - j \left( \frac{\omega M_{aD}^2 L_D}{R_D^2 + \omega^2 L_D^2} \right)$$

$$= R_a + R_e + j\omega(L_a + L_e)$$

$$R_e = R - R_a$$

$$L_e = L - L_a$$

$$L_D = -\frac{L_e R_D}{R_e} \quad (\text{compare values})$$

$$M_{aD}^2 = \frac{R_e (R_D^2 + \omega^2 L_D^2)}{\omega^2 L_D^2}$$

APPENDIX D  
USERS MANUAL

Computer Software/Computer Program/Computer Data Base Configuration Items

D.1. INTRODUCTION

This appendix is the Program Documentation or the User's Manual. It contains a listing of the following SCEPTRE programs including necessary subroutines.

1. The three phase AC generator program model
2. The three phase transformer program model
3. The AC resonant charging program
4. The DC resonant charging program

Data are also given for numerical examples so that simulations can be run to test the operation of the models. The data are the same as that used in examples in the body of the report. The data are included in the card decks and in the program listings as well as in line by line description of the program statements in this User's Manual.

Sufficient detail is given in the description of the generator program so that anyone with a minimum knowledge of SCEPTRE should be able to use it in this application. Less detail is given in the documentation of the transformer, the AC resonant charging circuit and DC resonant charging circuit where the detail would be a duplication.

D.2 THREE PHASE GENERATOR MODEL

D.2.1 Introduction

A three phase generator has been modeled using SCEPTRE. The generator

model includes the three stator windings, the field winding, the quadrature axis damper winding and the direct axis damper winding. Also included in the model is variable speed representation. While not included, field voltage control may be applied with small modifications to the existing program. All discussion refers to the attached program listing and elements shown in Figure 78.

#### D.2.2 Job Control Cards

SCEPTRE requires the use of job control cards. Each computer installation must determine the proper job control cards to be used. The job control cards required for use with the IBM 370-3033 installed at Clemson University are included in the program listing.

The first card is for accounting purposes. The record card allows for execution of the SUPERSCEPTRE program. The second card may be appended with additional information to produce a listing of all function subprograms. As listed, no listing of function subprograms is provided. In order to obtain a listing, the card should be changed to

```
//STEP 1 EXEC SUPERSEP, OUT=(SYSOUT=A)
```

The third card causes input data to be read into SCEPTRE.

Immediately following the "END" card are the fourth and fifth job control cards. the "/\*" card denotes the end of program data in SCEPTRE format. If no function subprograms are used, this is the last job control card. If function subprograms are to be included, the fifth job control card must be included.

#### D.2.3 Header Cards

These cards must be included in the program in the sequence shown and must be spelled correctly.. The header cards are listed.

"CIRCUIT DESCRIPTION"  
"ELEMENTS"  
"DEFINED PARAMETERS"  
"FUNCTIONS"  
"OUTPUTS"  
"INITIAL CONDITIONS"  
"RUN CONTROLS"  
"END"

While SCEPTRE allows the use of additional header cards, only those header cards required for the generator model are included or discussed.

#### D.2.4 Description of Input Data

##### D.2.4.1 "ELEMENTS" Section

The "ELEMENTS" section contains all circuit element information required in the generator model. The first character of each circuit element identifies the element types.

"E": voltage source	(e.g., EFI)
"R": resistor	(e.g., RAL)
"L": inductor	(e.g., LII)
"C": capacitor	(e.g., CI)
"J": current source	(e.g., JFI)
"M": mutual inductance	(e.g., M12)

Each circuit element must be identified by a unique alpha-numeric label. The one or two character label is located adjacent to the element type. Several examples are given for illustrative purposes.

EFI: element type = "E"  
label = "FI"

RD-A123 730

DYNAMIC SIMULATION OF AIRBORNE HIGH POWER SYSTEMS(U)  
CLEMSON UNIV SC DEPT OF ELECTRICAL AND COMPUTER  
ENGINEERING R W GILCHRIST ET AL NOV 82

3/3

UNCLASSIFIED

AFWAL-TR-82-2092 F33615-79-C-2047

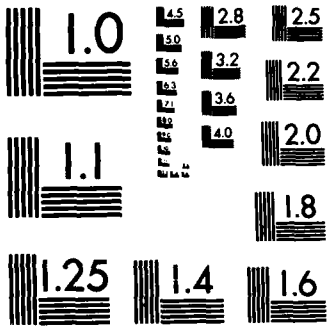
F/G 10/2

NL


END

FORMED

12/82



MICROCOPY RESOLUTION TEST CHART  
NATIONAL BUREAU OF STANDARDS-1963-A

EFI = voltage source number "FI"

LII = inductor number "ll"

RAL = resistor number "AL"

Each circuit element is connected to two nodes. Node connection information is adjacent to the circuit element label. The circuit element label is always separated from the node connection information by a comma. The node connection information includes the "from" node and "to" node connections. The "from" node and "to" node are each two character alpha numeric values and are always separated by a dash.

EFI, 34-0: voltage source number "FI" is connected to "from" node 34 and "to" node 0

RA, 1-11: resistor number "A" is connected to "from" node 1 and "to" node 11.

Designation of "from" node and "to" node determines polarity of voltage across the element and current through the element. SCEPTRE assumes that current always enters the "from" node. Voltage polarity is assumed to be;

a) passive elements (resistor, inductor, capacitor)

"from" node is positive

"to" node is negative

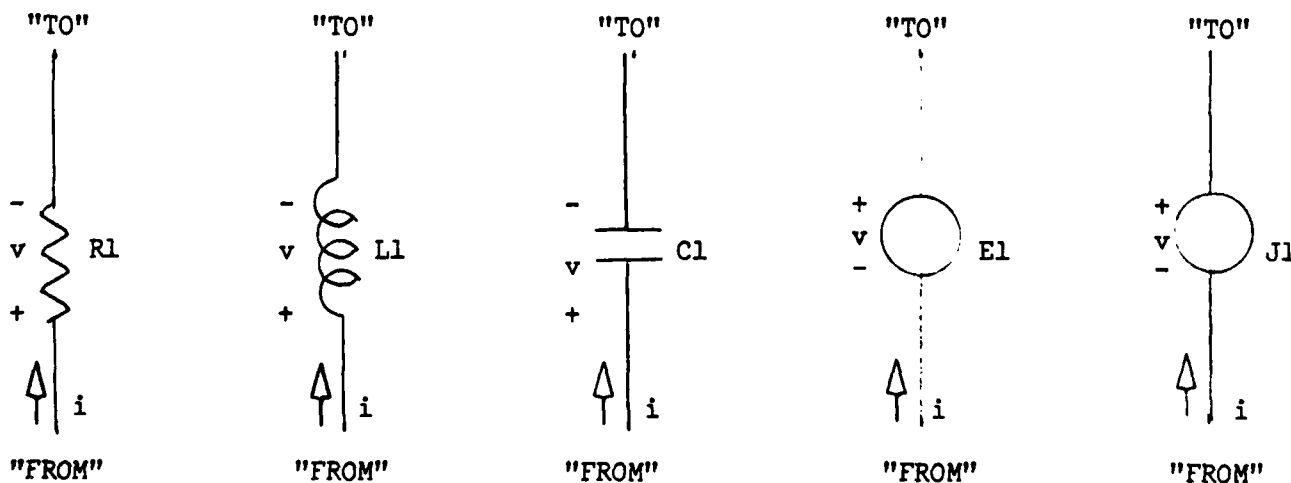


FIGURE 76. SCEPTRE CIRCUIT ELEMENTS WITH VOLTAGE AND CURRENT DIRECTIONS

b) active elements (voltage source, current source)

"from" node is negative

"to" node is positive

Voltage across a circuit element is determined by SCEPTRE by use of the label "V" and the labeled circuit element.

VR1 = voltage across resistor number "1"

VL1 = voltage across inductor number "1"

VC1 = voltage across capacitor number "1"

VJ1 = voltage across current source number "1"

voltage across voltage source (E1) is E1.

Current through a circuit element is determined by SCEPTRE by use of the label "I" and the labeled circuit element.

IR1 = current through resistor number "1"

IL1 = current through inductor number "1"

IC1 = current through capacitor number "1"

Mutual inductance elements do not have actual circuit connections and consequently no "from" node and "to" node data is used. However, a mutual inductance does link two inductors. These two inductors (labeled circuit elements) replace the "from" node and "to" node connections.

M12, L11-L22: mutual inductance number "12" links  
inductor number "11" (L11) to inductor  
number "22" (L22)

The value of any circuit element may be one of the following.

1) Double Precision Constant

EF1, 34-0 = 375.00

2) Defined Parameter

RA, 1-11 = PRA

(Defined parameters will be discussed later)

### 3) Table

RAL, 31-Ø = T1

(Table will be discussed later).

### 4) Expression

M45, L44-L55 = X13 (0.099 \* PCFD)

"X" is the symbol used by SCEPTRE to denote an expression. Each expression must have a unique expression number (e.g., X13). The value of an expression must be enclosed in parentheses. The expression value is an arithmetic statement. Variables used in an expression may be double precision constants, defined parameters, currents, or voltages. It should be noted that any constant enclosed in parentheses must be in double precision format. SCEPTRE in no case will recognize integer values.

### 5) Double Precision Function

E1, 11-21 = FM1 (IL11, ILZZ,...,PCAQ, PCFD)

Elsewhere in the input data is included a double precision function (e.g., FM1). Enclosed in parentheses is a calling list of parameters. This list of parameters may include double precision constants, defined parameters, currents, or voltages. No integer values are allowed. The double precision function is discussed in detail later. It should be noted that function subprograms return a single value. However, if the value of any variable included in the calling list of parameters is replaced by a new value within the function subprogram, then that variable will assumed its new value outside the function subprogram. The function subprogram may in this way be used to change many variable values.

## 6) Equation

M12, L11-L22 = Q2 (1.9D-3, PCAA)

"Q" is the symbol used by SCEPTRE to denote an equation. Alternately, the symbol "EQUATION" may be used. Each equation must have a unique equation number (e.g., Q2). An equation is defined elsewhere in the program and will be discussed later. Enclosed in parentheses is a calling list of parameters. This list may include double precision constants, defined parameters, currents or voltages. No integer values are allowed.

### D.2.4.2 Defined Parameters

"P" is the symbol used by SCEPTRE to denote a defined parameter. A defined parameter is determined only in the defined parameter section of the program. Defined parameters are, in general, values or variables used in several locations in a program. Two uses are of immediate concern.

A generator model uses many constants which are related to actual machine construction and which are measurable. If SCEPTRE is used as a design tool, the defined parameter value of a constant allows for changing of the constant throughout the program by changing only one data entry.

An application may include the formulation of the same algebraic expression many times. A defined parameter will allow for evaluation of that expression once, and will save subsequent evaluations.

Also included under defined parameters is the solution of differential equations.

DPS = X1 (FD2THT(IL11,...,PS))

PS = 376.988D0

The solution of this differential equation is

$$PS = \int_{t_0}^t DPS + \text{constant}$$

where:  $t_0$  = start time

$t_t$  = stop time

constant = initial value

DPS = time derivative of PS

PS = integrated value of DPS and initially contains the  
initial value of PS.

"D" is the symbol used by SCEPTRE to denote a differential equation. Each differential equation must have as its value an expression. This expression must possess a unique statement number and must be followed in the data by an accompanying defined parameter.

#### D.2.4.3 Functions

The Functions section defines both equations and tables. A description of the calling procedure for equations and tables was presented earlier.

EQUATION 1 (A,B,C,D)=(D\*(A+B\*DCOS(2.0D\*PT+C))

"Q" is the symbol used by SCEPTRE to denote an equation. Alternately, the symbol "EQUATION" may be used. Each equation must have a unique equation number (e.g., Q1). Enclosed in parentheses is the symbolic list of calling parameters. To the right of the equality is the equation, enclosed in parentheses, to be evaluated. All arithmetic statement functions and constants must be expressed in double precision form.

Since an equation uses symbolic parameters, the user may use a given equation many times in a program by providing different sets of calling parameters. Defined parameters are assigned to common statements internally to SCEPTRE and consequently may be used in an equation.

TABLE 1

0.D0, 0.D0, 0.5D0, 1.0D0, 0.5D0, 2.0D0, 3.0D0, 3.0D0

"T" is the symbol used by SCEPTRE to denote a table. Alternately, the symbol "TABLE" may be used. Each table must have a unique table number (e.g., T1). The data card immediately following a table identification card contains the data necessary for construction of a table. A table describes a piece-wise linear function as a function of time. Odd-numbered data are values of time while even-numbered data are values of the described function. The example given above may be plotted.

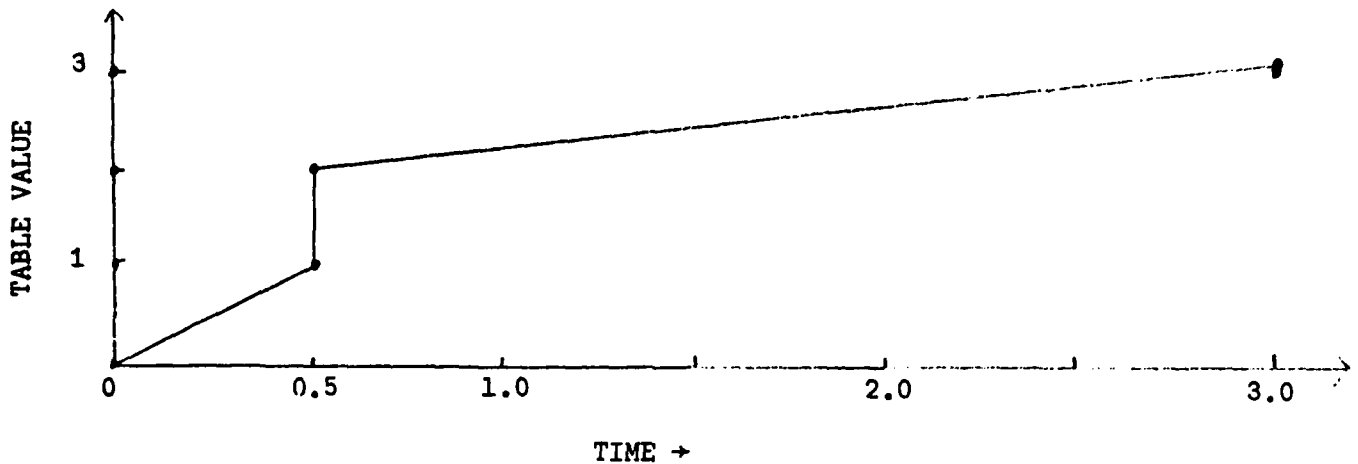


FIGURE 77. ILLUSTRATION OF SCEPTRE TABLE OF VALUES

At any given time (time=t), SCEPTRE will use linear interpolation to determine the value of table.

#### D.2.4.4 Outputs

Plots of any variable -vs- time may be obtained. In order to obtain a plot of a single variable, the statement "PLOT" is used

IL11, IL22, IL33, PLOT

This statement will provide a separate plot of each variable. Plots of more than one variable may be obtained as well as plots of one variable -vs- a second variable.

#### D.2.4.5 Run Controls

SCEPTRE may be controlled by use of input data for any allowable control function. Included in the listing are a few of the allowed controls.

INTEGRATION ROUTINES = IMPLICIT

SCEPTRE allows numerical integration by the Backward Euler Algorithm (IMPLICIT), the Forward Euler Algorithm (XPO), and the Trapezoidal Algorithm (TRAP). Because of numerical stability consideration, the implicit algorithm is used in generator modeling.

MINIMUM ABSOLUTE ERROR = 1.D-8

This statement controls relative error (local truncation error) and is the relative error tolerance.

STOP TIME = 0.495D0

This statement must be included with an appropriate value of stop time.

#### D.2.4.6 Generator Model Element Values

In the elements section of the program data, several resistors, voltage sources, current sources, inductors and mutual inductances are defined. A detailed explanation of each element follows. Since an explanation of "from" node, "to" node, and assumed voltage and current polarities has been previously presented and since a sketch illustrating the connections of each element has also been presented, no further discussion will be made of circuit connections.

EF1 = 375.D0

The external field voltage in this model is 375 volts (D.C.).

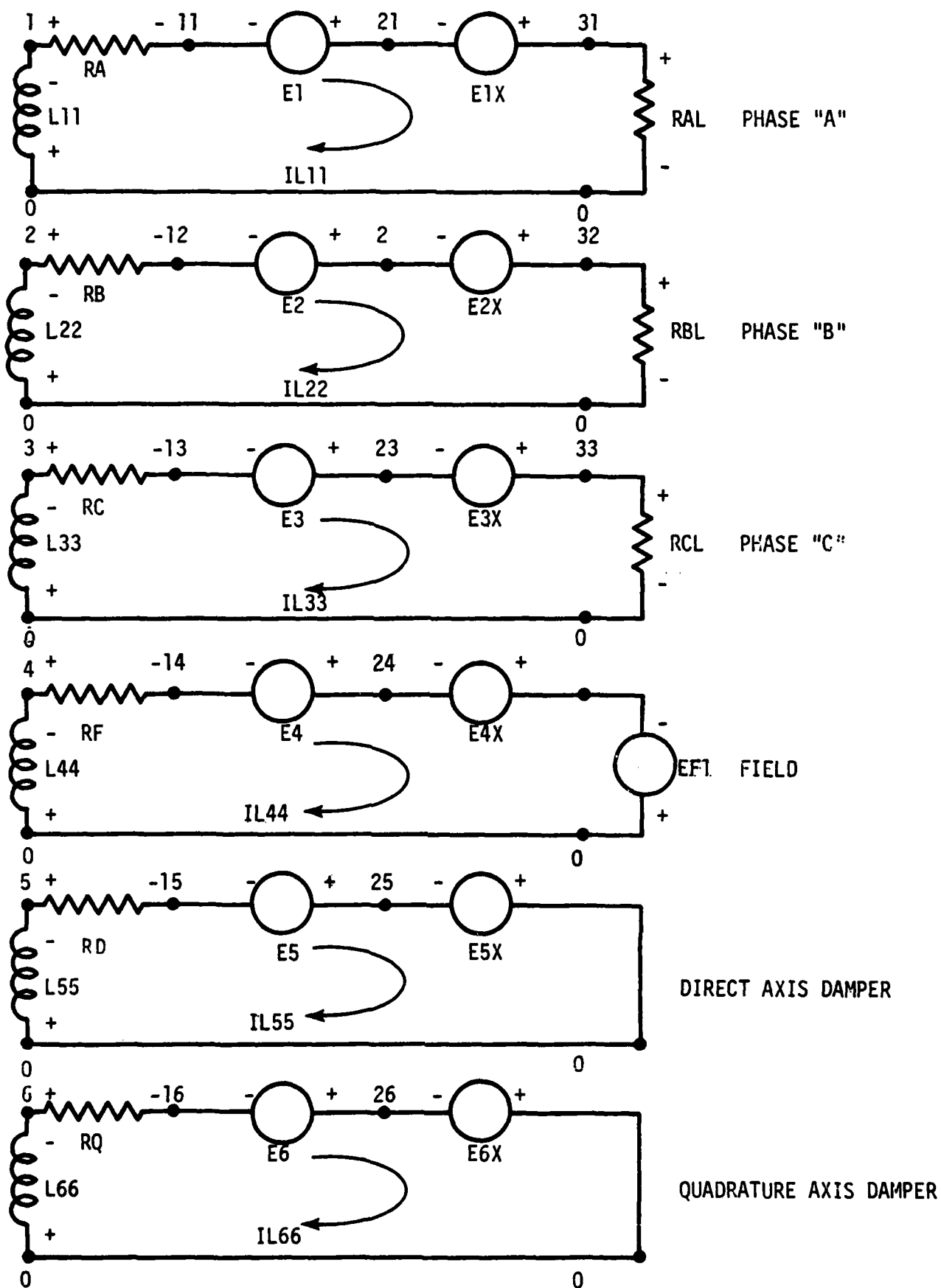


FIGURE 78. SCEPTRE NODE NUMBERING THREE PHASE GENERATOR ELEMENTS

RAL = T1            This model uses resistors to provide a load to each phase of  
RBL = T1            the generator. The value of the load resistors is provided  
RCL = T1            by table T1. These resistors are, therefore, a function of  
                     time and can be manipulated to provide various short circuit,  
                     or open circuit tests.

RA = 1.542D-3      These resistors represent the stator winding resistance of  
RB = 1.542D-3      each phase.

RC = 1.542D-3

RF = 0.61D0        The field winding resistance plus any external field  
                     resistance is represented by RF.

RD = 18.421D-3    The direct axis damper winding resistance is represented by  
                     RD.

RQ = 18.969D-3    RQ is the quadrature axis damper winding resistance.

E1 = FM1 (IL11, IL22, IL33, IL44, IL55, IL66, PS, PT, PCAA, PCFF, PCDD, PCAF,  
                     PCAD, PCAQ, PCFD)

E1 is the speed voltage term of the phase "A" circuit. Since E1  
is a complicated expression, function subprogram FM1 is used to  
determine its value. The required list of parameters is defined.

IL11 - current through inductance L11

(Phase "A" current)

IL22 - current through inductance L22 (Phase "B")

IL33 - current through inductance L33 (Phase "C")

IL44 - current through inductance L44 (field current)

IL55 - current through inductance L55

(direct axis damper current)

IL66 - current through inductance L66

(quadrature axis damper current)

PS - rotor speed in radians/second

PT - rotor angle in radians

PCAA - saturation multiplier of inductance L11 (Phase "A")

All saturation multipliers will be further defined in defined parameter section.

PCFF - saturation multiplier of inductance L44. (field)

PCDD - saturation multiplier of inductance L55. (direct axis damper)

PCAF - saturation multiplier of mutual inductance M14.

(mutual inductance between field and phase "A")

PCAD - saturation multiplier of mutual inductance M15.

(mutual inductance between direct axis damper and phase "A")

PCAQ - saturation multiplier of mutual inductance M16.

(mutual inductance between quadrature axis damper and phase "A")

PCFD - saturation multiplier of mutual inductance M45.

(mutual inductance between field and direct axis damper)

The remaining speed voltage terms follow in the data. The calling list of parameters in each voltage term is identical to that for E1.

E2 = speed voltage term of phase "B" circuit

E3 = speed voltage term of phase "C" circuit

E4 = speed voltage term of phase field circuit

E5 = speed voltage term of direct axis damper circuit

E6 = speed voltage term of quadrature axis damper circuit

Each of the function subprograms used in calculation of each of the six speed voltage terms will be described in detail later.

E1X = FM1X (IL11, IL22, IL33, IL44, IL55, IL66, PS, PT, PCEQ, PDEQ)

E1X is the saturation voltage term of phase "A" circuit which contains saturation effects involving  $\frac{\partial L}{\partial I}$  terms. Since E1X is a complicated expression, function subprogram FM1X is used to determine its value. The required list of parameters is defined.

- IL11 - current through inductance L11 (phase "A" current)
- IL22 - current through inductance L22 (phase "B" current)
- IL33 - current through inductance L33 (phase "C" current)
- IL44 - current through inductance L44 (field current)
- IL55 - current through inductance L55 (direct axis damper current)
- IL66 - current through inductance L66 (quadrature axis damper current)
- PS - rotor speed in radians/second
- PT - rotor angle in radians
- PCEQ - equivalent direct axis current. This term will be defined in detail later
- PDEQ - time derivative of equivalent direct axis current. This term will be defined in detail later

The remaining saturation voltage terms follow in the data. The calling list of parameters in each voltage term is identical to that for E1X.

- E2X - saturation voltage term of phase "B"
- E3X - saturation voltage term of phase "C"
- E4X - saturation voltage term of field circuit
- E5X - saturation voltage term of direct axis damper circuit
- E6X - saturation voltage term of quadrature axis damper circuit

Each of the function subprograms used in the calculation of each of the six saturation voltage terms will be described in detail later.

NOTE: In any study in which the full effects of saturation are not required, the user may set each of the six saturation voltage terms to zero.  
(e.g.,  $E1X = 0.00$ )

This must be done for both linear model and the partially saturated model. Significant improvement in computation time with minimal loss of accuracy may be obtained.

M12, L11-L22 = EQUATION 2 (MS, LM, PCAA, PM2P3)

M12 is the mutual inductance between inductance L11 and L22. Since M12 is an expression, its value is determined by an equation. M12 is defined to be  $PCAA * (-MS + Lm * \cos(2\theta - 2\pi/3))$ .

The constants Ms and Lm are measured unsaturated machine inductance values as described by Anderson and Fouad.

The calling list of parameters is defined.

MS - the value of Ms

LM - the value of Lm

PCAA - the normalized saturation multiplier applicable to stator inductances. PCAA will be defined in detail later.

PM2P3 - the defined parameter constant equalled to  $-2\pi/3$  radians.

M13, L11-L33 = EQUATION 2 (MS, LM, PCAA, P2P3)

M13 is the mutual inductance between inductance L11 and L33. M13 is defined to be

$PCAA * (-Ms + Lm * \cos(2\theta + 2\pi/3))$ .

The calling list of parameters is defined.

MS - the value of Ms

LM - the value of Lm

PCAA - the normalized saturation multiplier used in stator self inductances.

P2P3 - the defined parameter constant equal to  $2\pi/3$ .

M14, L11-L44 = EQUATION 9 (1., MAF, PCAF, 0.)

M14 is the mutual inductance between inductance L11 and L44. M14 is defined to be

$$1. * PCAF * MAF * \cos(\theta + 0.)$$

The calling list of parameters is defined

1. - a constant

MAF - the value of  $M_{AF}$ . The constant  $M_{AF}$  is the measured unsaturated generator mutual inductance between phase "A" and field as described by Anderson and Fouad.

PCAF - the normalized saturation multiplier applicable to stator - field mutual inductance. PCAF will be defined in detail later.

0. - a constant

M15., L11-L55 = EQUATION 9 (1., MAD, PCAD, 0.)

M15 is the mutual inductance between inductance L11 and L55. M15 is defined to be

$$1. * PCAD * MAD * \cos(\theta + 0.)$$

The calling list of parameters is defined

1. - a constant

MAD - the value of  $M_{AD}$ . The constant  $M_{AD}$  is the measured unsaturated generator mutual inductance between phase "A" and direct axis damper as described by Anderson and Fouad.

PCAD - the normalized saturation multiplier applicable to stator - direct axis damper mutual inductance. PCAD will be defined in detail later.

0. - a constant

M16, L11-L66 = EQUATION 8 (1., MAQ, 0., PCAQ)

M16 is the mutual inductance between inductance L11 and L66. M16 is defined to be

$$1. * PCAQ * MAQ * \sin(\theta + 0.)$$

The calling list of parameters is defined

1. - a constant

MAQ - the value of MAQ. The constant MAQ is the measured unsaturated generator mutual inductance between phase "A" and quadrature axis damper as described by Anderson and Fouad.

0. - a constant

PCAQ - the normalized saturation multiplier applicable to stator - direct axis damper mutual inductance. PCAD will be defined in detail later.

M23, L22-L33 = EQUATION 2 (MS, LM, PCAA, 0.)

M23 is the mutual inductance between inductance L22 and L33. M23 is defined to be

$$PCAA * (-MS + LM * \cos(2\theta + 0.))$$

All entries in the calling list of parameters are previously defined.

M24, L22-L44 = EQUATION 9(1., MAF, PCAF, PM2P3)

M24 is defined to be

$$1. * PCAF * MAF * \cos(\theta - 2\pi/3)$$

All entries in the calling list of parameters are previously defined.

M25, L22-L55 = EQUATION 9 (1., MAD, PCAD, PM2P3)

M25 is defined to be

$$1. * PCAD * MAD * \cos(\theta - 2\pi/3)$$

All entries in the calling list of parameters are previously defined.

M26, L22-L66 = EQUATION 8 (1., MAQ, PM2P3, PCAQ)

M26 is defined to be

$$1. * PCAQ * MAD * \sin(\theta - 2\pi/3)$$

All entries in the calling list of parameters are previously defined.

M34, L33-L44 = EQUATION 9 (1., MAF, PCAF, P2P3)

M34 is defined to be

$$1. * PCAF * MAF * \cos(\theta + 2\pi/3)$$

All entries in the calling list of parameters are previously defined.

M35, L33-L55 = EQUATION 9 (1., MAD, PCAD, P2P3)

M35 is defined to be

$$1. * PCAD * MAD * \cos(\theta + 2\pi/3)$$

All entries in the calling list of parameters are previously defined.

M36, L33-L66 = EQUATION 8(1., MAQ, P2P3, PCAQ)

M36 is defined to be

$$1. * PCAQ * MAQ * \sin(\theta + 2\pi/3)$$

All entries in the calling list of parameters are previously defined.

M45, L44-L55 = X13 (MFD \* PCFD)

M45 is defined to be

$$PCFD * MFD.$$

The terms in the expression are defined.

MFD - the value of  $M_{FD}$ . The constant  $M_{FD}$  is the measured unsaturated generator mutual inductance between field and direct axis damper as described by Anderson and Fouad.

PCFD - the normalized saturation multiplier used in field-direct axis damper mutual inductance.

L11 = EQUATION 1 (LS, LM, 0., PCAA)

L11 is defined to be

$$PCAA * (LS + LM * \cos(2\theta + 0.))$$

The calling list of parameters is defined

LS - the value of  $L_s$ . The constant  $L_s$  is the measured unsaturated generator inductance value associated with stator self-inductance.

LM - the previously defined constant  $L_m$ .

0. - a constant

PCAA - the previously defined saturation multiplier.

L22 = EQUATION 1 (LS, LM, P2P3, PCAA)

L22 is defined to be

$$PCAA * (LS + LM * \cos(2\theta + 2\pi/3))$$

All entries in the calling list of parameters are previously defined.

L33 = EQUATION 1 (L%, LM, PM2P3, PCAA)

L33 is defined to be

$$PCAA * (LS + LM * \cos(2\theta - 2\pi/3))$$

All entries in the calling list of parameters are previously defined.

L44 = X11 (LFF \* PCFF)

L44 is defined to be

$$PCFF * LFF.$$

The terms in the expression are defined.

LFF - the measured unsaturated field self-inductance

PCFF - the normalized saturation multiplier applicable to field self-inductance.

L55 = X12 (LDD \* PCDD)

L55 is defined to be

$$PCDD * LDD$$

The terms in the expression are defined.

LDD - the measured unsaturated direct-axis damper self-inductance.

PCDD - the normalized saturation multiplier applicable to direct axis damper self-inductance.

L66 = LQQ

LQQ - the measured unsaturated quadrature-axis damper self-inductance.

This model assumes no quadrature axis saturation effect.

#### D.2.4.7 Defined Parameters

PCEQ = FIEQ (IL11, IL22, IL22, IL33, IL44, IL55, NFA, NFD, PT)

PCEQ is the equivalent direct axis current and is defined to be

$$IL44 + NFD * IL55$$

$$+ NFA * (IL11 * \cos(\theta) + IL22 * \cos(\theta - 2\pi/3) + IL33 * \cos(\theta + 2\pi/3))$$

The value of PCEQ is determined by the function subprogram FIEQ. The calling list of parameters is defined.

IL11, IL22, IL33, IL44, IL55 - previously defined values of current in phase "A", phase "B", phase "C", field, and direct axis damper  
 NFA - turns ratio of phase "A" stator winding to field winding  
 NFD - turns ratio of direct axis damping winding to field winding  
 PT - rotor angle in radians.

PDEQ = FDEQ (DL11, DL22, DL33, DL44, DL55, NFA, NFD, PS, PT, IL11, IL22, IL33)

PDEQ is the time derivative of the equivalent direct axis current and is defined to be.

$$\begin{aligned} & \frac{d}{dt} (IL44) + NFD * \frac{d}{dt} (IL55) \\ & + NFA * [\cos(\theta) * \frac{d}{dt} (IL11) + \cos(\theta - 2\pi/3) * \frac{d}{dt} (IL22) + \\ & \quad \cos(\theta + 2\pi/3) * \frac{d}{dt} (IL33)] \\ & - PS * NFA * [IL11 * \sin(\theta) + IL22 * \sin(\theta - 2\pi/3) \\ & \quad + IL33 * \sin(\theta + 2\pi/3)] \end{aligned}$$

The value of PDEQ is determined by the function subprogram FDEQ. The calling list of parameters is defined.

DL11 - the label assigned by SCEPTRE to the time derivative of current through inductor L11. (i.e.,  $DL11 = \frac{d}{dt} (IL11)$ )

DL22, DL33, DL44, DL55 - the time derivatives of current through inductors L22, L33, L44, and L55.

NFA, NFD - previously defined turns ratios.

PS - rotor speed in radians/second.

PT - rotor angle in radians

IL11, IL22, IL33 - stator currents.

PCAA = FPOLY (A1, A2, A3, A4, PCEQ, LIM, A0)

PCAA is the normalized saturation multiplier which is applicable to each stator self-inductance and to each stator - stator mutual inductance. The value of PCAA is determined by the function subprogram FPOLY. Function subprogram FPOLY is used for all saturation multipliers. Each saturation multiplier is defined by the polynomial

$$A0 + A1 * PCEQ + A2 * PCEQ ** 2 + A3 * PCEQ ** 3 + A4 * PCEQ ** 4.$$

A1, A2, A3, A4, A0 - linear regression constants.

A table of experimental measurements is required to be made. These measurements relate saturated values of inductance or mutual inductance to equivalent direct axis current (PCEQ). Linear regression analysis is applied to the data. After the "best fit" is determined using polynomials of order 1 through order 4, the regression constants are determined.

PCEQ - equivalent direct axis current

LIM - in general, the derived polynomial is applicable only in the range of current  $PCEQ = 0$  to  $PCEQ = LIM$ . If during solution, a current PCEQ is greater than its limit, then the value of FPOLY will be determined at  $PCEQ = LIM$ .

All saturation multipliers must be set equal to zero in the linear generator model.

$PCFF = FPOLY (A1, A2, A3, A4, PCEQ, LIM, A0)$

PCFF is the normalized saturation multiplier applicable to field self inductance.

The following normalized saturation multipliers are listed.

PCDD - direct axis damper

PCAF - stator-field mutual inductance

PCAD - stator-direct axis damper mutual inductance

PCAQ - stator-quadrature axis damper mutual inductance

PCFD - field-direct axis damper mutual inductance

P2P3 =  $2\pi/3$  = a constant

PM2P3 =  $-2\pi/3$  = a constant

DPS = X1 (FD2THT (IL11,...,IL66, E1,...,E6, PS))

DPT = X2 (PS)

PS = 376.998

PT = 2.455

SCEPTRE provides for the solution of differential equations under the defined parameter section. These four statements provide for the solution of two nested differential equations.

PS - Rotor speed in radians/second

Initial value of rotor speed is input as 376.998 radians/second.

PS is the evaluation of the integral

$$PS = \int DPS.$$

PT - Rotor angle in radians.

Initial value of rotor angle is input at 2.455 radians.

PT is the evaluation of the integral

$$PT = \int DPT = \int PS$$

DPS is determined by function subprogram FD2THT and is expressed as the following equation.

$$DPS = \frac{d}{dt} (PS) = \frac{TM - TE}{J}$$

where TM = constant mechanical torque

J = polar moment of inertia

TE = variable electrical torque as calculated by the equation.

$$TE = \frac{1}{2} \frac{\partial}{\partial \theta} [I^T L I]$$

I = the vector containing six currents

$I^T$  = the transpose of I

L = the inductance matrix

After performing the indicated matrix multiplication using symbolic notation and after finding the derivative with respect to theta ( $\theta$ ), certain simplifications are evident. The speed voltage terms ( $E_1, \dots, E_6$ ) have been previously calculated. These derived terms are also present in the derivation of TE. For this reason the speed voltage terms are used in the parameter list and in the calculations of TE. TE is derived to be

$$TE = (E_1 * IL11 + E_2 * IL22 + E_3 * IL33 \\ + E_4 * IL44 + E_5 * IL55 + E_6 * IL66) / (2 * PS)$$

Accelerating torque is TM-TE.

$$DPS = \frac{d}{dt} (PS) = \frac{d^2}{dt^2} (PT) - \frac{d^2 \theta}{dt^2} \\ = \frac{TM - TE}{J}$$

TM = SB3 \* PM/OMEGAR

SB3 - MVA rating of the generator

PM - per unit generation level at which the generator is operating

OMEGAR - rated rotor speed in radians/second

The calling list of parameters has been previously defined.

IL11, IL22, IL33, IL44, IL55, IL66 - current through each of six inductors

E1, E2, E3, E4, E5, E6 - speed voltage terms appearing in each of the six circuits in the generator model.

PS - rotor speed in radians/second.

#### D.2.4.8 Functions

The previously discussed mutual-inductances and self-inductances made use of equations. A list of parameters was provided in the evaluation of each inductance. Each equation is evaluated by the use of symbolic notation. In this manner, one equation function may be used to evaluate any number of terms. Since each of the four equations were discussed previously, no further discussion is made here.

#### TABLE 1

This table is used in the evaluation of load resistors RAL, RBL, and RCL during certain system disturbances. For a three phase fault applied at time = 0.05 second, all three load resistors should be equal to Table 1 (T1). For a line-to-ground fault on phase "C", load resistors RAL and RBL should be set equal to a constant while RCL should be equal to T1.

The operation of the table function has been discussed previously.

#### D.2.4.9 Outputs

This section contains the variable names whose values are to be plotted for output.

#### D.2.4.10 Initial Conditions

Initial values are required of all state variables. SCEPTRE will default to a value of zero for any missing initial values. In the generator model formulation, the state variables are the six self-inductance currents (IL11,...,IL66). Initial values of each of these currents are calculated by hand or by a separate program of the user's design.

#### D.2.4.11 Run Controls

Integration Routine = Implicit

The Backward Euler integration routine (Implicit) is used in this model and is recommended.

Minimum Absolute Error = 1.D-8

The relative error tolerance is set to 1.D-8 and a value of the user's discretion.

Computer Save Interval = 5

Specification of this parameter can result in the output of results even though certain abnormal stop conditions may have occurred.

Plot Interval = 1.67D-2

The value of the plot interval is at the user's discretion and is specifically used in multiple plots.

Stop Time = .049500

Stop time is the user specified time at which calculations are halted.

#### D.2.4.12 Function Subprograms

Several function subprograms have been previously discussed. These are listed.

FD2THT

FIEQ

FDEQ

FPOLY

Function subprograms FM1X, FM2X, FM3X, FM4X, FM5X, FM6X call upon function subprogram FPOLY. FPOLY1 determines the slope of a saturation multiplier function. The same regression constants used in the evaluation of FPOLY are used in FPOLY1.

If  $FPOLY = A0 + A1 * CEQ + AZ * CEQ **Z + A3 * CEQ ** 3$ , then  $FPOLY1 = A1 + 2.*AZ * CEQ + 3.*A3 * CEQ ** 2$ .

If current (PCEQ) is greater than a user defined upper limit (LIM), FPOLY1 is set to zero.

FPOLY1 is used to evaluate the values of the terms PDAA, PDAF, PDAD, and PDAQ. It is understood that PDAA, PDAF, PDAD, PDAQ are the instantaneous slopes ( $\frac{d}{d(CEQ)}$ ) of PCAA, PCAF, PCAD, and PCAQ.

FM1X is the function subprogram used to evaluate E1X. Each of the calling parameters has been previously discussed. All required machine constants are listed in the subprogram.

$$P2P3 = 2\pi/3$$

$$PM2P3 = -2\pi/3$$

$$PLS = Ls$$

$$PMS = Ms$$

$$PLM = Lm$$

$$PMAF = M_{AF}$$

$$PMAD = M_{AD}$$

$$PMAQ = M_{AQ}$$

Since a long involved calculation is made, the resultant is expressed as the sum of several parts.

$$FM1X = PDEQ * (CL11 + CL12 + CL13 + CL14 + CL15 + CL16)$$

Values of CL11, CL12, CL13, CL14, CL15, and CL16 are separately determined.

Inspection of each of these six terms may be readily performed by the user and compared with the derivation.

FM2X, FM3X, FM4X, FM5X, FM6X - the saturation voltage terms E2X, E3X, E4X, E5X, E6X are determined by these function subprograms. Analysis of each subprogram is similar to that for FM1X.

FM1 is the function subprogram used to evaluate E1. Each of the calling parameters has been previously defined. All required machine constants are listed in the subprogram.

$$P2P3 = 2\pi/3$$

$$PM2P3 = -2\pi/3$$

$$PLM = Lm$$

$$PMAF = M_{AF}$$

$$PMAD = M_{AD}$$

$$PMAQ = M_{AQ}$$

The function is evaluated piecewise.

$$SL1 = 2. * PCAA * Lm * SIN(2\theta) * IL11$$

$$SL2 = 2. * PCAA * Lm * SIN(2\theta - 2\pi/3) * IL22$$

$$SL3 = 2. * PCAA * Lm * SIN(2\theta + 2\pi/3) * IL33$$

$$SL4 = PCAF * M_{AF} * SIN(\theta) * IL44$$

$$SL5 = PCAD * M_{AD} * SIN(\theta) * IL55$$

$$SL6 = PCAQ * M_{AD} * COS(\theta) * IL66$$

$$E1 = FM1 = PS * (SL1 + SL2 + SL3 + SL4 + SL5 + SL6)$$

The remaining function subprograms (FM2, FM3, FM4, FM5, FM6) are similarly analyzed.

D.2.4.13 GENERATOR MODEL

```
//GFBL3 JOB (0915-5-200-GB- ,30), 'G F BELL', REGION=1024K
//STEP1 EXEC SUPERSEP
//G.SYSIN DD *
CIRCUIT DESCRIPTION
ELEMENTS
EF1,34-0=375.DD
RAL,31-0=T1
RBL,32-0=T1
RCL,33-0=T1
RA,1-11=1.542D-3
RB,2-12=1.542D-3
RC,3-13=1.542D-3
RF,4-14=0.61DD
RD,5-15=18.421D-3
RQ,6-16=18.969D-3
E1,11-21=FM1(IL11,IL22,IL33,IL44,IL55,IL66,PS,
PT,PCAA,PCFF,PCDD,PCAF,PCAD,PCAQ,PCFD)
E2,12-22=FM2(IL11,IL22,IL33,IL44,IL55,IL66,PS,
PT,PCAA,PCFF,PCDD,PCAF,PCAD,PCAQ,PCFD)
E3,13-23=FM3(IL11,IL22,IL33,IL44,IL55,IL66,PS,
PT,PCAA,PCFF,PCDD,PCAF,PCAD,PCAQ,PCFD)
E4,14-24=FM4(IL11,IL22,IL33,IL44,IL55,IL66,PS,
PT,PCAA,PCFF,PCDD,PCAF,PCAD,PCAQ,PCFD)
E5,15-25=FM5(IL11,IL22,IL33,IL44,IL55,IL66,PS,
PT,PCAA,PCFF,PCDD,PCAF,PCAD,PCAQ,PCFD)
E6,16-26=FM6(IL11,IL22,IL33,IL44,IL55,IL66,PS,
PT,PCAA,PCFF,PCDD,PCAF,PCAD,PCAQ,PCFD)
E1X,21-31=FM1X(IL11,IL22,IL33,IL44,IL55,IL66,PS,PT,PCEQ,PDEQ)
E2X,22-32=FM2X(IL11,IL22,IL33,IL44,IL55,IL66,PS,PT,PCEQ,PDEQ)
E3X,23-33=FM3X(IL11,IL22,IL33,IL44,IL55,IL66,PS,PT,PCEQ,PDEQ)
E4X,24-34=FM4X(IL11,IL22,IL33,IL44,IL55,IL66,PS,PT,PCEQ,PDEQ)
E5X,25-0=FM5X(IL11,IL22,IL33,IL44,IL55,IL66,PS,PT,PCEQ,PDEQ)
E6X,26-0=FM6X(IL11,IL22,IL33,IL44,IL55,IL66,PS,PT,PCEQ,PDEQ)
M12,L11-L22=EQUATION 2 (1.75945D-3,7.433D-5,PCAA,PM2P3)
M13,L11-L33=EQUATION 2 (1.75945D-3,7.433D-5,PCAA,PM2P3)
M14,L11-L44=EQUATION 9 (1.0DD,89.006D-3,PCAF,0.0DD)
M15,L11-L55=EQUATION 9 (1.0DD,4.22098D-3,PCAD,0.0DD)
M16,L11-L66=EQUATION 8 (1.0DD,1.96904D-3,0.0DD,PCAQ)
M23,L22-L33=EQUATION 2 (1.75945D-3,7.433D-5,PCAA,0.0DD)
M24,L22-L44=EQUATION 9 (1.0DD,89.006D-3,PCAF,PM2P3)
M25,L22-L55=EQUATION 9 (1.0DD,4.22098D-3,PCAD,PM2P3)
M26,L22-L66=EQUATION 8 (1.0DD,1.96904D-3,PM2P3,PCAQ)
M34,L33-L44=EQUATION 9 (1.0DD,89.006D-3,PCAF,PM2P3)
M35,L33-L55=EQUATION 9 (1.0DD,4.22098D-3,PCAD,PM2P3)
M36,L33-L66=EQUATION 8 (1.0DD,1.96904D-3,PM2P3,PCAQ)
M45,L44-L55=X13(.09901383*PCFD)
L11,0-1=EQUATION 1 (4.47005D-3,7.433D-5,0.0DD,PCAA)
L22,0-2=EQUATION 1 (4.47005D-3,7.433D-5,PM2P3,PCAA)
L33,0-3=EQUATION 1 (4.47005D-3,7.433D-5,PM2P3,PCAA)
L44,0-4=X11(2.189*PCFF)
L55,0-5=X12(5.989D-3*PCDD)
L66,0-6=1.423D-3
DEFINED PARAMETERS
FCEQ=FIER(IL11,IL22,IL33,IL44,IL55,4.C66D-4,4.98007D-2,PT)
FDER=FDER(DL11,DL22,DL33,DL44,DL55,4.C66D-4,4.98007D-2,PS,PT,
IL11,IL22,IL33)
PCAA=FPOLY(-2.9246D-5,-1.0771D-7,2.0394D-11,0.0D,PCEQ,3.D3,.9E367DD)
PCFF=FPOLY(-2.9867D-5,-1.0519D-7,1.8699D-11,0.0D,PCEQ,3.D3,1.0080D)
PCDD=FPOLY(-2.1569D-5,-7.9586D-8,1.593D-11,0.0D,PCEQ,3.D3,.97827DD)
PCAF=FPOLY(-6.9202D-5,-8.4719D-8,1.6303D-11,0.0D,PCEQ,3.D3,1.DD)
PCAD=FPOLY(-8.012D-5,-6.1443D-8,1.2983D-11,0.0D,PCEQ,3.D3,.9F860C)
PCAQ=FPOLY(-2.6322D-5,-5.5511D-8,1.0182D-11,0.0D,PCEQ,3.D3,.99419DD)
PCFD=FPOLY(-6.9355D-5,-6.6653D-8,1.3054D-11,0.0D,PCEQ,3.D3,1.DD)
P2P3=2.0943951J24DD
PM2P3=-2.0943951024DD
DPS=X1(FD2THT(IL11,IL22,IL33,IL44,IL55,IL66,E1,E2,E3,E4,E5,E6,PS))
```

D.2.4.13 GENERATOR MODEL (Continued)

```

DPT=X2(PS)
PS=375.998D0
PT=2.45500D0
FUNCTIONS
EQUATION 1 (A,B,C,D)=(D*(A+B*DCOS(2.0D0*PT+C)))
EQUATION 2 (A,B,C,D)=(C*(-A + B*DCOS(2.0D0*PT+D)))
EQUATION 3 (A,B,C,D)=(A*B*D*DSIN(PT+C))
EQUATION 9 (A,B,C,D)=(A*B*C*DCOS(PT+D))
TABLE 1
0.0D0,1.75781D0,.05D0,1.75781D0,.05D0,0.0D0,.1D0,0.0D0,.1D0,1.75781D0,
10.0D0,1.75781D0
OUTPUTS
IL11,IL22,IL33,PL0T
IL44,IL55,IL66,PS
E1X,E2X,E3X,E4X,E5X,E6X
INITIAL CONDITIONS
IL11=6967.35D0
IL22=-3483.675D0
IL33=-3483.675D0
IL44=633.378D0
IL55=0.0D0
IL66=0.0D0
RUN CONTROLS
INTEGRATION ROUTINE=IMPLICIT
MINIMUM ABSOLUTE ERROR=1.D-8
COMPUTER SAVE INTERVAL = 5
PLOT INTERVAL = 1.67D-2
STOP TIME=.0495D0
ND
/*
/FORT,FORTSRC DD *
DOUBLE PRECISION FUNCTION FD2THT(IL11,IL22,IL33,IL44,IL55,IL66,
1 E1,E2,E3,E4,E5,E6,PS)
IMPLICIT REAL*8(A-Z)
THIS SUBPROGRAM COMPUTES ROTOR ANGLE ACCELERATION
DATA SB3,PM,OMEGAR/160.0D0,C.8D0,2.37D0,375.998D0/
TE=IL11*E1 +IL22*E2 +IL33*E3 +IL44*E4 +IL55*E5 +IL66*E6
TE=TE/(2.0D0 * PS)
TM=SB3 * PM/OMEGAR
FD2THT = (TM - TE)/5335.0D0
RETURN
END
DOUBLE PRECISION FUNCTION FIEQ(IL11,IL22,IL33,IL44,IL55,
1 PNFA,PNFD,PT)
IMPLICIT REAL*8(A-H,I,O-Z)
THIS SUBPROGRAM COMPUTES THE EQUIVALENT CURRENT ALONG THE ROTOR AXIS.
REFER TO PAPER BY SMITH AND SNIDER FOR THEORETICAL FORMULATION.
A = DCOS(PT)
B = DCOS(PT-2.094395102393D0)
C = DCOS(PT+2.094395102393D0)
STEP1 = (IL11*A + IL22*B + IL33*C)*2.0D0/3.0D0
STEP2 = PNFD*IL55 + PNFA*STEP1
FIEQ= IL44 + STEP2
FIEQ= DABS(FIEQ)
RETURN
END
DOUBLE PRECISION FUNCTION FDEQ(DL11,DL22,DL33,DL44,DL55,
1 PNFA,PNFD,PS,PT,IL11,IL22,IL33)
IMPLICIT REAL*8(A-H,I,J-Z)
A = DCOS(PT)
B = DCOS(PT-2.094395102393D0)
C = DCOS(PT+2.094395102393D0)
PM2P3=-2.094395102393D0
P2P3= 2.094395102393D0
STEP1 = (DL11*A + DL22*B + DL33*C)
STEP2 = IL11*DSIN(PT) + IL22*DSIN(PT+PM2P3) + IL33*DSIN(PT+P2P3)

```

D.2.4.13 GENERATOR MODEL (Continued)

```

FDEQ = DL44 + PVFD*DL55 + PVFA*(STEP1 - PS * STEP2)
RETURN
END
DOUBLE PRECISION FUNCTION FPOLY(A1,A2,A3,A4,PCEQ,LIM,A0)
IMPLICIT REAL*8(A-Z)
C1=PCEQ
IF(PCEQ.GT.LIM)C1=LIM
C2=C1*C1
C3=C1*C2
C4=C1*C3
FPOLY=A0 + A1*C1 +A2*C2 +A3*C3 +A4*C4
RETURN
END
DOUBLE PRECISION FUNCTION FPOLY1(A1,A2,A3,A4,PCEQ,LIM)
IMPLICIT REAL*8(A-Z)
C1=PCEQ
C2=C1*C1
C3=C1*C2
C4=C1*C3
FPOLY1= A1 +2.00*A2*C1 +3.00*A3*C2 +4.00*A4*C3
IF(PCEQ.GT.LIM)FPOLY1=0.00
RETURN
END
DOUBLE PRECISION FUNCTION FM1X(IL11,IL22,IL33,IL44,IL55,IL66,PS,
PT,PCEQ,PDE2)
IMPLICIT REAL*8(A-Z)
P2P3=2.094395102400
PM2P3=-2.094395102400
PLS=4.473050-3
PMS=1.759450-3
PLM=0.074330-3
PMAF=89.3060-3
PMA0=4.223980-3
PMA2=1.959040-3
PDAA= FPOLY1(-2.92460-5,-1.07710-7,2.03940-11,0.00,PCEQ,3.03)
PDAF= FPOLY1(-6.92020-5,-8.47190-8,1.63030-11,0.00,PCEQ,3.03)
PDAD= FPOLY1(-8.0120-5,-6.14430-8,1.29830-11,0.00,PCEQ,3.03)
PDAQ= FPOLY1(-2.63220-5,-5.55110-8,1.01820-11,0.00,PCEQ,3.03)
CL11= -PDAA * (PLS + PLM * DCOS(2.00 * PT)) * IL11
CL12= -PDAA * (-PMS + PLM * DCOS(2.00* PT + PM2P3)) * IL22
CL13= -PDAA * (-PMS + PLM * DCOS(2.00* PT + P2P3)) * IL33
CL14= -PDAF * PMAF * DCOS(PT) * IL44
CL15= -PDAD * PMA0 * DCOS(PT) * IL55
CL16= -PDAQ * PMA2 * DSIN(PT) * IL66
FM1X= PDE2*(CL11 +CL12 +CL13 +CL14 +CL15 +CL16)
RETURN
END
DOUBLE PRECISION FUNCTION FM2X(IL11,IL22,IL33,IL44,IL55,IL66,PS,
PT,PCEQ,PDEQ)
IMPLICIT REAL*8(A-Z)
P2P3=2.094395102400
PM2P3=-2.094395102400
PLS=4.473050-3
PMS=1.759450-3
PLM=0.074330-3
PMAF=89.3060-3
PMA0=4.223980-3
PMA2=1.959040-3
PDAA= FPOLY1(-2.92460-5,-1.07710-7,2.03940-11,0.00,PCEQ,3.03)
PDAF= FPOLY1(-6.92020-5,-8.47190-8,1.63030-11,0.00,PCEQ,3.03)
PDAD= FPOLY1(-8.0120-5,-6.14430-8,1.29830-11,0.00,PCEQ,3.03)
PDAQ= FPOLY1(-2.63220-5,-5.55110-8,1.01820-11,0.00,PCEQ,3.03)
CL21= -PDAA * (-PMS + PLM * DCOS(2.00* PT + PM2P3)) * IL11
CL22= -PDAA * (PLS + PLM * DCOS(2.00* PT + P2P3)) * IL22
CL23= -PDAA * (-PMS + PLM * DCOS(2.00* PT )) * IL33
CL24= -PDAF * PMAF * DCOS(PT + PM2P3) * IL44

```

D.2.4.13 GENERATOR MODEL (Continued)

```

CL25= -PDAQ * PMAQ * DCOS(PT + PM2P3) * IL55
CL26= -PDAQ * PMAQ * DSIN(PT + PM2P3) * IL66
FM2X=PDE2*(CL21 +CL22 +CL23 +CL24 +CL25 +CL26)
RETURN
END

```

```

1 DOUBLE PRECISION FUNCTION FM3X(IL11,IL22,IL33,IL44,IL55,IL66,PS,
PT,PCEQ,PDE2)
IMPLICIT REAL*8(A-Z)
P2P3=2.094395102400
PM2P3=-2.094395102400
PLS=4.470050D-3
PMS=1.759450D-3
PLM=0.074330D-3
PMAF=89.0060D-3
PMAD=4.220980D-3
PMAQ=1.959040D-3
PDAA= FPOLY1(-2.92460D-5,-1.07710D-7,2.03940D-11,0.00,PCEQ,3.03)
PDAF= FPOLY1(-6.92020D-5,-8.47190D-8,1.63030D-11,0.00,PCEQ,3.03)
PDAD= FPOLY1(-8.0120D-5,-6.14430D-8,1.29830D-11,0.00,PCEQ,3.03)
PDAQ= FPOLY1(-2.63220D-5,-5.55110D-8,1.01820D-11,0.00,PCEQ,3.03)
CL31= -PDAA * (-PMS + PLM * DCOS(2.00* PT + P2P3)) * IL11
CL32= -PDAA * (-PMS + PLM * DCOS(2.00* PT )) * IL22
CL33= -PDAA * (PLS + PLM * DCOS(2.00* PT + PM2P3)) * IL33
CL34= -PDAF * PMAF * DCOS(PT + P2P3) * IL44
CL35= -PDAD * PMAD * DCOS(PT + P2P3) * IL55
CL36= -PDAQ * PMAQ * DSIN(PT + P2P3) * IL66
FM3X=PDE2*(CL31 +CL32 +CL33 +CL34 +CL35 +CL36)
RETURN
END

```

```

1 DOUBLE PRECISION FUNCTION FM4X(IL11,IL22,IL33,IL44,IL55,IL66,PS,
PT,PCEQ,PDE2)
IMPLICIT REAL*8(A-Z)
P2P3=2.094395102400
PM2P3=-2.094395102400
PMAF=89.0060D-3
PLFF=2.18900D0
PMR=.0990138300
PDAA= FPOLY1(-2.98670D-5,-1.05190D-7,1.86090D-11,0.00,PCEQ,3.03)
PDAF= FPOLY1(-6.92020D-5,-8.47190D-8,1.63030D-11,0.00,PCEQ,3.03)
PDAD= FPOLY1(-6.93550D-5,-6.66630D-8,1.30540D-11,0.00,PCEQ,3.03)
CL41= -PDAF * PMAF * DCOS(PT) * IL11
CL42= -PDAF * PMAF * DCOS(PT + PM2P3) * IL22
CL43= -PDAF * PMAF * DCOS(PT + P2P3) * IL33
CL44= -PDFF*PLFF * IL44
CL45= -PDFD*PMR * IL55
CL46=0.00
FM4X=PDE2*(CL41 +CL42 +CL43 +CL44 +CL45)
RETURN
END

```

```

1 DOUBLE PRECISION FUNCTION FM5X(IL11,IL22,IL33,IL44,IL55,IL66,PS,
PT,PCEQ,PDE2)
IMPLICIT REAL*8(A-Z)
P2P3=2.094395102400
PM2P3=-2.094395102400
PMAD=4.220980D-3
PMR=.0990138300
PLDD=5.9890D-3
PDD= FPOLY1(-2.15690D-5,-7.95860D-8,1.5930D-11,0.00,PCEQ,3.03)
PDAD= FPOLY1(-8.0120D-5,-6.14430D-8,1.29830D-11,0.00,PCEQ,3.03)
PDFD= FPOLY1(-6.93550D-5,-6.66630D-8,1.30540D-11,0.00,PCEQ,3.03)
CL51= -PDAD * PMAD * DCOS(PT) * IL11
CL52= -PDAD * PMAD * DCOS(PT + PM2P3) * IL22
CL53= -PDAD * PMAD * DCOS(PT + P2P3) * IL33
CL54= -PDFD*PMR * IL44
CL55= -PDD*PLDD * IL55
CL56=0.00

```

D.2.4.13 GENERATOR MODEL (Continued)

```

FM5X=PDE3*(CL51 +CL52 +CL53 +CL54 +CL55)
RETURN
END
DOUBLE PRECISION FUNCTION FM6X(IL11,IL22,IL33,IL44,IL55,IL66,PS,
1 PT,PCEQ,PDEQ)
IMPLICIT REAL*8(A-Z)
P2P3=2.094395102400
PM2P3=-2.094395102400
PMAQ=1.959040-3
PDAQ=FPJLY1(-2.63220-5,-5.55110-8,1.01R20-11,0.00,PCEQ,3.03)
CL61=-PDAQ * PMAQ * DSIN(PT) * IL11
CL62=-PDAQ * PMAQ * DSIN(PT +PM2P3) * IL22
CL63=-PDAQ * PMAQ * DSIN(PT +P2P3) * IL33
CL64=0.00
CL65=0.00
CL66=0.00
FM5X=PDE3*(CL61 +CL62 +CL63)
RETURN
END
DOUBLE PRECISION FUNCTION FM1(IL11,IL22,IL33,IL44,IL55,IL66,PS,
1 PT,PCAA,PCFF,PCDD,PCAF,PCAD,PCAQ,PCFD)
IMPLICIT REAL*8(A-Z)
P2P3=2.094395102400
PM2P3=-2.094395102400
PLM=0.074330-3
PMAF=89.00060-3
PMAD=4.220980-3
PMAQ=1.959040-3
SL1=2.00 * PCAA * PLM * DSIN(2.00 * PT) * IL11
SL2=2.00 * PCAA * PLM * DSIN(2.00 * PT + PM2P3) * IL22
SL3=2.00 * PCAA * PLM * DSIN(2.00 * PT + P2P3) * IL33
SL4=PCAF * PMAF * DSIN(PT) * IL44
SL5=PCAD * PMAD * DSIN(PT) * IL55
SL6=-PCAQ * PMAQ * DCOS(PT) * IL66
FM1=PS*(SL1 +SL2 +SL3 +SL4 +SL5 +SL6)
RETURN
END
DOUBLE PRECISION FUNCTION FM2(IL11,IL22,IL33,IL44,IL55,IL66,PS,
1 PT,PCAA,PCFF,PCDD,PCAF,PCAD,PCAQ,PCFD)
IMPLICIT REAL*8(A-Z)
P2P3=2.094395102400
PM2P3=-2.094395102400
PLM=0.074330-3
PMAF=89.00060-3
PMAD=4.220980-3
PMAQ=1.959040-3
SL1=2.00 * PCAA * PLM * DSIN(2.00 * PT + PM2P3) * IL11
SL2=2.00 * PCAA * PLM * DSIN(2.00 * PT + P2P3) * IL22
SL3=2.00 * PCAA * PLM * DSIN(2.00 * PT) * IL33
SL4=PCAF * PMAF * DSIN(PT + PM2P3) * IL44
SL5=PCAD * PMAD * DSIN(PT + PM2P3) * IL55
SL6=-PCAQ * PMAQ * DCOS(PT + PM2P3) * IL66
FM2=PS*(SL1 +SL2 +SL3 +SL4 +SL5 +SL6)
RETURN
END
DOUBLE PRECISION FUNCTION FM3(IL11,IL22,IL33,IL44,IL55,IL66,PS,
1 PT,PCAA,PCFF,PCDD,PCAF,PCAD,PCAQ,PCFD)
IMPLICIT REAL*8(A-Z)
P2P3=2.094395102400
PM2P3=-2.094395102400
PLM=0.074330-3
PMAF=89.00060-3
PMAD=4.220980-3
PMAQ=1.959040-3
SL1=2.00 * PCAA * PLM * DSIN(2.00 * PT + P2P3) * IL11
SL2=2.00 * PCAA * PLM * DSIN(2.00 * PT) * IL22

```

D.2.4.13 GENERATOR MODEL (Continued)

```

SL3=2.D0 * PCAA * PLM * DSIN(2.D0* PT +PM2P3) *IL33
SL4=PCAF * PMAF * DSIN(PT + P2P3) *IL44
SL5=PCAD * PMAD * DSIN(PT + P2P3) *IL55
SL6=-PCAA * PMAQ * DCOS(PT +P2P3) *IL66
FM3=PS*(SL1 +SL2 +SL3 +SL4 +SL5 +SL6)
RETURN
END
DOUBLE PRECISION FUNCTION F4(IL11,IL22,IL33,IL44,IL55,IL66,PS,
1 PT,PCAA,PCFF,PCDD,PCAF,PCAD,PCAQ,PCFD)
IMPLICIT REAL*8(A-Z)
P2P3=2.0943951024D0
PM2P3=-2.0943951024D0
PMAF=99.306D-3
SL1=PCAF * PMAF * DSIN(PT) *IL11
SL2=PCAF * PMAF * DSIN(PT + PM2P3) *IL22
SL3=PCAF * PMAF * DSIN(PT + P2P3) *IL33
FM4=PS*(SL1 +SL2 +SL3)
RETURN
END
DOUBLE PRECISION FUNCTION F5(IL11,IL22,IL33,IL44,IL55,IL66,PS,
1 PT,PCAA,PCFF,PCDD,PCAF,PCAD,PCAQ,PCFD)
IMPLICIT REAL*8(A-Z)
P2P3=2.0943951024D0
PM2P3=-2.0943951024D0
PMAD=4.22398D-3
SL1=PCAD * PMAD * DSIN(PT) *IL11
SL2=PCAD * PMAD * DSIN(PT + PM2P3) *IL22
SL3=PCAD * PMAD * DSIN(PT + P2P3) *IL33
FM5=PS*(SL1 +SL2 +SL3)
RETURN
END
DOUBLE PRECISION FUNCTION F6(IL11,IL22,IL33,IL44,IL55,IL66,PS,
1 PT,PCAA,PCFF,PCDD,PCAF,PCAD,PCAQ,PCFD)
IMPLICIT REAL*8(A-Z)
P2P3=2.0943951024D0
PM2P3=-2.0943951024D0
PMAQ=1.96904D-3
SL1=-PCAQ * PMAQ * DCOS(PT) *IL11
SL2=-PCAQ * PMAQ * DCOS(PT +PM2P3) *IL22
SL3=-PCAQ * PMAQ * DCOS(PT +P2P3) *IL33
FM6=PS*(SL1 +SL2 +SL3)
RETURN
END

```

### D.3. TRANSFORMER MODEL

Previous discussion has illustrated the use of SCEPTRE, the required JCL cards, and other general information concerning a SCEPTRE program. For this reason, that information is not repeated. The user should refer to the User's Guide for the Generator Model for specific detailed descriptions.

A schematic representation illustrating node connections for the three phase transformer model is shown in Figure (79). A description of each term of the transformer model is now presented.

$$EA = X1 (340. * COS (2513 * TIME))$$

The voltage source EA provides excitation for the transformer. This source is connected to the phase "A" primary winding. Since the value of EA is a sinusoid, an expression is used. The connection of EA indicates that the transformer primary is wye-connected. By changing node connections of EA, EB, and EC the transformer primary may be converted to delta-connection. The magnitude of this line - ground voltage source is 340 volts and its frequency is 400 HZ.

$$R22 = 0.12$$

R22 is the resistance of primary phase "A" winding L22.

L22 = FINDI (P1X, P2X, P3X, A0, A11, A12, A13, A21, A22, A23, A31, A32, A33)

L22 is the phase "A" primary winding inductance. In general, all transformer inductances and mutual inductances are functions of all six transformer currents. Function subprogram FINDI is used to calculate the saturated value of each inductance and mutual inductance. Each entry in the calling list of parameters is defined.

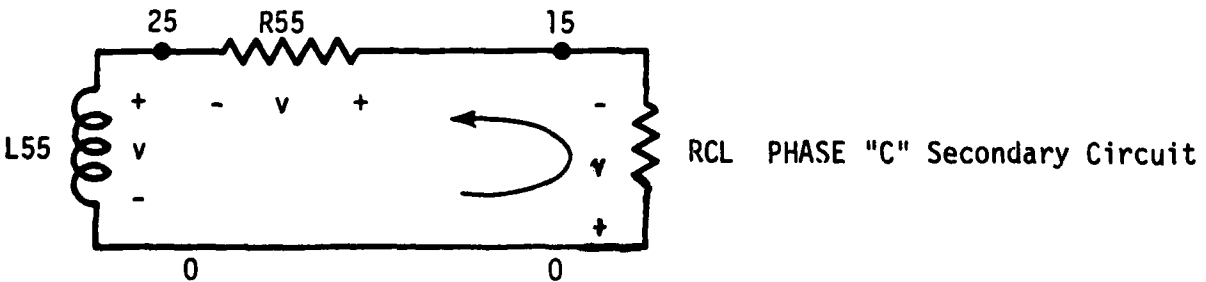
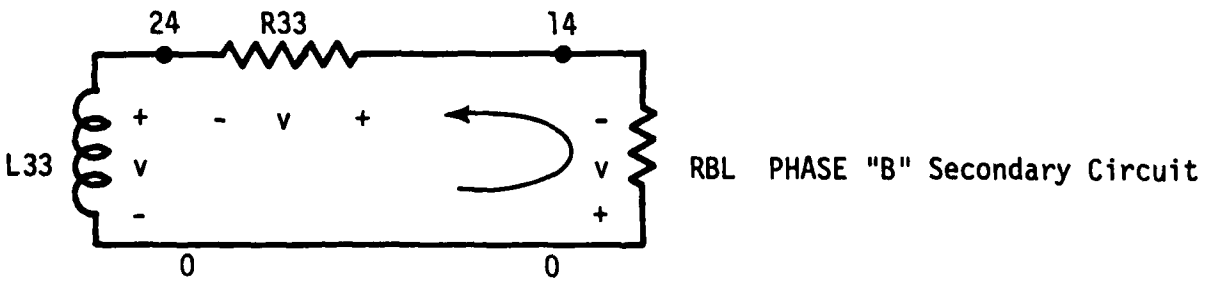
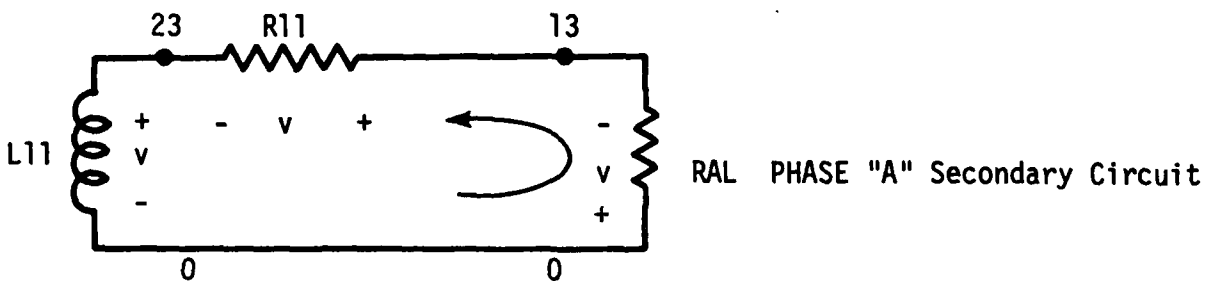
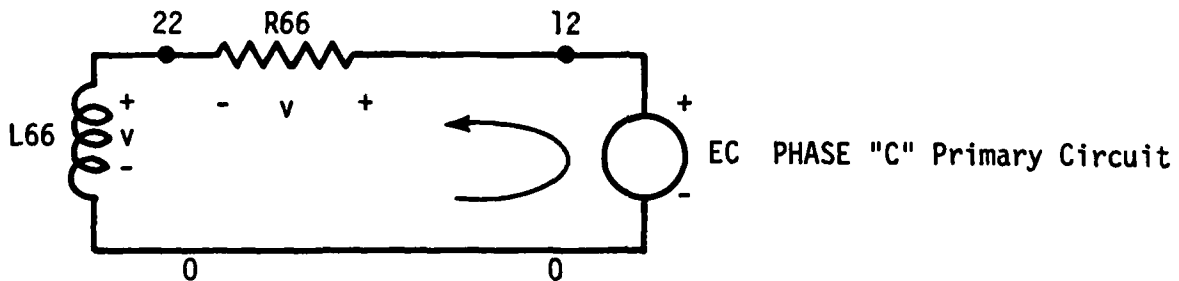
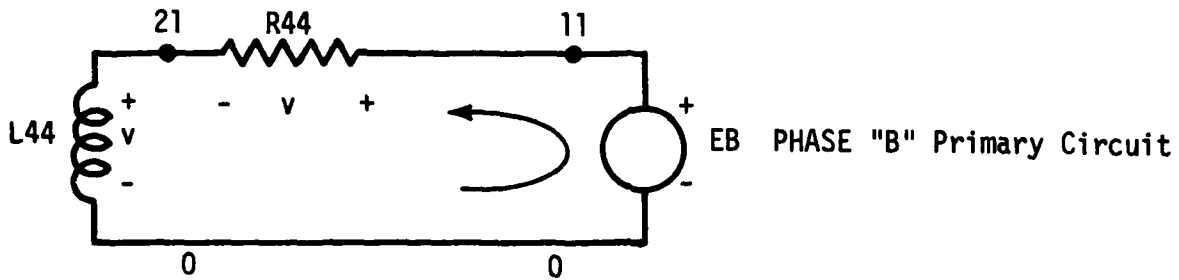
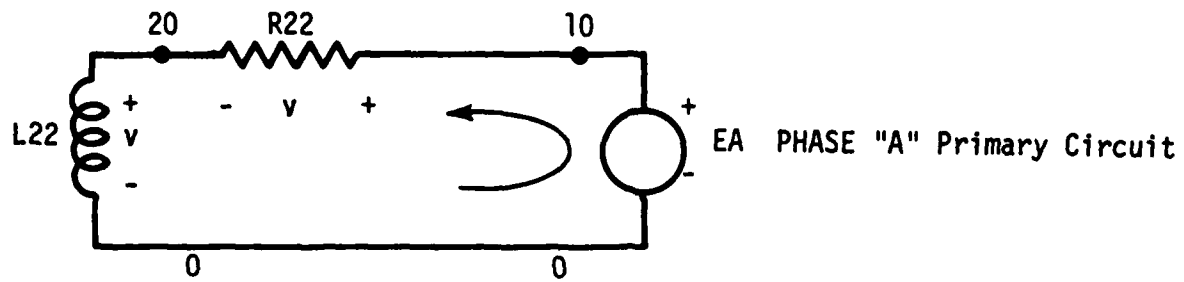


FIGURE 79. SCEPTRE NODE NUMBERING FOR THREE PHASE TRANSFORMER

P1X - By assuming a constant primary-to-secondary turns ratio the model may be simplified greatly. This assumption allows each inductance to be a function of three currents. P1X is the phase "A" magnetizing current. Specific details of P1X will be offered later.

P2X - phase "B" magnetizing current

P3X - phase "C" magnetizing current

A0 - unsaturated value of inductance

A11, A12, ..., A33 - regression coefficients.

Experimental measurements of each inductance and mutual inductance as a function of three magnetizing currents are conducted. By application of linear regression analysis, the "best fit" is determined using a polynomial model.

$$L = A0 + A11 * P1X + A12 * P1X ** 2 + A13 * P1X ** 3 \\ + A21 * P2X + A22 * P2X ** 2 + A23 * P2X ** 3 \\ + A31 * P3X + A32 * P3X ** 2 + A33 * P3X ** 3$$

From this model, each of the regression coefficients are determined.

The remaining circuit elements are similar to these previously defined.

EB - phase "B" transformer excitation voltage

R44 - phase "B" primary winding resistance

L44 - phase "B" primary winding inductance

EC - phase "C" transformer excitation voltage

R66 - phase "C" primary winding resistance

L66 - phase "C" primary winding inductance

RAL - phase "A" secondary load resistance

R11 - phase "A" secondary winding resistance

L11 - phase "A" secondary winding inductance

RBL - phase "B" secondary load resistance  
R33 - phase "B" secondary winding resistance  
L33 - phase "B" secondary winding inductance  
RCL - phase "C" secondary load resistance  
R55 - phase "C" secondary winding resistance  
L55 - phase "C" secondary winding inductance

M12 Mutual inductance terms which link each of the six winding

M13 inductances. Representation of a three phase transformer model

M14 requires the inclusion of each of these mutual inductance terms.

M15 In representation of a bank of three single phase transformers,

M16 only those mutual inductances which link phase primary to phase

M23 secondary are included. These are M12, M34, M56.

M24

M25

M26

M34

M35

M36

M45

M46

M56

PN1 - the number of primary winding turns

PN2 - the number of secondary winding turns

P1X - phase "A" magnetizing current referenced to secondary current

P2X - phase "B" magnetizing current referenced to secondary current

P3X - phase "C" magnetizing current referenced to secondary current

Each magnetizing current is defined to be secondary current plus turns ratio times primary current.

#### D.3.1 Integration of the Transformer Model

The transformer model may be coupled to models of other equipment by altering certain elements.

#### D.3.2 Generator-Transformer Model

The three generator load resistors (RAL, RBL, RCL) must be removed. The three transformer primary voltage sources (EA, EB, EC) must be removed. The two models are then connected to each other. Care must be taken to insure that duplicate element names and node connections are not used.

#### D.3.3 Transformer - Load Model

The three transformer load resistors (RAL, RBL, RCL) must be removed. The transformer secondary connections are mated to the input connections of the load model.



## D.4 THE RESONANT CHARGING PROGRAMS

The resonant charging part of the user's manual is in three parts. First, an SCR model is created in SCEPTRE with parameters for the GE C602LM used in later circuit models. Second, the AC charging circuit and program are given and last the DC charging circuit and program are given.

Tables are included to identify the particular numerical values in the example problems of the programs included.

### D.4.1 The SCR Model

A permanent SCR model is entered into SCEPTRE. The numerical values are for the particular SCR used in subsequent simulations.

Figure 80 gives the SCR circuit in SCEPTRE format with nodes and element name corresponding to those used in the SCR model program of Figure 81.

Tables 12, 13 and 14 give the numerical values used in the model and relate these to the circuit elements of Figure 80 and the program of Figure 81.

The model requires two FORTRAN subroutines. One of these, FIS, is used to simulate junction breakdown the other, FCJ, is used to compute a non-linear breakdown capacitance. These are given in Figures 83 and 82.

The subroutines are in FORTRAN and are function subprograms.

The model is named SCR by the statement

```
MODEL SCR (A-G-K)
```

and the A-G-K are dummy variables of the three terminal device or element. When listing elements the nodes to which these terminals are connected in a circuit are specified.

The resistors are listed first under elements in standard SCEPTRE format described at the beginning of this appendix.

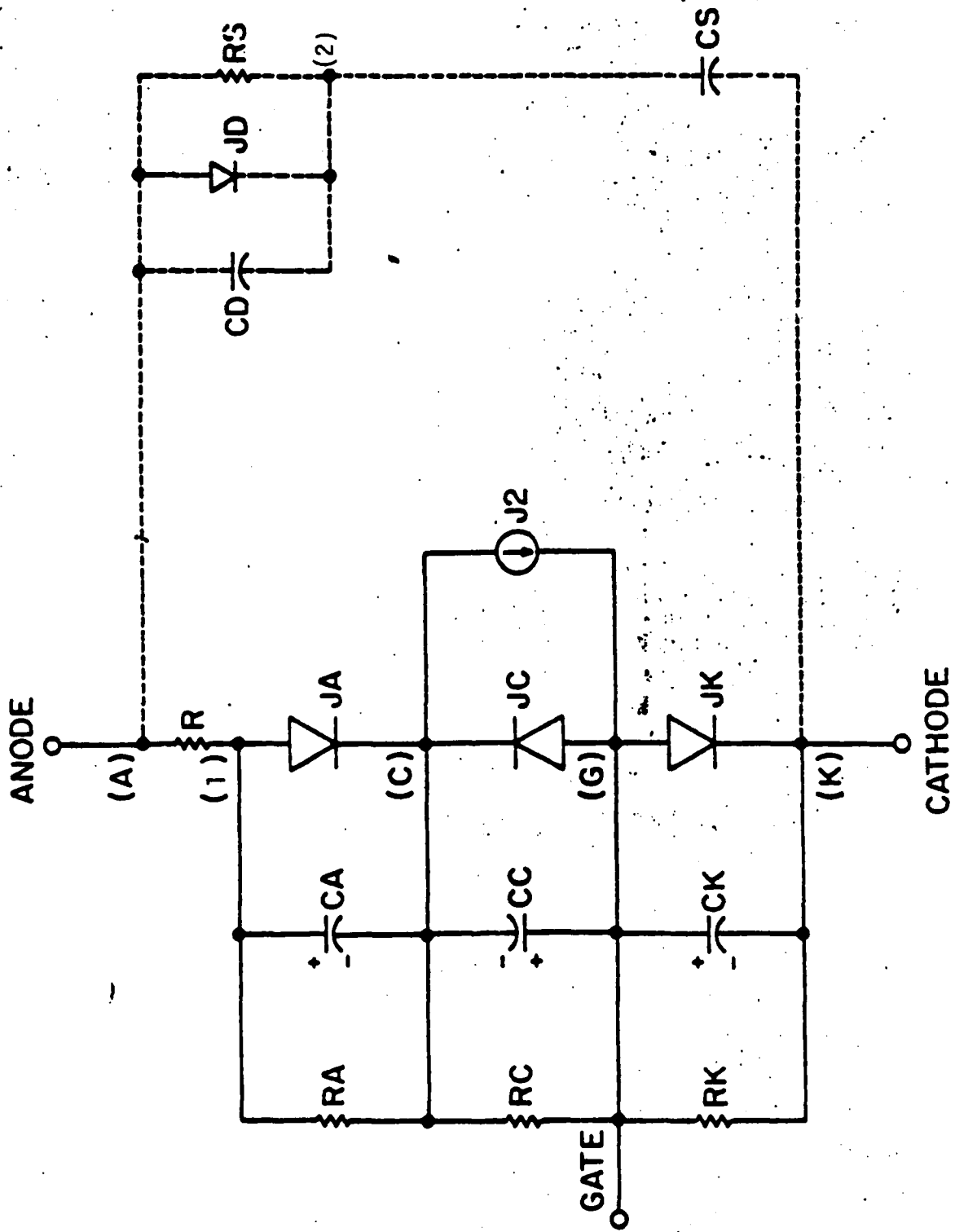


FIGURE 80. THE SCPTRE REDUCED 3-JUNCTION SCR MODEL WITH A REDUCED NUMBER OF CURRENT SOURCES IN THE MODEL. (—) model. (---) optional snubber.

MODEL DESCRIPTION  
MODEL SCR(A-G-K)

THIS IS A REDUCED ELEMENT VERSION OF THE 3-JUNCTION SCR MODEL DEVELOPED FOR USE WITH SCEPTRE. THE PARAMETER DETERMINATION PROCEEDURE FOR THIS MODEL IS THE SAME AS FOR THE 3-JUNCTION MODEL.

UNITS: OHMS, FARADS, HENRIES, SECONDS, AMPS, VOLTS

ELEMENTS

R, A-1=5. D-3

RA, 1-C=1. D6

RC, C-G=1. D6

RK, G-K=9. 375

JA, 1-C=DIODE Q(2.488D-17, 38.61)

JC, C-C=DIODE Q(PX1, PX2)

JK, G-K=DIODE Q(PX3, PX2)

J2, C-G=X1(.9\*JA+.9\*JK)

CA, 1-C=FCJ(1.78D-5, 2.488D-17, 38.61, JA, VCA, 4. D-9, 1. D-10)

CC, G-C=FCJ(4.95D-6, 5.65D-15, 38.61, JC, VCC, 4. D-9, 1. D-10)

CK, G-K=1. D-9

RS, A-2=100.

CS, 2-K=. 1D-6

DEFINED PARAMETERS

PX1=FIS(5.65D-15, VCC, 2.7D3)

PX2=38.61

PX3=FIS(2.488D-17, VCK, 5.)

OUTPUTS

VCA, VCC, VCK, PLOT

FIGURE 81. SCEPTRE MODEL DESCRIPTION  
INPUT FOR A GE C602 LM

DOUBLE PRECISION FUNCTION FIS(IS, VJ, VBD)  
C SUBROUTINE FIS IS USSD TO SIMULATE JUNCTION BREAKDOWN BY VARYING THE  
C SATURATION CURRENT, IS, INPUT TO THE DIODE EQUATION FOR PRIMARY DEPENDENT  
C CURRENT SOURCES. IS = JUNCTION REVERSE SATURATION CURRENT: VJ =  
C CAPACITOR STATE VARIABLE VOLTAGE FOR JUNCTION: VBD = BREAKDOWN VOLTAGE:  
IMPLICIT REAL\*8(A-K, O-Z)  
FIS=IS  
IF(VJ.GE.-VBD) RETURN  
A=100.\*(-VBD-VJ)  
IF(A.LE.40.) GO TO 10  
A=40.  
10 FIS=IS\*DEXP(A)  
RETURN  
END

FIGURE 82. SUBROUTINE FIS USED TO  
CALCULATE PX1 & PX2 OF  
TABLE 9.

```

      DOUBLE PRECISION FUNCTION FCJ(TAU, IS, THT, J, VC, CJO, CMIN)
C SUBROUTINE FCJ CALCULATES THE NON-LINEAR INCREMENTAL CAPACITANCE ASSOCIATED
C WITH THE CHARGE STORAGE OCCURRING ABOUT A PN JUNCTION. IF THE JUNCTION IS
C FORWARD BIASED THE DEPLETION LAYER TERM IS HELD CONSTANT WHILE THE DIFFUSION
C CALCULATED. CONVERSELY IF THE JUNCTION IS REVERSE BIASED ONLY A DEPLETION
C TERM IS CALCULATED. FOR A REVERSED BIASED JUNCTION THE CAPACITANCE IS LIMITED
C TO A MINIMUM VALUE, CMIN, TO AVOID UNREASONABLY SMALL TIME CONSTANTS IN THE
C CIRCUIT SIMULATION. PARAMETERS ARE; TAU = THE EXCESS CARRIER LIFETIME IN THE
C NEUTRAL REGIONS ABOUT THE JUNCTION, IS = JUNCTION SATURATION CURRENT, THT =
C EINSTEIN'S CONSTANT (Q/KT = 38.61 @ 300 DEG K.), J = CURRENT SOURCE SIMULATING
C THE PN JUNCTION FOR WHICH CAPACITANCE IS BEING CALCULATED, VC = VOLTAGE ACROSS
C CAPACITOR WHOSE VALUE IS BEING CALCULATED, CJO = ZERO BIAS VALUE OF THE
C DEPLETION LAYER CAPACITANCE, CMIN = MINIMUM VALUE OF JUNCTION CAPACITANCE TO
C BE ALLOWED.
      IMPLICIT REAL*8(A-Z)
      IF(VC.GT.0.) GO TO 10
      FCJ=CJO/(1.-VC)**.5
      IF(FCJ.GE.CMIN) RETURN
      FCJ=CMIN
      RETURN
10 FCJ=TAU*THT*(J+IS)+CJO
      RETURN
      END

```

FIGURE 83. SPECIAL SUBROUTINE FCJ USED TO CALCULATE NON-LINEAR JUNCTION CAPACITANCES OF THE SCEPTRE 3-JUNCTION SCR MODEL.

TABLE 12. SCEPTRE 3-Junction SCR Model Parameters Obtained Using The Procedure of Table 6 For a GE C602 LM SCR.

$R_K = 9.375 \Omega$	$I_{CS} = 5.65D-15 A$
$\alpha_{R_2} = 0.5$	$P_3 = 4.4D-3$
$\alpha_{f_2} = 0.9$	$R = 5.D-4 \Omega$
$\alpha_{f_1} = 0.9$	$\tau_{R_1} = 4.95D-6 S$
$\alpha_{R_1} = 0.9$	$C_{JC_0} = 4.D-9 F$
$\tau_{f_1} = 1.780-5 S$	$C_{JA_0} = 4.D-9 F$
$\theta = 38.61 V^{-1}$	$CK = 1.D-9 F$
$I_S = 2.239D-17 A$	$V_{BOC} = 2.7D3$
$I_{AS} = 2.488D-17 A$	$V_{BOK} = 5.$
$I_{KS} = 2.488D-17 A$	$C_{MIN} = 1.D-10$

TABLE 13. Manufacturer's Specifications For a GE C602 LM SCR And SCEPTRE Computer Simulation Specification Predictions.

<u>Quantity</u>	<u>Manufacturer's specifications</u>	<u>SCEPTRE simulation value</u>
$I_H$	100 ma	100 ma
$I_{GT}$	80 ma	87 ma
$t_r(t_{on})$	3.6 $\mu s$ (5.4 $\mu s$ )	4 $\mu s$ (7 $\mu s$ )
$V_T$	1.1V	1.1V
$V_{BO}$	2700V	2700V
dv/dt	G.T.500V/ $\mu s$	G.T.500V/ $\mu s$
$t_q$	L.T.125 $\mu s$	L.T.125 $\mu s$

TABLE 14. SCEPTRE SCR Model Circuit Element Description For The 3-Junction Model of Figure 24.

RESISTORS

R, A-1 = R  
 RA, 1-C = 1.D6  
 RC, C-6 = 1.D6  
 RK, G-K = RK

PRIMARY DEPENDENT SOURCES (PN JUNCTIONS)

JA , 1-C = DIODE Q(I<sub>AS</sub>, θ)  
 JC , G-C = DIODE Q(PX1, PX2)  
 JK , G-K = DIODE Q(PX3, PX2)

SECONDARY DEPENDENT SOURCES (COLLECTED CURRENTS & REVERSE BREAKDOWN CURRENTS)

J2 = X1(α<sub>f1</sub>\*JA + α<sub>f2</sub>\*JK)

CAPACITANCES (JUNCTION DEPLETION LAYER AND NEUTRAL REGION EXCESS CHARGE STORAGE [DIFFUSION])

CA, 1-C = FCJ(τ<sub>f1</sub>, I<sub>AS</sub>, θ, JA, VCA, C<sub>JAO</sub>, C<sub>MIN</sub>)  
 CC, G-C = FCJ(τ<sub>r1</sub>, I<sub>CS</sub>, θ, JC, VCC, C<sub>JCO</sub>, C<sub>MIN</sub>)  
 CK, G-K = CK

DEFINED PARAMETERS (REVERSE BREAKDOWN MULTIPLIERS)

PX1 = FIS(I<sub>CS</sub>, VCC, VBOC)  
 PX2 = θ  
 PX3 = FIS(I<sub>KS</sub>, VCK, VBOK)

SNUBBER ELEMENTS (OPTIONAL)

RS , A-2 = VALUE IN OHMS  
 CS , 2-K = VALUE IN FARADS

ALSO IF USING DIODE SNUBBER:

-----

JD , A-2 = DIODE Q(DIODE SAT. CURRENT, THERMAL VOLTAGE)  
 CD , A-2 = VALUE IN FARADS

The J current sources are defined by terminals to which they are connected and by the SCEPTRE internal diode model or by an equation. For example

$$JA, 1 - C = DIODE Q(X1,X2)$$

$$J2, C - G = X1(.9 * KA + .9 * JK)$$

The JA is defined by the SCEPTRE diode model when X1 and X2 are supplied.

X1 is the diode saturation current  $I_{AS}$  of Table 12 and X2 is the VD of the diode equation

$$I_D = I_S (e^{\theta V_D} - 1)$$

The J2 is defined by the expression in the parentheses.

The capacitors CA and CC are defined by the FORTRAN function subprogram FCJ. The CA for example is a capacitor connected between nodes 1 and C defined by

$$CA, 1 - C = FCJ (1.78D-5, 2.488D-17, 38.61, JA, VCA, 4.D-9, 1.D-10)$$

The required numbers can be identified from Table 12.

Under the defined parameter header the FORTRAN function subprogram calculates PX1. This and  $PX2 = 38.61$  are used in the diode equation for defining JC. JK is similarly computed.

#### D.4.2 The AC Resonant Charging Circuit

Figure 85 gives the program for a simulation of an AC resonant charging circuit. The node coding and the element name designations are shown on the circuit diagram of Figure 84. Table 15 gives the element values not already given in the SCR model.

In the program the voltage sources EAN, EBN, and ECN, the resistors RA, RB, RC, R1A, R2A, R1B, R2B, R1C, and R2C, the inductors LA, LB, and LC, and the capacitors C1A, C2A, C1B, C2B, C1C, and C2C are read in the manner previously described in Section D.2.4.1 for entering circuit elements.

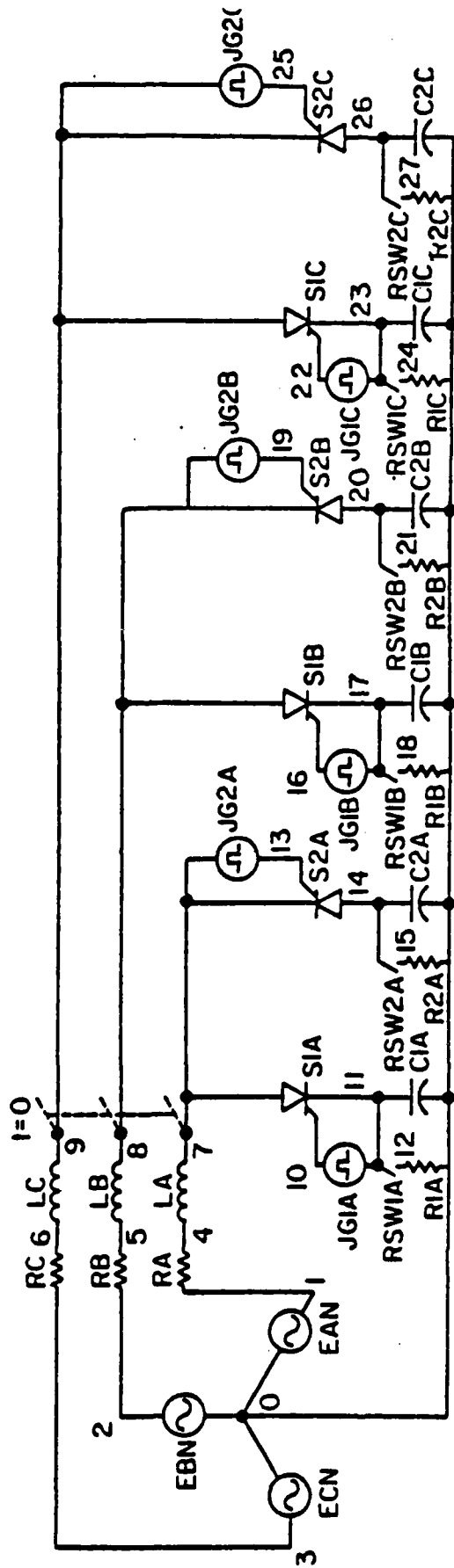


FIGURE 84. 3- $\phi$  AC RESONANT CHARGING CIRCUIT.

```

CIRCUIT DESCRIPTION
ELEMENTS
EAN,0-1=X1(1.D3*DSIN(6285.18*TIME))
RA,1-4=1.
LA,4-7=5.897E-2
EBN,0-2=X2(1.D3*DSIN(6285.18*TIME-2.094))
RB,2-5=1.
LB,5-8=5.897E-2
ECN,0-3=X3(1.D3*DSIN(6285.18*TIME+2.094))
RC,3-6=1.
LC,6-9=5.897E-2
S1A,7-10-11=MODEL SCR
S2A,14-13-7=MODEL SCR
C1A,11-0=.43D-6
C2A,0-14=.43D-6
R1A,12-0=11.
R2A,15-0=11.
JG1A,11-10=FGEN(.2,0.,0.,1.D-4,1.D-3,TIME,0)
JG2A,7-13=FGEN(.2,0.,5.D-4,1.D-4,1.D-3,TIME,0)
RSW1A,11-12=FGEN(1.D7,0.,-2.25D-4,9.75D-4,1.D-3,TIME,1)
RSW2A,14-15=FGEN(1.D7,0.,-7.25D-4,9.75D-4,1.D-3,TIME,1)
S1B,8-16-17=MODEL SCR
S2B,20-19-8=MODEL SCR
C1B,17-0=.43D-6
C2B,0-20=.43D-6
R1B,18-0=11.
R2B,21-0=11.
JG1B,17-16=FGEN(.2,0.,3.33D-4,1.D-4,1.D-3,TIME,0)
JG2B,8-19=FGEN(.2,0.,-1.67D-4,1.D-4,1.D-3,TIME,0)
RSW1B,17-18=FGEN(1.D7,0.,-8.92D-4,9.75D-4,1.D-3,TIME,1)
RSW2B,20-21=FGEN(1.D7,0.,-3.92D-4,9.75D-4,1.D-3,TIME,1)
S1C,9-22-23=MODEL SCR
S2C,26-25-9=MODEL SCR
C1C,23-0=.43D-6
C2C,0-26=.43D-6
R1C,24-0=11.
R2C,27-0=11
JG1C,23-22=FGEN(.2,0.,6.67D-4,1.D-4,1.D-3,TIME,0)
JG2C,9-25=FGEN(.2,0.,1.67D-4,1.D-4,1.D-3,TIME,0)
RSW1C,23-24=FGEN(1.D7,0.,-5.58D-4,9.75D-4,1.D-3,TIME,1)
RSW2C,26-27=FGEN(1.D7,0.,-5.58D-4,9.75D-4,1.D-3,TIME,1)
OUTPUTS
EAN,VC1A,VC2A,ILA,PLOT1
EBN,VC1B,VC2B,ILB,PLOT2
ECN,VC1C,VC2C,ILC,PLOT3
RUN CONTROLS
INTEGRATION ROUTINE = IMPLICIT
PLOT INTERVAL = 1.E-5
MAXIMUM PRINT POINTS=0
STOP TIME=1.E-3
MINIMUM STEP SIZE = 1.E-30
END

```

FIGURE 85. SCEPTRE INPUT CIRCUIT DESCRIPTION FOR THE CIRCUIT OF FIGURE 84.

```

      DOUBLE PRECISION FUNCTION FGEN(HIGH,LOW,TD,TON,TP,TIME,MNEG)
C FGEN IS A PULSE GENERATOR SUBROUTINE. THE PARAMETERS ARE AS FOLLOWS;
C HIGH = MAXIMUM VALUE OF FUNCTION , LOW = MINIMUM VALUE OF FUNC-
C TD = TIME DELAY UNTIL START OF FIRST PULSE, TON = TIME OF PULSE DURA-
C TION , TP = TIME OF PULSE CYCLE PERIOD, TIME = TIME POINT OF CIR-
C CUIT BEING SIMULATED. PULSE VALUE IS SET TO LOW FOR TIME LESS THAN
C OR EQUAL TO ZERO IF MNEG IS NOT EQUAL TO 1. MNEG = 1 IF PULSE MAY HAVE
C NON-ZERO VALUE AT OR PRIOR TO TIME EQUAL ZERO.
      IMPLICIT REAL*8(A-L,N-Z)
      FGEN=LOW
      IF(TIME.LE.0..AND.MNEG.NE.1) GO TO 20
      N=(TIME-TD)/TP
      IF(N.LT.0.0) GO TO 20
      M=IDINT(N)
      P=(N-M)*TP
      IF(P.GT.TON) GO TO 10
      FGEN=HIGH
      GO TO 20
10 FGEN=LOW
20 RETURN
      END

```

FIGURE 86. SUBROUTINE FGEN IS A PULSE GENERATOR SUBROUTINE USED IN CIRCUIT SIMULATIONS TO SIMULATE GATE DRIVES AND CAPACITOR DISCHARGE SWITCHES.

TABLE 15. DC Resonant Charging Scaling

Quality	Silva's Diode Circuits (unscaled)	SCR Facsimile Circuits (scaled)
3-Phase <u>AC</u> System (section 6.2)		
Source Voltage	6465.85V per phase	1000V per phase
Source Frequency	400 hertz	1000 hertz.
Resonant load inductance	0.327 henries	0.05897 henries
Resonant load capacitance	0.43 micro-farads	0.43 micro-farads
DC Resonant Load on 3-phase Source (section 7.1)		
Source voltage	6465.85V per phase	1000V
Source frequency	400 hertz.	1000 hertz.
Resonant load inductance	2.58 henries	0.173 henries
Resonant load capacitance	2.58 micro-farads	0.586 micro-farads

The current sources for triggering the SCR's JG1A, JG2A, JG1B, JG2B, JG1C, and JG2C are defined by a FORTRAN function subprogram given in Figure 86, FGEN. The SCR's S1A, S2A, S1B, S2B, S1C, and S2C are defined by the SCR model described in Section D.4.1. For example the statement

S1A, 7-10-11 = MODEL SCR

indicates to the program that a device described by a model called SCR is connected to nodes 7-10-11. The order of the nodes listed must properly correspond to the nodes of the model of Section D.4.1.

The switches RSW1A, RSW2A, RSW1B, RSW2B, RSW1C and RSW2C are defined by the FORTRAN function subprogram given in Figure 86, FGEN.

The outputs are optional and are determined as defined in Section D.4.2.9. Similarly, the run control options are defined in Section D.4.2.11.

### D.4.3 The DC Resonant Charging Circuit

Figure 88 gives the programs for a simulation of a DC resonant charging circuit. The node coding and the element name designations are shown on the circuit diagram of Figure 87. Table 15 gives the element values not already given in the SCR model.

The only element entries different in form from those already described in Section D.4.2 are the switches or relays defined by entering a model element for each switch K2 and SW1.

The switch K2 for example is defined by the model statements

```
MODEL RLY(1-2)
ELEMENTS
R, 1-2 = TABLE 1
FUNCTIONS
TABLE 1
0., 1.E8, 2.5E-5, 1.E8, 2.5E-5, 0., 2.E-3, 0.
```

These statements model a resistor which takes on values varying with time as defined by Table 1.

The use of function tables is described in Section D.4.2.3.

In the program the statement

```
K2, 11-12 = MODEL RLY 1
```

tells the program the device designated as K2 is connected between nodes 11 and 12 and is defined by previously entered model RLY 1.

All other elements are similar to the ones described in Section D.4.2 but for the circuit arrangement of Figure 87.

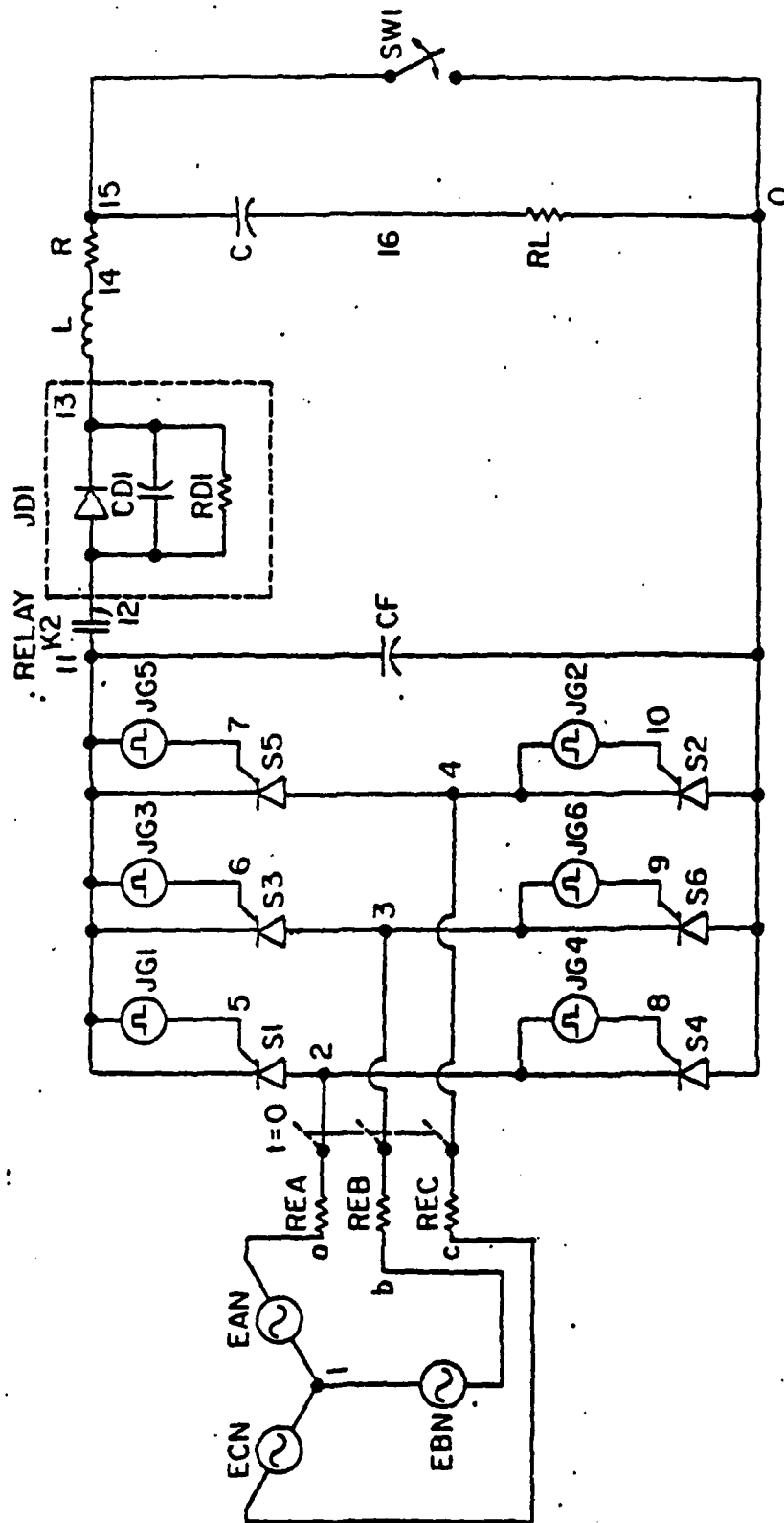


FIGURE 87. A DC RESONANT CHARGING SYSTEM.

```

MODEL DESCRIPTION
MODEL RLY1(1-2)
THIS MODEL REPRESENTS RELAY K2 IN JAMIE SILVA'S CIRCUIT
ELEMENTS
R,1-2=TABLE 1
FUNCTIONS
TABLE 1
0.,1.E8,2.5E-5,1.E8,2.5E-5,0.,2.E-3,0.
MODEL DESCRIPTION
MODEL RLY2(1-2)
THIS MODEL REPRESENTS SWITCH SW1 IN JAMIE SILVA'S CIRCUIT
ELEMENTS
R,1-2=TABLE 1
FUNCTIONS
TABLE 1
0.,0.,2.0E-5,0.,2.5E-5,1.E8,1.E-3,1.E8,1.E-3,0.,1.02E-3,0.,1.02E-3,
1.E8,2.E-3,1.E8
CIRCUIT DESCRIPTION
THIS CIRCUIT SIMULATES A 1000V/1KHZ RESONANT CHARGING PULSE POWER
SYSTEM.
ELEMENTS
EAN,1-A=X1(1.D3*DSIN(6285.18*TIME-5.236D-1))
REA,A-2=1.
EBN,1-B=X2(1.D3*DSIN(6285.18*TIME-2.618))
REB,B-3=1.
ECN,1-C=X3(1.D3*DSIN(6285.18*TIME+1.5708))
REC,C-4=1.
S1,2-5-11=MODEL SCR
S2,0-10-4=MODEL SCR
S3,3-6-11=MODEL SCR
S4,0-8-2=MODEL SCR
S5,4-7-11=MODEL SCR
S6,0-9-3=MODEL SCR
JG1,11-5=FGEN(.2,0.,1.67E-4,3.33E-4,1.E-3,TIME,1)
JG2,4-10=FGEN(.2,0.,3.33E-4,3.33E-4,1.E-3,TIME,1)
JG3,11-6=FGEN(.2,0.,5.00E-4,3.33E-4,1.E-3,TIME,1)
JG4,2-8=FGEN(.2,0.,6.67E-4,3.33E-4,1.E-3,TIME,1)
JG5,11-7=FGEN(.2,0.,-1.67E-4,3.33E-4,1.E-3,TIME,1)
JG6,3-9=FGEN(.2,0.,0.,3.33E-4,1.E-3,TIME,1)
CF,11-0=7.5E-9.
K2,11-12=MODEL RLY1
JD1,12-13=DIODE Q(1.D-8,38.61)
CD1,12-13=5.D-9
RD1,12-13=1.D4
L,13-14=.173
R,14-15=1.E-2
SW1,15-0=MODEL RLY2
CO,15-16=.586E-6
RL,16-0=1.82
OUTPUTS
EAN,VCF,IRL,VCO,PLOT1
IREA,IREB,IREC,PLOT2
RUN CONTROLS
RUN INITIAL CONDITIONS
INTEGRATION ROUTINE = IMPLICIT
PLOT INTERVAL = 1.E-5
MAXIMUM PRINT POINTS=0
STOP TIME=1.02E-3
MINIMUM STEP SIZE = 1.E-30
END

```

FIGURE 88. SCEPTRE INPUT LISTING FOR THE DC RESONANT CHARGING SYSTEM OF FIG. 69.

## REFERENCES

1. R.H. Park and B.L. Robertson, "The Reactances of Synchronous Machines," Trans. AIEE, Vol. 471, No. 21, pp. 514-536.
2. S.R. Sedore and J. Bowers, "SCEPTRE: A Computer Program for Circuits and Systems Analysis," Prentice-Hall, Inc., Englewood Cliffs, N.Y., 1971.
3. I.R. Smith and L.A. Snider, "Prediction of Transient Performance of Isolated Saturated Synchronous Generators," Proc. IEEE (London), Vol. 119, No. 9, pp. 1309-1318, September, 1972.
4. L.A. Snider and I.R. Smith, "Measurement of Inductance Machines," Proc. IEEE, Vol. 119, No. 5, May 1972.
5. E.W. Kimbark, "Power System Stability," (Vol. III, Synchronous Machines) 1956, Wiley.
6. P.M. Anderson and A.A. Foad, "Power Systems Control and Stability," Iowa State University Press, 1977.
7. Charles Concordia, "Synchronous Machines - Theory and Performance," Wiley 1951.
8. H.L. Nakra and T.H. Barton, "Three Phase Transformer Transient," IEEE Winter Power Meeting, New York, N.Y. 1973.
9. W.A. Manly Jr., "An Appraisal of Several Nonlinear Hysteresis Loop Models," IEEE Trans. on Magnetics, Vol. No. 3, May 9, Sept. 1973.
10. H.L. Nakra and J.H. Barton, "The Dynamics of Coupled Circuits with Ferromagnetic Non-Linearity. IEEE Winter Power Meeting, New York, N.Y., 1971.
11. Leon O. Chua and Pen-Min Lin, "Computer-Analysis of Electronic Circuits," Englewood Cliffs, New Jersey, Prentice Hall, 1975.
12. D.A. Calahan, "Computer-Aided Analysis of Electronic Circuits," Englewood Cliffs, New Jersey: Prentice Hall, 1975.
13. W.K. Macfadyen, R.R.S. Simpson, R.D. Slater, W.S. Wood, "Representation of Magnetization Curves by Exponential Series." PROC. IEEE, Vol. 120, No. 8, August 73.
14. AFAPL-TR-76-102 "Development of Lightweight Transformers for Airborne High Power Supplies," Thermal Technology Laboratories, Inc. December, 1976.
15. G.E. Forsythe, M.A. Malcom and C.B. Moler, Computer Methods for Mathematical Computations - Englewood Cliffs, New Jersey: Prentice Hall, 1977.
16. L.O. Chua and P.M. Lin, Computer-Aided Analysis of Electronic

Circuits: Algorithms and Computational Techniques. Englewood Cliffs, New Jersey: Prentice Hall, 1975.

17. C.W. Gear, Numerical Initial Value Problems in Ordinary Differential Equations. Englewood Cliffs, New Jersey: Prentice Hall, 1971.
18. A. Ralston and P. Rabinowitz, A First Course in Numerical Analysis 2nd ed. New York: McGraw-Hill, 1978, 1965, Chap. 5.
19. S.W. Director, Computer-Aided Circuit Design: Simulation and Optimization. Stroudsburg, Pennsylvania: Dowden, Hutchinson and Ross, 1974.
20. D.A. Calahan, "Numerical Considerations for Implementation of a Nonlinear Transient Circuit Analysis Program," IEEE Trans. Circuit Theory, CT-18, pp. 66-73, Jan. 1971.
21. R.K. Brayton, F.G. Gustafson and G.D. Hachtel, "A New Efficient Algorithm for Solving Differential-Algebraic Systems Using Implicit Backward Differentiation Formulas," PROC. IEEE, 60, pp. 98-108, Jan. 1972.
22. G.N. Glasoe, J.V. Lebacqz, "Pulse Generators" Radiation Laboratory Series, McGraw-Hill, 1948.
23. F.H. Branin, Jr., G.R. Hogsett, R.L. Lunde, and L.E. Kugal, "ECAP II A New Electronic Circuit Analysis Program," IEEE J. Solid-State Circuits, SC-6, pp. 146-166, Aug. 1971.
24. Avant, R.L., R. Ramanathan, and F.C. Lee, "Computer Simulation of DC and AC Resonant Charging Circuits for Pulse Power Applications", PCI/MOTOCON March 1983 Conference Record.
25. Stephenson, R.E., "Computer Simulation for Engineers", Harcourt Brace, Javonovich, Inc., New York, 1971.
26. Collilla, A.M., M.J. O'Sullivan, D.J. Carlino, "Systems Simulation", Lexington Books, D.C. Heath and Company, Lexington, MA, 1974.
27. "Subsystem Design Analysis Lightweight Alternator" (Model Test Program). Final Report, March 1977, AFWL-TR-75-66, Add 2.
28. Sedore, Stephen R., "Sceptre Support II, Volume I: Revised Users Manual", NTIS Publication AD-882 384, July 1970.
29. Sedore, Stephen R., "Sceptre Support II, Revised Mathematical Formulation", NTIS Publication AD-882 385.
30. Becker, David, "Extend Scepter Volume II - Mathematical formulation", NTIS Publication AD-A009 595, Dec. 1974.
31. Sedore, Stephen R., "Sceptre Support II, Volume I: Revised User's Manual (supplement)", NTIS Publication AD-751 518, Sept. 1972.

32. Temple, V.A.K., F.W. Holroyd, M.S. Adler, P.V. Gray, "The Effect of Carrier Lifetime Profile on Turn-off Time and Turn-off Losses", IEEE PESC '80 Record.
33. Avant, R.L., F.C. Lee and D.Y. Chen, "A Practical SCR Model for Computer Aided Analysis of AC Resonant Charging Circuits", Proceedings, IEEE Power Electronics Specialists Conference, 1981.
34. Waiman, F., Ki, "A SPICE Model for the SCR", Master Thesis, Department of Electrical and Computer Science, University of California-Berkeley, Dec. 1979.
35. Hu, C. and W.F. Ki, "Toward a Practical Computer Aid for Thyristor Circuit Design", IEEE Power Electronics Specialists Conference, 1980.
36. Maggetto, Gaston, "Le Thyristor: Definitions, Protections, Commands", Presses Universitaires de Bruxelles, Avenue Paul Higer 42, 1050, Bruxelles, 1971.
37. Bowers, James C. and Stephen R. Sedore, "SCEPTRE: A Computer Program for Circuit and Systems Analysis, Prentice-Hall, Inc., Englewood Cliffs, New Jersey, 1971.
38. Getreu, I.E., "Modeling the Bipolar Transistor", Elsevier Scientific Publishing Company, New York, 1978.
39. Blicher, Adolf, "Thyristor Physics", Springer-Verlag, New York, 1976.
40. G.E. SCR Manual, 6th Edition, 1979.
41. Becker, David, "Extended Sceptre, Volume I", NTIS Publication AD/A-009 594, Dec. 1974.
42. Silva, Jaime R., "Prime Power to Pulse Conditioning Interface Methods", Thesis for M.S.E.E., Dec. 1980, Air Force Institute of Technology, WPAFB, Dayton, Ohio.
43. Bowers, James C., et al., "User's Manual for SUPER-SCEPTRE", Final Report on Contract No. DAAA-21-73-C-0655, Fuse Development and Engineering Division, Picatinny Arsenal, Dover, New Jersey, May 1975.
44. Nienhus, H.A., and J.C. Bowers, "A General Purpose Computer Model for a High Power SCR", Technical Report AFAPL-TR-76-82, USAF Aero Propulsion Laboratory, AFAPL/POD, Wright-Patterson Air Base.
45. Dougherty, M., "A Series Resonant Inverter Simulation using SUPER-SCEPTRE", Proceedings of the IEEE 1979 National Aerospace and Electronics Conference, NAECON 1979.
46. Lee, F.C., D.Y. Chen, R.L. Avnat, and R. Ramanathan, Report on Phase I of the Dynamic Simulation of Airborne High Power Systems", Elec. Eng. Dept., VPI & SU, Sept. 18, 1980.

47. "A Computer Model for a High Power SCR", Final Report, AFAPL-TR-75-106, Dec. 1975.
48. "Silicon Controlled Rectifier Large Signal Model", Report No. AFAPL-TR-75-89, Oct. 1975.
49. Nagel, W.W., "SPICE2: A Computer Program to Simulate Semiconductor Circuits", Electronic Research Laboratory, College of Engineering, University of California, Berkeley, CA, Memo No. ERL-M520.
50. Bowers, James et al., "A Survey of Computer Aided-Design and Analysis Programs", Technical Report, AFAPL-TR-76-33, USAF Aero Propulsion Laboratory, AFAPL/POD, Wright-Patterson Air Force Base, Ohio, April 1976.

INITIAL DISTRIBUTION LIST

DTIC-DDA-1	CONDENSER PRODUCTS CORPORATION
AFWAL/PS	DOUGLAS AIRCRAFT COMPANY
AFWAL/TST/LIBRARY	ENGINEERING SOCIETIES LIBRARY
AFWAL/TST/PO	FILM CAPACITORS, INC.
AFWAL/NTYP	FICHER ENGINEERING
AFWL/CA	AIRESEARCH MANUFACTURING CO
AIR UNIVERSITY LIBRARY	GENERAL ELECTRIC COMPANY
USA FOR SCI AND TECH CTR	GEORGIA TECH
ERADCOM	DON BCSACK
US ARMY ELECTRONICS COMMAND	HUGHES AIRCRAFT COMPANY
MERADCOM	HUGHES RESEARCH LAB
USA FAC ENGR SUPPORT AG	IAN SMITH, INC.
NAVAL AVIONICS CENTER	KGS ELECTRONICS
NAVAL MATERIAL COMMAND	LOCKHEED MISSILES AND SPACE CO.
NAVAL OCEAN SYSTEMS CENTER	LOS ALAMOS SCIENTIFIC LAB
NAVAL INTEL SUPPORT CTR	MAXWELL LABORATORIES
NAVAL SEA SYSTEMS COMMAND	McGRAW EDISON COMPANY
DTNSRDC	NATIONAL RESEARCH GROUP
NASA LEWIS RESEARCH CENTER	PHYSICS INTERNATIONAL CO
NASA JOHNSON SC, CODE EH-5	RAYTHEON CO, MISSILE SYSTEMS DIV
NASA GODDARD SPACE FLT CTR	RCA/GOVERNMENT SYSTEMS DIV
NASA MARSHALL SPACE FLT CTR	SPRAGUE ELECTRIC CO
U.S. DOE, FUSION ENERGY OFFICE	TECH-TRAN CORP
DOD PROJ MGR-MOB ELECT PWR	THERMAL TECHNOLOGY LAB
NASA JET PROPULSION LAB	TOBE DEUTSCHMANN LABS
CENTRAL INTELLIGENCE AGENCY	UNITED AIRCRAFT CORPORATION
AEROVOX INC.	ST UNIV OF NY, BUFFALO
BOEING MILITARY AIRPLANE CO.	UNIVERSITY OF MICHIGAN
BROOKHAVEN NATIONAL LAB	UNIVERSITY OF TOLEDO
CSI TECHNOLOGIES, INC.	UNIVERISTY OF WASHINGTON
CLARENCE CONTROLS, INC.	UNIVERSITY OF WISCONSIN
CLEMSON UNIVERSITY	VPI & SU, DEPT OF EE
COMPONENTS RESEARCH CORP.	WESTINGHOUSE ELECTRIC, AEROSPACE DIV